UNIVERSIDADE FEDERAL DO CEARÁ
CENTRO DE TECNOLOGIA
DEPARTAMENTO DE ENGENHARIA DE TRANSPORTES
PROGRAMA DE PÓS-GRADUAÇÃO EM ENGENHARIA DE TRANSPORTES

LARISSA VIRGÍNIA DA SILVA RIBAS

THERMOCHROMIC FUNCTIONALIZATION OF ASPHALT MIXTURES AS AN URBAN HEAT ISLAND MITIGATION STRATEGY: ASSESSING SPRAY-COATING PERFORMANCE AND MICROCLIMATIC IMPACTS IN A TROPICAL ENVIRONMENT

FORTALEZA
2026

LARISSA VIRGÍNIA DA SILVA RIBAS

THERMOCHROMIC FUNCTIONALIZATION OF ASPHALT MIXTURES AS AN URBAN HEAT ISLAND MITIGATION STRATEGY: ASSESSING SPRAY-COATING PERFORMANCE AND MICROCLIMATIC IMPACTS IN A TROPICAL ENVIRONMENT

Dissertation document submitted as part of the requirements to obtain the Doctor's Degree in Transportation Engineering at Federal University of Ceará. Graduate Program in Transportation Engineering. Subarea: Transportation Infrastructure.

Advisor: Verônica Teixeira Franco Castelo Branco, Ph.D.

FORTALEZA

2026

LARISSA VIRGÍNIA DA SILVA RIBAS

THERMOCHROMIC FUNCTIONALIZATION OF ASPHALT MIXTURES AS AN URBAN HEAT ISLAND MITIGATION STRATEGY: ASSESSING SPRAY-COATING PERFORMANCE AND MICROCLIMATIC IMPACTS IN A TROPICAL ENVIRONMENT

Dissertation document submitted as part of the requirements to obtain the Doctor's Degree in Transportation Engineering at Federal University of Ceará. Graduate Program in Transportation Engineering. Subarea: Transportation Infrastructure.

Approved in: 26/05/2026.

COMMITTEE MEMBERS

____

Verônica T. F. Castelo Branco, Ph.D. (Advisor)
Universidade Federal do Ceará (UFC)

____

Prof. Dr. Pierre Basílio Almeida Fechine
Universidade Federal do Ceará (UFC)

____

Profa. Dr. Elisabete Fraga de Freitas
Universidade do Minho (UMinho)

____

Profa. Jamilla Emi Sudo Lutif Teixeira Ph.D.
University of Nebraska – Lincoln (UNL)

____

Dr. Isabel Lavrador Ribeiro
Swedish Meteorological and Hydrological Institute (SMHI)

ACKNOWLEDGMENTS

Um trabalho científico dessas proporções não se constrói de forma independente, e eu, afortunadamente, pude contar com o apoio de muitos. Aos que contribuíram, seja com a mão na massa, seja com o incentivo pessoal, deixo aqui meus inestimáveis agradecimentos:

À Mainha, Dinha, Lilian e Elvis que sempre oportunizaram e incentivaram minha educação. Um salve, pois finalmente teremos uma doutora na família!!

Ao TRAMA, o grupo de pesquisa que me recebeu e que "vesti a camisa", sinto que contribuímos mutuamente para nosso amadurecimento científico, levo um pouco e deixo um tanto de mim. Em nome dos colegas que entretiveram esses anos de doutoramento, em especial, Marina Soriano, Henrique Pinto, Victor Cardoso, Bruno Brito, Levi Chaves, Amanda Alcântara, Karina de Lima, com quem dividi "as dores e as delícias" da vida acadêmica.

A Rob, o IC mais interessado e interessante do TRAMA, por toda a dedicação e comprometimento com essa pesquisa.

À minha orientadora, Verônica, carinhosamente apelidada de Rainha, por toda a dedicação dentro e fora da universidade. Por comprar minhas ideias, por todas as discussões científicas, por oportunizar caminhos para que a pesquisa tivesse a minha cara e por acreditar mais em mim do que eu mesma. Mas, principalmente, por me inserir culturalmente em Fortaleza (lado B), por abrir o coração e me deixar entrar. A quem hoje eu considero uma amiga.

Ao IMPAR, o grupo de pesquisa da University of Nebraska – Lincoln, em nome da Profa. Jamilla Teixeira, por abrir as portas e viabilizar meu período de estágio no exterior, que notoriamente frutificaram o desenvolvimento dessa pesquisa e o meu crescimento pessoal. Também destaco as relações que tornaram tudo mais leve, em especial, Taísa Medina, Isabela Bueno, Kaylee Cunning, Erik Harada, Richard Ngarnim e Alex Tamayo.

Ao GQMat, grupo de pesquisa da Química/UFC, especialmente em nome do doutorando Emanuel Queiroz, por aceitar o desafio de sintetizar as cápsulas termocromáticas.

À Kelvia de Assunção Ferreira Barros (vulgo Kéké), por toda a paciência para lidar com o meu caos, sempre com apoio, calmaria e amor, se transformou em família e em lar.

Aos meus amigos: Cris (Tina), por me receber abertamente em Fortaleza e ter se tornado referência para mim; Bobinho e Tchelly, por sempre "chegarem junto" mesmo à distância; Jacinha, por todo o empenho na revisão das minhas citações e referências.

Ao apoio institucional da UFBA, pela oportunidade de capacitação enquanto servidora pública e ao incentivo dos colegas do DETG.

Aos órgãos de fomento, FUNCAP, CAPES e CNPq, pelo apoio financeiro ao longo deste doutorado.

“Cheguei com meu universo e aterrizo no seu pensamento; trago as luzes dos postes nos olhos, rios e pontes no coração. Pernambuco embaixo dos pés e minha mente na imensidão.” (Chico Science e Nação Zumbi, 1996).

ABSTRACT

Urban heat has become one of the most critical environmental challenges in contemporary cities. The extensive presence of impervious surfaces, particularly asphalt pavements, intensifies solar absorption and heat storage, significantly contributing to the formation and persistence of urban heat islands (UHIs). Because pavements occupy large portions of urban areas, they constitute a strategic surface for implementing sustainable cooling solutions. In this context, the thermochromic functionalization of asphalt pavements emerges as a promising cool pavement strategy, as it enhances the surface's capacity to modulate temperature. Thermochromic materials reversibly change color according to temperature, modifying surface albedo and increasing solar reflectance under high thermal conditions. The main objective of this research is to evaluate how the thermochromic capacity of asphalt pavement surfaces, functionalized through a surface spraying technique, influences the formation and mitigation of UHI effects. This dissertation is organized into four main parts. First, a bibliometric analysis followed by a systematic literature review investigates the current scientific panorama of thermochromic asphalt pavements' functionalization, identifying research trends and knowledge gaps. Second, experimental studies evaluate the effects of thermochromic spray coatings applied to recycled asphalt mixtures on surface texture and cracking resistance. Laboratory analyses include colorimetry, texture characterization, pull-off adhesion tests, accelerated aging, and semi-circular bending (SCB) tests under long-term aging conditions. Third, outdoor experiments assess optical-thermal balance, cooling performance, and durability under environmental exposure. Finally, a case study simulates the microclimatic impacts of the thermochromic strategy, including pedestrian thermal comfort, in different urban morphologies of a tropical city using computational fluid dynamics (CFD)-based modeling. Results indicate that thermochromic coatings reduce surface temperatures by 5–9 °C during peak solar radiation. The functionalization shows good adhesion, minimal changes in surface texture, and improved cracking resistance in aged specimens with 6% thermochromic content. However, accelerated weathering reveals reductions in solar reflectance over time, highlighting durability challenges. At the urban scale, simulations demonstrate surface temperature reductions of up to 9.6 °C and air temperature reductions of 1.7 °C. Nevertheless, thermal comfort analysis using the universal thermal climate index (UTCI) reveals that lower thermophysical variables do not necessarily result in improved daytime comfort, due to increased mean radiant temperature and the influence of urban canyon geometry. The findings confirm the potential of thermochromic pavements for UHI mitigation, while emphasizing the need for context-sensitive and integrated urban climate strategies.

Keywords: thermochromic pavements; urban heat island mitigation; microclimate impact.

RESUMO

O calor urbano tornou-se um dos desafios ambientais mais críticos nas cidades contemporâneas. A extensa presença de superfícies impermeáveis, especialmente pavimentos asfálticos, intensifica a absorção e o armazenamento de energia solar, contribuindo significativamente para a formação das Ilhas de Calor Urbanas (ICUs). Como os pavimentos ocupam grandes porções do espaço urbano, constituem uma interface estratégica para a implementação de soluções sustentáveis de arrefecimento. Nesse contexto, a funcionalização termocromática de pavimentos asfálticos surge como uma estratégia promissora, pois amplia a capacidade da superfície de modular sua temperatura. Materiais termocromáticos alteram reversivelmente sua cor em função da temperatura, modificando o albedo superficial e aumentando a refletância solar. O principal objetivo desta pesquisa é avaliar como a capacidade termocromática de superfícies asfálticas, funcionalizadas por meio da técnica de aspersão superficial, influencia a formação e a mitigação dos efeitos de ICUs. Esta tese está organizada em quatro partes principais. Primeiro, realizou-se uma análise bibliométrica seguida de uma revisão sistemática da literatura, a fim de investigar o panorama científico atual sobre a funcionalização termocromática de pavimentos asfálticos, identificando tendências e lacunas de pesquisa. Em seguida, estudos experimentais avaliaram a textura superficial e a resistência ao trincamento em misturas asfálticas recicladas funcionalizadas por aspersão superficial. As análises laboratoriais incluíram colorimetria, caracterização de textura, ensaios de aderência por arrancamento (*pull-off*), envelhecimento acelerado e ensaios de flexão semicircular (SCB) sob envelhecimento de longo prazo. Experimentos em ambiente externo avaliaram o balanço óptico-térmico, o desempenho de resfriamento e a durabilidade sob exposição ambiental. Por fim, um estudo de caso simulou os impactos microclimáticos da estratégia termocromática, incluindo o conforto térmico de pedestres, em diferentes morfologias urbanas de uma cidade de clima tropical, por meio de modelagem CFD (do inglês, *computational fluid dynamics*). Os resultados indicaram que a solução termocromática reduz a temperatura superficial entre 5 e 9°C durante os períodos de pico de radiação solar. A funcionalização apresentou boa aderência, alterações mínimas na textura superficial e melhoria na resistência ao trincamento em amostras envelhecidas para solução com 6% de material termocromático. Entretanto, o envelhecimento acelerado revelou redução da refletância solar ao longo do tempo, evidenciando desafios relacionados à durabilidade. Em escala urbana, as simulações demonstraram reduções de até 9,6°C na temperatura superficial e 1,7°C na temperatura do ar. Contudo, a análise de conforto térmico pelo índice UTCI (do inglês, *universal thermal climate index*) indicou que a redução de variáveis termofísicas nem sempre resulta em melhoria do conforto diurno, devido ao aumento da temperatura radiante média e à influência da geometria dos cânions urbanos. Os resultados confirmam o potencial dos pavimentos termocromáticos na mitigação de ICUs, ressaltando a necessidade de estratégias integradas e sensíveis ao contexto urbano e climático.

Palavras-chave: pavimentos termocromáticos; mitigação de ilhas de calor urbanas; impacto microclimático.

LIST OF FIGURES

Figure 1 – Research Framework ... 24
Figure 2 – Flowchart of the schematic structure. ... 29
Figure 3 – TRL scales and respective definition. ... 31
Figure 4 – Evolution of the thermochromic asphalt mixtures publications through the years. 32
Figure 5 – Co-occurrence network of the most frequent terms present in titles, abstracts and keywords of scientific papers published on thermochromic asphalt mixtures; (i) red cluster related to mechanical properties and aging resistance; (ii) green cluster related to environmental impact of thermochromic solutions; (iii) blue cluster related to laboratory tests and energy efficiency. ... 33
Figure 6 – Network map of co-authorship by author. ... 34
Figure 7 – Network map of co-authorship by institutions. ... 36
Figure 8 – Number of published papers by country. ... 37
Figure 9 – Bibliographic coupling by sources with temporal metrics. ... 38
Figure 10 – Schematic thermochromic mechanism in Leuco dyes. ... 39
Figure 11 – Schematic optical-thermal balance on the pavement surface. ... 45
Figure 12 – Technology Readiness Levels for thermochromic pavements' future perspectives. ... 56
Figure 13 – Experimental testing program. ... 65
Figure 14 – Particle size distribution curve of asphalt mixture SLX. ... 66
Figure 15 – Specimens preparation steps to an experimental program. ... 69
Figure 16 – Flowchart of 3D Computer Vision through PCR. ... 70
Figure 17 – Types of fracture damage in pull-off adhesion test: (a) cohesive; (b) adhesive; (c) glue failure. ... 71
Figure 18 – SEM testing results of (a) TCM pigment (magnification factor: 2086); (b) TCM pigment (magnification factor: 9716). ... 73
Figure 19 – FTIR spectrum of blue TCM pigment. ... 73
Figure 20 – Visual color differential as a function of temperature. ... 74
Figure 21 – Thermochromic activation by variation of b* coordinates as a function of temperature. ... 75
Figure 22 – Macrotexture Results. ... 76
Figure 23 – S_a, S_q, S_p, and S_v parameters before and after functionalization. ... 77
Figure 24 – S_{sk} and S_{ku} parameters before and after functionalization. ... 78

Figure 25 – Bonding Strength of TCM coating: (a) before and after aging; (b) cohesive failure after test at 3%TCM specimen; and (c) 6%TCM specimen. 79
Figure 26 – Variation in load-displacement curves in SCB test at 25°C. 81
Figure 27 – Fracture Parameters of HMA for different conditions in SCB test at 25°C, (a) Flexibility index; (b) Fracture energy; (c) Maximum peak-load. 82
Figure 28 – Experimental testing program. 88
Figure 29 – (a) Color change of TCM pigments; (b) Spectral reflectance of TCM powder before and after TT. 90
Figure 30 – (a) Scanning Electron Microscope (SEM) of TCM pigment (magnification factor: 2,086); (b) FTIR spectrum of TCM powder. 90
Figure 31 – Spectral power distribution of UVA-340 lamp and sunlight. 91
Figure 32 – (a) Thermochromic samples conditioning before colorimetry analysis; and (b) position of specimen in reflectance measurements. 93
Figure 33 – Schematic optical-thermal balance on the thermochromic pavement surface...... 95
Figure 34 – The reflection spectra of HMA_2 specimens after the QUV test at room temperature (a (t=0h), c (t=24h), and e (t=48h)) and above transition temperature (b (t=0h), d (t=24h), and f (t=48h)). 99
Figure 35 – The outdoor solar radiation test results: (a) the surface temperature and (b) the surface temperature differences between functionalized specimens and control specimen. 100
Figure 36 – Thermal photograph of HMA specimens at (a) 7 a.m.; (b) 12 p.m.; (c) 4 p.m.; and (d) 6 p.m. 101
Figure 37 – The outdoor solar radiation test results: a) the net radiation between functionalized specimens and control specimen and b) the total amount of net radiation during the time test. 103
Figure 38 – Flowchart of research. 109
Figure 39 – Location of the study area: (a) City of Fortaleza; (b) Case study neighborhoods and temperature measurement stations. 110
Figure 40 – LCZ classification sample from Fortaleza and the quantity of training areas for each LCZ type. 112
Figure 42 – (a) LCZ classification map of Fortaleza; (b) LCZ classes percentage distribution. 119
Figure 43 – LCZ- Air temperature interpolation maps in Fortaleza on November 19, 2021, at: (a) 12 p.m.; (b) 10 p.m. 120

Figure 44 – Daily air temperature anomalies across different LCZ classes in Fortaleza on November 19, 2021: a) LCZ-temperature anomalies map; b) total deviation graph. 121
Figure 45 – a) Low-rise (LR) street view's borders; b) LR building heights distribution. 123
Figure 46 – a) High-rise (HR) street view's borders; b) HR building heights distribution. .. 123
Figure 47 – Comparison between simulated and measured air temperature for different dates: a) and b) LR (h = 1.4 m); c) and d) HR (h = 1.4 m). 125
Figure 48 – Maps of air temperature at a height of 1.4 m at noon on 19th November, 2021: (a) LR and (b) HR. 127
Figure 49 – Maps of ground surface temperature (z = 0 m) at noon on 19th November, 2021: (a) LR and (b) HR. 128
Figure 50 – Maps of absolute differences in potential air temperature (h = 1.4 m) between RP and CO simulations at 8:00 a.m., 12:00 p.m., 4:00 p.m., and 8:00 p.m. on 19th November, 2021 129
Figure 51 – Maps of absolute differences in ground surface temperature (z = 0 m) between RP and CO simulations at 8:00 a.m., 12:00 p.m., 4:00 p.m., and 8:00 p.m. on 19th November, 2021 130
Figure 52 – Maps of absolute differences in ground surface temperature (z = 0 m) between RP and CO simulations at 8:00 a.m., 12:00 p.m., 4:00 p.m., and 8:00 p.m. on 19th November, 2021 131
Figure 53 – Maps of absolute differences of MRT (h = 1.4 m) between RP and CO simulations at 8:00 a.m., 12:00 p.m., 4:00 p.m., and 8:00 p.m. on 19th November, 2021...... 133
Figure 54 – Diurnal profiles of UTCI for all scenarios. 134
Figure 55 – Maps of absolute differences in UTCI (h = 1.4 m) between RP and CO simulations at 8:00 a.m., 12:00 p.m., 4:00 p.m., and 8:00 p.m. on 19th November, 2021...... 135
Figure 56 – Diurnal profiles of UTCI for all scenarios with an alternative acclimation threshold. 137
Figure 57 – Diurnal profiles of UTCI for all scenarios with an alternative acclimation threshold. 137
Figure 58 – Hourly matrix of adjusted UTCI values organized by street orientation (N/S and E/W) and canyon geometry (H/W ratio) for: (a) LR and (b) HR. 138

LIST OF TABLES

Table 1 – Most productive authors on the theme. 35
Table 2 – Most cited documents in the Scopus database on the theme. 35
Table 3 – Main thermal and optical results of the use of thermochromic material in asphalt binders and mixtures. 48
Table 4 – Main cooling effect results of the use of thermochromic material in asphalt binders and mixtures. 51
Table 5 – Main cooling effect results of the use of thermochromic material in asphalt binders and mixtures. 58
Table 6 – Colorimetry test results between 20°C and 60°C 74
Table 7 – Results of colorimetry test. 97
Table 8 – Total solar reflectance (%) of thermochromic HMA2 before and after QUV test. 100
Table 9 – Detailed input parameters for simulated areas (LR and HR). 115
Table 10 – Input layer parameters used in the ENVI-met simulation. 116
Table 11 – UTCI equivalent temperature classification. 118
Table 12 – Morphological parameters of the LR and HR neighborhoods by LCZ4r. 122
Table 13 – Validation indices of the ENVI-met model for simulated base scenarios. 126

TABLE OF CONTENTS

1. INTRODUCTION 14

1.1 Problem Statement, Rationale, and Research Questions 21

1.2 Objectives 22

1.3 Dissertation Structure 22

2. RESEARCH TRENDS ON THERMOCHROMIC ASPHALT MIXTURE FUNCTIONALIZATION: BIBLIOMETRIC ANALYSIS AND REVIEW 25

2.1 Introduction 25

2.2 Methods 28

2.3 Results 31

2.3.1 Bibliometric Results and Discussions 31

2.3.2 Main Terms 31

2.3.3 Co-Authorship 33

2.3.4 Sources 37

2.3.5 Systematic Review Results 38

2.3.5.1 Raw materials, obtaining, and incorporation methods 38

2.3.5.2 Thermal and optical performance of thermochromic asphalt mixture 44

2.3.5.3 Mechanical performance of thermochromic asphalt mixtures 52

2.4 Technology Readiness Level of Thermochromic Pavements' Future Perspectives 55

2.5 Conclusions 56

3. EVALUATION OF SURFACE CHARACTERISTICS AND LONG-TERM FRACTURE BEHAVIOR OF ASPHALT MIXTURES FUNCTIONALIZED BY THERMOCHROMIC SPRAYING COATING 61

3.1 Introduction 61

3.2 Objectives and Scope 64

3.3 Materials and Methods 65

3.3.1 Materials 65

3.3.1.1 Aggregates, Asphalt Binder, and RAP 65

3.3.1.2 Thermochromic Pigment and Coating 66

3.3.1.3 Specimen Preparation with Thermochromic Coating 67

3.3.2 Methods 67

3.3.2.1 Physical, Chemical, and Thermal Characterization 67

3.3.2.2 Colour Parameters Measurement ... 68
3.3.2.3 3D Computer Vision through the Close-Range Photogrammetry (CPR) ... 70
3.3.2.4 Pull-off Adhesion Test ... 71
3.3.2.5 Semi-circular Bending (SCB)n Test ... 72
3.4 Results and Discussion ... 72
3.4.1 Physical, Chemical, and Thermal Characterization of TCM Pigments ... 72
3.4.2 Thermal Differential and Colorimetry on TCM Coating ... 74
3.4.3 Surface Properties ... 75
3.4.3.1 Macrotexture ... 75
3.4.3.2 Microtexture ... 76
3.4.4 Bonding Strength ... 78
3.4.5 Mid-Temperature Cracking Resistance ... 80
3.5 Conclusions ... 82
4. ASSESSMENT OF OPTICAL-THERMAL BALANCE AND ENVIRONMENTAL DEGRADATION OF A THERMOCHROMIC-COATED ASPHALT MIXTURE FOR URBAN HEAT MITIGATION ... 85
4.1 Introduction ... 85
4.2 Research Objective and Scope ... 88
4.3 Materials and Methods ... 89
4.3.1 Thermochromic Material Characterization and TC treated HMA Preparation ... 89
4.3.2 Simulation of environmental degradation ... 91
4.3.3 Reflectance spectrum test ... 92
4.3.4 Outdoor solar radiation test ... 94
4.3.4.1 Optical-thermal balance on pavement surfaces theory ... 94
4.3.4.2 Thermal performance evaluation ... 96
4.4 Results and Discussions ... 97
4.4.1 Environmental Degradation and Color coordinates on HMA2 ... 97
4.4.2 Optical characterization results ... 98
4.4.3 Thermal performance of thermochromic HMA1 in indoor solar radiation test ... 100
4.5 Conclusions ... 103
5. EVALUATING THE MICROCLIMATIC AND THERMAL COMFORT IMPACT OF HIGH-REFLECTIVE PAVEMENTS ACROSS DIFFERENT URBAN CANYON SETTINGS IN A TROPICAL CITY ... 105
5.1 Introduction ... 105

5.2 Methods 109
5.2.1 Case Study Area 109
5.2.2 Local Climate Zone Classification 111
5.2.3 UHI analysis by LCZ4r 113
5.2.4 Microclimate modelling and calibration 114
5.2.4.1 Modelling Areas Selection 114
5.2.4.2 Envi-met Settings and Scenarios 114
5.2.4.3 Model Calibration 116
5.2.4.4 Assessment of Thermal Comfort 117
5.3 Results 118
5.3.1 LCZ Maps and UHI analysis 118
5.3.2 Urban Characteristics of Modeled Areas 121
5.3.3 Validation of Envi-met modelling results with field measurements 124
5.3.4 Air and ground surface temperatures in the control simulation (CO) 126
5.3.5 Impacts of the heat mitigation strategy (RP) on the air and surface temperatures 128
5.3.6 Impacts of the heat mitigation strategy (RP) on surface energy balance 130
5.3.7 Impacts of the heat mitigation strategy (RP) on outdoor thermal comfort 132
5.3.8 Consideration of Local Acclimatization and Perception of Thermal Comfort ... 135
5.5 Conclusions 141
6. FINAL THOUGHTS AND CONCLUSIONS 143
6.1 Session 2 (Bibliometric Analysis and Literature Review) 143
6.2 Session 3 (Considerations of Surface Characteristics and Long-term Fracture Behavior of Functionalized Asphalt Mixtures) 145
6.3 Session 4 (Consideration of Optical-Thermal Balance and Durability of Functionalized Asphalt Mixtures) 147
6.4 Session 5 (Considerations of Microclimatic Simulations) 149
REFERENCES 152

1 INTRODUCTION

Extreme events rank among the most lethal natural hazards globally, and their occurrence and severity are expected to rise under ongoing climate change (IPCC, 2023; Martín; Paneque, 2022). Among the main human activities that accelerate climate change, the operation of transportation systems stands out as the third most polluting sector, accounting for about 25% of global greenhouse gas (GHG) emissions (IEA, 2021). Although atmospheric pollution is the most widely recognized externality of the transportation sector, it is not the only one. The rise in temperatures caused by the high impermeabilization of natural areas due to transportation infrastructure is particularly evident in cities, where the proportion of paved surfaces is substantial.

In this context, pavements contribute to the emergence and intensification of an environmental phenomenon known as urban heat islands (UHIs). This phenomenon is characterized by higher temperatures in urbanized areas compared to surrounding rural zones, primarily as a result of the high heat-absorption and retention capacity of materials used in urban infrastructure (Cheela *et al*., 2021). Additional factors that exacerbate localized warming are related to urban morphology and human activities, including high-density occupation, the formation of urban canyons, concentration of industrial uses, and limited green spaces. Common construction materials, such as asphalt and concrete, further intensify UHIs, as they absorb and store considerably more solar energy than natural surfaces, releasing this heat, especially during the afternoon and nighttime periods (Garland, 2010).

In the urban atmosphere, different microclimatic realities coexist; elements of climatic variation can be detected from the perspective of thermodynamic subsystems, such as areas of higher or lower humidity, temperature, and pollution levels (Monteiro, 1990). Different landscapes can influence climatic dynamics at various scales, with direct effects on the radiation balance of cities, promoting an increase in urban area temperatures relative to the atmosphere (Stewart; Oke, 2012). Among the climatic modifications observed, the increase in air temperature is the most noticeable, since it directly affects population health and well-being, energy consumption, and worsens environmental issues (Xu *et al*., 2021).

Future trends and actions have been debated worldwide, including a better understanding of the causes and consequences of climate change as identified in reports from the Intergovernmental Panel on Climate Change (IPCC). The major challenge for cities is to rethink their urban infrastructure, balancing continued socioeconomic activities with the implementation of actions that promote sustainable, conscious, and less environmentally aggressive development (IPCC, 2023). In this regard, one important milestone was the establishment of the Sustainable Development Goals (SDGs) (United Nations, 2015), which call for global strategies to protect the climate and the environment. The recognized effects of human development activities on the environment have become increasingly intense and recurrent (IPCC, 2023), motivating the need for sustainable and resilient solutions. Several studies discuss the role of urban infrastructure strategies, propose approaches to measure their impacts, and suggest ways to align infrastructure investment with the SDGs (Hartley, 2022; Mansell *et al*., 2024). In the Brazilian context, one milestone in this direction is the recent publication of climate action plans by major cities such as Fortaleza, Recife, Salvador, São Paulo, Rio de Janeiro, Curitiba, etc. However, these plans generally direct efforts primarily toward reducing/controlling emissions and electrifying the transportation sector (Soriano; Castelo Branco, 2025).

Resilience, in the context of transportation infrastructure, is a broad concept with implications that go far beyond the structural integrity of pavements. In Brazil, there is no single standardized definition for sustainable pavements established by national regulatory bodies such as the DNIT (In Portuguese, *Departamento Nacional de Infraestrutura de Transportes*). Instead, the concept is addressed through technical guidelines and research, generally referring to pavement systems that minimize environmental impacts throughout their life cycle while ensuring adequate functional and structural performance. Within this context, sustainability is operationalized through practices such as the use of recycled materials (e.g., reclaimed asphalt pavement - RAP), the adoption of warm mix asphalt technologies, the reduction of energy consumption during production and construction, and the enhancement of pavement durability. Likewise, the Federal Highway Administration (FHWA) defines resilience as the ability to anticipate, prepare for, adapt to, withstand, respond to, and recover quickly from disruptions (Muench *et al.,* 2023).

Even based on this definition, it becomes evident that infrastructure resilience extends beyond physical durability. In practice, when considering extreme weather events of increasing frequency and intensity, the primary concerns of transportation infrastructure sectors are centered around a concept of resilience aimed at making the system more resistant to these changes. According to FHWA, the idea of sustainable pavements arises from practices encompassing strategies to reduce environmental impacts, optimize resource efficiency, and enhance the social value of pavement systems throughout their life cycle. These practices include: (1) achieving engineering objectives; (2) preserving and ideally restoring surrounding ecosystems; (3) using financial, human, and environmental resources wisely; and (4) meeting basic human needs such as health, safety, equity, employment, comfort, and happiness (Muench *et al.,* 2023).

The gap between current levels of adaptation and mitigation and the levels required for sustainable urban infrastructures is, however, considerable. In light of increasingly frequent extreme weather events, there remains a clear need for more comprehensive and effective planning, especially in the pursuit of alternatives that serve the needs of the most vulnerable communities (Salvador, 2020), such as Indigenous groups, riverine populations, low-income communities, as well as specific demographic groups such as children and the elderly.

The technical and scientific community has directed efforts toward the development of more sustainable materials, solutions, methods, and construction techniques. In the field of transportation infrastructure, potential technological and application strategies for cooling pavements have been adopted to mitigate UHI effects. Among the various innovative paving technologies used in urban areas, the solutions are commonly grouped into reflective pavements, permeable pavements, thermally modified pavements, and pavements for energy generation/capture (Xu *et al.*, 2021). In this context, research on functionalized asphalt mixtures stands out (Saadeh *et al.*, 2019; Rocha Segundo *et al.*, 2021; Xu *et al.*, 2021).

Pavement functionalization consists of endowing pavements with new capabilities or functions beyond conventional ones, while guaranteeing at least the same mechanical performance and resistance to weathering originally required (Rocha Segundo *et al.*, 2021. Among these capabilities is thermochromic functionalization, which modifies the physical properties of asphalt pavements' surfaces when exposed to external temperature variations (Rossi; Simeoni; Quaranta, 2021). Thermochromic pavements, in particular, offer a significant advantage by acting as smart coatings. These pavements are highly reflective in summer and less reflective in winter, providing an important thermoregulation feature that can more efficiently modulate pavement surface temperatures (Karlessi *et al.*, 2009). The reversible color change of thermochromic pavements in response to ambient temperature variations alters the surface albedo, i.e., the ratio of solar radiation reflected by a surface to the total incident radiation, with potentially positive effects on the overall thermal balance of the surface–atmosphere system.

Thermochromic functionalization is a relatively new cool pavement strategy, with some studies focused on temperature control and reduction of energy absorption by the pavement, since high temperatures can negatively affect pavement durability (Du; Chen; Zhang, 2019; Li; Zhang; Chen, 2018; Zhang *et al.*, 2018; Zhang *et al.*, 2017). Although still scarcely explored in literature, scientific interest in thermochromic asphalt pavements has grown, particularly in the last decade (Ribas *et al.*, 2022; Rocha Segundo *et al.*, 2022; Rocha Segundo *et al.*, 2021).

Asphalt materials have thermal sensitivity and, due to their dark coloration, absorb substantial solar radiation on hot days, reaching temperatures above 70°C, which accelerates the appearance of functional and structural defects. Thermochromic functionalization modifies material reflectivity through reversible color change in response to temperature variations. These reversible changes in optical properties occur at a specific transition temperature (TT), meaning the material is colored below the TT and becomes lighter above it. Results from Karlessi *et al*. (2009) indicate a 43% increase in albedo when a thermochromic pavement shifts from the colored to the colorless phase. Paved surfaces with higher reflectance in summer and lower reflectance in winter are desirable, since composite temperature control can produce asphalt mixtures that exhibit better thermal performance and aging resistance, helping mitigate UHI effects (Hu; Yu, 2013).

Pavement functionalization using nano- and micromaterials can be achieved through different methods, such as bulk incorporation, in which the functionalizer becomes part of the asphalt mixture, or prior modification of the asphalt binder (Rocha Segundo *et al.*, 2019a). Although both techniques ensure immobilization of the functionalizing agent, they may also affect mechanical pavement performance (Du; Chen; Zhang, 2019; Hu; Gao; Yu, 2015; Li, Q. *et al.*, 2020b; Li; Zhang; Chen, 2018; Zhang; Li; Chen, 2020). In this regard, the surface spraying technique, i.e., applying a solution on the surface of the compacted pavement, has advantages, such as: not altering pavement structural layers; requiring less functionalizing material; ensuring greater thermochromic efficiency; applying to pavements at different temperatures (Rocha Segundo *et al.*, 2019a); and being usable at any construction stage or even on in-service pavements, which increases its versatility. Additionally, functionalization can act as a protective layer, delaying aging and potentially reducing atmospheric pollutant emissions from pavement heating cycles (Ribas *et al.*, 2025b). However, the main challenges of surface spraying are: guaranteeing proper immobilization of the solution on the substrate (Carneiro *et al.*, 2013; Rocha Segundo *et al.*, 2019a), reduction of functional characteristics (friction and surface texture) of the pavement (Hu *et al.*, 2021; Rocha Segundo *et al.*, 2019b), and loss of solution efficiency after abrasion from traffic (Lima *et al*., 2023; Yi *et al*., 2022).

To improve immobilization conditions for the use of thermocapsules on asphalt substrates, some studies have developed epoxy resin–based solutions, with promising results even after weathering and abrasion tests (Li *et al*., 2019; Lima *et al.,* 2023). However, the efficiency of these solutions after UV degradation and abrasion, as well as their impacts on functional characteristics such as pavement friction and texture, remains a research gap (Hu *et al*., 2021a; Lima *et al*., 2023; Rocha Segundo *et al*., 2019b; Yi *et al*., 2022). While surface spraying acts as a physical barrier that increases reflective area and potentially improves thermochromic efficiency, it also exposes the functionalized layer to environmental degradation and traffic wear, inevitably compromising durability. Additionally, this approach may lead to the leaching of functionalization components into nearby water bodies, raising concerns about potential pollutant release, while the use of binders or adhesives required to ensure coating adhesion may introduce further environmental issues.

Surface texture is important to pavement functional characteristics, influencing factors such as friction, noise, drainage, and light reflection. It is therefore important to investigate the effects of functionalization on pavement functional characteristics to ensure less adverse impacts on road safety, the environment, or urban quality of life. Chen, Y. *et al.* (2022) evaluated surface characteristics, friction, and texture changes of an asphalt pavement after surface spraying with an epoxy-based reflective solution. The British Pendulum test showed a 21.5% reduction in pavement friction. However, the resulting 51 BPN (British pendulum number) still met Chinese safety standards (BPN ≥ 45). The same was observed in the sand patch test, where the reflective film reduced pavement texture by 17.3%, yet remained within local regulatory recommendations (≥0.55mm).

Although increased reflectance is desirable for reducing pavement surface temperatures, it also raises concerns about the use of thermochromic pavements in urban areas. In densely built areas, radiation reflected by highly reflective pavements may be blocked by surrounding buildings, resulting in its absorption or re-emission into the local environment rather than being returned to the atmosphere, potentially exacerbating UHIs (Jia; Siqi; Wang, 2021; Xu *et al.*, 2021). Additionally, reflected energy during the day can affect thermal comfort for people and animals near reflective pavements (Jia; Siqi; Wang, 2021). Increased reflection may also cause visual discomfort for pedestrians and drivers if radiation is not adequately directed toward the atmosphere (Erell; Pearlmutter; Williamson, 2011). Therefore, thermochromic pavement studies must consider land-use characteristics and urban configuration to determine suitable application locations and maximize microclimate and well-being benefits. More specifically, microclimate simulation studies using numerical models to analyze the effects of replacing conventional pavements with thermochromic ones can provide valuable decision support for deploying these sustainable strategies in urban areas.

Given the complexity of the urban environment, both morphological and anthropogenic, microclimate prediction and control require a holistic approach. Numerical simulation tools have gained prominence (Tsoka; Tsikaloudaki; Theodosiou, 2018), enabling investigation of mitigation and adaptation strategies to address UHIs (Santamouris *et al.*, 2012; Sen *et al.*, 2019; Taleghani *et al.*, 2019; Wang; Berardi; Akbari, 2016; Zhang *et al.*, 2022). The meta-analysis by Tsoka, Tsikaloudaki, and Theodosiou (2018) demonstrated the importance of microclimate models in simulating and analyzing urban climate. According to the authors, peak air temperature reductions resulting from reflective pavement strategies and new tree planting average 2.0°C. Air temperature (T_a) is the most widely evaluated microclimate variable, with evidence that the model generally captures the diurnal microclimatic profile accurately. However, for mean radiant temperature (T_{mrt}), mainly in pedestrian comfort studies, models tend to overestimate daytime T_{mrt} by 6°C on average (Tsoka; Tsikaloudaki; Theodosiou, 2018), which can compromise human comfort analyses, especially in regions with naturally warm climates.

Reflective pavements are among the most efficient pavement strategies in reducing T_a and surface temperature (T_s). Simulations of increased pavement albedo from 0.1 to 0.4 have shown varying air temperature reduction performance, from 0.4°C (Jia; Wang, 2021; Sen *et al.*, 2019) to 1.5°C (Zeeshan; Ali, 2022; Zhang *et al.*, 2022). These reductions can be even more significant under low-wind conditions (< 4 m/s), with decreases up to 5°C (Lu *et al.*, 2022; Synnefa; Santamouris; Apostolakis, 2011). In terms of T_s, albedo has an even more substantial effect, with reductions between 6 and 12°C (Synnefa; Santamouris; Apostolakis, 2011; Zhang *et al.*, 2022).

Although widely used, studies emphasize the local nature of microclimate simulation results, with urban morphology and climatic conditions being key factors in UHI mitigation (Rahmani; Sharifi, 2023; Zeeshan; Ali, 2022; Pigliautile *et al.*, 2020; Sen *et al.*, 2019). Even though reflective pavements appear more efficient in high-insolation climates, most studies are concentrated in the Northern Hemisphere, in regions with subtropical (Jia; Wang, 2021; Zhang *et al.*, 2022), semi-arid (Sen *et al.*, 2019), temperate (Taleghani *et al.*, 2019), and Mediterranean climates (Kolokotsa *et al.*, 2018; Kyriakodis; Santamouris, 2018; Pigliautile *et al.*, 2020; Synnefa *et al.*, 2011). There is scope to expand research into sustainable strategies, such as thermochromic pavements in tropical urban climates, where higher baseline temperatures often exceeding those of temperate regions by 5 – 10°C, along with elevated solar radiation, persistent humidity, and reduced diurnal thermal variation, may significantly influence thermochromic activation thresholds, cooling efficiency, and long-term material performance.

Understanding the behavior of cooling strategies is challenging because numerous variables influence the phenomenon, from local meteorological conditions to intrinsic material properties and their interactions. In fact, the relationship between air temperature and pavement temperature is highly complex. Aldrich (1956) described the primary variables affecting heat transfer between air and pavement as: longwave solar radiation, which varies with geographic location; atmospheric vapor pressure, which influences solar absorption and diffusion; cloud presence and type, which block sunlight and create shading; atmospheric conditions, including pollutant concentrations; and pavement surface characteristics, primarily color and texture. Dempsey and Thompson (1970) reported that the quality of input data is essential for accurate surface temperature predictions. This is particularly relevant in the context of climate change, since ambient temperatures are increasingly high, making it essential to understand how these conditions affect pavement thermal behavior when defining sustainable paving strategies. Additionally, calibration and boundary conditions are important factors for simulation accuracy (Tsoka; Tsikaloudaki; Theodosiou, 2018). These examples highlight the importance of advancing microclimate simulation as a decision-support tool in urban planning and infrastructure investment. Simulation quality depends on accurate input data, such as local meteorological conditions and urban morphological characteristics, to ensure the model reliably represents real-world conditions.

The occurrence of UHIs is a reality affecting different areas with varying intensities and consequences. Understanding the mechanisms that drive the formation and intensification of these phenomena is an urgent and challenging task. Tropical cities are really susceptible to the increased thermal discomfort caused by UHIs, as their geographic location already subjects them to naturally high temperatures for most of the year.

Given the influence of transportation infrastructure on the physical and dynamic characteristics of cities, the scientific community plays a critical role in proposing more sustainable solutions. Asphalt pavements cover large areas of the urban environment, usually more than 60% of the impermeable area (Tsoka; Tsikaloudaki; Theodosiou., 2018), and absorb significant heat, making them relevant systems for implementing solutions aimed at mitigating climate effects. Within this framework, thermochromic pavements align with Brazilian and FHWA's sustainability principles, as their ability to reduce surface temperatures may lower heat-induced degradation, support preservation practices by slowing aging processes, and improve social well-being by enhancing thermal comfort, especially in vulnerable urban areas. Thermochromic coatings can further strengthen sustainability outcomes by reducing maintenance needs and contributing to safer, more equitable, and climate-responsive transportation infrastructure.

Therefore, this dissertation focuses on evaluating thermochromic functionalization using the surface spraying technique, investigating the cooling effects of thermochromic solutions, and assessing the impacts of thermochromic pavements on UHI formation, aiming to contribute to the development of more sustainable paving solutions in the face of contemporary climate challenges. Finally, it is noted that the proposal aligns with the United Nations' 2030 Agenda for Sustainable Development, particularly SDG 3, which aims to ensure healthy lives and promote well-being for all, highlighting the need for controlled temperatures and reduced thermal stress in urban areas; SDG 9, which promotes resilient infrastructure, sustainable industrialization, and innovation, objectives that align strongly with thermochromic pavement functionalization; SDG 11, which aims to make cities and human settlements resilient and sustainable; and SDG 13, which seeks to strengthen climate resilience and adaptation to climate-related risks and natural disasters.

1.1 Problem Statement, Rationale, and Research Questions

The central hypothesis of this research is that the thermochromic functionalization of asphalt pavements strategy applied in tropical climate regions improves the urban microclimate. Based on this hypothesis and the scientific gaps identified in the literature, the following research questions were formulated:

- What is the current state of the art regarding thermochromic functionalization in asphalt pavements?
- How does the spray-applied thermochromic solution modify the surface characteristics and cracking resistance of asphalt mixtures?
- What are the thermal effectiveness and weathering resistance of the thermochromic-functionalized asphalt mixtures?
- What are the microclimatic impacts of the thermochromic functionalization strategy across different urban settings in a tropical climate context?

This research aimed to cover the thermochromic functionalization of asphalt pavements' surfaces, ranging from a comprehensive review of the state of the art to investigating its application in different aspects, including effectiveness, performance, and microclimatic impact.

1.2 Objectives

The main objective of this research is to evaluate the thermal and functional performance of thermochromic coating solutions and the microclimatic impacts of spray-applied functionalization of asphalt pavements as an urban heat island mitigation strategy in tropical environments. To achieve this main objective, the following specific objectives were established:

1. To investigate the current scientific overview concerning thermochromic functionalization in asphalt pavements;
2. To evaluate the effects of the thermochromic spray (TS) on the surface characteristics and cracking resistance of asphalt mixtures;
3. To assess the TS outdoor thermal effectiveness and the durability against accelerated environmental degradation;
4. To assess the microclimatic impacts, including pedestrians' thermal comfort, of the TS strategy applied in different urban morphologies in a tropical climate city.

1.3 Dissertation Structure

This dissertation was organized into relatively independent sessions. **Session 1** outlines the general context of the research proposal, comprising the Introduction, Research Problem, Justification, Research Questions, and Objectives. Sessions 2 to 5 were structured in the format of complete scientific papers, each with its own subsections (Introduction, Materials and Methods, Results, and Conclusions), addressing the specific objectives defined in Session 1, as follows:

- **Session 2**, corresponding to Objective 1, presents a bibliometric and literature review on the key topics that supported the definition of this dissertation's objectives (scientific paper published in *Cleaner Materials*, https://doi.org/10.1016/j.clema.2024.100273).
- **Session 3**, corresponding to Objective 2, analyzes the surface characteristics of functionalized asphalt mixtures and their potential resistance to cracking under long-term aging conditions (scientific paper published in *International Journal of Pavement Engineering*, https://doi.org/10.1080/10298436.2025.2544897).
- **Session 4**, corresponding to Objectives 3, evaluates the cooling performance of the thermochromic solution under outdoor conditions and resistance to accelerated

environmental degradation (scientific paper published in *Road Materials and Pavement Design*, https://doi.org/10.1080/14680629.2025.2482846).

- **Session 5**, corresponding to Objective 4, integrates spatial analysis and microclimate modeling to bridge the gap between theoretical knowledge and practical heat mitigation strategies in tropical urban environments, offering actionable guidance to planners and policymakers on *where* and *how* to implement the thermochromic reflective pavement strategy for maximum benefit (scientific paper submitted to Building and Environment Journal, in progress).

Finally, **Session 6** presents the concluding remarks, interconnecting the preceding sessions within the overarching framework of this dissertation, followed by the references. The overall research framework of this dissertation is presented in Figure 1.

Figure 1 – Research Framework

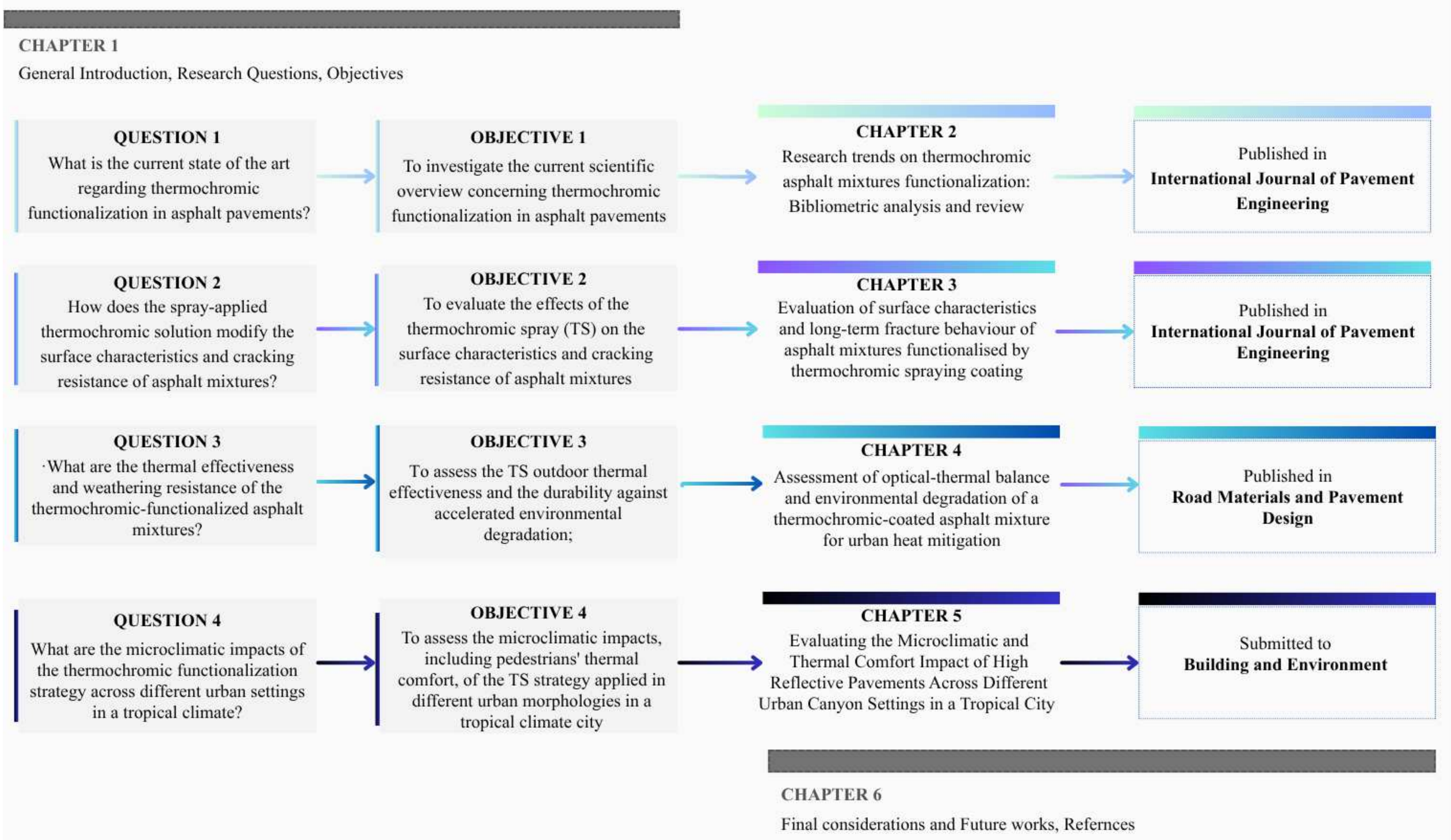

Source: Author, 2026.

2 RESEARCH TRENDS ON THERMOCHROMIC ASPHALT MIXTURE FUNCTIONALIZATION: BIBLIOMETRIC ANALYSIS AND REVIEW

This is a Manuscript of an article published by Elsevier in Cleaner Materials on 8th October 2024, available online: https://doi.org/10.1016/j.clema.2024.100273.

Abstract

Asphalt mixtures absorb high levels of solar light, increasing their internal temperatures and negatively affecting their behavior. In urban areas, this leads to the urban heat island (UHI) phenomenon, where extensive asphalt coverage raises microclimate temperatures. Integrating thermochromic properties into asphalt could provide a sustainable solution to mitigate UHI while maintaining the necessary mechanical performance. This research reviews literature, scientific advances, gaps, and future perspectives on thermochromic (TCM) asphalt mixtures through bibliometric analysis and systematic review. The analysis highlights that thermochromic asphalt has recently gained significant scientific interest, with an increasing number of publications from 2013 to 2023. Notably, Hunan University in China has emerged as a leading contributor to thermochromic-related publications. The findings identify the wet method as a prevalent form of thermochromic functionalization, with 4-6% TCM content considered most suitable for thermal performance. Adding TiO_2 improves optical characteristics due to its high reflectance in the Near-infrared solar spectrum. Studies using TCM binders typically show asphalt mixtures with better resistance to rutting and cracking, likely due to enhanced thermoregulation. The key knowledge gaps identified include the lack of consistent procedures across studies, the feasibility of scaling lab-based methods to field applications, and the need for experiments to assess their impact on road safety, surface characteristics, and the durability of thermochromic properties over the pavement's service life. This review highlights the promise of TCM for urban heat management and emphasizes the importance of additional research to achieve the ideal balance between thermal and mechanical properties.

2.1 Introduction

Asphalt mixtures are commonly used in road pavements, covering a large impermeable area of urban surfaces. They absorb a significant amount of solar radiation, which poses environmental, social, and economic challenges (Golden; Kaloush, 2006; Rosenfeld *et* *al.*, 1996). This fact exacerbates the formation of urban heat islands (UHIs), among other adverse effects. UHI is a phenomenon where urban areas experience higher temperatures compared to surrounding and rural areas. This is mainly caused by the replacement of natural land with built surfaces. In this context, pavements with low reflectance and high heat retention may alter the local microclimate, affecting environmental conditions, human health, and the demand for electricity and water consumption to maintain thermal comfort.

Asphalt materials are sensitive to temperature changes, which affect their mechanical behavior and performance. During summer, asphalt mixtures absorb high amounts of solar radiation due to their black color, reaching temperatures up to 70°C (Qin; Hiller, 2014). In Transportation Engineering, efforts have been made to develop sustainable materials, solutions, methods, and construction processes to low-down in-service mixture temperature, as this directly impacts their durability and accelerates deterioration. An example of such technology is the development of thermochromic asphalt mixtures (Rocha Segundo *et al.*, 2021), which has been used to mitigate UHI effects.

The use of thermochromic materials in asphalt mixtures enhances their reflectance by undergoing reversible color changes from colored to colorless states in response to temperature fluctuations. These color changes occur at a specific transition temperature (TT), below which the material is colored and above which it becomes colorless, resulting in a modification of the material's optical properties. The temperature coefficient of the TT is typically consistent with that of the construction sector (Berardi; Garai; Morselli, 2020). This makes it suitable for use in the production of paints, roofs, and external coatings of buildings, among others and additionally tends to reduce the material’s deterioration.

Although thermochromic capacity is a relatively new subject in the transportation infrastructure area and still little explored in the literature (Rocha Segundo *et al.*, 2021), the number of publications on this theme has shown an increasing trend in the last decade (Cheng *et al.*, 2018; Rocha Segundo *et al.*, 2022). A few examples are the functionalization of asphalt pavements through the use of modified asphalt binder or mixtures to minimize temperature variation (Hu; Yu, 2020a; Li, Q. *et al.*, 2020b; Xie *et al.*, 2023), resulting in materials with greater mechanical performance and better resistance to aging and the proposed of innovative road engineering applications using thermochromic sensors through functionalized road markings to improve road safety (Lima Jr. *et al.*, 2022). This has been a widely researched topic (Hu; Yu, 2016b).

The investigations have focused on controlling temperature variation and reducing heat absorption by the pavement. According to Hu (Hu; Yu, 2013), the surface temperature of a thermochromic asphalt binder can be reduced by up to 6.6°C compared to the base binder (Hu; Yu, 2013). Similarly, thermochromic hot mix asphalt (HMA) can keep surface temperatures an average of 5 to 15°C cooler than base HMA during summer (Hu; Yu, 2020a). Despite these promising results, there is significant variation in the TCM content, methods, and procedures used for functionalization, which complicates the standardization and comparison of thermal improvement results in these scientific studies and hinders the practical application of thermochromic technology in road engineering.

Few studies have explored the combination of different cool pavement techniques to mitigate UHI effects. Zhang *et al.* (2022) initiated an analysis combining open-graded asphalt layers with a thermochromic spray coating on the surface. Their key findings showed a reduction in surface temperature by 10.57°C in an experimental indoor solar radiation simulation and a maximum air temperature decrease of 1.5°C at a height of 1.5 meters when a CFD simulation applied the thermochromic coating across all paved areas of Shanghai, China (Zhang *et al.*, 2022). These findings highlight the importance and necessity of using combined techniques, such as permeable and reflective layers, to improve the thermal balance of pavement. It also emphasizes the need for further research into obtaining thermodynamic parameters of materials and predicting the interactions within the pavement-atmosphere system and the feasibility of scaling lab-based methods to field applications.

In addition to thermal benefits, researchers have also investigated the mechanical and rheological performance of thermochromic asphalt. Most findings suggest that thermochromic powders can enhance the high-temperature stability of asphalt binder, as evidenced by improvements in softening point, viscosity, complex modulus, penetration, phase angle, and dynamic shear rheological tests (Chen *et al.*, 2019; Li, Q. *et al.*, 2020b; Zhang *et al.*, 2017). According to (Li; Zhang; Chen, 2018; Zhang *et al.*, 2018), the additions of thermochromic powders had only a slightly impact on the physical and rheological properties of SBS-modified asphalt compared to the base binder. Furthermore, Du *et al.* found that the use of thermochromic microcapsules improved the fatigue and aging resistance of both the base asphalt and SBS-modified asphalt (Du; Chen; Zhang, 2019). However, there is still a significant lack of knowledge regarding the durability and long-term aging resistance of thermochromic asphalt mixtures in current literature.

The evidence suggesting that controlling the temperature of asphalt composites can enhance their mechanical performance and increase resistance to aging (Du; Chen; Zhang, 2019), combined with the fact that this also helps to mitigate the effects of UHI by reducing heat absorption (Hu; Yu, 2013), indicates that the thermochromic approach could offer both environmental and economic benefits. These benefits include improving ambient thermal comfort, reducing energy consumption, and promoting the well-being and health of the population, especially in regions with hot climates (Garshasbi; Santamouris, 2019; Xu *et al.*, 2021; Zhang *et al.*, 2022). Therefore, analyzing the impacts of maintenance and rehabilitation frequency, reductions in air temperature, and life cycle assessments are among the understudied areas that should be considered in this field.

The purpose of this paper is to characterize the scientific scenario concerning the research in thermochromic asphalt mixtures. To achieve this, a bibliometric analysis and a systematic review of the available literature will be conducted. The review will discuss the state-of-the-art in terms of thermal, optical, and mechanical performance. Additionally, the main scientific gaps will be inferred, and future perspectives will be considered. Thus, the first approach will address the publication evolution, co-authorship, leading countries, and institutions. The second approach will identify and compare materials, thermochromic incorporation methods, changes in thermochromic asphalt mixture properties, and the potential to mitigate UHI effects.

2.2 Methods

Figure 2 presents the flowchart of the schematic structure of this review, which comprises two main parts: the bibliometric approach and the literature review approach.

The methodology used for this bibliometric analysis can be summarized in three steps. To begin the research, Scopus was selected as the citation database due to its significance, multidisciplinarity, and status as one of the largest international peer-reviewed databases. Search criteria were defined to refine the results, including language and document type. Only papers and reviews written in English were included in the search to avoid duplicates and false-positive records (Rocha Segundo *et al.*, 2022; Santos; Bento-Gonçalves; Vieira, 2021). The search strings were then defined as "thermochrom*" AND "asphalt" OR "bitum*" to find literature on the application of thermochromism in asphalt/bituminous binders and mixtures. The term 'asphalt binder' is commonly used by American researchers, while 'bitumen' is preferred by Europeans. Therefore, geographic restrictions were not considered in this study. A search was conducted on Scopus using this string combination, with no limitation on the period, on January 25, 2024. The bibliometric analysis included 35 papers and searched titles, abstracts, and keywords.

The data mining process involved manually filtering papers to ensure alignment with the purpose of this work and removing any duplicates. After reviewing all abstracts, the final database consisted of 31 documents.

Figure 2 – Flowchart of the schematic structure.

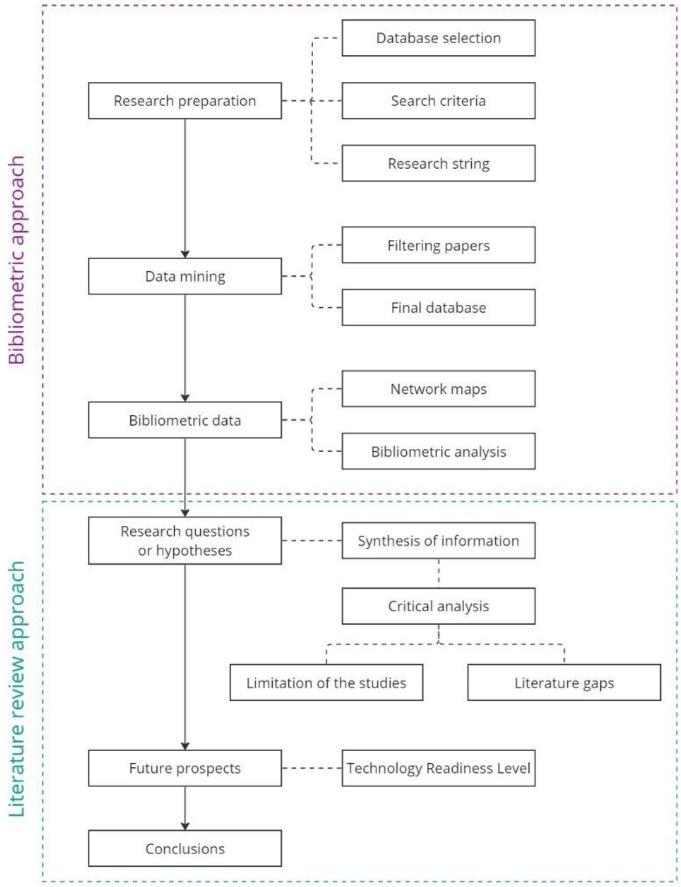

Source: Ribas et al. (2024).

The third part of this approach involved developing a bibliometric analysis with statistical tool support using the free software VOSviewer. This software can generate network maps from bibliometric data, such as bibliographic coupling, citation, co-authorship, and co-citation. To guide the bibliometric analysis, the following research questions were defined:

- What is the temporal evolution of this theme?
- What are the most frequently used keywords in the papers?
- Who are the most relevant authors?
- What are the most important papers in the scientific community?
- Which are the most relevant research institutions? And where are they located?
- What are the most important sources (scientific journals) for this area?

Moreover, the results of visual maps were analyzed to characterize the current panorama of the scientific research of thermochromic asphalt mixture worldwide.

The systematic review focuses on the state-of-the-art in terms of thermal, optical, and mechanical performance of thermochromic asphalt pavements. Therefore, the methodology used for the literature review analysis in the final database involved answering to the following guiding questions:

- Which thermochromic materials were used? And what are their main physical characteristics?
- What were the incorporation methods of the thermochromic powders into the asphalt binder or mixture?
- Regarding thermal, optical, and mechanical performance, what were the main results achieved with the thermochromic asphalt materials?
- What are the main research gaps in the literature? And what are the main future perspectives?

To enhance the comparison and synthesis of key information in papers, three tables were generated. The first and second tables presents the thermal and optical outcomes concerning the incorporation of the thermochromic materials into asphalt binders and mixtures respectively, while the second table summarizes the mechanical results. The tables provide a summary of the type, composition, and physical characteristics of thermochromic materials, as well as the incorporation methods used, highlighting the outcomes of each study. A critical analysis was conducted on the main outcomes, discussing, comparing, and evaluating them from a research progress perspective associated with cooler pavements results and UHI impacts. The limitations of the studies and research gaps between these mitigation technologies and their effects on the urban environment were also discussed. Finally, this study proposes prospects and conclusions by evaluating the current status of research on mitigating the urban heat island (UHI) impact of thermochromic pavement technologies by the Technology Readiness Level (TRL) method adapted. TRL is a formalized tool originally developed by NASA to assess and communicate the maturity of technologies during the development process. This method employs a scale ranging from 1 to 9, with each level reflecting a progressive advancement in technological development. Level 1 indicates the initial observation of basic principles, while Level 9 signifies a fully mature technology, proven through successful deployment in its operational environment (Figure 3). In this work, the scientific gaps and suggestions for future work were grouped into blocks according to TRL: research lab (TRL 1 - 3); simulated world (TRL 4 - 7); and real world (TRL 8 - 9).

Figure 3 – TRL scales and respective definition.

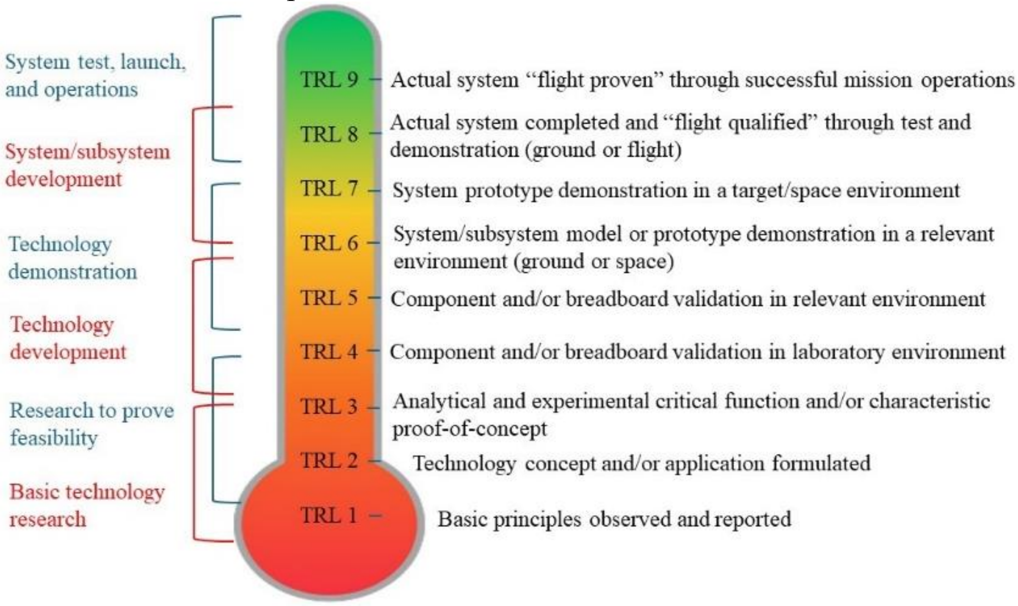

Source: Ribas et al. (2024)

2.3 Results

2.3.1 Bibliometric Results and Discussions

Figure 4 shows the evolution over time of the number of publications on thermochromic asphalt mixtures in the Scopus database. It is evident that there was no published paper before 2013, indicating a growing trend of research on this theme. An increase in the number of papers since 2018 is also observed. The highest number of publications was recorded in 2023, with six papers. It is worth noting that one paper has already been published in 2024, despite the year has just started (the search was conducted on January 25, 2024). This information suggests that thermochromic capability is a recent and innovative subject that has generated interest in scientific investigations of asphalt materials and structures.

2.3.2 Main Terms

The network map presented in Figure 5 plots the main index keywords of each assessed document and their co-occurrence frequency. Only terms that occurred at least twice are included, and there are no duplicated or similar terms on the map. The most frequently used terms in the text are 'asphalt mixtures', 'chromogenic', and 'thermochromic materials', with 15, 13, and 11 occurrences, respectively. These terms are highly relevant to all clusters and are strongly connected to most other terms. Chromogenic materials are materials that can change color reversibly due to variations in certain properties, such as pH, temperature, pressure, and electrical charge. Thermochromic materials are a type of chromogenic material that changes its optical properties in response to changes in temperature. The terms 'binders' and 'asphalt mixtures' are also related to this topic.

Figure 4 – Evolution of the thermochromic asphalt mixtures publications through the years.

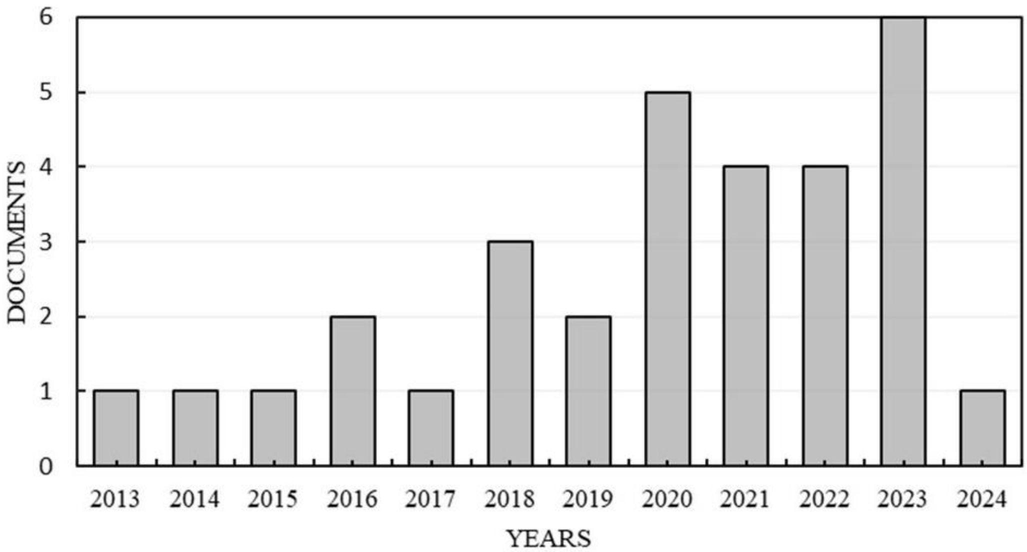

Source: Ribas et al. (2024).

The study identified three clusters based on color and main terms: (i) RED - 'powders', 'rheological property', 'temperatures', 'physical properties', 'SBS-modified asphalt', and 'aging resistance'; (ii) GREEN - 'atmospheric temperature', 'surface properties', 'urban heat island effects', 'microstructure', and 'durability'; and (iii) BLUE - 'surface temperatures', 'Fourier Transform Infrared Spectroscopy', 'solar energy', 'differential scanning calorimeter', and 'specific heat'. Cluster (i) is related to the mechanical properties and aging resistance of asphalt binders and mixtures, as well as thermochromic materials. Cluster (ii) contains terms related to the environmental effects of thermochromic solutions. The keywords in cluster (iii) are mainly related to laboratory tests and measures of energy efficiency of functionalized capabilities.

Figure 5 – Co-occurrence network of the most frequent terms present in titles, abstracts and keywords of scientific papers published on thermochromic asphalt mixtures; (i) red cluster related to mechanical properties and aging resistance; (ii) green cluster related to environmental impact of thermochromic solutions; (iii) blue cluster related to laboratory tests and energy efficiency.

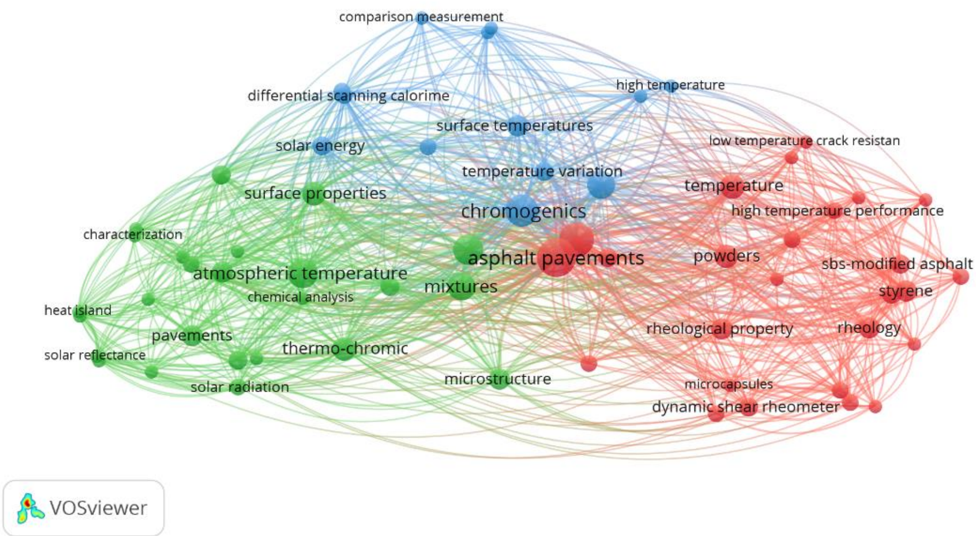

Source: Ribas et al. (2024).

2.3.3 Co-Authorship

Figure 6 shows the results of the co-authorship network. The network map displays clusters of authors who have co-authored at least two papers, forming five distinct clusters. The nodes show the names of the authors, the lines represent co-authorship relations, and each color corresponds to authors who worked together in the same paper. The red cluster, composed of Chinese authors, is the most strongly connected and accounts for the largest number of publications (big node size). Zhan H. and Chen Z. can be considered the most productive researchers, with thirteen co-authored papers and over 410 citations. The primary focus of Zhang H. and Chen Z.'s work was the investigation of the mechanical and cooling performance of thermochromic binders and asphalt mixtures.

On the other hand, it can be observed that the other clusters have a low number of co-authorship links, which may indicate a high variability of co-authors across publications. When different research teams authored each paper, the authors did not meet the threshold to appear on the network map. This is likely the case for the light blue, light purple, and yellow clusters, which are composed of Chinese, American, and Brazilian-Portuguese researchers, respectively. It is important to highlight the emerging hub for researching the use of thermochromic material in paving applications with Brazilian co-authorship, due to the completely different climate conditions of this country deal comparing to China and the USA, which can strongly contribute to increasing the knowledge of its performance as innovative and sustainable material.

Figure 6 – Network map of co-authorship by author.

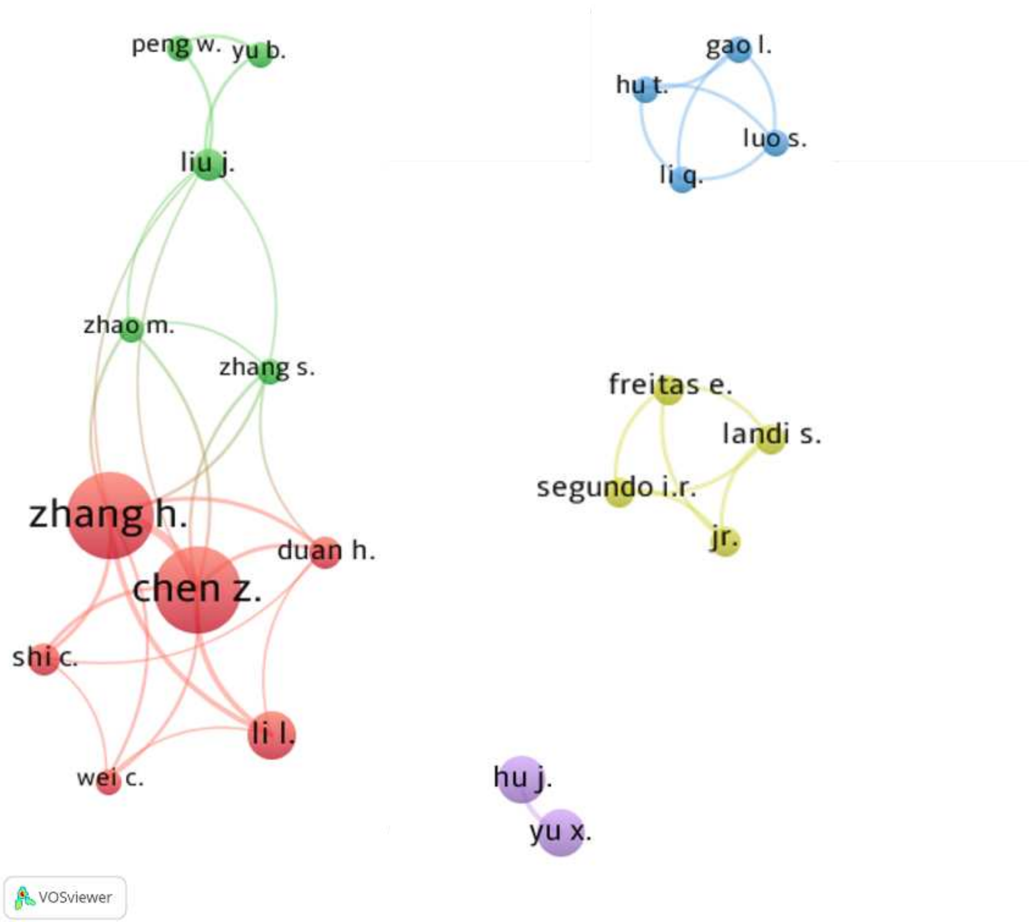

Source: Ribas et al. (2024).

A total of forty-nine authors have written about thermochromic asphalt mixtures, and the top five most productive individual authors have been selected. Table 1 shows the authors with the highest number of publications and citations related to the topic. The authors are from Chinese and American organizations, which indicates that these institutions can be the main centers of scientific knowledge on this topic.

Table 1 – Most productive authors on the theme.

Author	Documents	Citations	Country	Affiliation
CHEN, Z. ZHANG, H.	13	410	China	Hunan University
HU, J. YU, X.	6	202	US	Case Western Reserve University
LI, L.	5	93	China	Hunan University

Source: Ribas et al. (2024).

The five most relevant scientific papers according to the number of citations in the Scopus database are listed in Table 2. These papers were primarily published by two research groups from Hunan University (China) and Case Western Reserve University (USA), aligning with the aforementioned analysis of scientific productivity. They had at least 40 citations each, and all the papers were mainly concerned with thermochromic asphalt binders' mechanical and optical performance, aging behavior, and combination with a warm-mix technology. Here, it is possible to see the tendency for research works to use thermochromic asphalt functionalization in the current literature.

Table 2 – Most cited documents in the Scopus database on the theme.

Title	Authors	Journal	Citations	Year
Physical, rheological, and chemical characterization of aging behaviors of thermochromic asphalt binder	Zhang, H., Chen, Z., Xu, G., Shi, C.	Fuel	138	2018
Improvement of thermal and optical responses of short-term aged thermochromic asphalt binder by warm-mix asphalt technology	Chen, Z., Zhang, H., Duan, H., Shi, C.	Journal of Cleaner Production	68	2021
Evaluation of aging behaviors of asphalt with different thermochromic powders	Zhang, H., Chen, Z., Li, L., Zhu, C.	Construction and Building Materials	52	2017
Experimental study of sustainable asphalt binder	Hu, J., Yu, X.	Transportation Research Board	48	2013
Characterization of the optical and mechanical properties of innovative multifunctional thermochromic asphalt binders	Hu, J., Gao, Q., Yu, X.	Jour. of Materials in Civil Engineering	43	2015

Source: Ribas et al. (2024).

Regarding the network map of co-authorship by organizations (Figure 7), seven clusters of institutions that have developed research on thermochromic asphalt mixtures can be observed. Although there are links between different organizations, they are mostly between groups of researchers from the same university/nationality, which indicates a weak geographical spread of collaboration.

Key Laboratory for Green & Advanced Civil Engineering Materials and Application Technology, from Hunan University - China, is the most relevant organization with the largest number of partnership publications. However, these network links are only with other Chinese groups. Two clusters have links with groups of different nationalities: Portugal - Brazil and China - United States. Therefore, in addition to weak links, there is a low geographical spread of research.

The map of the co-authorship network by country was also examined, and it showed only eight countries, divided into two clusters with no connections between them. The first one is composed of China and the United States, and they represent the most productive countries with at least 70% and 29% co-authorship in the papers, respectively. The link between Portugal and Brazil (the second cluster) has only one document for each. This scene reinforces the incipient partnership research and the concentration of published papers in a few countries. The number of published papers by country can be seen in Figure 8.

Figure 7 – Network map of co-authorship by institutions.

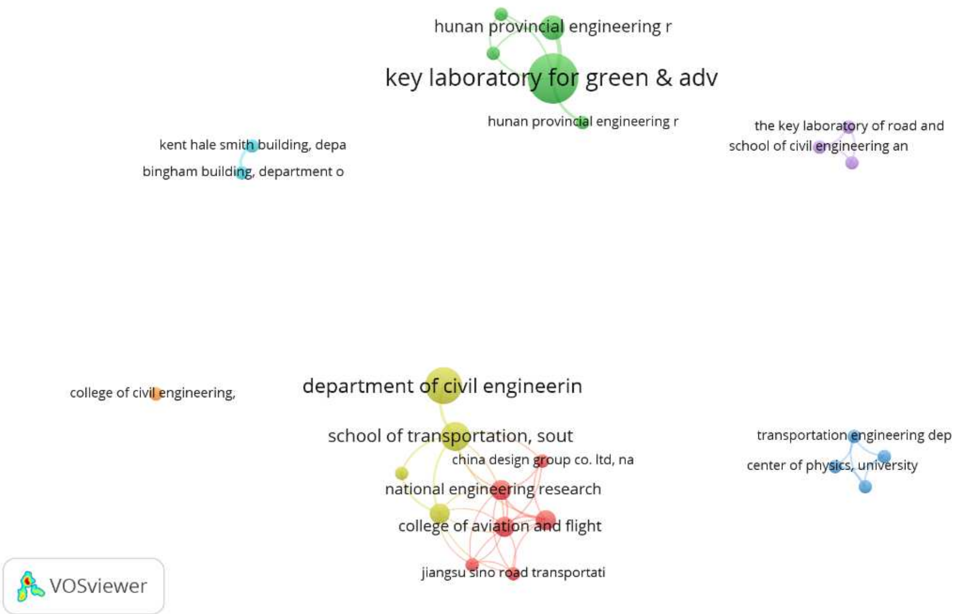

Source: Ribas et al. (2024).

2.3.4 Sources

Figure 9 shows the bibliographic coupling network by source, presented using a temporal metric. The most important journal is Construction and Building Materials with 10 published documents and the highest number of citations (181), followed by the Journal of Materials in Civil Engineering with 3 published documents on the topic. The main fields of knowledge from which the sources come are Civil Engineering, Materials Science and Energy.

More recently, due to the multidisciplinary nature of the topic, other scholarly sources have published papers in a variety of areas, such as sustainable/environmental and smart/technology cities. Examples include the Journal of Cleaner Production and Sustainable Cities and Society.

Figure 8 – Number of published papers by country.

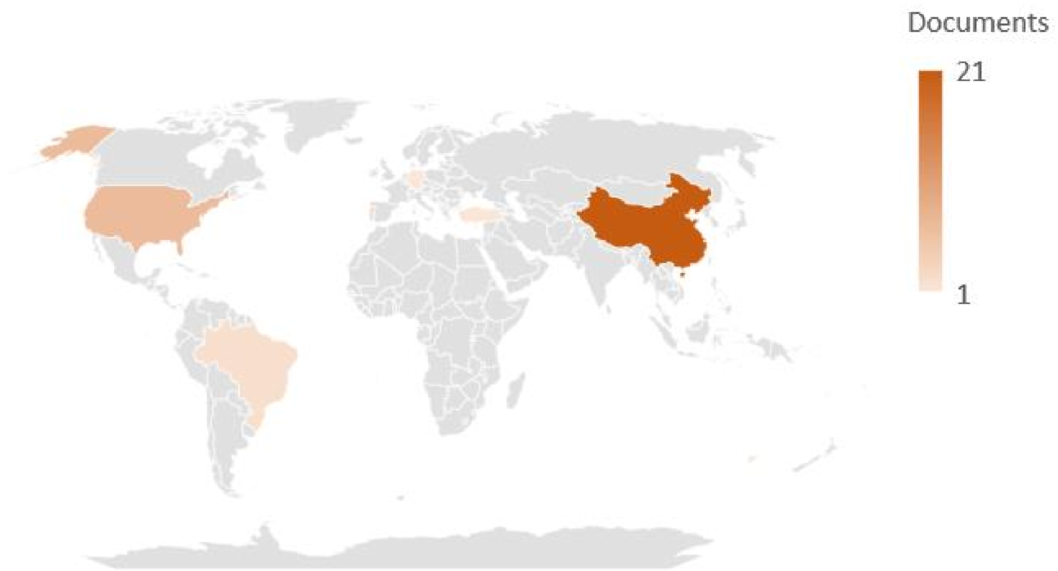

Source: Ribas et al. (2024).

Figure 9 – Bibliographic coupling by sources with temporal metrics.

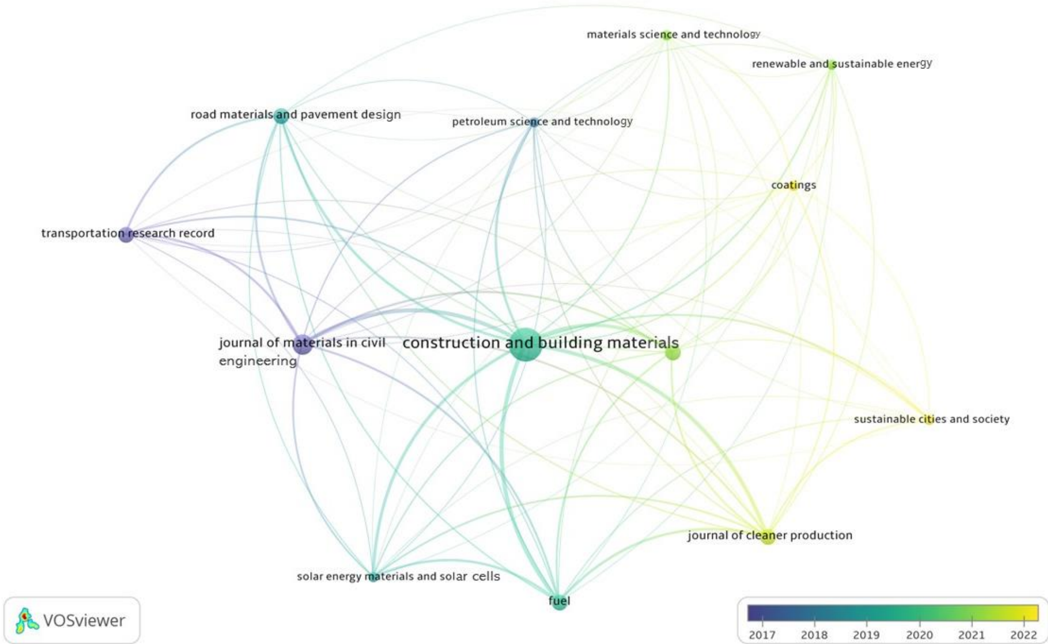

Source: Ribas et al. (2024).

2.3.5 Systematic Review Results

The following sections provide a summary of the information gathered through a bibliometric approach from the final database. They present the main results related to the use of thermochromic materials in asphalt binders or asphalt mixtures. The analyses focused on three performance approaches: thermal, optical, and mechanical properties.

2.3.5.1 Raw materials, obtaining, and incorporation methods

Thermochromic materials (TCM) are based on color changes in their visible optical properties upon temperature changes, due to a chromogenic core. TCM are organic mixtures composed of at least a color former (Leuco dye), color developer, and co-solvent. The color change mechanism is reversible and occurs at a specific transition temperature (TT), determined by the co-solvent melting point. Below TT, the leuco dye reacts with the developer, causing the material to become colored due to the absorption peak in the visible range. When the material is heated, the solvent-developer interaction becomes dominant, and above the TT, the color is lost (Figure 10) (Hu; Wanasekara; Yu, 2014; Hu; Yu, 2013).

Figure 10 – Schematic thermochromic mechanism in Leuco dyes.

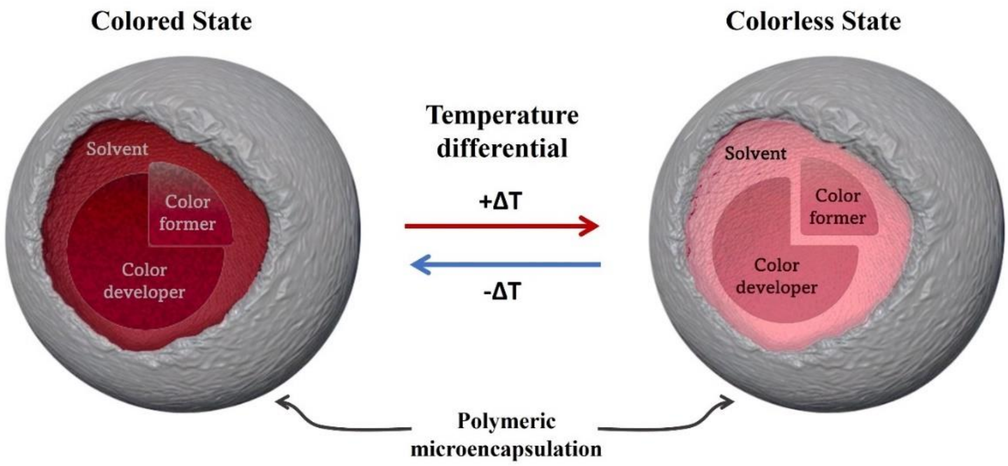

Source: Ribas et al. (2024).

The characterization of the chromogenic core is crucial for understanding the behavior of thermochromic materials. In the articles reviewed, the TCM are primarily of industrial origin, making it challenging to fully understand their composition, quantities, and the proportion of the materials involved. However, the chemical analysis of the chromogenic core has been mostly conducted using Fourier Transform Infrared (FTIR) spectroscopy (Chen, Z. *et al.*, 2019, 2022; Li, Q. *et al.*, 2020b; Zhang *et al.*, 2017, 2018). The main results of the FTIR spectrum identified key chemical bonds through absorption bands centered around 3,365 cm^{-1} and 1,511 cm^{-1}, corresponding to hydroxyl (-OH) and benzene skeleton vibrations, respectively. These are likely derived from bisphenol A (BPA). The characteristics of methyl stearate were identified by the presence of functional groups such as methyl ($-CH_3$), methylene ($-CH_2$), and carbonyl (C=O), indicated by peaks at 2,923 cm^{-1}, 2,848 cm^{-1}, and 1,740 cm^{-1}, respectively. Peaks centered around 1,556 cm^{-1} and 813 cm^{-1} were attributed to the melamine-formaldehyde resin used as the microcapsule shell. More specifically, the main chemical composition of the leuco dyes includes varying proportions different materials: 3-Diethylamino-6-methyl-7-2,4-xylidinofluoran, 3-N-p-tolyl-N-ethylamino-7-methyl-fluoran, and 3-(4-(diethylamino)-2-(hexyloxy)phenyl)-3-(1-ethyl-2-methyl-1H-indol-3-yl)-4-azaphthalide, for black, red, and blue pigments, respectively (Chen *et al.*, 2019; Chen Z. *et al.,* 2022; Li, Q. *et al.*, 2020b; Zhang *et al.*, 2017; Zhang *et al* 2018).

Studies indicate that BPA is commonly used as a color developer in thermochromic pigments due to its ability to produce darker tones and higher color contrast. However, BPA is known to be toxic and carcinogenic, raising concerns about its environmental impact. This is particularly relevant for TCM applications in pavements, where surface damage to microcapsules can release BPA into the environment. In the textile industry, Tözüm; Alay Aksoy; Alkan, (2021) explored the synthesis of thermochromic microcapsules using phenolphthalein (PP) as an alternative color developer. Their findings demonstrated that these PP-based microcapsules have significant potential for use in textile materials, offering reversible color change and thermal indication without the harmful effects associated with BPA

The thermochromic core is typically microencapsulated with polymer materials, such as trioctanoinand (Hu; Gao; Yu, 2015; Hu; Wanasekara; Yu, 2014; Hu; Yu, 2016b; Hu; Yu, 2020; Li, Q., *et al.*, 2020a) or Melamine-formaldehyde resin (Chen *et al.*, 2019; Du; Chen; Zhang, 2019; Li, Q. *et al.*, 2020a; Zhang *et al.*, 2022), serving as a shell. The aim of the microencapsulation strategy is to extend the thermochromic capacity, hold the entire thermochromic system together, and protect it from ultraviolet (UV) radiation exposure and physical disruption (Du; Chen; Zhang, 2019). The susceptibility of TCM microcapsules poses a significant challenge for road applications. The primary drawback of using these materials in practice is their rapid aging (Garshasbi; Santamouris, 2019), with UV radiation being the main degradation mechanism that reduces thermochromic reversibility (Karlessi *et al.*, 2009). Environmental exposure can cause the capsules to break, resulting in the loss of the core material and, consequently, the thermochromic capability. Zhang *et al.*'s (Zhang *et al.*, 2022) physical analysis of TCM materials revealed that during transportation, changes in environmental conditions (such as direct solar radiation) caused some microcapsules to break, leading to the leakage of the color-changing content. No studies have been found on the potential effects on mechanical performance of leaking encapsulated material into the binder or asphalt concrete regarding its mechanical performance and durability, highlighting a possible opportunity for future research.

Initial results indicate that microcapsules with shells made of melamine-formaldehyde resin tend to be more susceptible to damage during heating or binder mixing compared to those made with trioctanoin (Li, Q. *et al.*, 2020a). Furthermore, studies suggest that TCMs have been manually stirred into paint cool coatings to prevent damage to the microcapsules (Berardi; Garai; Morselli, 2020; Zhang; Zhai, 2019), which can also increase the heterogeneity of the final product. This caution was not observed in studies involving the modification of asphalt binders, where the use of magnetic stirrers and high rotation speeds prevailed (Hu; Gao; Yu, 2015; Zhang *et al.*, 2022). This underscores the need for improvements in the photoaging resistance and durability of microencapsulated thermochromic materials. Exploring the use of biopolymers in the chemical composition and synthesis of microcapsules could be a valuable research opportunity to enhance their durability and sustainability.

However, raw thermochromic powders demonstrate good thermal stability even when subjected to high temperatures. According to Hu and Yu (Hu; Yu, 2016a), thermogravimetric analysis shows that the main pyrolysis of TCM occurs after 200°C, indicating that this temperature is the material's critical point and minimal thermal weight loss occurs below it. Even after heating for 2 hours at 200°C, the TCM powder maximum weight loss observed was only 7.8% (Hu; Yu, 2016a). This suggests a high likelihood that these capsules will perform well within the typical temperature range experienced by in-service pavements. All the reviewed papers used commercial thermocapsules with a transition temperature (TT) of 31°C, indicating that this temperature is likely suitable for asphalt material applications. There have been successful reports of modifying binder and asphalt mixtures for different climate regions, including China (Chen, 2021b) and the US (Hu; Yu, 2013, 2020a). There is, therefore, room for contributions focused on the synthesis and application of thermochromic microcapsules with higher TT to better accommodate the realities of naturally hotter tropical climates, as well as the increasing frequency of heat waves due to climate change.

Regarding to physical characteristics, TCM powder consists of spherical microcapsule particles, with sizes predominantly ranging from 1 to 10 μm. The particle size can have controversial effects on thermochromic coatings. On one hand, larger particles can negatively impact reflectivity by reducing the surface area available to reflect sunlight. On the other hand, the spherical shape of the particles prevents them from highly interacting particles or agglomeration, leading to better dispersion in the coating. This improved dispersion allows the optical and thermal effects of the thermochromic material to be fully realized (Zhang *et al.*, 2022). Li *et al.* (Li, Q. *et al.*, 2020a) analysis of two thermochromic additives with different particle sizes (TM_1 = 3~10 μm; TM_2 =1~10 μm) confirms that, following the same mixing process, TM_2 (smaller sizes) particles adhered to the surface of the binder, resulting in better uniformity dispersion and diffusivity compared to TM_1 particles. The differential diffusivity caused by particle size significantly affects the mechanical performance of additives and it is likely the reason why TM_2 particles presented better rutting resistance and cooling effects (Li, Q. *et al.*, 2020a; Li, Q. *et al.*, 2020b). Therefore, controlling the particle size of additives used to modify the binder is a fundamental scientific and technical issue that can significantly influence the performance of thermochromic asphalt binder.

In terms of optical characteristics, after the TT, the TCM color changes increases the spectral reflectance in the visible and near-infrared (NIR) spectrum (Hu; Gao; Yu, 2015) and it is dependent of their specific color pigment (Hu; Yu, 2016b). The study conducted by Zhang *et al*. evaluated the effects of six different thermochromic powder colors on the optical and thermal properties of coatings. The results showed that TCM has a higher total solar reflectance compared to traditional cool materials. Red and black TCM powders were found to be more suitable for use in thermoregulation coating pavements, considering both reflectance characteristics and visual effect (glare) (Zhang *et al.*, 2022). Similar results were found by Hu & Yu's to thermochromic asphalt binder, which the reflectance increase was the highest for black powders, followed by blue and red (Hu; Gao; Yu, 2015). Additionally, it was found that the optical properties improved with an increase in powder content (Hu; Yu, 2016b).

Some studies combine thermochromic powders and semiconductors to improve the optical characteristics of modified binder or asphalt mixtures. According to Hu & Yu's optical characterization, nano-TiO_2 particles have a solar reflectance of up to 90% in the NIR solar spectrum, while the thermochromic powder reflectance range is 60-80% (Hu; Yu, 2020a). Zhang *et al.* investigation of the effect of different rutile TiO_2 contents on the optical properties of thermochromic coatings found that 2% and 5% TiO_2 contents are the optimal levels for thermoregulation at high and low temperatures for red and black coatings, respectively (Zhang *et al.*, 2022). TiO_2 is a semiconductor widely used in pavement applications due to its photocatalytic properties (Rocha Segundo *et al.*, 2019b; Rocha Segundo *et al.*, 2021). It also possesses other characteristics, such as hydrophobicity and the ability to degrade adsorbed organic materials (Rocha Segundo *et al.*, 2021). These properties could contribute to the development of thermochromic solutions with multiple capabilities, such as photocatalytic, super hydrophobicity, and self-cleaning, which have not yet been widely explored in the literature of the field.

Regarding the incorporation of thermochromic powders, most studies have utilized a wet mixing process to modify asphalt binders (Bo *et al.*, 2021; Chen, Z. *et al.*, 2019; 2021a; 2021b; 2022; Civan; Kurama, 2021; Du; Chen; Zhang, 2019; Hu; Gao; Yu, 2015; Hu; Wanasekara; Yu, 2014; Hu; Yu, 2013, 2016a; 2016b; 2020a; 2020b; Li, L. *et al.*, 2018; Li; Zhang; Chen, 2018; Li, Q. *et al.*, 2020a; 2020b; Yu *et al.*, 2022; Zhang, *et al.*, 2017, 2018; Zhang; Li; Chen, 2020; Zhang *et al.*, 2022). This process involves mixing the heated binder with the thermochromic additive until a homogeneous mixture is produced, using the weight of the base asphalt binder. Thermochromic asphalt mixtures also can be produced using the bulk incorporation dry mixing process, which involves replacing a portion of the fine aggregate or filler with thermochromic materials. Chen *et al.* (Chen, Z. *et al.*, 2022) investigated both functionalization techniques, and their key findings indicated that the wet process promotes a more uniform distribution of thermochromic microcapsules within the mixtures, while the dry process is more effective in preserving the integrity of the microcapsules. The distinct characteristics of the wet and dry methods, along with different mixing procedures in the dry process, can significantly impact the mechanical performance of thermochromic asphalt mixtures. Overall, the asphalt mixtures prepared using the wet process generally exhibit better mechanical performance and a superior cooling effect compared to those prepared using the dry process (Chen, Z. *et al.*, 2022). While both functionalization likely ensures the best TCM immobilization, they can also impact pavement performance. Mastering the mechanical behavior of thermochromic asphalt mixtures and binders is a primary focus of current research (Du; Chen; Zhang, 2019; Hu; Gao; Yu, 2015; Li, L. *et al.*, 2018; Li; Zhang; Chen, 2018; Li, Q. *et al.*, 2020b; Zhang; Li; Chen, 2020).

The technique of spraying coating is another possibility for functionalization, and it involves applying a TCM solution over the surface of the compacted pavement (Lima *et al.*, 2023; Zhang *et al.*, 2022). However, this technique has rarely been evaluated in recent literature on thermochromic asphalt. In the study of photocatalytic solutions, the surface spraying functionalization technique was found to be more efficient. It requires less semiconductor and does not cause mechanical alterations in the asphalt concrete (Rocha Segundo *et al.*, 2019b). However, ensuring proper immobilization of the solution to the substrate remains a challenge (Carneiro *et al.*, 2013; Rocha Segundo *et al.*, 2019a). To improve immobilization conditions of thermocapsules to the asphalt substrate, some studies have developed solutions based on epoxy resin. These solutions maintain the thermochromic capacity even after weathering tests (Li *et al.*, 2019; Lima *et al.*, 2023). Yi *et al*. investigated the friction reduction characteristics of reflective asphalt mixtures and demonstrated adherence to an asymptotic model, with the reduction stabilizing at 48 BPN after 150,000 cycles (Yi *et al.*, 2023). Prior to the abrasion process, an increase in the volume of the sprayed solution resulted in reduced friction, and consequently in a smoother microtexture. However, the efficiency of the solutions after abrasion and the impact of functional characteristics such as friction and texture of the coatings remain a research gap in surface spraying functionalization (Hu *et al.*, 2021b; Lima *et al.*, 2023; Rocha Segundo *et al.*, 2019a; Yi *et al.*, 2022).

On one hand, functionalization through spray coating acts as a physical barrier on the pavement surface, which increases the reflective area and potentially enhances thermochromic efficiency. On the other hand, this technique leaves the material more exposed to the elements, making it more susceptible to environmental degradation and traffic wear, which inevitably compromises its durability. Furthermore, investigating how changes in pavement surface characteristics, particularly friction and texture, impact road safety aspects (such as increased stopping distances and the number of traffic incidents) represents a gap in the literature regarding the surface spraying technique.

2.3.5.2 Thermal and optical performance of thermochromic asphalt mixture

Thermochromic asphalt pavements should, in principle, exhibit different responses to solar radiation than regular asphalt pavement due to their characteristics. Figure 11 compares a conventional asphalt pavement to a thermochromic pavement in terms of changes in optical and thermal characteristics. Conventional asphalt pavement absorbs and stores most of the incident solar radiation due to its black color, contributing to the heating of urban centers. In contrast, thermochromic pavement has a colorless surface that reflects large amounts of solar energy after TT. This higher solar reflectivity lowers the surface temperature and reduces energy absorption in the form of heat by the pavement (Zhang *et al.*, 2022). However, issues to prevent glare and other adverse visual effects in order to ensure safety on colorless road surfaces need to be considered, such as colorimetry analysis of thermochromic solutions and lightness control (Zhang *et al.*, 2022).

Thermochromic pavements are a type of passive cool pavement technology that can modify the heat absorption and structural performance of pavements. This is achieved by increasing the solar reflectance and thermal emissivity of the materials (Xu *et al.*, 2021). The pavement harvests solar energy in three ways, through: sensible heat and latent heat released by the pavement, and conductive heat that travels through the pavement structure, as showed in Figure 10. The release of sensible heat is a significant contributor to the urban heat island (UHI) phenomenon (Fortuniak, 2008; Qin; Hiller, 2014), due to the heat exchange directly influences the temperature of the pavement surface and surrounding air. Prospective technologies aimed at reducing the UHI effect focus on minimizing the release of sensible heat (Xu *et al.*, 2021).

There are several innovative pavement technologies used in urban areas to mitigate the effects of the UHI phenomenon. These technologies can be categorized into four main types based on the pavement solution studied: highly reflective, permeable, thermally modified, and energy-harvesting pavement systems (Xu *et al.*, 2021).

Figure 11 – Schematic optical-thermal balance on the pavement surface.

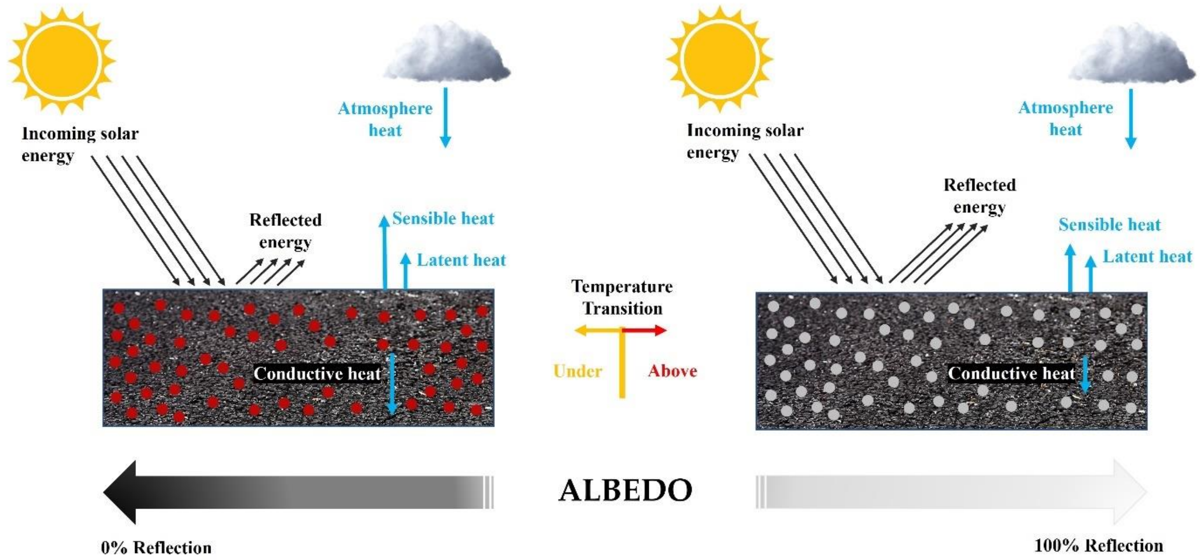

Source: Ribas et al. (2024).

Thermochromic pavements, in particular, offer a significant advantage by acting as smart sealing layers. These pavements are highly reflective in summer and less reflective in winter, giving to them an important characteristic of thermoregulation, which could modulate the pavement surface temperature more efficiently (Karlessi *et al.*, 2009). The reversible color change of thermochromic pavements in response to external temperature variations alters the surface albedo, i.e., the ratio of visible solar radiation reflected by a surface to the total visible radiation incident on it. There are reports of the maximum albedo increase of thermochromic coating was measured to be 43% when it transferred from colored to colorless phase (Karlessi *et al.*, 2009). Once functionalized, thermochromic pavements are ready for full operation, unlike other types of cool pavements. In comparison, permeable pavements rely on water for cooling, and in dry conditions, their surface temperature tends to be high (Asaeda; Ca, 2000). Additionally, these pavements are prone to pore clogging under high traffic loads and from vegetation, leading to a quickly reduced efficiency. Permeable paving, however, has other significant advantages such as drainage capacity and reduced surface runoff, increased friction and reduced noise pollution effects (Asaeda; Ca, 2000). Another kind of technology, such as thermally modified pavements (high thermal conductivity) stores heat during the day, causing remission of the heat during nighttime (Dawson *et al.*, 2012), which is the opposite of the desired effect. Finally, energy-harvesting pavement systems come with high initial and maintenance costs, are mostly non-recyclable, and have a high potential for voids between the pipes, that contain circulating liquid to harvest the heat energy, and the asphalt mixture, increasing the risk of debonding (Mallick; Chen; Bhowmick, 2009).

Regarding thermochromic optical performance, the functionalized asphalt materials exhibit a similar trend to thermochromic powder. Specifically, thermochromic asphalt binder and thermochromic asphalt mixtures reflect more near-infrared light than conventional pure asphalt due to temperature-induced color changes (Chen, Z. *et al.*, 2022; Hu; Gao; Yu, 2015). In the visible wavelength range of 350 to 550 nm, the reflectance values can increase by over 50% in the colorless thermochromic phase (Chen, Z. *et al.*, 2022). Hu and Yu's main findings indicate that the spectral reflectance properties of thermochromic asphalt binder increase as the powder content increases from 10 to 40% (Hu; Yu, 2016b). To predict the reflectance spectra of thermochromic asphalt binder based on powder content levels, optical mixing formulas such as Maxwell, Mori-Tanaka, and effective medium theory (EMT) were tested. These models provide a reasonable description of the phenomenon and can assist in the multifunctional design and optimization of the thermochromic binder (Hu; Yu, 2016b).

Enhanced solar reflectance is preferred because it reflects more solar radiation through the thermochromic effect, resulting in lower asphalt surface temperatures. However, heat exposure, even during production, can affect the thermochromic properties of powders and coatings. Conventional high-temperature asphalt preparation methods may harm the durability of thermochromic microcapsules in the asphalt matrix, undermining the temperature regulation capabilities of thermochromic asphalt materials (Chen Z. *et al.* 2021b). Hu; Gao; Yu (2015) found that subjecting thermochromic binders to 200°C for 2 hours resulted in a decrease in solar reflectance percentages of 4% for black, 8.5% for blue, and 15.8% for red asphalt coatings due to thermal treatment. To minimize excessive reductions in solar reflectance, it is advisable to produce black thermochromic asphalt using the WMA technique, while blue and red asphalt can employ both HMA and WMA technologies (Hu; Yu, 2016a). Chen *et al.* found that WMA technology can reduce the mixing and compaction temperatures of thermochromic asphalt mixture by 16°C (Chen Z. *et al.* 2021b). Additionally, the use of Sasobit® additive was shown to be effective in preserving the structural integrity of thermochromic microcapsules, reducing the leakage of core materials, and enhancing the optical reflectance in short-term aged thermochromic asphalt (Chen Z. *et al.* 2021b). This highlights that the optical properties of thermochromic microcapsules can vary based on the powder's chemical characteristics and ambient temperature.

While increasing reflectance is desirable for reducing pavement surface temperatures, it is also a huge concern associated with the use of thermochromic pavements.

Large areas of highly reflective pavement in urban settings could cause surrounding buildings to absorb the reflected light, potentially exacerbating the UHI effect (Jia; Wang, 2021; Xu *et al.*, 2021). Additionally, during the daytime, the reflected light may lower thermal comfort for people and animals near these pavements (Jia; Wang, 2021). It is essential that studies on thermochromic pavements take these issues into account to determine suitable locations for their application, enhancing to improve local microclimatic conditions and enhance the well-being of the population. More specifically, microclimate simulation studies using software to investigate the effects of replacing conventional pavement surfaces with thermochromic pavement may offer a valuable tool for informing the decision-making process when applying resilient strategies in urban areas.

The addition of thermochromic material to asphalt binder also modifies its thermal properties and performance. The latent heat of thermochromic asphalt can also be up to 3 times higher than that of conventional asphalt (Hu; Yu, 2013). According to Hu & Yu, the specific heat capacity of thermochromic binder is 21-33% higher than pure binder in the air temperature range from 20°C to 50°C. A higher heat capacity can help regulate temperature fluctuations by reducing the maximum surface temperature and increasing the minimum surface temperature (Hu; Gao; Yu, 2015). Additionally, the thermal conductivity and thermal diffusivity are lower by 5-35% and 3-45%, respectively. (Hu; Wanasekara; Yu, 2014), indicating that it takes longer to heat or cool these materials compared to conventional asphalt pavements.

The specific heat capacity and thermal conductivity properties were modeled as a linear function with different angular coefficients for low temperatures (-20°C to 20°C) and intermediate temperatures (20°C to 50°C) (Hu; Wanasekara; Yu, 2014). These empirical models can be used to forecast the specific heat capacity and thermal conductivity of asphalt binders under conditions that include low and intermediate pavement service temperatures, as well as scenarios with low powder concentrations. However, further research is needed to develop models for high temperatures and higher concentrations of thermochromic pavements. This is a relevant issue from the perspective of climate change, as ambient temperatures and pavement surface temperatures are increasing.

As a great significance to the improvement of urban microclimate and the sustainable development of city, Table 3 summarizes the main outcomes of using thermochromic materials in asphalt binders and mixtures, regarding optical and thermal properties. This article focuses on the results of applying thermochromic asphalt in hot weather conditions.

Table 3 – Main thermal and optical results of the use of thermochromic material in asphalt binders and mixtures.

Ref.	Technol. details	Optical properties	Thermal properties
(Hu, J. e Yu, 2013)		Not Evaluated	TCM binder has higher latent heat (3x), heat capacity (1.2x), and thermal conductivity (1.4x) than pure binder
(Hu, Wanasekara e Yu, 2014)	TCM asphalt binder with red, blue, and black powder content of 10% by weight, wet mixing	Not Evaluated	From -20°C to 50°C, the specific heat capacity of TCM binder is from 21% to 33% higher, while the thermal conductivity is from 5% to 35% and the thermal diffusivity is from 3% to 45% lower than pure binder
(Hu, J e Yu, 2016)		TCM binder is more reflective in the near-IR range than pure binder, and it increases with temperature; thermal treatment reduces the solar reflectance of TCM binder by at least 4% to 15.8% under 200°C for 2 h.	To keep thermal stability, it is suggested that the blue and red binder should be prepared below 200°C and less than 2 h, to control the weight losses in production conditions
(Hu, J. e Yu, 2016a)	TCM binder incorporating powder contents of 10, 20, 30, and 40% by weight, wet mixing	The spectral reflectance of TCM binder increases as the powder content increases, especially in IR range;	Not evaluated
(Hu, J. e Yu, 2020)	TCM binder incorporating powder 6%, or 1% powder + 3% TiO2 by weight, wet mixing	6% powder increases in 43% the HMA's solar reflectance; After rutting, TCM HMA presents 13-25% lower solar reflectance;	Not evaluated
(Chen, Zhang, Duan e Shi, 2021)	TCM binder incorporating powder 6% by weight and 4% Sasobit®, wet mixing	6% TCM + 4% Sasobit® exhibits the highest optical reflectance (especially within UV and visible light regions) among pure and 6% TCM short-term aged asphalt binders	Not evaluated
(Zhang, X. *et al.*, 2022)	TCM coating composed by 20% of red/black and TiO2 total mass fraction; the water-based silicone acrylic emulsion was used as the binder accounting for 55wt% of the coating	Increasing TiO_2 content, the reflectance spectra are improved; Considering hiding power, optical reflective characteristics, visual effects, and optical reflective characteristics, the optimal TiO_2 contents in the red and black TCM coating are 2wt% and 5wt%, respectively.	Not evaluated
(Chen, Z. *et al.*, 2022)	TCM binder incorporating powder content of 6% by weight, wet process; TCM mixture incorporating powder content of 0.326% by mass of the aggregates, dry	To wavelength range from 350 to 550 nm, the reflectance values can be increased by more than 50% in colorless thermochromic phase	Not evaluated

	process		
(Lima *et al.*, 2023)	TCM aqueous solution coating composed by powder 3% w/v, dye 0.5% w/v, and epoxy resin 20 mL, superficial sprayed	The addition of resin contributed to an increase in 3 times the colorimeters parameters (ΔE*, ΔL*), indicating higher luminosity	Not evaluated
(Xie *et al.*, 2023)	5% incorporating novel thermochromic pellets, with a TT 45°C, 55°C, and 65°C, to prepare ultra-thin wear layer (UTWC) asphalt mixtures	Not Evaluated	The thermochromic pellets have smaller thermal conductivity (9.5%) and thermal diffusion coefficient (23%), but higher specific heat capacity (17.5%) compared to the reference mixtures.
(Chen *et al.*, 2024b)	TCM binder incorporating powder content of 6% by weight, wet mixing	At a temperature larger than 31 °C, the solar albedo of TCM HMA is 0.30, which is six times larger than that of the conventional asphalt pavement material	Not evaluated

Source: Ribas et al. (2024).

Regarding to promotion a cooling effect, previous studies have exposed thermochromic binder to open spaces during hot summer days in Cleveland, OH, US. At temperature ranges between 20 - 70°C, the thermochromic binders consistently exhibited lower surface temperatures than the conventional asphalt binder. The maximum reduction in surface temperature was 6.6°C, 2.7°C, and 4.9°C for the black, blue, and red asphalt coatings, respectively (Hu; Gao; Yu, 2015; Hu; Yu, 2013). The laboratory tests have shown that the addition of thermochromic additives to HMA mixtures with binder modification results in a linear reduction of the maximum temperature. The average temperature reductions in the top asphalt layer (0 ~ 4 cm) are approximately 2, 4, and 5 °C for 4%, 6%, and 8% of thermochromic additive content, respectively (Li, Q. *et al.*, 2020a). During experimental outdoor tests, the maximum temperature reduction in HMA depths showed absolute errors of less than 3°C between laboratory and field results, satisfying the accuracy requirements of engineering practice (Li, Q. *et al.*, 2020a). Zhang *et al.* achieved better results for the cooling effect in indoor experiments by covering the HMA with thermochromic coating, resulting in a surface temperature 10.5°C lower than the conventional HMA (Zhang *et al.*, 2022). Furthermore, the study found that the cooling effect of TCM coating was 2-5 degrees Celsius lower than that of cool coating with the same color (Zhang *et al.*, 2022), suggesting that thermochromic coating is more effective among reflective pavements.

Although the initial results are promising, the studies remain in the early stages. One major limitation is the duration of field trials, which typically range from just days to a few months, and are often conducted in summer. Long-term environmental exposure is crucial for understanding the behavior of thermochromic asphalt pavements over the course of annual weather variations. Moreover, no studies have yet examined the application of thermochromic asphalt pavements on a full-scale, presenting a valuable opportunity for further scientific investigation with practical implications. In laboratory tests, incandescent lamps are used to simulate the effects of solar irradiation in controlled settings. However, this approach neglects the influence of other environmental factors, such as wind, cloud cover, humidity, and air pollution, which may lead to discrepancies between field and laboratory results.

On the other hand, computer simulations have been employed to estimate and to evaluate the cooling effects of thermochromic asphalt applications. Chen *et al*. found promising results using an interpolation methodology to match numerical simulation with experimentally monitored specimen temperature data. In summer conditions, a cooling effect of 6.26°C was obtained when the thermochromic surface of the asphalt mixture had an albedo six times higher than the base asphalt (Chen *et al.*, 2024). Zhang *et al*. (2022) utilized Computational Fluid Dynamics (CFD) simulations to evaluate the impact of replacing all traditional asphalt pavements in a typical residential area of Shanghai, China, with thermochromic pavement. The results, modeled for an extremely hot summer day, indicated a maximum reduction of 1.5°C in air temperature measured at a height of 1.5m. The use of simulations to study thermochromic pavements remains underexplored in the current literature, particularly in terms of quantifying their potential to reduce UHI effects on human health, well-being, air pollution, and smog formation. Additionally, the relationship between the cooling effects of thermochromic pavements and energy consumption in urban centers represents a significant knowledge gap. It's important to note that the relationship between environmental impact and cost is highly complex due to the presence of several indirect benefits, and because environmental costs are not easily quantified. Addressing these areas could offer valuable insights into urban planning and environmental enhancement.

The use of additives has been also explored to assess their combined effects with thermochromic materials. Zhao *et al*. (2023) found that incorporating 7% by weight of thermochromic powder and 25% of low freezing point materials in HMA specimens reduced surface temperature by 4–9ºC. This was due to the internal differential temperature caused by the additives, which lowered the internal temperature of the modified asphalt mixture compared to the unmodified specimen. This delay in high-temperature distress of asphalt pavement has important implications for pavement durability and performance (Zhao *et al.*, 2023). However, given the early stage of thermochromic asphalt research, several promising areas warrant further investigation. These include exploring the integration of thermochromic capabilities with environmentally friendly materials, such as phase change materials (PCM) and reclaimed asphalt pavement (RAP), among others. PCM is already well-established in asphalt materials applications due to its broad phase change temperature range and substantial enthalpy during transitions (Pinheiro *et al.*, 2023), which can enhance cooling effects and help mitigate UHI impacts. Additionally, combining asphalt pavements recycling techniques with cooling strategies could represent an innovative approach to improving sustainability.

The potential of thermochromic cooling performance is also affected by the production process. This is relevant when choosing strategies to efficiently mitigate UHI. For instance, the use of WMA technology to prepare thermochromic asphalt mixture can reduce pavement temperature by 2°C compared to traditional thermochromic HMA mixture (Chen *et al.* 2021b). The asphalt mixture modified with thermochromic microcapsules, prepared using the wet process, exhibits a superior cooling effect compared to those prepared using three dry processes, with a difference of at least 2°C (Chen, Z. *et al.*, 2022).

To advance in this area, the underlying theory of pavement design for thermochromic pavements must be thoroughly understood and requires further investigation. Table 4 summarizes the key findings on the cooling effects from the thermochromic studies discussed here, detailing the methods used and highlighting the main scientific gaps.

Table 4 – Main cooling effect results of the use of thermochromic material in asphalt binders and mixtures.

Ref.	Cooling effect	Study method	Gaps
(Hu, J. e Yu, 2013)	Surface temperature reduction of as much as 6.6°C during summer	Experimental outdoor (surface temperatures were recorded for 24 h during a typical hot summer day in Cleveland, Ohio)	Possible reductions in high temperature–related performance degradation
(Hu, J e Yu, 2016)	Surface temperature reduction of as much as 6.6°C during summer	Outdoor temperature was measured experimentally at 60-second intervals.	Improvements in the temperature meter instrument in the range of temperature control
(Hu, J. e Yu, 2020)	TCM HMA keeps 5–15 °C cooler during daytime and 1°C warmer during nighttime in summer	Outdoor temperature test (24h on a typical hot day in Cleveland, OH.)	Design optimization of TCM asphalt mixture by conducting field evaluation during both summer and winter seasons

(Li, Q., Hu, *et al.*, 2020)	The average temperature reductions in the whole top asphalt layer (0 ~ 4 cm) are approximately 2, 4, and 5 °C for TCM additive contents of 4%, 6%, and 8%, respectively	Laboratory solar radiation simulation (typical summer day in Nanjing - China, from 5:30 to 18:30)	Comparison with outdoor experiments
(Chen, Zhang, Duan e Shi, 2021)	TCM asphalt mixture prepared by WMA technology can achieve 2°C decrease in pavement temperature compared with pure asphalt mixture.	Outdoor solar radiation in hot summer (from 9:00 a.m. to 5:00 p.m. on a summer day in the city of Changsha-China)	The durability of TCM asphalt materials prepared by WMA technology by indoor accelerated long-term aging or long-term outdoor weathering aging test / the effects of mechanical blending and aggregates movement, during mixing and paving procedures, on the integrity of microcapsules
(Zhang, X. *et al.*, 2022)	Under experimental indoor high temperatures, the cooling effect of TCM coating on road surfaces could reach 10.57°C; The CFD simulation results lead to a maximum 1.5m air temperature drop of 1.5°C.	Indoor solar radiation simulation experiment / CFD simulation method applied to a typical extremely hot summer day in Shanghai	The combination of TCM and suitable phase change materials for improvement in the heating effect of TCM coatings / to explore the effect of TCM coating on the improvement of urban microclimate considering using it in more areas and a wider variety of urban surfaces (roofs and walls) as well as in combination with greening.
(Chen, Z. *et al.*, 2022)	Maximum decrease of 4–7°C in pavement surface temperature during the daytime	Outdoor experiments, 72 h during summertime in the city of Changsha, China	Influence of wet/dry process on the cooling function sustainability of thermochromic microcapsule modified road materials
(Zhao *et al.*, 2023)	During the day, the internal temperature was greater than the outside temperature, and in the early afternoon, the discrepancy between the two temperatures reached about 30°C to 7%TCM + 25% Low freezing point materials.	The temperature data inside different asphalt mixtures exposed to outdoor solar radiation from 8:00–19:00 in hot summer	Investigation of different asphalt mixture types and long-term performance evaluation
(Xie *et al.*, 2023)	The UTWC with thermochromic pellets exhibits a maximum temperature reduction of 5.5°C	Indoor radiation solar simulation with infrared light from a Tungsten iodide lamp (500W).	Investigation of road safety performance (skid resistance)
(Chen *et al.*, 2024b)	The average temperature reduction of TCM compared with the pure asphalt pavement material in different regions is 6.26 ℃	Outdoor solar radiation test for successive three days in hot summer and numerical simulation for outdoor solar radiation test (heat transfer theory of asphalt pavement)	The influence of the cooling function of TCM on the temperature and modulus distribution inside pavement structure, as well as the pavement mechanical response and service life

Source: Ribas et al. (2024).

2.3.5.3 Mechanical performance of thermochromic asphalt mixtures

The use of thermochromic materials in pavements has been shown to have an impact on their mechanical performance mainly due to the potential effects of these materials on temperature control (Chen, Z. *et al.*, 2019, 2022; Chen, Z. *et al.*, 2021a; 2021b; Du; Chen; Zhang, 2019; Hu; Gao; Yu, 2015; Hu; Yu, 2020a; Li, L. *et al.*, 2018a; 2018b; 2020; Li, Q. *et al.*, 2020a; 2020b; Zhang *et al.*, 2017; Zhang; Li; Chen, 2020). Therefore, it is relevant to consider these factors when incorporating thermochromic materials into pavement design.

Experimental results on the physical and rheological properties of asphalt binders with the addition of thermochromic materials indicate that the softening point, viscosity, complex modulus, rutting resistance, fatigue resistance, and stiffness of the asphalt binder increase with the addition of the thermochromic additive. Conversely, the penetration, phase angle, and creep rate decrease (Hu; Gao; Yu, 2015; Hu; Yu, 2016a). The addition of 3-10% black powder can improve the high temperature of performance grade (PG) by 8.6-15.8% (Hu; Gao; Yu, 2015; Hu; Yu, 2016a). Furthermore, increasing the thermochromic powder content can enhance the high-temperature stability of asphalt (Hu; Gao; Yu, 2015; Hu; Yu, 2016a) and its resistance to weathering and aging (Chen *et al.*, 2019; Hu; Yu, 2016a). Thermochromic asphalt binders are greatly less influenced by sunlight than base asphalt binders, which is attributed to the best solar radiation reflection that protects the asphalt matrix from sunlight influence, leading to higher weathering aging resistance of thermochromic asphalt binder (Chen *et al.*, 2019). The study also suggests that the weathering aging behavior of thermochromic asphalt binders is influenced by both the characteristics of the asphalt matrix and the thermochromic powder.

This suggests that thermochromic asphalt binders may be a resilient alternative for use in cities with hot climates. Given the increasing frequency of climate change-induced extreme events, such as heat waves, the importance of pavements with enhanced thermal stability is growing. This increased stability can directly impact the durability of asphalt materials, reducing the frequency of maintenance and repairs needed for pavements. This represents a significant knowledge gap in applying thermochromic materials in paving. More broadly, conducting a life cycle analysis of thermochromic asphalt materials remains an open challenge in the current literature.

Controversially, studies have shown that the use of thermochromic materials in SBS-modified asphalt binders can slightly weaken their high-temperature performance compared to pure asphalt binders (Li, L. *et al.*, 2018a; 2018b; 2020). Specifically, the addition of 4% TCM to SBS-modified binders resulted in a change in PG from 82.6-24.7 (pure SBS-modified binder) to 81.6-38, reflecting a decrease in high-temperature performance and an improvement in low-temperature performance. Additionally, adding 2% TCM to SBS-modified asphalt binders enhances their low-temperature crack resistance by approximately 24%, their resistance to natural aging by over 5% (Du; Chen; Zhang, 2019; Li, L. *et al.*, 2020), and their deformability by up to 22% (Li; Zhang; Chen, 2018).

Despite research into the combined effects of thermochromic materials and asphalt binders, there has been limited analysis of the impact of TCM nanomaterials on long-term pavement aging performance. Long-term aging, caused by prolonged exposure to high temperatures and continuous oxidation, can increase the susceptibility of HMA to intermediate-temperature cracking (Wu *et al.*, 2017). Thus, performance-based approaches for the design and selection of materials that resist cracking are crucial. Furthermore, the incorporation of additives that reduce cracking potential remains an area of significant interest.

The semicircular bending (SCB) test on notched samples has attracted significant attention from pavement researchers for assessing the fracture resistance and cracking parameters of thermochromic HMA. Li *et al*. (Li, Q. *et al.*, 2020b) observed that TCM-modified asphalt mixtures exhibited an increase in failure strain and a decrease in tensile strength as the additive content increased during SCB tests conducted at -10°C to evaluate low-temperature cracking resistance. These TCM-modified mixtures absorbed more solar heat by changing color at low temperatures, which softened the binders and improved low-temperature performance in conditions exposed to sunlight. However, while the study found statistically significant effects of TCM additives, with smaller particle sizes having a greater stiffening effect on asphalt binders, the overall impact of TCM additives was minimal when the same base binder was used (Li Q. *et al.*, 2020b).

Li *et al.* also investigated the effects of two different thermochromic particle sizes on SBS-asphalt binders. The study found adding powder with small particle size can improve the rutting resistance as it hardens the pure binders and ensures a better cooling effect (Li *et al.*, 2020b). However, the complex modulus of the asphalt decreases with the addition of powder, likely due to the thermochromic powder negatively affecting the rutting resistance (Zhang; Li; Chen, 2020). The mechanical performance of asphalt mixture is influenced by the modification process used. Both dry and wet mixing method showed similar moisture susceptibility (Chen, Z. *et al.*, 2022) and an increase of 30% in the dynamic modulus when compared to the base samples. In this context, the complexity of the impacts of adding nanomaterials to the mechanical performance of asphalt materials becomes evident, highlighting the importance of optimizing the percentage of thermochromic additives to balance both mechanical behavior and cooling effects.

Concerning the encapsulation strategy, the same effects were achieved using microcapsules composed of trioctanoinand compared with shells made by melamine-formaldehyde resin to thermochromic asphalt mixtures (Li, Q. *et al.*, 2020a). However, the potential impact of leakage from thermochromic core components on the mechanical behavior of asphalt mixtures remains unknown. For example, methyl stearate, similar to oil released from TCM microcapsules, compensates for flexibility loss but reduces the ability of asphalt binders to resist thermal stress at low temperatures (Li, Q. *et al.*, 2020a).

To sum up, by reducing the inner asphalt temperature, the mechanical properties of certain asphalt materials can be improved. The mechanical behavior of thermochromic binders and mixtures remains a relevant research subject with many opportunities for improvement and development. There is a lack of studies on the mechanical performance of thermochromic alternatives under long-term use and weathering conditions, field application studies, as well as further numerical studies are necessary to quantify the impacts of thermochromic additives. Cost assessments including the impact on maintenance and restoration interventions and a life cycle assessment are also essential. It could be inferred that the thermochromic capability has a relevant potential to improve the mechanical conditions of asphalt pavements while mitigating UHI effects. Table 5 presents the primary findings regarding the mechanical performance of thermochromic asphalt materials.

2.4 Technology Readiness Level of Thermochromic Pavements' Future Perspectives

From the bibliometric and systematic analyses conducted throughout this work, it has been possible to ascertain that the thermochromic asphalt pavements' functionalization represents an innovative theme with significant potential for relevant scientific investigation. Certain scientific gaps have been identified as potential contributions to the field of transportation infrastructure, particularly within the paving sector.

In this context, the Technology Readiness Level (TRL) method was adapted to estimate the technological maturity level best suited for each proposed future work perspective. The nine TRL levels were grouped into three categories: laboratory research; simulation world; and real world, as illustrated in Figure 12. It is evident that there is potential for scientific contribution at all TRL levels, which aligns with the state of the art of the thermochromic asphalt technology in question.

Figure 12 – Technology Readiness Levels for thermochromic pavements' future perspectives.

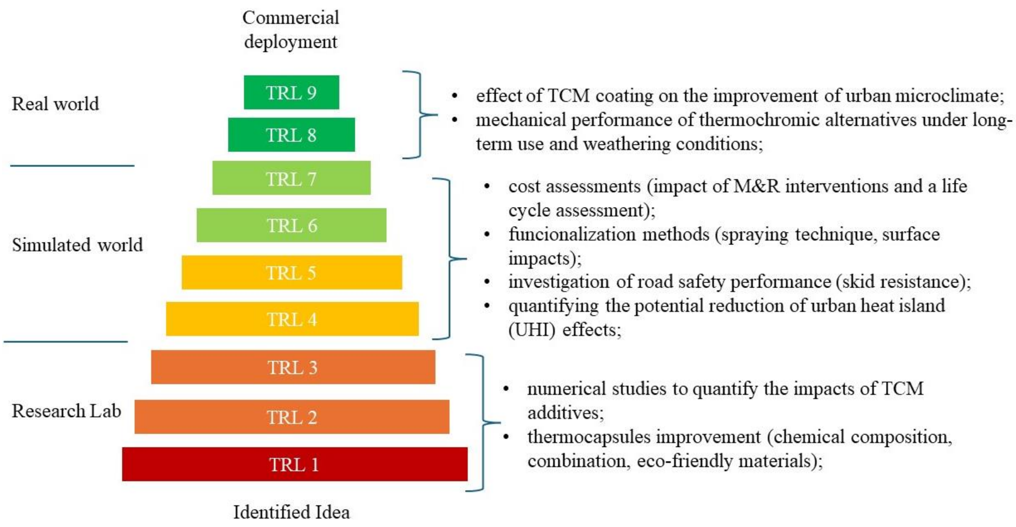

Source: Ribas et al. (2024).

2.5 Conclusions

This document presents a literature review dedicated to thermochromic asphalt binders, mixtures, and pavements used to mitigate UHI effects. To achieve this goal, two approaches were taken: first, a bibliometric analysis was conducted to produce network maps and analyze the current literature. Second, a systematic review was performed and a state of the art was elaborated basing a discussion on the thermal, optical, and mechanical performance of thermochromic asphalt mixtures, identifying the present scientific gaps, and outlining future perspectives. The results indicate that the theme has been a popular subject of scientific research, with a growing number of publications since 2013. The analysis revealed the following key findings:

China is the most productive country, with a relevant and well-established group of researchers. There is an initial connection among organizations, highlighted by a few numbers of partnerships between authors and scientific groups. Research papers were mostly published in the Journal of Construction and Building Materials.

Most studies available that investigated organic powders as TCM reported that the color, content, particle size, chemical composition, and method incorporation are crucial aspects to define the behavior of asphalt functionalization. Black thermochromic powders typically exhibit the best spectral reflectance in the visible and near-infrared spectra. The optimal content of TCM for achieving optimal optical and thermal performance is 4-6%. Smaller particle sizes improve the dispersion and intactness of thermochromic microcapsules in base binders, resulting in better physical properties and rutting resistance. The shell materials composed of trioctanoin showed less damage during heating or mixing, preventing leakage and loss of thermochromic efficiency. The incorporation of TCM using the dry process results in higher reflectance compared to the wet process, indicating that the dry process better preserves the integrity of thermochromic microcapsules. Additionally, the addition of TiO_2 to thermochromic coatings has been shown to improve optical characteristics due to its high reflectance in the NIR solar spectrum.

In laboratory tests, temperatures dropped by up to 10°C in terms of thermal performance. Experimental outdoor tests on a typical sunny day showed a cooling effect between 3-7°C for the thermochromic binder and 5-15°C for HMA. These results demonstrate that thermochromic asphalt is particularly effective in hot weather for improving thermal comfort and mitigating the UHI effect. The technology known as WMA can lower the mixing and compaction temperatures of thermochromic asphalt mixture by 16°C. This suggests that combining sustainable strategies can be an effective method for enhancing cooling efficiency and decreasing pollutant emissions.

The mechanical properties of thermochromic binders are improved compared to the base samples. This is especially true for the high-temperature performance grade, which reinforces the recommendation to use it in cities with hot climates. The reversibility of TCM can slow down the oxidation of the bitumen matrix, ensuring greater stability to UV aging for thermochromic asphalt binder, including SBS-modified binder. WMA can also provide benefits by reducing the short-term aging temperature of thermochromic asphalt binders. Therefore, thermochromic asphalt pavements have the potential to serve as a thermoregulation alternative, helping to mitigate temperature-related distresses, improve durability, and reduce the frequency of maintenance needs.

In summary, thermochromic technology shows to be promising in mitigating the urban heat island effect, particularly in hot weather locations, while also enhancing the mechanical performance of asphalt pavements by changing color in high temperatures. However, there are still relatively few studies on this topic, and further scientific research is needed. The methods of incorporation, particularly the spraying coating technique, should be further investigated due to their versatility and functionalization of new and old pavements ease. Particularly, the immobilization of thermocapsules in the asphalt substrate under weathering conditions, the impact of the solutions on road safety, and the superficial characteristics of thermochromic coatings must be further studied to increase the level of readiness of this technology and give confidence on its use in field.

Table 5 – Main cooling effect results of the use of thermochromic material in asphalt binders and mixtures.

Ref.	Technological Details	High-Temperature Performance / Rutting Resistance	Low-Temperature Performance / Cracking Resistance	Water Stability	Aging Analysis
(Chen, Zhang, Duan e Shi, 2021)	Asphalt binder incorporating 6%TCM by weight and 4% Sasobit®, wet mixing	The larger complex modulus of modified binder indicates Sasobit can improve its high-temperature stability	-	-	The WMA technology can mitigate the adverse effects of short-term aging on functionality of modified asphalt binder
(Chen, Zhang, Duan, Wu, *et al.*, 2021)	Asphalt binder incorporating 6%TCM by weight, wet mixing	Modified asphalt binder after 20 Day of UV exposition decreased rutting resistance due to leakage of methyl stearate	DSRFn of the control asphalt binder is 3.25 higher than modified asphalt binder and, thus, more susceptible of cracking	-	Modified asphalt binder can slow down the oxidation of the bitumen matrix during long-term aging condition
(Li, L. *et al.*, 2018)	SBS-modified asphalt binder incorporating 2, 4, 6 and 8%TCM by weight, wet mixing	TCM slightly affected the high-temperature stability (from PG 82.6-24.7 to PG 81.6-38 with 4% TCM)	Analysis of BBR test indicates adding 4%TCM of modified asphalt binder represented the best low-temperature performance	-	Considering short- and long-term aging by TFOT test, 2% and 4% red TCM asphalt binders showed superior aging resistance
(Li, Q., Hu, *et al.*, 2020)	SBS-modified asphalt binder incorporating 4, 6, and 8% TCM by weight, wet mixing	The small TCM particles (1-10 µm) cause hardening and further improve rutting resistance by URLPD test	The addition of TM additive has little effect on the low-temperature cracking resistance of asphalt mixtures using SCB test	Higher particle sizes TCM-modified asphalt mixtures show slightly better moisture resistance than small TCM by T-IDT test.	-
(Li, L. *et al.*, 2020)	SBS-modified asphalt binder incorporating 2%TCM by weight, wet mixing. Thermochromic HMA	Modified HMA presents a slightly (~5%) reduction in high-temperature performance according to results of Rutting test	Low-temperature splitting test showed the addition of TCM can improve the low-temperature performance of SBS-modified HMA	TSR results of the TCM with SBS-modified HMA is 6.8% better than that of the control HMA	TCM can improve the antinatural aging ability of SBS-modified HMA, and 2% red powder has the best antinatural aging effect
(Li, L., Zhang e Chen, 2018)	SBS-modified asphalt binder incorporating 2 and 4%TCM by weight, wet mixing	Ductility test showed TCM improved the deformability by up to 22% of modified asphalt binder compared to the control asphalt binder	-	-	the anti-aging properties of modified asphalt binders are better than control binder. 2% of black TCM showed the best aging resistance (TFOT test)

(Chen, Z. *et al.*, 2022)	Asphalt binder incorporating TCM content of 6% by weight, wet process; and HMA incorporating TCM content of 0.326% by mass of the aggregates, dry process	Considering tensile strength, tensile deformation and rutting resistance, modified HMA prepared by wet process can display a better performance than dry process. Both are better than control HMA	-	Freeze-thaw ITS test showed the addition of TCM improves the adhesion between asphalt binder and aggregates for both processes, which reduces moisture susceptibility	-
(Hu, J., Gao e Yu, 2015)	Asphalt binder incorporating 3, 6 and 10%TCM by weight, wet mixing	TCM is found to increase the Superpave high-temperature performance grades of modified asphalt binder; TCM helps to improve rutting resistance at the corresponding service temperatures in DSR test	The increase of TCM content reduces the resistance of modified asphalt binder to low temperature cracking	-	The stiffness and rutting resistance of modified asphalt binder increased after short-term aging (RTFO test).
(Zhang, H. *et al.*, 2017)	Asphalt binder incorporating 4 and 6% TCM by weight, wet mixing	TCM can improve high-temperature stability of asphalt binder by increasing its softening point, viscosity, complex modulus while decreasing penetration and phase angle.	The stiffness of modified asphalt binder was lower than control asphalt binder, which could improve capacity of deformability of modified asphalt binder in low temperatures.	-	6% red TCM represented good anti-aging performance after long-term thermal oxidation aging (PAV aging test).
[16]	Asphalt binder incorporating 6% TCM by weight, wet mixing	Modified asphalt binder exhibits lower Jnr and higher ZSV than control asphalt binder, manifesting TCM can improve the high-temperature stability; the rutting resistance is gradually decreased until 6 months of weathering aging, but after which the rutting resistance begins to be improved	The stronger solar reflection of red TCM and heat absorption of methyl stearate mitigate thermal aging effect on cracking resistance	-	Rheological indexes of modified asphalt binder are not always increasing or decreasing with growth of weathering aging time but there is a turning point that is at the sixth month

(Hu, J. e Yu, 2020)	Asphalt binder incorporating 6% TCM, or 1% TCM + 3% TiO_2 by weight, wet mixing; Thermochromic HMA	The addition of nano-TiO_2 improves rutting resistance of thermochromic HMA according to APA rutting test	-	TSR results and stripping observed show the addition of nano-TiO_2 improves the moisture resistance of thermochromic HMA	-
(Li, Q., Jiang, *et al.*, 2020)	Asphalt binder incorporating 4, 6, and 8% TCM by weight, wet mixing	According to TFS test and MSCR test, the small TCM particles (1-10 μm) cause hardening and further improve rutting resistance	-	-	-
(Zhang, H. *et al.*, 2018)	Asphalt binder incorporating 2, 4, 6, and 8% TCM by weight, wet mixing	-	Creep stiffness modulus indicates low-temperature properties are improved along with an increment of TCM content first and then decline, and optimum content is 6%.	-	4% is the optimal content in which modified asphalt binder exhibits the best aging resistance measured by FTIR analysis,
(Du, P., Chen e Zhang, 2019)	SBS-modified asphalt binder incorporating 6%TCM by weight, wet mixing	According MSCR test results, TCM microcapsule weakens rutting resistance of base asphalt binder, and has few effects on rutting of SBS modified asphalt binder	Thermochromic microcapsule improves fatigue of base and SBS asphalt modified binder	-	Thermochromic microcapsule can also improve thermal and photo oxidation aging resistance of SBS modified asphalt binder
(Chen *et al.*, 2024b)	Asphalt binder incorporating TCM content of 6% by weight, wet mixing; Thermochromic HMA	Considering the cooling effect, the dynamic modulus at 1.59 Hz of the modified HMA is 12.4% higher than control HMA	The Failure Tensile Strain (FTS) of modified HMA is 30% over the control HMA after aging.	-	Relaxation strength spectra of modified HMA do not significantly change after aging, indicates the cooling effect can mitigate the aging degree of HMA
(Zhao *et al.*, 2023)	Asphalt binder incorporating TCM content of 3, 5 and 7% by weight, wet mixing; + low freezing point materials replaced 25, 50, and 75% of the mineral filler volume in HMA specimens	The content of 5 %TCM + 25 % low freezing point additive achieved the best highest dynamic stability results to modified HMA	ITS test of modified HMA increased with a 25% of low freezing point, and the inclusion of TCM has little impact on that. The bending test of modified HMA is 2 - 8% lower than control HMA.	Modified HMA freeze-thaw splitting strength fell to a maximum of 10.19% compared to control HMA, with the increase of low freezing point materials	-

Source: Ribas et al. (2024).

3 EVALUATION OF SURFACE CHARACTERISTICS AND LONG-TERM FRACTURE BEHAVIOR OF ASPHALT MIXTURES FUNCTIONALIZED BY THERMOCHROMIC SPRAYING COATING

This is a manuscript of an article published by Taylor & Francis Group in the International Journal of Pavement Engineering on 14th August 2025, available online: https://doi.org/10.1080/10298436.2025.2544897.

Abstract

Flexible pavement surfaces absorb and retain heat, leading to heat island formation, affecting users' well-being and health. The adoption of reflective pavements, particularly thermochromic (TCM) functionalization of asphalt materials, is a recognized cooling strategy. However, the effects of TCM coating on pavement surface characteristics and durability needs to be evaluated. This study aimed to evaluate the efficiency of the TCM spray functionalization and its effects of on RAP-recycled asphalt mixture surface and cracking resistance. For that, the surface of a reference mixture was functionalized with two TCM spray coating contents (3% and 6%). Key physical, chemical, and thermal characteristics of TCM powders were assessed. Surface characteristics of functionalized mixtures were analysed through colorimetry and texture measurements. The cracking potential of the studied mixtures was assessed using the Semi-Circular Bending (SCB) test while subjected to long-term aging (LTA) conditioning. Furthermore, the bond strength between the TCM coating and HMA was determined based on pull-off adhesion test. Results from the thermal differential test indicated that the TCM coating activates at about 30°C, significantly changing surface colour and potentially reducing urban heat island (UHI) effects. Spray functionalization slightly smoothed the macrotexture and minimal impact on microtexture. Good adhesion between TCM coating and mixture surface was observed, presenting only cohesive failure and some increase in bond strength. From SCB results, it was observed that mixtures functionalized with 6% TCM coating reduced the stiffness and improved the ductility of the LTA specimens. Findings imply that higher contents of TCM could improve the cracking resistance of LTA specimens more significantly.

3.1 Introduction

Urban areas are characterized by large extensions of artificial surfaces that absorb and retain heat. Combined with the lack of vegetation, these factors play a key role in the formation and intensification of urban heat islands (UHI) (Xu *et al.*, 2021). UHI leads to increase ambient temperatures and thermal stresses, reduces air quality, and higher electricity consumption (Akbari; Menon; Rosenfeld, 2009; Xu *et al.,* 2021), resulting in social, economic, and environmental consequences. Since paved areas cover, on average, more than 60% of urban surfaces (Tsoka; Tsikaloudaki*;* Theodosiou*,* 2018), the use of materials with different thermal properties has garnered considerable interest as a resilient strategy for dealing with climate changes (Akbari; Menon; Rosenfeld, 2009). Conventional asphalt pavements, due to their black color and low albedo, absorb and store most of the incident solar radiation, raising its internal temperatures and contributing to the warming of urban centers (Rocha Segundo *et al*., 2021). To face this problem, one widely recognized cooling strategy is the use of reflective pavements, among which thermochromic (TCM) functionalization of asphalt materials stands out (Rocha Segundo *et al*., 2021; Xu *et al*., 2021).

The TCM can modify some properties of the pavement surface materials when exposed to external temperature variations (Rossi; Simeoni; Quaranta, 2021). The main concept is based on material color change occurring at a specific transition temperature (TT), below which the material is colored and above which it becomes colorless, resulting in a modification of the material's optical properties. In asphalt paving, TCM functionalization is a "cool pavement" strategy, with some studies focusing on controlling temperature variations and reducing the absorption of thermal energy by the pavement to mitigate the effects of UHI (Jiang *et al*., 2019; Shamsaei; Carter; Vaillancourt., 2022). Additionally, by lowering pavement temperatures through the reduction of the heat absorption on the surface layer materials, TCM can positively impact the durability of these structures by increasing their resistance to thermal oxidation aging, and consequently, making them less susceptible to cracking, including fatigue and thermal cracking (Li *et al*., 2018a; Zhang *et al*., 2018; Du *et al*., 2019).

TCM nanocapsules consist of a polymeric shell encapsulating an organic mixture of three core components: leuco dye (3-Diethylamino-6-methyl-7-2,4-xylidinofluoran), bisphenol as the developer, and methyl stearate as the solvent. Microencapsulation aims to enhance thermochromic capacity, maintain system integrity, and protect against UV radiation and physical damage (Du *et al*., 2019). TCM asphalt functionalization can be achieved through various methods, including wet mixing, where the heated binder is mixed with the TCM additive (Hu; Yu 2016a, 2020a; Du *et al*., 2019; Li, Q. *et al*., 2020b), and bulk incorporation dry mixing, which replaces a portion of the fine aggregate or filler with TCM materials (Chen Z. *et al*., 2022). Both methods likely ensure optimal TCM immobilization but can impact pavement performance (Hu; Gao; Yu, 2015; Li *et al*., 2018b; Du; Chen; Zhang, 2019; Li, Q. *et al*., 2020b). Another technique is spray coating, which involves applying a TCM solution to the compacted pavement surface (Zhang *et al*., 2022). The temperature of a TCM asphalt binder can be reduced by up to 6.6°C compared to the base binder (Hu; Yu, 2013). Similarly, TCM hot mix asphalt (HMA) can keep surface temperatures an average of 5 to 15°C cooler than conventional HMA during summer (Hu; Yu, 2020a). Moreover, open-graded asphalt concrete functionalized with TCM coating was found to reduce surface temperature by 10°C in an experimental indoor solar radiation simulation (Zhang *et al*., 2022). The surface spraying functionalization stands out for its greater efficiency in reducing surface temperatures (Zhang *et al*., 2022) without compromising the mechanical performance of pavements (Rocha Segundo *et al*., 2019b). However, the efficiency of functionalization can be reduced due to exposure to weather conditions and traffic-induced wear (Carneiro *et al*., 2013; Rocha Segundo *et al*., 2019a; Yi *et al*., 2022). Lima Jr. (2023) used the accelerated polishing test and found that the asphalt mixture functionalized with TCM solution showed dye traces on the surface, which indicates that the functionalization resisted wear, even under the severe conditions of the test.

In terms of material's performance and durability, the use of TCM nanomaterials has proven their effectiveness in improving the asphalt binder rheological properties and the mechanical properties of asphalt mixtures. Some studies have shown that the addition of 3-10% of black TCM powder by total weight of asphalt binder can improve the high-temperature performance grade (PG) of binder by 8.6-15.8%, which suggests that thermochromic asphalt binders may be suitable for use in hot climate regions (Hu; Gao; Yu, 2015; Hu; Yu, 2016a). Furthermore, increasing the TCM powder content can enhance the high-temperature stability of asphalt binder and its resistance to weathering and aging (Hu; Yu, 2016; Chen *et al*., 2019). In other research works, it was shown that the incorporation of 2% TCM to SBS-modified asphalt binders improved binder's low-temperature crack resistance by approximately 24%, as well as their antinatural aging ability by more than 5% (Du; Chen; Zhang, 2019; Li, Chen, *et al*., 2020), and their deformability by up to 22% (Li *et al*., 2018a). Although researchers have examined the combined effect of thermochromic materials and asphalt binders, there has been limited analysis of the long-term aging performance of pavements incorporating TCM nanomaterials.

Long-term aging (LTA) can be caused by prolonged exposure to high temperatures and continuous oxidation, as a result, HMA become more susceptible to intermediate-temperature cracking (Wu *et al*., 2017; Yazdipanah *et al*., 2025). Cracking is among the primary distresses that could significantly affect the serviceability of flexible pavements. That said, many performance-based methods are incorporated into the design and selection of asphaltic materials to account for cracking resistance, particularly under LTA conditions which is critical for evaluating this property. The semicircular bending (SCB) test has garnered significant attention from pavement researchers for determining the fracture resistance and/or cracking parameters of HMA materials (Yin; West, 2021). Considering the great ongoing efforts to develop more eco-friendly and sustainable asphalt mixtures, the use of reclaimed asphalt pavement (RAP) stands out in the United States as a recycling strategy (Williams; Willis; Shacat, 2022). Using RAP in the design of new HMA reduces the need for new aggregates and asphalt binder, which lower the costs and environmental impacts. It also minimizes landfill waste and promotes sustainability in asphalt pavement construction (Yang *et al.*, 2014). More than that, using RAP can enhance mechanical properties like stiffness and rutting resistance of HMA due to the presence of aged binder in RAP, which can improve the load-bearing capacity of the pavement (Al-Qadi *et al.*, 2012). However, RAP materials that have undergone LTA during a pavement's service life can cause premature cracking distresses while being used in the design of new asphalt mixtures. Therefore, it is fundamental to combine innovative solutions with sustainable practices to minimize the LTA effects. In this context, characterizing the indirect effect of spraying a thermochromic coating solution on RAP-recycled HMA surfaces as an aging barrier remains unexplored in the current scientific literature. The impact of functionalization on the surface characteristics of asphalt mixtures, the efficiency of the coating to adhere in the HMA subtract and the potential benefits related to the reduction of aging effects (volatilization and oxidation) on the cracking performance of HMA has practical significance for achieving long-lasting asphalt pavements and mitigating the effects of UHI.

3.2 Objectives and Scope

The main objective of this study is to evaluate the efficiency of the TCM spray functionalization and its effects on RAP-recycled asphalt mixtures surface and cracking resistance. Figure 13 summarizes the experimental plan adopted in this study.

Initially, the physical, chemical, and thermal characteristics of the selected TCM powder were assessed based on scanning electronic microscopy (SEM), Fourier-Transformed Infrared spectroscopy (FTIR), and thermogravimetric analysis (TGA), respectively. This step was important to identify the microstructure characteristics, chemical composition and thermal stability of the selected TCM powder.

To verify the efficiency of TCM coating and its impact on the asphalt concrete surface and cracking resistance, a control RAP-recycled HMA containing 25% RAP, approximately the average RAP content used in the U.S., was utilized (Williams; Willis; Shacat, 2022). Then, compacted HMA samples, both with and without TCM spray coating (using two dosages of TCM powder: 3% and 6% w/v), were long-term aged according to the AASHTO R30 protocol and subjected to different testing protocols. The surface characteristics of the studied coatings were analyzed by colorimetry using digital image processing (DIP), and texture measurements of HMAs using close-range photogrammetry (CRP). Pull-off test was used to verify the bond strength of asphalt concrete treated with TCM spray coating. Finally, the long-term effects of TCM spray coating on cracking-related parameters (peak load, fracture energy, and flexibility index) were assessed based on SCB Test.

Figure 13 – Experimental testing program.

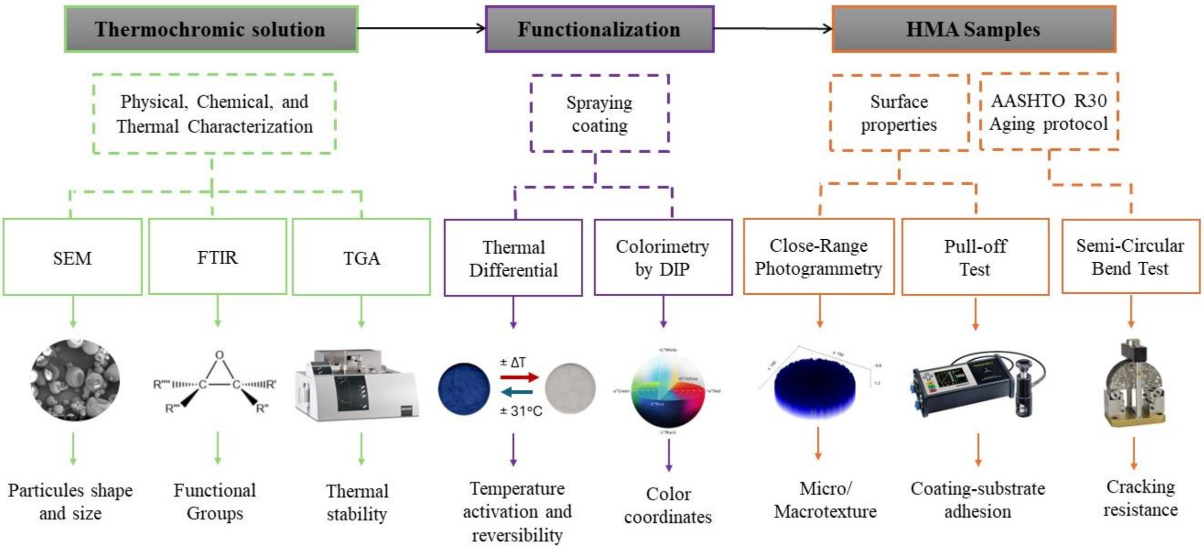

Source: Ribas et al. (2025c).

3.3 Materials and Methods

3.3.1 Materials

3.3.1.1 Aggregates, Asphalt Binder, and RAP

Virgin limestone aggregates with a nominal maximum aggregate size (NMAS) of 9.5 mm, PG 58V-34 asphalt binder, and RAP were combined in specified proportions to produce one control HMA mixture. The mixtures were produced with 25% RAP and 4.03% virgin binder, which resulted in a total binder content of 5.30% by weight. This mixture meets the Nebraska department of transportation (NDOT) requirements for mixtures applied in thin surface lift overlays, SLX mixtures.

It is important to mention that RAP was artificially produced in the laboratory for a better control of RAP characteristics. For that, a loose mixture was produced using the same aggregates and binder type and maintaining the aggregate gradation as in the control mixture. The RAP binder content was 5.3% (by weight of the mixture). The loose mixture was subjected to NCHRP 09-54 protocol (Kim *et al.*, 2017). Accordingly, loose mixtures were long-term aged in the oven for two days at 95ºC, simulating aging during four years of service life at 20 mm below the surface. Figure 14 indicates the gradation of aggregates (virgin and RAP blended) along with the higher and lower limits set by NDOT (Yazdipanah; Khedmati; Haghshenas, 2023).

Figure 14 – Particle size distribution curve of asphalt mixture SLX.

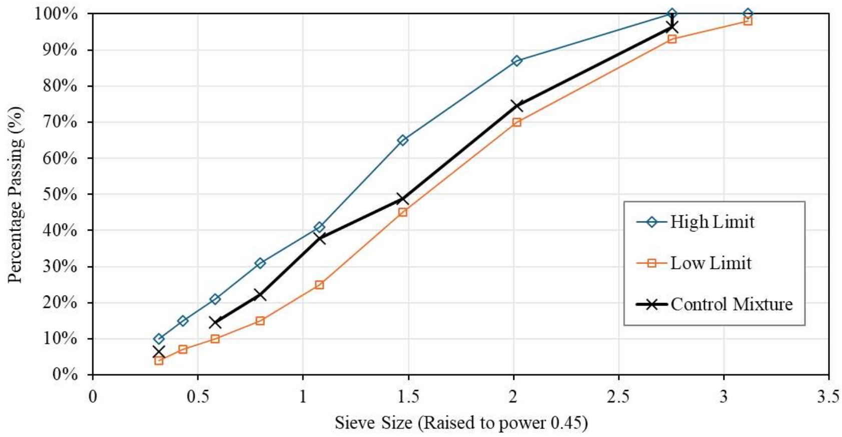

Source: Ribas et al. (2025c).

3.3.1.2 Thermochromic Pigment and Coating

The selected TCM pigment is the organic thermochromic microcapsule powder with a color change temperature of 31°C (LCR Hallcrest, thermochromic ChromaZone, USA). The TCM used in this study has a high sensitivity to temperature and the completed color transformation occurs within a few seconds after the temperature rose/fell to TT, exhibiting a reversible color change process from blue to colorless.

Based on the concentrations recommended by suppliers and previously indicated in the literature for optical, mechanical, and surface performances (Hu; Gao; Yu, 2015a; Zhang *et al.*, 2022a), two concentrations of blue TCM (3% and 6% w/v) and 1% (w/v) rutile TiO_2 (high purity, 30nm) were used to prepare the coating. Epoxy resin characterized by low viscosity, high transparency, advanced UV protection, and good mechanical resistance suitable for coating applications was utilized to enhance the immobilization of TCM on the HMA specimens in a mixing ratio recommended by the supplier (100:45 resin to hardener by weight).

3.3.1.3 Specimen Preparation with Thermochromic Coating

Cylindrical specimens with a diameter of 150 mm, height of 170 mm and 7±0.5% air voids were prepared by Superpave Gyratory Compactor (SGC) method in the height control mode, following AASHTO T 312 Standard, and using the loose mixtures discussed in preceding section. Then, the compacted HMA specimens were functionalized by spraying the surface with two TCM coating concentrations (3 and 6%) at a rate of 0.8 kg/m², each. In order to ensure uniform spray distribution, the spray gun was set 15cm above the HMA specimen and activated until the coating content was finished. The HMA cores were entirely (top, sides, and base) coated with the thermochromic solution. This comprehensive coating approach ensures that the entire specimen is subjected to the aging process, allowing for a more uniform assessment of the coating's performance and its interaction with the asphalt substrate under accelerated aging conditions.

After coating, the specimens were cured at room temperature at 25°C for 24 hours before undergoing subsequent tests. To simulate long-term aging (LTA) in the laboratory, the compacted HMA specimens were kept in a forced draft oven for 5 days at 85°C, following AASHTO R30 (AASHTO, 2002). The reason for choosing this LTA protocol was to evaluate the long-term effect of thermochromic coating on the cracking resistance of compacted specimens. The initial hypothesis is that if the pavement surface TCM functionalization in the field may reduce the long-term thermal-oxidative aging of HMA surface layer. The upper and lower surfaces of each specimen were used to acquire images using the CRP and then pull-off test method. AASHTO TP124-20 standard (AASHTO, 2020) was adopted to prepare the SCB specimens. Figure 15 summarizes the main steps involved in preparing, functionalizing, cutting, and cracking the HMA specimens under both unaged and long-term aging conditions.

3.3.2 Methods

3.3.2.1 Physical, Chemical, and Thermal Characterization

To characterize the microstructure of the microcapsules, the Nova NanoSEM™ equipment was utilized to collect, magnify, and obtain the final image of the TCM pigment. To enhance observations, the TCM pigment was first coated with a thin gold film, enabling magnification up to hundreds of thousands of times and resolution at the nanometer level.

The functional and chemical groups of the thermochromic powder material were characterized using Fourier Transform Infrared Spectroscopy (FTIR). FTIR analysis was conducted using a Nicolet iS20 spectrometer with a Smart iTX accessory featuring a diamond ATR crystal. The spectral data were collected over a wavenumber range of 4,000 to 400 cm^{-1}, ensuring comprehensive coverage of the infrared spectrum to identify all relevant functional groups. The measurements were performed with a resolution of 0.16 cm^{-1} and an average of 32 scans per sample to enhance signal-to-noise ratio and accuracy.

The thermal behavior of the TCM powder material was investigated using thermogravimetric analysis (TGA) to assess its stability and decomposition characteristics. The TGA tests were conducted using a TGA 209 F1 Libra instrument under a nitrogen atmosphere to prevent oxidation and other reactions that could interfere with the analysis. The thermochromic powder (5mg) was heated from 20°C to 100°C at a controlled rate of 2°C/min, which enroll the entire temperature range typically experienced by pavement surfaces. This controlled heating allowed for the precise measurement of weight changes as a function of temperature, providing insights into the material's thermal stability and potential weight loss due to decomposition. This analysis is critical for understanding the performance of the thermochromic powder when applied in pavement applications.

3.3.2.2 Colour Parameters Measurement

To demonstrate the thermochromic capacity and color variation of the surface coating, the 3% and 6% TCM coating samples were first spread on a metal disk and subjected to varied temperature conditions, ranging from 20 to 60°C. A digital hotplate and an infrared thermometer were used to heat and control the surface temperature of the samples. Starting in the colored phase (20°C), the samples were photographed every 5 min until reached the colorless phase. The colorimetry test analysis was performed by measuring the color coordinates using DIP with ImageJ 1.54g software, providing a perception of the color values of the samples at the end of this temperature range. For that, the color space specified by CIE (*Commision Internationale del'Eclairage*) methodology (International Commission on Illumination, 1976) was used, in terms of Lightness (L*) and chromaticity coordinates (a*, b*). The coordinates L*, a*, and b* indicates the position of the color in the color space. The L*-axis gives the lightness (0 black to 100 white), and the chromatic colors are described by two axes in the horizontal plane: a* the variation from red (+) to green (-), and b* the variation from yellow (+) to blue (-). After that, the color difference value ΔE*, which works as a perceptibility factor, was calculated according to Equation (1).

$$\Delta E^* = \sqrt{(\Delta L^*)^2 + (\Delta a^*)^2 + (\Delta b^*)^2} \quad (1)$$

Figure 15 – Specimens preparation steps to an experimental program.

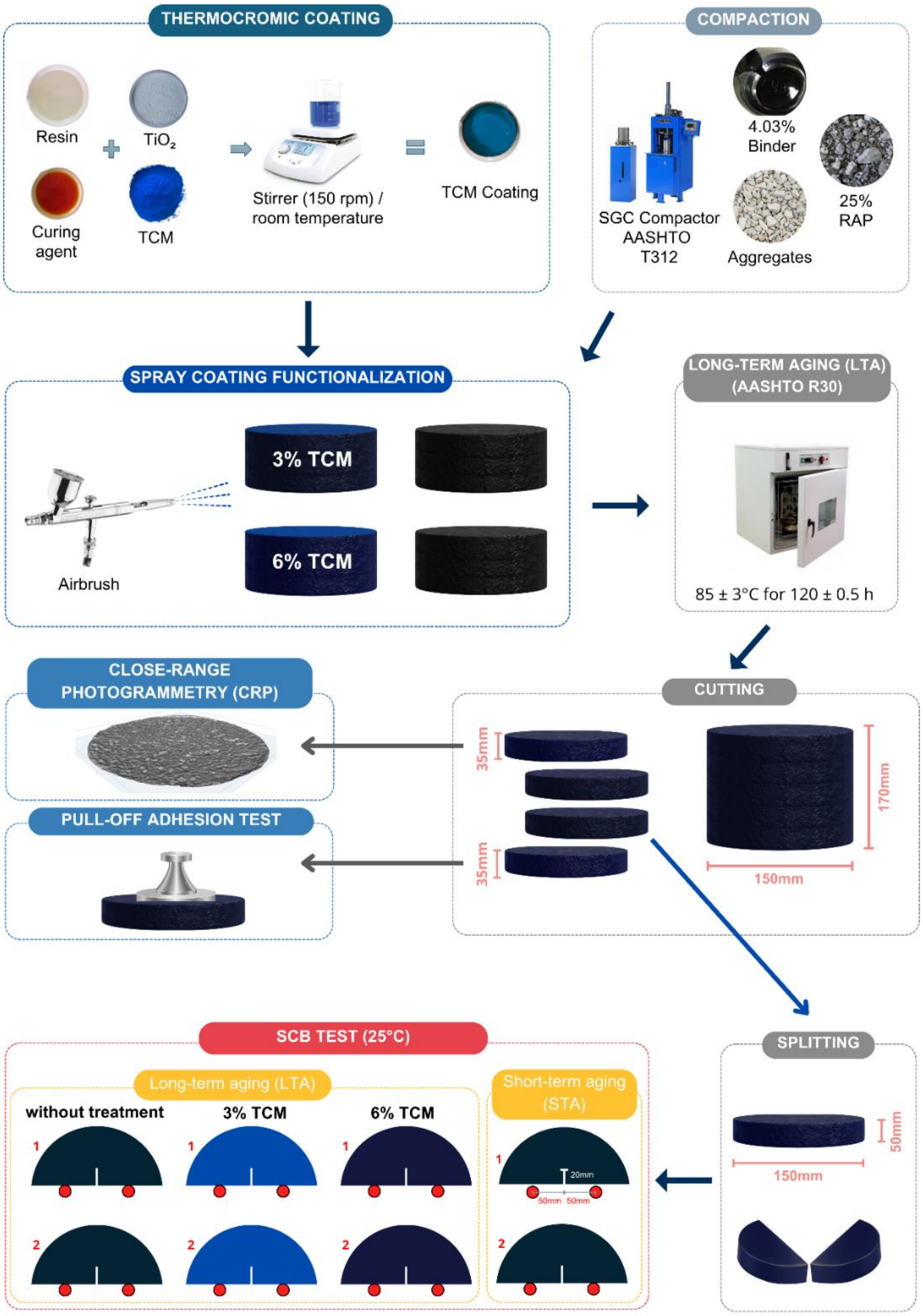

Source: Ribas et al. (2025c).

3.3.2.3 3D Computer Vision through the Close-Range Photogrammetry (CPR)

The surface texture of the HMA functionalized with the thermochromic solution were evaluated using CRP combined with DIP techniques. Three specimens of each coating concentration (3% and 6%TCM) and a control sample (without treatment) were part of this step. The main methodology allowed to obtain the texture parameters is summarized in Figure 16.

The main microtexture parameters from ISO 25178-12 calculated were: arithmetic mean deviation of the surface (Sa), root-mean-square deviation of surface (Sq), maximum peak height of the surface (Sp), maximum valley depth of the surface (Sv), skewness (Ssk), and kurtosis (Sku). These parameter variations between the control specimen (without TCM coating) and the functionalized specimens were compared to analyze texture characteristics changes. Analysis of variance (ANOVA), considering the treatment as a factor, was carried out to determine the main effect between the independent variables (Sa, Sq, Sp, Sv, Ssk, and Sku) over the parameters for a significance level of 5%. Turkey post-hoc analysis was also carried out to find patterns by testing if there was significant difference in the average of the parameters between the control and functionalized specimens.

Figure 16 – Flowchart of 3D Computer Vision through PCR.

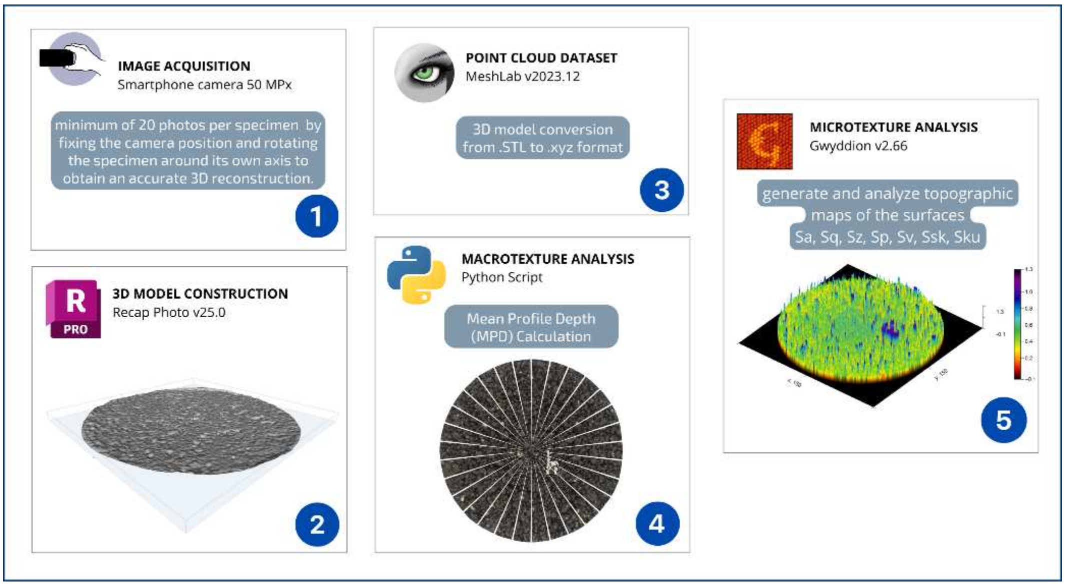

Source: Ribas et al. (2025c).

Regarding the macrotexture analysis, a Phyton script was developed to calculate the mean profile depth (MPD, ASTM E 1845-15) before and after the specimens' functionalization. Using x, y, and z coordinates from the point cloud file, profiles were calculated along the sample diameter at every 1-degree interval with a tolerance of 0.05 mm. To mitigate border effects, 10% of the outermost data points were excluded from the analysis. The MPD for each profile was determined by dividing the profile height baseline into two segments. The peak values for each segment were then arithmetically averaged to obtain the mean segment depth (Equation 2). The macrotexture of each specimen was calculated by averaging the MPD values from all profiles.

$$MPD = \frac{1stPeak + 2ndPeak}{2} - average\ level \tag{2}$$

3.3.2.4 Pull-off Adhesion Test

A digital display adhesion tester was used to measure the bond strength of the TCM coating using the pull-off principle with hydraulic pressure. The test measured the force required to pull at a rate of 24 psi/s a specified test diameter (50mm) of the TCM coating away from the coated HMA substrate and analyzed the fracture damage between them according to ASTM D4541-22. At the end of the test, three main types of fracture damage could be observed (Figure 17): (a) cohesive, when the fracture occurs within a coating layer; (b) adhesive, when the fracture occurs at the interface between layers; and (c) glue failure, when there is a visible separation of the glue from itself, the coating, or the dolly.

Figure 17 – Types of fracture damage in pull-off adhesion test: (a) cohesive; (b) adhesive; (c) glue failure.

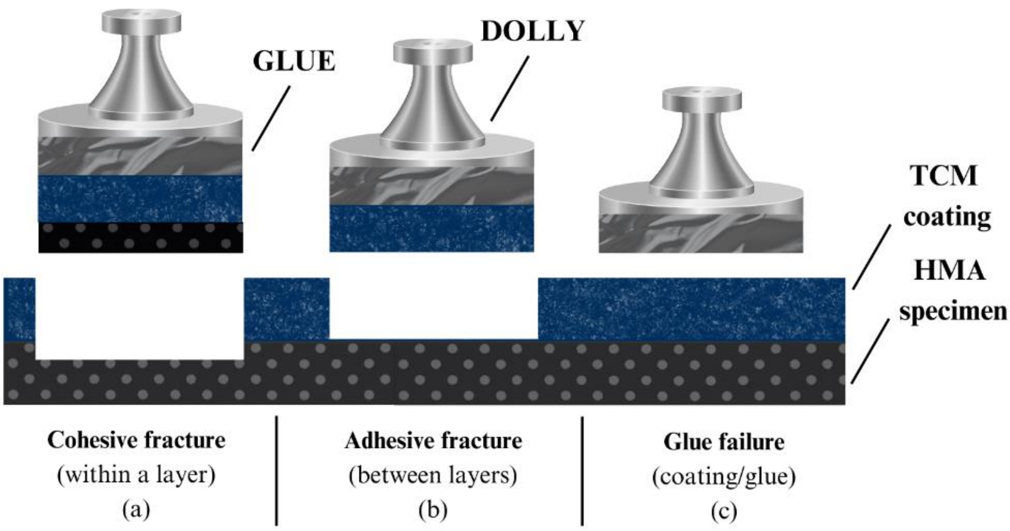

Source: Ribas et al. (2025c).

3.3.2.5 Semi-circular Bending (SCB)n Test

The SCB was conducted following the AASHTO TP124-20 standard. The semicircular specimens were positioned in the test fixture and loaded along the vertical radius at a rate of 50 mm/min at a testing temperature of 25±0.5°C. The load and load line displacement (LLD) were recorded throughout the process to determine the fracture energy (G_f) and post-peak slope (|m|), which were then used to develop the Flexibility Index (FI) as an indicator of cracking resistance for HMA. To determine the |m|, a tangential curve was drawn at the inflection point, and its slope provided the |m| value. FI can be calculated using Equation (3) from AASHTO TP 124-20:

$$FI = \frac{G_f}{|m|} \times A \tag{3}$$

where G_f is the fracture energy (J/m²), $|m|$ is the absolute value of the post-peak load slope (kN/mm), and A is a unit conversion and scaling factor equal to 0.01. For each studied case, 4 specimens were tested and average results, standard deviation, and coefficient of variation are presented.

3.4 Results and Discussion

3.4.1 Physical, Chemical, and Thermal Characterization of TCM Pigments

SEM micrographs and FTIR spectrum are presented in Figure 18 and 19, respectively. It can be observed that the TCM powder consists of spherical microcapsule particles, with the particle sizes predominantly ranging from 1 to 3 µm (Figure 18a). Some particle agglomeration or interaction was observed, potentially affecting coating dispersion and, consequently, its reflectivity. Additionally, a few microcapsules were found to be broken (Figure 18b), probably due to environmental conditions during transportation. This damage may lead to a reduction in thermochromic properties due to the leak of core material. From FTIR spectrum (Figure 19), it can be identified the absorption bands centered around 3,365 cm^{-1} and 1,511cm^{-1}, corresponding to hydroxyl (-OH) and benzene skeleton vibration, respectively, probably derived from bisphenol A, a color developer commonly utilized in TCM pigments (Zhang *et al.*, 2017). The characteristics of methyl stearate are identified by functional groups such as methyl (-CH_3), methylene (-CH_2), and carbonyl (C=O), indicated by peaks at 2,923cm^{-1} 2,848 cm^{-1}, and 1,740cm^{-1} separately. Peaks centered around 1,556 cm^{-1} and 813 cm^{-1} are attributed to the melamine-formaldehyde resin used as a microcapsule shell.

Finally, the TGA was conducted to confirm the thermal stability of TCM pigment. From room temperature (~25°C) to 100°C, the residual mass of TCM pigment was 99.23%. This result shows an 88% lower weight loss compared to the blue TCM pigment from Hu and Yu (2016a) at the same maximum temperature, indicating that it is thermally stable for the proposed coating's application in in-service pavement temperatures.

Figure 18 – SEM testing results of (a) TCM pigment (magnification factor: 2086); (b) TCM pigment (magnification factor: 9716).

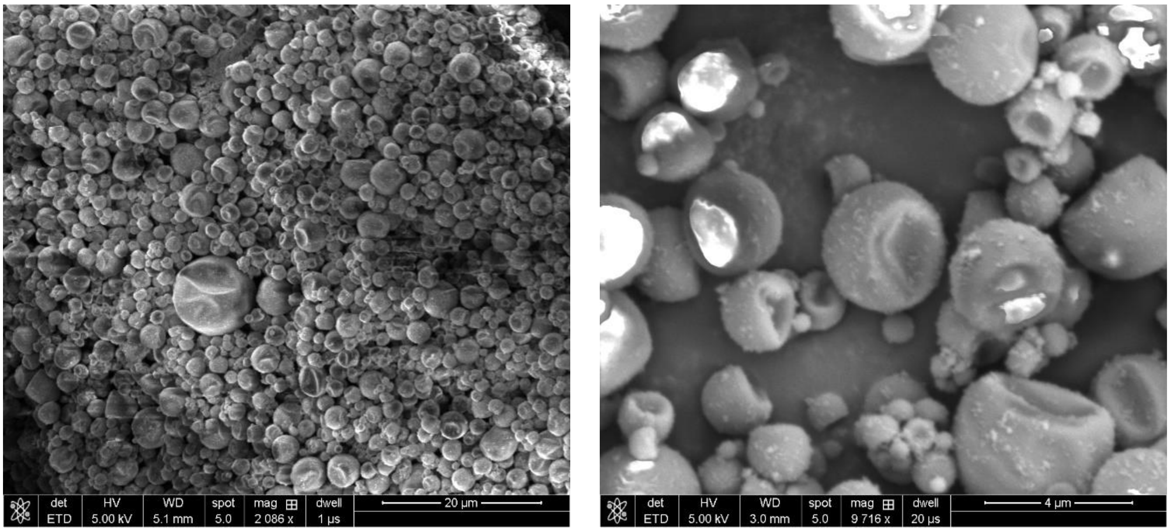

(a) (b)

Source: Ribas et al. (2025c).

Figure 19 – FTIR spectrum of blue TCM pigment.

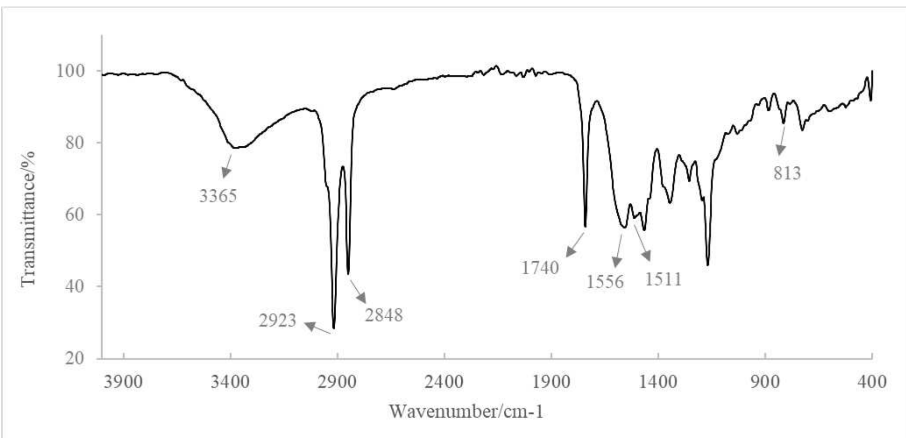

Source: Ribas et al. (2025c).

3.4.2 Thermal Differential and Colorimetry on TCM Coating

Visual analysis allowed to observe the thermal activation and color change during this process, as shown in Figure 20. Initially, at 20°C, both samples exhibited predominantly blue colors, indicating that the thermocapsules were still in their colored phase. From 30 to 60°C, significant changes in coloration were observed, with the samples becoming lighter as the thermocapsules transitioned from their colored to colorless phase.

The color coordinates values L*, a*, and b* were collected from post-processed images. The variations ΔE*, ΔL*, Δa*, and Δb* were calculated, as shown in the colorimetry results in Table 1. The 3%TCM coating had a higher color difference (ΔE*) before and after color change. The lower 6%TCM coating's ΔE* is contrary to expectations. It could be attributed to a possible agglomeration of the nanocapsules, which reduces thermochromic efficiency.

Figure 20 – Visual color differential as a function of temperature.

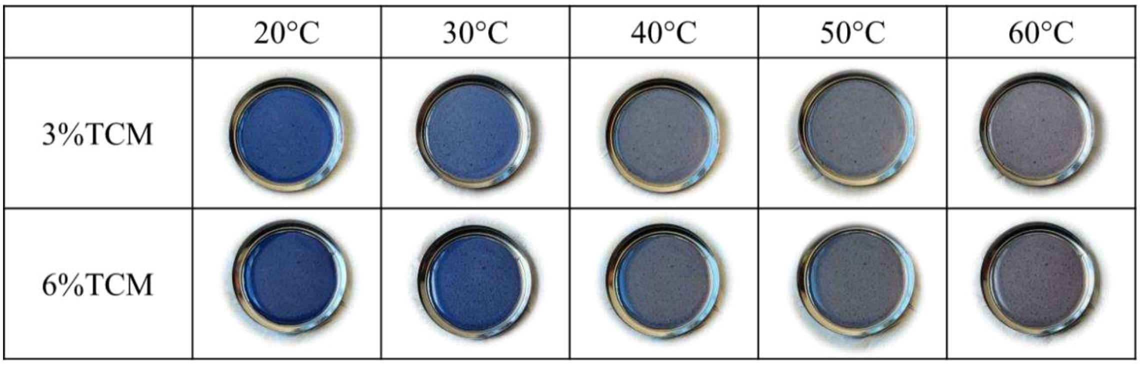

Source: Ribas et al. (2025c).

Table 6 – Colorimetry test results between 20°C and 60°C

Coordinates	3%TCM coating	6%TCM coating
ΔL*	16.36	12.35
Δa*	-5.41	-4.70
Δb*	29.08	23.51
ΔE*	33.80	26.97

Source: Ribas et al. (2025c).

Figure 21 – Thermochromic activation by variation of b* coordinates as a function of temperature.

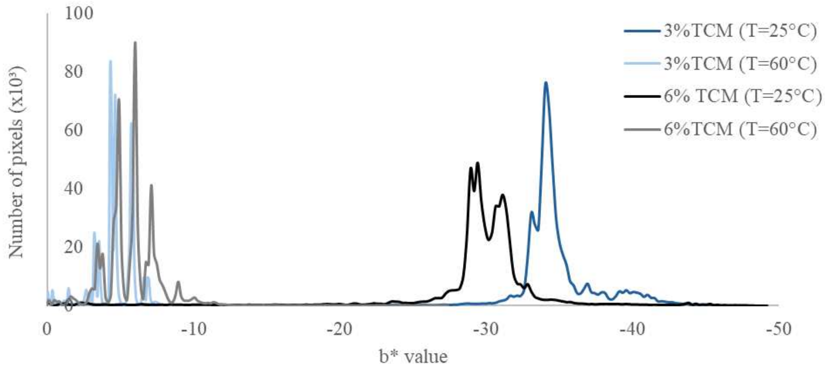

Source: Ribas et al. (2025c).

The Δb*parameter is particularly relevant in this colorimetry test as it represents the color variation from yellow to blue. A high positive variation in the Δb* parameter is desirable for this functionalization, aiming to change the coating surface color to a light shade to reduce heat absorption and, consequently, the UHI effects. Figure 21 presents the pixel histogram of b* coordinates for TCM coating as a function of temperature. After discoloration at higher temperatures, the TCM coatings showed a significant change: the chroma of blue was weakened confirming the activation of the thermochromic effect.

3.4.3 Surface Properties

3.4.3.1 Macrotexture

Figure 22 shows the macrotexture results before and after functionalization process. The spraying coating technique affected the macrotexture of HMA specimens by smoothing it by an average of 21-25% for the functionalized specimens. The reductions in MPD were expected due to the likely resin-filled micro-voids and irregularities on the surface of the asphalt mixture, thereby decreasing the surface microtexture and macrotexture. Although the ANOVA test carried out in this study to the MPD averages indicates significant differences (p value <0.05) among uncoated and functionalized results, dependence on the TCM content of the nanomaterial was not observed. It may be correlated with the fact that the pigment concentration added, both lower than the maximum recommended by the resin manufacturer, did not affect the coating viscosity. Water-based coatings have been shown as an alternative to lower MPD reduction, with spraying coating functionalization smoothing the HMA surface on an average of 7% compared with the control sample (Rocha Segundo *et al*., 2019b).

Figure 22 – Macrotexture Results.

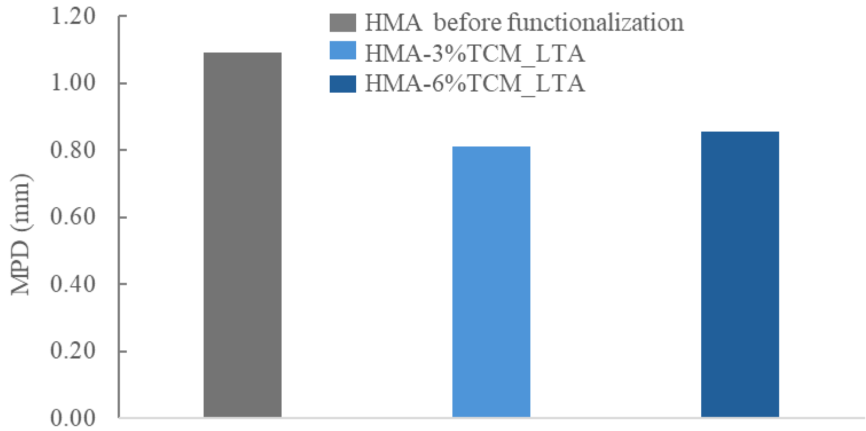

Source: Ribas et al. (2025c).

3.4.3.2 Microtexture

Figure 23 shows the results of the microtexture assessment for the following parameters: Sa, Sq, Sp, and Sv. The parameters Sa and Sq were used to quantify significant deviations of textures. They show the same trend for the difference between the specimens, which is because both are related to the distribution of the heights of all the points in relation to an average plane. The Sp >0 parameter indicates a predominance of peaks, which is compatible with the characteristics of positive coatings, such as dense asphalt mixtures. Sp showed a 40% reduction for samples functionalized with 6%TCM compared to the control HMA, which may be associated with the coverage and levelling of the surface after functionalization. The Sv parameter, however, showed practically identical values before and after functionalization of the specimens.

Figure 23 – S_a, S_q, S_p, and S_v parameters before and after functionalization.

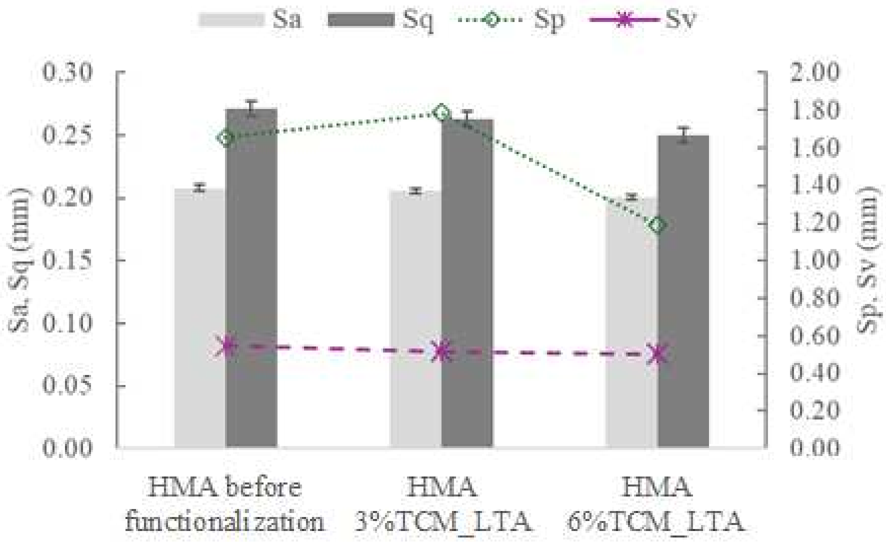

Source: Ribas et al. (2025c).

The average values of the parameters related to the shape of the height distribution curve, Ssk and Sku, are shown in Figure 24. The symmetry of peaks and valleys of the surface is established for Ssk = 0: normal distribution, that is, symmetry about the average line; Ssk<0: predominance of valleys (negative texture); and Ssk>0: indicates a higher number of peaks (positive texture). All the Ssk averages are positive and this result is in line with the concept of positive microtexture mentioned above. The Kurtosis (Sku) characterizes the presence of extremely deep valleys/high peaks for Sku=3: normal distribution; Sku>3: extremely deep valleys/high peaks; and Sku<3: lack of them. The control HMA (before functionalization) showed a high value for the average Sku parameter (5.14), which means that there is a predominance of extremely high peaks or deep valleys. On the other hand, for the functionalized specimens (3%TCM and 6%TCM) the heights are normally distributed, which is suggested by the average values assumed by Sku, close to 3. This result suggests the coexistence of higher peaks and/or deep valleys with parts free of these extreme values, probably due to the presence of the resin.

This reduction in kurtosis may indeed lead to a slight decrease in microtexture-related friction, especially under dry conditions where asperity interaction is a dominant factor. However, it is important to note that the surfaces maintained a positive skewness (Ssk>0), meaning that the predominance of peaks was preserved, which still contributes positively to friction. Nonetheless, further investigation, such as direct friction measurements, would be necessary to fully quantify the practical impact of this change in surface morphology on skid resistance.

Figure 24 – S_{sk} and S_{ku} parameters before and after functionalization.

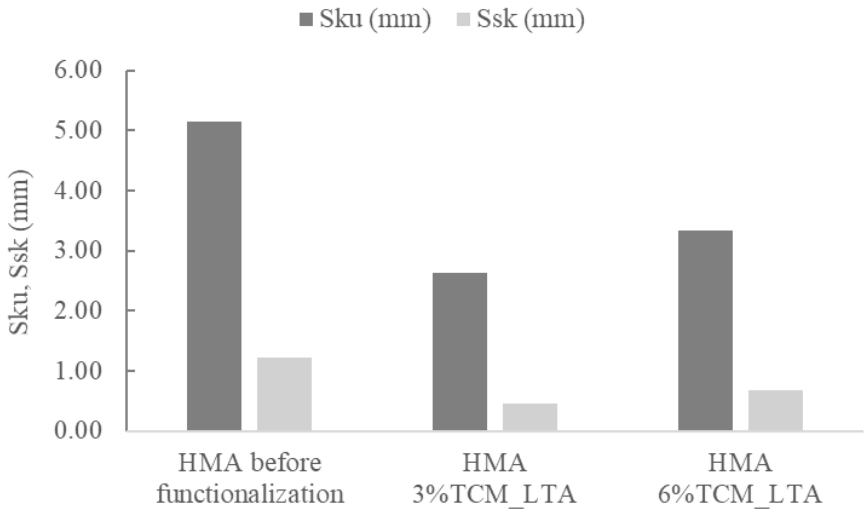

Source: Ribas et al. (2025c).

The ANOVA analysis of the factors influencing the microtexture parameters indicates that the independent variable of functionalization had no significant effect on Sa, Sq, Sp, and Sv ($p > 0.05$). A significant main effect of Group on Ssk (Skewness) was observed, $F(3, 4) = 7.77$, $p = 0.038$, indicating that surface skewness varied according to the coating condition. However, no significant main effect of Group was found for Sku (Kurtosis), $F(3, 4) = 4.06$, $p = 0.105$. The normality assumption was satisfied for both Ssk ($p = 0.148$) and Sku ($p = 0.583$) according to the Shapiro-Wilk test. Despite the significant ANOVA result for Ssk, post-hoc Tukey's test did not reveal statistically significant pairwise differences among the groups. Therefore, the functionalization had a minimal impact on these surface characteristics.

3.4.4 Bonding Strength

The bond strengths of functionalized specimens before and after aging are shown in Figure 25(a). Each test was repeated three times. The average bond strengths before aging were 0.83 MPa, 0.88 MPa, and 1.09 MPa for 3%TCM, 6% TCM, and Uncoated specimens, respectively. After aging, both TCM coating contents exhibited a slight increase in bond strengths, rising by 12% and 22%, respectively, while the uncoated sample presented a reduction lower than 2%. It is interesting to observe that the bond strength of the TCM coating did not lose its bonding capacity due to thermal-oxidative aging, as cohesive failure was observed in all tests (Figure 25(b) and (c)). This indicates that the asphalt layer failed before the bond between the TCM coating and the substrate. There is good adhesion between the TCM coating and the HMA, even under severe aging conditions.

The observed enhancement in bond strength post-aging can probably be attributed to the post-curing behavior of the epoxy resin. During thermal-oxidative aging, residual reactive groups within the epoxy resin may continue to react, leading to an increased cross-linking density. This post-curing process results in a more robust and cohesive resin network, thereby enhancing the adhesion between the coating and the asphalt concrete substrate. Such behavior has been documented in studies examining the thermal aging of epoxy asphalt systems, where post-curing contributes to improved mechanical properties and adhesion performance (Apostolidis *et al.*, 2022; Wang *et al.*, 2022).

Figure 25 – Bonding Strength of TCM coating: (a) before and after aging; (b) cohesive failure after test at 3%TCM specimen; and (c) 6%TCM specimen.

a)

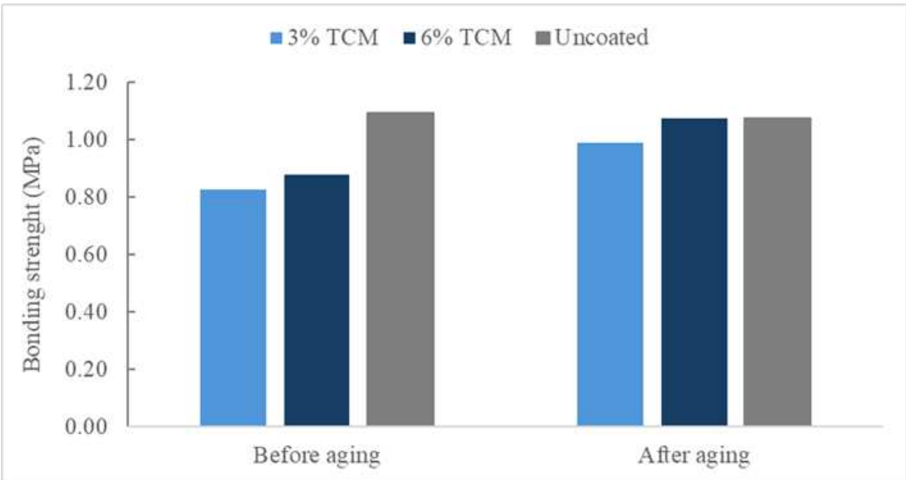

b)

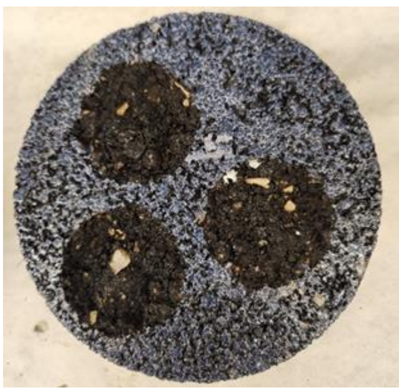

c)

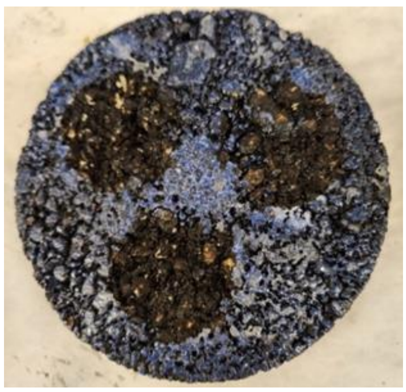

Source: Ribas et al. (2025c).

3.4.5 Mid-Temperature Cracking Resistance

Figure 26 depicts the variation of load-displacement curves in the SCB fracture test based on three replicates for different conditions: short-term aged (HMA_STA), long-term aged (HMA_LTA), and long-term aged functionalized with two contents of TCM coating (HMA-3%TCM_LTA, HMA-6%TCM_LTA). As expected, HMA_STA specimens have significantly lower fracture force (based on peak load) and higher flexibility (based on pre- and post-peak slopes) compared to the HMA_LTA ones. This trend is expected since the LTA process increases the stiffness of HMA, leading to less capability of mixtures in relaxing the applied stresses and making the materials more brittle and susceptible to cracking (Ozer *et al.*, 2016). To be more specific, the average peak load value increased by about 40% and the displacement associated with the peak load reduced by about 60% in the HMA_LTA when compared to HMA_STA specimen, illustrating less ductile material with a faster rate of crack initiation (Al-Qadi *et al.*, 2022; Bastola *et al.*, 2024).

Regarding the effects of TCM functionalization on mid-temperature cracking resistance after LTA conditioning, it was observed that the use of 3% TCM spray coating resulted in similar cracking behavior as the HMA_LTA specimen. HMA-3%TCM_LTA shows almost similar peak load (slightly higher) compared to the HMA_LTA, indicating that 3%TCM content is not sufficient to combat the LTA effects on HMA cracking performance. Another explanation could be related to the coating dosage issue or TCM powder degradation under LTA condition, suggesting that the low dosages of thermocapsules are more susceptible to weathering when subjected to a long thermal oxidating process. On the other hand, HMA-6%TCM_LTA showed 18% reduction in peak load value compared to the HMA_LTA specimen. Additionally, both the pre- and post-peak slopes indicated a more ductile behavior of this treated specimen compared to the HMA-LTA. This highlights the significant impact of the 6%TCM coating layer in improving the fracture behavior of HMA after exposure to the LTA condition.

Figure 27 shows various parameters derived from load-displacement curves including peak-load, fracture energy (G_f), and flexibility index (FI). The average coefficient of variation (COV) for the FI is about 15%, which is higher than for G_f (about 5%). This is expected, as FI is associated with the shape of the post-peak segment of the curve, while G_f represents an average value derived from the area under the curve. Therefore, the FI is more sensitive to changes in sample density, material variability, equipment, and the operator (Keymanesh *et al.*, 2023).

Figure 26 – Variation in load-displacement curves in SCB test at 25°C.

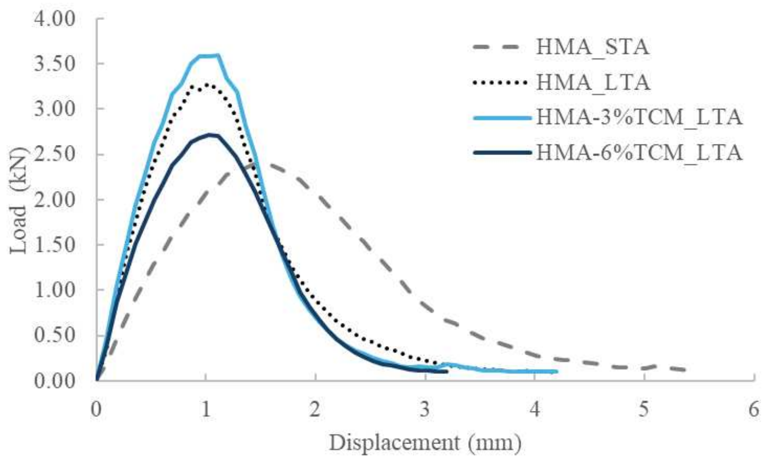

Source: Ribas et al. (2025c).

As shown in Figure 27c, compared to HMA-STA, LTA process increased the specimens' peak-load by 39.7% and 54.7% for HMA_LTA and HMA-3%TCM_LTA, respectively. However, for HMA-6%TCM-LTA, this increase is only limited to 15% when compared to HMA-STA. This implies that the 6% TCM coating effectively enhances cracking resistance and toughness after LTA conditioning, likely due to its ability to protect the surface layer of HMA, reduce binder brittleness, and improve the viscoelastic response of the asphalt mixture. The statistical analysis of the average of the results using Tukey's HSD test (95% confidence level) indicates that the differences between peak load of HMA_STA and HMA-6%TCM_LTA is not statistically significant ($p < 0.05$), which further verifies the positive impact of 6% TCM coating on cracking resistance of mixtures.

However, the FI parameter, which depends largely on the post-peak slope behavior, did not show significant improvement for the TCM-treated specimens compared to the control LTA specimen. This discrepancy can be explained by the FI's sensitivity to the entire post-peak region of the load-displacement curve. While TCM coatings help reduce peak load and improve ductility (as seen in Figure 14), they may not substantially affect the overall shape and decay of the post-peak region captured by the FI. Consequently, although 6% TCM could reduce the stiffness of LTA mixtures significantly by reducing the peak load value, it couldn't change the post-peak slope enough so to improve the FI as a cracking resistance index. The lowered stiffness and improved ductility obtained from TCM coating after LTA conditioning could potentially show its positive impact on another performance indicator such as cracking tolerance index (CT_{index}) obtained from IDEAL-CT test. This difference in terms of practical results could be attributed to the crack development and propagation mechanisms in strength-based and fracture-based tests, as reported by other researchers (Al-Qadi *et al*., 2022; Teixeira *et al*., 2023). Overall, the results imply that higher contents of TCM (more than 6%) might potentially have more significant impact on the improved cracking resistance of LTA specimens.

Figure 27 – Fracture Parameters of HMA for different conditions in SCB test at 25°C, (a) Flexibility index; (b) Fracture energy; (c) Maximum peak-load.

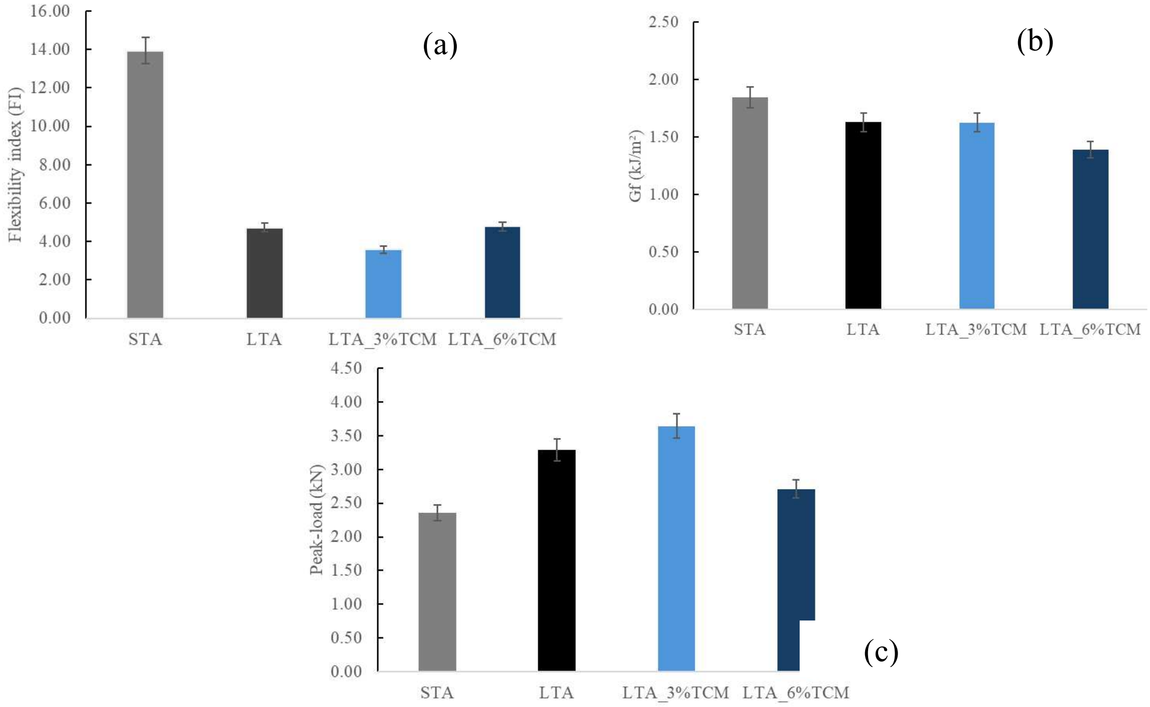

Source: Ribas et al. (2025c).

3.5 Conclusions

This study evaluated the effects of TCM spray functionalization on the performance of RAP-recycled asphalt mixtures subjected to long-term thermal oxidation aging. The investigation focused on the efficiency of TCM coatings concerning surface characteristics, specifically macrotexture and microtexture, bond strength adhesion, and fracture performance of HMA. Followings are the major conclusions from this research:

- The thermal differential test results confirmed that the activation temperature of the TCM coating occurs at approximately 30 °C. The significant positive variation in the color coordinate b* ensures a noticeable change in the coating's surface color to a lighter shade. Notably, the 3% TCM coating exhibited a higher color difference (ΔE*) before and after the color change. These results suggest the potential of TCM coatings to reduce heat absorption, thereby contributing to the mitigation of UHI effects.

- Regarding surface characteristics, spray functionalization of specimens slightly smoothed the macrotexture by an average of 21-25%, particularly evident with the 6% TCM coating. The impact on microtexture surface characteristics indicates that the functionalization does not significantly alter the microtexture of the pavement surface.
- Pull-off test results for HMAs functionalized with TCM spray coating exhibited only cohesive failure, and bond strengths remained the same after aging. This indicates strong adhesion between the TCM coating and the HMA, even under severe aging conditions, suggesting the durability of the coating in long-term applications.
- The mid temperature cracking test results showed that 6% TCM coating improved the cracking resistance of LTA specimens by reducing the peak load, pre- and post-peak slope in the load-displacement graph, indicating its potential impact on reducing mixture stiffness due to aging. The effect on post-peak behavior was minimal, resulting in similar (slightly lower) FI as the non-treated specimen. These findings imply that higher contents of TCM might improve the cracking resistance of asphalt mixtures after LTA conditioning.

The implications of these findings are significant for the development of sustainable pavement materials. The ability of TCM coatings to reduce surface temperatures can contribute to mitigating UHI effects, enhancing urban thermal comfort, and potentially extending pavement lifespan by reducing thermal-induced distresses. The maintained adhesion and slight improvements in fracture resistance suggest that TCM coatings can be integrated into existing pavement systems without compromising structural integrity.

Future research should further explore the long-term aging performance of TCM coated HMAs. It is important to highlight the necessity of incorporating additional factors such as ultraviolet radiation and moisture to more accurately simulate field aging. Adding an assessment of the surface temperatures of functionalized pavements is needed to verify the actual benefits in terms of reducing energy absorption and mitigating UHI effects. Field performance of TCM-functionalized pavements should assess their effectiveness in various climatic conditions, evaluate their durability over the service life of pavement, and examine their economic feasibility for large-scale implementation. Additionally, future research should examine the effect of functionalization on pavement friction values, including assessments after mechanical wear. It is strongly recommended to study the impact of aging protocols on the fracture properties of different asphalt mixtures, incorporating micro-structural simulations to provide comprehensive information on cracking resistance.

4 ASSESSMENT OF OPTICAL-THERMAL BALANCE AND ENVIRONMENTAL DEGRADATION OF A THERMOCHROMIC-COATED ASPHALT MIXTURE FOR URBAN HEAT MITIGATION

This is an Manuscript of an article published by Taylor & Francis Group in Road Materials and Pavement Design on 27th March 2025, available online: https://doi.org/10.1080/14680629.2025.2482846.

Abstract

Thermochromic coatings offer a promising solution to reduce pavement heat absorption and mitigate urban heat island (UHI) effects. While surface spray techniques enhance thermochromic performance by creating a reflective top layer, environmental exposure can significantly diminish their durability. This study evaluates the cooling performance and durability of an innovative thermochromic solution (TS) applied to hot mix asphalt (HMA) by analyzing its optical-thermal properties and resistance to environmental degradation. Outdoor experiments conducted over a 12-hour summer day demonstrated that the functionalized HMA achieved surface temperature reductions of 5–9°C during peak solar radiation periods compared to the control HMA. Accelerated weathering tests revealed a notable decrease in solar reflectance, with a reduction of 32% observed after 24 hours of exposure. Despite this loss, the TS continued to demonstrate cooling potential. The findings provide a scientific basis for the application of TS pavements, addressing urban climate change strategies and enhancing resilience.

4.1 Introduction

The urban environment is characterized by extensive artificial surfaces that absorb and store heat. Coupled with limited vegetation and intensive human activities, these conditions contribute to the formation and intensification of urban heat islands (UHI) (Xu *et al.*, 2021). UHIs result in elevated temperatures, greater thermal discomfort, lower air quality, and increased energy demands (Akbari; Menon; Rosenfeld, 2009; Xu *et al.*, 2021), leading to considerable social, economic, and environmental consequences.

Asphalt pavements are particularly sensitive to heat. Due to their dark color, they absorb a large amount of solar radiation on hot days, reaching temperatures above 60°C (Jiang *et al.*, 2019). Throughout the day and night cycles, asphalt pavements absorb solar heat during the day and release it gradually at night due to their capacity to store thermal energy. This ongoing process of heating and cooling significantly contributes to the formation of UHI, as the stored heat is released back into the atmosphere, elevating nighttime temperatures in urban areas and exacerbating local warming effects (Xu *et al.*, 2021).

Since paved areas cover an average of over 60% of urban surfaces (Tsoka; Tsikaloudaki; Theodosiou, 2018), using materials with different thermal properties has gained considerable interest as a strategy to mitigate urban heat (Akbari; Menon; Rosenfeld, 2009), such as the thermochromic solutions used in functionalization of asphalt materials (Rocha Segundo *et al.*, 2021; Xu *et al.*, 2021). Conventional asphalt pavements, with their black color and low albedo, absorb and store most of the incident solar radiation, increasing internal temperatures and contributing also to urban heating (Rocha Segundo *et al.*, 2021). Thermochromic pavements change color reversibly in response to external temperature variations, which enhances solar reflection and the material's thermal emissivity (Rossi; Simeoni; Quaranta, 2021). According to Zhou and Shepherd (Zhou; Shepherd, 2010), several studies on reflective pavements reported improvements in urban albedo from 0.15 to 0.50, with a reduction of maximum ambient temperature by 0.5°C. Consequently, thermochromic asphalt mixtures have emerged as a potential solution for mitigating UHI effects (Rocha Segundo *et al*., 2021; Zhang *et al*., 2022).

All materials emit thermal radiation as a function of their temperature and emissivity, with wavelengths longer than solar radiation. This long-wave radiation can either contribute to heating or cooling the pavement, depending on the temperature difference between the pavement surface and the atmosphere (Xu *et al.*, 2021). Materials with higher emissivity release more absorbed solar energy as long-wave radiation. Synnefa; Santamouris; Livada (2006) highlighted the importance of emissivity in the thermal balance of pavement surfaces, finding that when the emissivity value increases from 0.35 to 0.93, nighttime surface temperatures decrease by 5°C.

Thermochromic functionalization is a "cool pavement" strategy for asphalt pavements. Several studies have focused on controlling temperature variations and reducing the absorption of thermal energy by pavements to alleviate the effects of UHI (Jiang *et al.*, 2019; Qin; Hiller, 2014; Sha *et al.*, 2017). Additionally, these approaches can offer structural benefits, as reducing pavement temperatures can positively impact their durability (Du; Chen; Zhang, 2019; Li *et al*., 2018; Zhang *et al*., 2017, 2018).

To evaluate cooling efficiency in laboratory settings, experimental setups were developed to simulate the exposure of functionalized asphalt mixtures to sunlight. Studies have used tungsten filament lamps under controlled intensity and duration of exposure to evaluate thermochromic behavior during heating and cooling cycles, and found good correlation and accuracy with field measurements, with the advantage of greater control over variables (Li Q. *et al*., 2020b; Zhang *et al*., 2022).

Research in outdoor environments presents greater challenges due to the addition of variables such as wind, air, sunlight angle, air pollution, and urban configuration. Despite these challenges, some studies have shown promising results. Open-air studies conducted on hot summer days in Cleveland, OH, USA, revealed that thermochromic binders consistently achieved lower surface temperatures compared to conventional asphalt binders, with maximum reductions of 6.6°C, 2.7°C, and 4.9°C for black, blue, and red asphalt coatings, respectively (Hu; Gao; Yu, 2015; Hu; Yu, 2013). In another study, Hu; Yu (2020a) verified that thermochromic HMA pavements exhibited significant surface temperature reductions, ranging from 5-15°C cooler than conventional asphalt concrete (Hu; Yu, 2020a). Another promising result was a maximum surface temperature decrease of 4-7°C during the day (Chen, Z *et al.*, 2022). However, these studies primarily focus on surface temperature reduction without evaluating the overall thermal balance of the environment, which involves factors such as solar radiation, albedo, and emissivity. Albedo and emissivity are the key factors controlling pavement heat sources during the day and night, respectively (Pisello, 2017; Synnefa, Santamouris; Livada, 2006), and therefore must be carefully considered when assessing the optical-thermal energy balance.

One of the pavement functionalization techniques the application of thermochromic solution to the surface of compacted pavement, also refer as spray coating (Li *et al*., 2018; Zhang *et al*., 2022). This method is notable for its simplicity, effectiveness in reducing surface temperatures, and minimum impact on the mechanical performance of pavements (Rocha Segundo *et al*., 2019a). However, the effectiveness of thermochromic materials is questionable, and might be reduced due to exposure to the climate and traffic-related wear (Carneiro *et al*., 2013; Rocha Segundo *et al*., 2019b; Yi *et al*., 2022). Ensuring proper immobilization of the solution to the substrate remains a challenge (Carneiro *et al.*, 2013; Lima *et al.*, 2023). Some studies have developed epoxy resin-based solutions to improve the immobilization of thermochromic capsules on HMA samples, maintaining thermochromic capacity even after weathering tests (Li *et al*., 2018b; Rocha Segundo *et al*., 2019a). However, despite its strong adhesion, epoxy resin tends to reduce the pavement surface's roughness and is harmful to the environment. In this regard, water-based thermochromic solutions have been investigated for being more environmentally friendly (Zhang *et al*., 2022).

Therefore, it is essential to study the resistance of thermochromic pavements to environmental degradation caused by sun exposure and traffic, as well as their ability to remain immobilized on the substrate. Evaluating the thermochromic durability of pavements over their lifetime is a critical challenge for incorporating these asphalt mixtures as an active technology for mitigating UHI effects (Lima *et al.*, 2023).

4.2 Research Objective and Scope

This research aims to address critical gaps in the understanding of thermochromic solution (TS) efficiency. To that aim, two goals are established:

Goal 1: Evaluate TS cooling effects and field performance through the application of optical-thermal balance, grounded in established heat transfer pavement surface theory.

Goal 2: Assesses the durability of TS by analyzing their resistance to accelerated environmental degradation, providing valuable insights into their long-term performance.

To meet the objectives, laboratory and outdoors tests were performed. Figure 28 shows the overall experimental plan, including materials, selected tests, and main outputs.

Figure 28 – Experimental testing program.

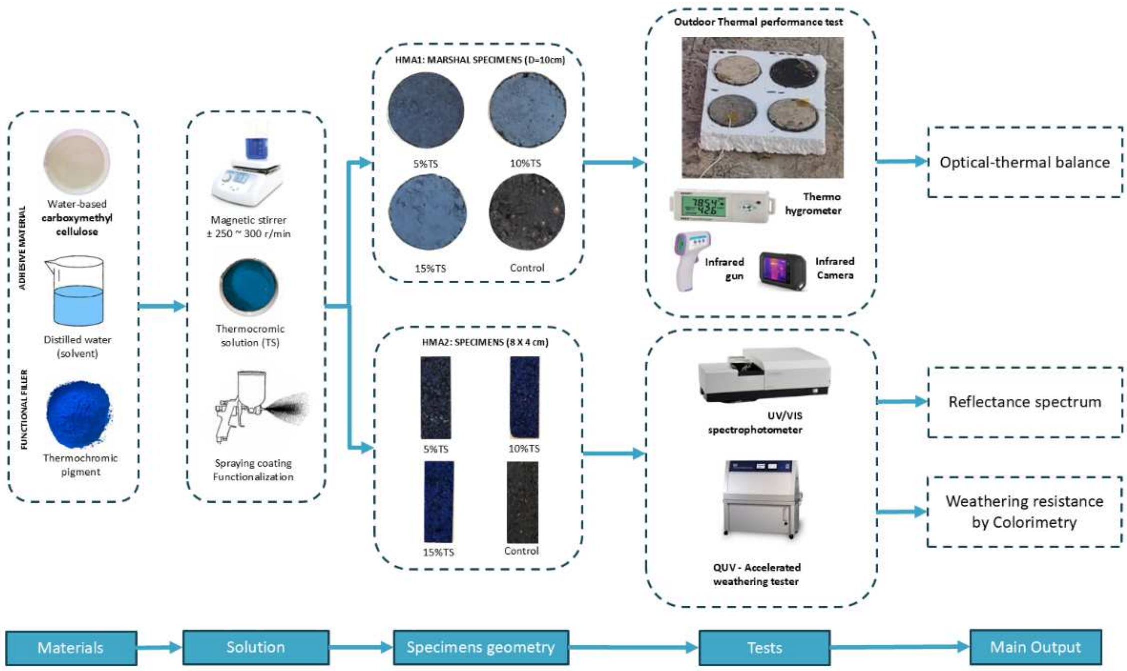

Source: Ribas et al. (2025a).

4.3 Materials and Methods

4.3.1 Thermochromic Material Characterization and TC treated HMA Preparation

The thermochromic material (TCM) selected for this study is an organic thermochromic microcapsule powder with a color transition temperature (TT) of 31°C (LCR Hallcrest, Thermochromic ChromaZone, USA). This TCM exhibits high sensitivity to temperature, with complete color transformation occurring within a few seconds upon reaching the TT. The reversible color change process involves a shift from blue to colorless (light grey), as illustrated in Figure 29a. Optical analysis shows that the TCM pigment is highly reflective, particularly after exceeding TT, in the visible range of the solar spectrum (Figure 29b). In the near-infrared (NIR) region, the solar reflectance values of the TCM particles range from approximately 60% to 80%, suggesting their potential use in heat-reflective applications (Hu; Yu, 2020a).

Initially, the physical and chemical properties of the selected thermochromic material (TCM) powder were characterized using scanning electron microscopy (SEM), Fourier-transform infrared spectroscopy (FTIR). These assessments were crucial to determine the microstructural features and chemical composition of the TCM powder.

The TCM powder is composed of spherical microcapsules with particle sizes primarily ranging from 1 to 3 µm (Figure 30a). The Fourier transform infrared (FTIR) spectrum (Figure 30b) reveals absorption bands at 3,365 cm^{-1} and 1,511 cm^{-1}, corresponding to hydroxyl (-OH) and benzene ring vibrations, respectively, likely derived from bisphenol A, a color developer commonly used in TCM pigments (Zhang *et al*., 2017).

Three concentrations of TCM were used to prepare the water-based TS solutions: 5%, 10%, and 15% (w/v). The concentrations were recommended by suppliers and previously indicated in the literature for optical, mechanical, and surface performances (Panák *et al*., 2018; Zhang *et al*., 2022). Thus, TCM powder was mixed into a 3% solution of carboxymethyl cellulose (Mw 250,000, ThermoScientific) to obtain the thermochromic solutions (TS) (Panák *et al*., 2018). The formulated TS was applied to the surface of compacted HMA specimens by spraying at a rate of 0.8 kg/m² (Yi *et al.*, 2022). After coating, the specimens were cured at room temperature (25°C) for 24 hours before undergoing subsequent tests.

Figure 29 – (a) Color change of TCM pigments; (b) Spectral reflectance of TCM powder before and after TT.

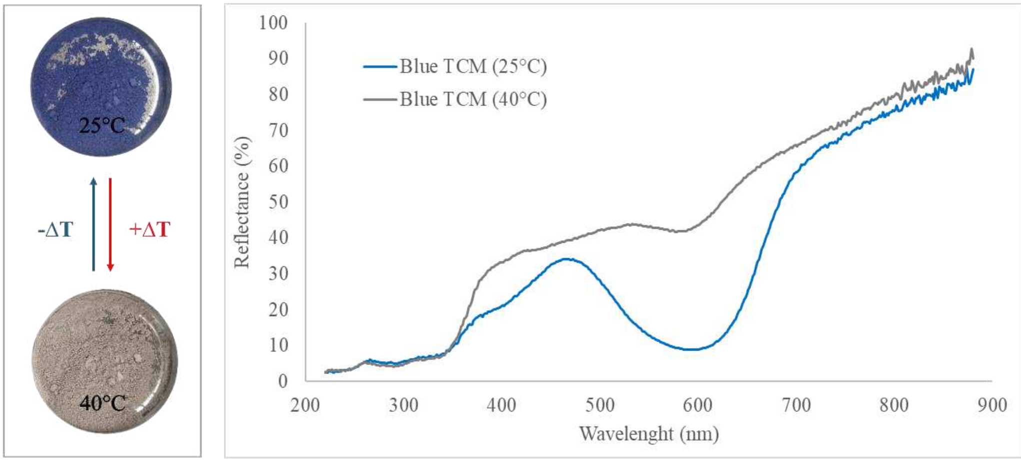

a) b)

Source: Ribas et al. (2025a).

Figure 30 – (a) Scanning Electron Microscope (SEM) of TCM pigment (magnification factor: 2,086); (b) FTIR spectrum of TCM powder.

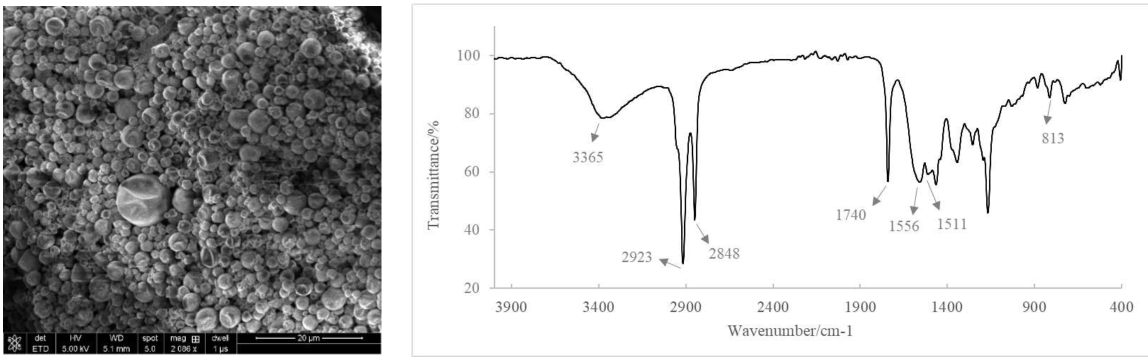

a) b)

Source: Ribas et al. (2025a).

To evaluate the effectiveness of the TS and its influence on the optical-thermal balance, an outdoor experiment was conducted. Three functionalized HMA specimens, along with an untreated control sample, were exposed to natural environmental conditions. For that, two types of asphalt mixtures were coated with TS in this study, with three replicates for each TCM concentration and a control (uncoated) HMA sample for each mixture. The first asphalt mixture (HMA1) was prepared using the Marshall asphalt mixture design method, with an optimal binder content of 4.5% and granitic coarse aggregates, fine aggregates, and mineral filler. The second asphalt mixture (HMA2) was designed using the Superpave volumetric mixture design method, with a PG 58V-34 binder content of 5.3% and limestone coarse aggregates, fine aggregates, and mineral filler, and 25% RAP. The samples were labeled as HMAn-X%TS, where "n" refers to the mixture type (1 or 2), and "X" indicates the percentage of TCM in the TS. The uncoated control specimens were labeled as HMA-control. For example, HMA1-5%TS refers to specimens of mixture type 1 functionalized with a thermochromic solution containing 5% TCM.

4.3.2 Simulation of environmental degradation

Environmental degradation was simulated using the Quick Ultraviolet Accelerated Weathering Test (Q-LAB, Model QUV/spray) to reproduce the damage caused by sunlight, rain, and dew. The test cycles applied to this study followed the ASTM G154-23 to simulate UV exposure and moisture. Each cycle consists of 8h UV at 60°C + 4h condensation at 50°C. The fluorescent lamps type UVA-340 were set to 0.89 W/(m².nm) irradiance and present the spectral power distribution as shown in Figure 31. HMA2 specimens were exposed to QUV cycles for 48h.

Figure 31 – Spectral power distribution of UVA-340 lamp and sunlight.

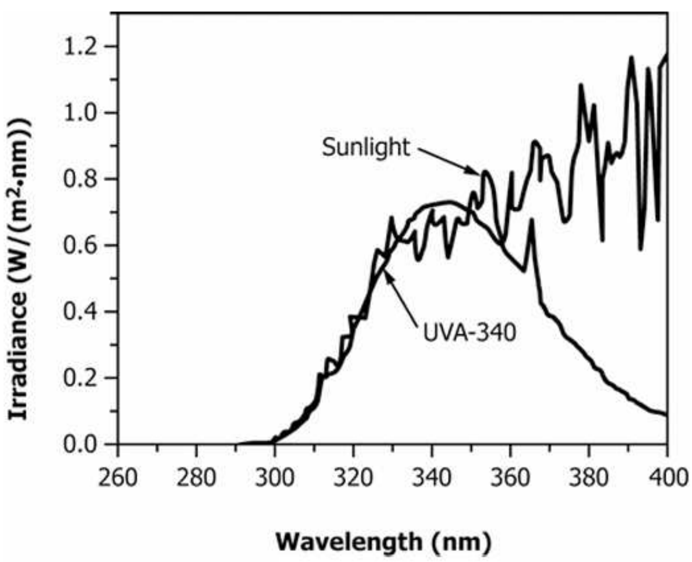

Source: Ribas et al. (2025a).

In order to investigate color changes of HMA2 specimens the colorimetry analysis was performed by measuring the color coordinates of the specimens at three key points: before the QUV test (0 hours) and after 24 and 48 hours of exposure. These measurements were taken using close-range photogrammetry, which provided precise color values at each stage of the testing period. To eliminate the influence of ambient light, the specimens were photographed inside a photobox with consistent camera settings that were not altered during the experiment.

The image processing procedure for quantitatively evaluating color changes was carried out using ImageJ® software. The color coordinates were measured in terms of L*, a*, and b*, as defined by the Commission Internationale de l'Éclairage (CIE). L* indicates the lightness, ranging from black (L* = 0) to white (L* = 100); a* represents the variation from red (positive values) to green (negative values); and b* captures the shift from yellow (positive values) to blue (negative values). Additionally, the ΔE* value was calculated as a perceptibility factor, quantifying the overall color difference without indicating the direction of the change according to Equation (4).

$$\Delta E^* = \sqrt{(\Delta L^*)^2 + (\Delta a^*)^2 + (\Delta b^*)^2} \quad (4)$$

The variation of each coordinate (L*, a*, and b*) was determined by comparing the initial and final color values of the functionalized HMA2 surfaces.

4.3.3 Reflectance spectrum test

To qualitatively evaluate the thermal responses of thermochromic functionalized HMA in the reflectance spectrum, a UV-VIS Shimadzu UV-2501PC spectrophotometer (operating in the 220–880 nm range) was used in accordance with ASTM E903 (ASTM International, 1996). Barium sulfate ($BaSO_4$) plates, with a total reflectance close to 100%, served as the reference, and the test wavelength interval was set to 5 nm. In this test, as illustrated in Figure 32a, the prepared HMA2 was cut into 8×4 cm rectangular samples to fit into the equipment and placed in the specimen position.

It is important to note that this analysis was limited to the UV-Vis range (220–850 nm) due to equipment availability, preventing the inclusion of the infrared (IR) spectrum, where a significant portion of thermal energy resides. While this limitation does not compromise the primary focus of this research step, which is related to optical changes, as the UV-Vis range captures most of the solar spectrum influencing the initial heating and activation behavior of the thermochromic asphalt surface, future studies should incorporate IR spectral analysis to provide a complete understanding of the solar spectrum.

To capture the reflectance spectrum in both the colored and colorless phases, the specimens were conditioned for 10 minutes at 25°C and 40°C before spectral testing. Reflectance measurements were conducted from repetition of three replicates specimens in test conditions. This conditioning allowed measurement of the reflectance variation due to the thermochromic effect, both below and above the TT. Furthermore, the specimens were analyzed after 24h and 48h of accelerated weathering conditions (explained in the section on *simulation of environmental degradation*). Reflectance measurements were obtained by testing three replicate specimens under these conditions. As shown in Figure 32b, the functionalized HMA were placed at the position of the specimen.

Figure 32 – (a) Thermochromic samples conditioning before colorimetry analysis; and (b) position of specimen in reflectance measurements.

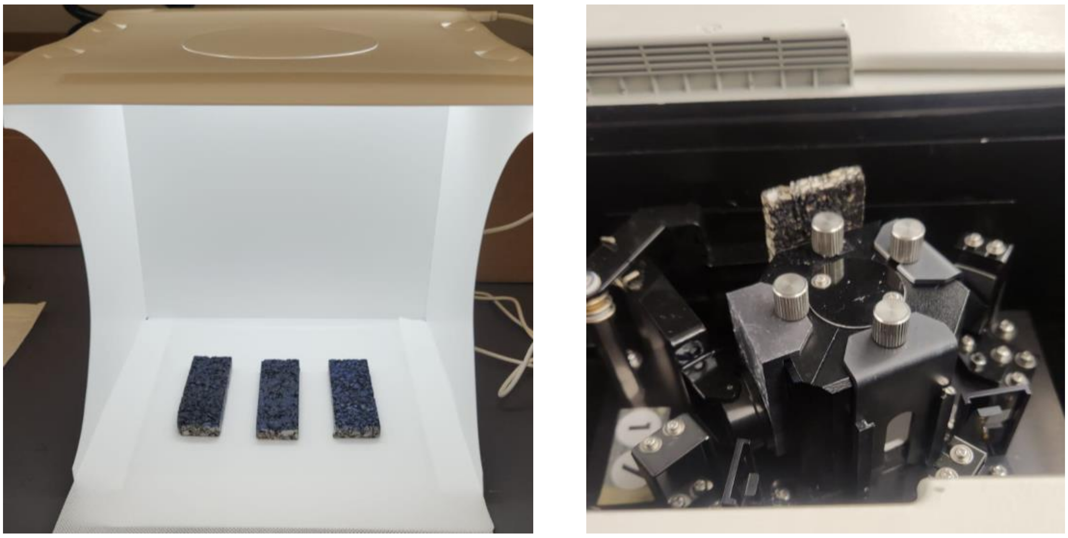

a) b)

Source: Ribas et al. (2025a).

In accordance with ASTM E490 (ASTM International, 2000), the total solar reflectance (R) of each specimen was calculated from the measured reflectance spectrum using the weighted-averaging method, based on the standard spectral irradiance distribution (E_λ) and the weighting function ($\Delta\lambda$), as in Equation 5:

$$R(\%) = \frac{\left(\sum_{i=1}^{n} R(\lambda_i) E_{\lambda i} \cdot \Delta\lambda_i\right)}{\sum_{i=1}^{n} E_{\lambda i} \cdot \Delta\lambda_i} \quad (5)$$

4.3.4 Outdoor solar radiation test

4.3.4.1 Optical-thermal balance on pavement surfaces theory

The modes of optical and thermal balance of the pavement surface are usually determined by the amount of solar radiation absorbed, also referred to as net radiation (Xu *et al.*, 2021). Net radiation, R_n, is defined as the arithmetic difference between the radiation received by the pavement and the outgoing terrestrial radiation, as expressed in Equation 6:

$$R_n = R_i - R_r + R_a - R_s \tag{6}$$

where R_n is the net radiation received by the pavement (W/m²), R_i is the incident radiation from solar energy (W/m²), R_r is the reflected radiation from the pavement (W/m²), R_a is the atmospheric radiation (W/m²), influenced by urban geometry and local atmospheric conditions, and R_s is the surface radiation emitted by the pavement. This equation governs the calculation of solar energy absorbed by pavement structures, which is crucial for evaluating the UHI effect and proposing UHI mitigation strategies.

The reflected R_r from the pavement is calculated using Equation (7):

$$R_r = \alpha \cdot R_i \tag{7}$$

where α is the surface albedo of the pavement surface. Albedo is defined as the fraction of incident light reflected by a surface and is used to characterize the reflectivity of a material's surface. It accounts for the hemispherical reflectance of solar radiation across the solar spectrum, including both diffuse and reflected components.

In pavement structures, solar radiation, primarily in the form of short-wave radiation, is the main heat source in the surface energy balance. The net short-wave radiation, R_{ns}, is expressed as:

$$R_{ns} = R_i - R_r = (1 - \alpha) \cdot R_i \tag{8}$$

where R_{ns} is the net short-wave radiation.

Materials continuously emit thermal radiation as a function of their temperature and emissivity, with wavelengths longer than solar radiation. This long-wave radiation can either add to or subtract from the heat in the pavement's energy balance, depending on the temperature difference between the atmosphere and the pavement surface. The net long-wave radiation, R_{nl}, including both atmospheric and surface radiation, was calculated using the Stefan-Boltzmann law:

$$R_{nl} = R_a - R_s = \epsilon \cdot \sigma \cdot (T_{sky}^4 - T_s^4) \quad (9)$$

where R_{nl} is the net long-wave radiation, ϵ is the emissivity of the pavement surface, σ is the Stefan-Boltzmann constant (5.67×10^{-8} W/m^{2}K^4), T_{sky} is the atmospheric temperature, and T_s is the pavement surface temperature, both in Kelvin.

By implementing Equations (7) and (8) into Equation (6), we obtain Equation (10), which represents the total heat exchange at the pavement surface:

$$R_n = R_{ns} + R_{nl} = (1 - \alpha) \cdot R_i + \epsilon \cdot \sigma \cdot (T_{sky}^4 - T_s^4) \quad (10)$$

In this study, the optical-thermal balance was assessed through the calculation of R_n. Figure 33 shows the schematic representation of thermochromic pavement and thermal-optical energy paraments in an outdoors environment.

Figure 33 – Schematic optical-thermal balance on the thermochromic pavement surface.

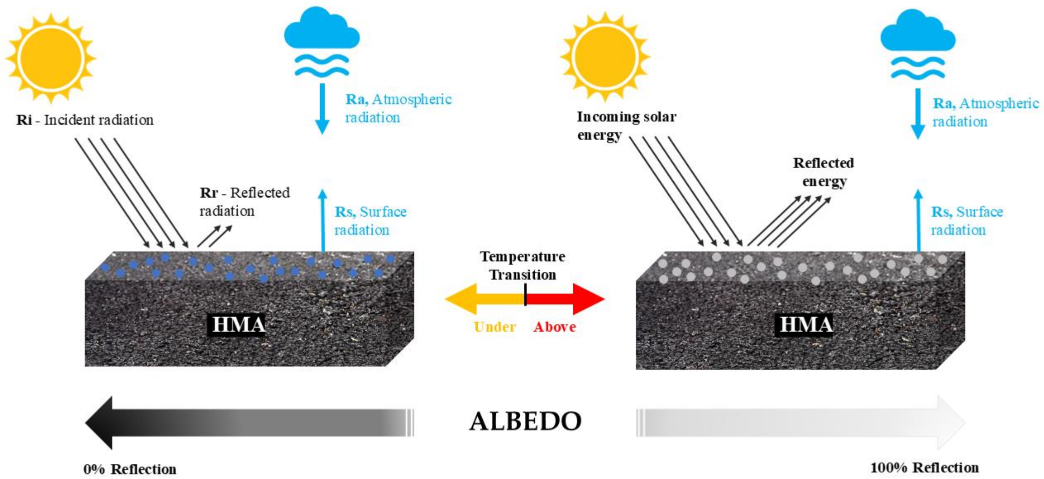

Source: Ribas et al. (2024).

When the pavement surface temperature is higher than the ambient air temperature, the absorbed solar radiation is, subsequently, released as a convective heat flux, which occurs at longer wavelengths. Sensible convective heat can be calculated based on Newton's cooling law, as shown in Eq. (11), which depends on the temperature difference between the pavement surface and the ambient air, as well as wind speed (Santamouris, 2013):

$$H_s = A \times h \times (T_s - T_{1.5m}) \tag{11}$$

where, A is the surface area (m²), h is the sensible heat transfer coefficient ($W/m^2 \cdot KW/m^2 \cdot K$), Ts is the temperature of the pavement surface, and $T_{1.5m}$ is the temperature of the ambient air at 1.5 m above the pavement surface.

The sensible heat transfer coefficient (h) is primarily determined by wind speed, and its calculation has been extensively studied through mathematical models by various researchers (Xu *et al.*, 2021a). However, in the present study, the contribution of convective heat transfer to the optical-thermal balance was not explicitly calculated. This decision was based on the relatively small surface area of the functionalized specimens used in the experiments (cylindric samples with a diameter of 10 cm). Given the limited surface area, the convective heat flux was considered negligible compared to the dominant radiative heat transfer mechanisms. For future studies involving larger pavements' surfaces or real-world applications, the inclusion of convective heat transfer will be essential to provide a more comprehensive understanding of the thermal balance and its implications for mitigating the UHI effects.

4.3.4.2 Thermal performance evaluation

To evaluate thermal performance, four HMA1 specimens were exposed to natural environmental conditions for 12 hours on a typical hot summer day in Fortaleza, Ceará, Brazil. Over this period, surface temperatures, incident and reflected radiations of each sample were measured every 30 minutes, while meteorological data was continuously recorded. In this test, specimens with a diameter of 100 mm and thickness of 25 mm were tested. Once this study focused exclusively on the surface effects of thermochromic coatings and based on the thermal-optical balance equations, the interior thermal analyses were not performed and, therefore, the sample mass does not significantly impact the heat transfer experiment. Functionalized specimens and an untreated HMA were completely thermally insulated to avoid the interferences from the environment, i.e., heat flowing from the surrounding and bottom, except by the exposed top surface. Surface temperatures of the studied HMA specimens were recorded using thermocouple type K sensors; the incident radiation (R_i) and reflected (R_r) radiation were measured in situ using a portable solar radiometer, following ASTM C1549-2016; while the meteorological data was obtained by a thermohygrometer HOBO® MX1101.

4.4 Results and Discussions

4.4.1 Environmental Degradation and Color coordinates on HMA2

The color coordinate values, L*, a*, and b*, were measured at three-time intervals: before the test start (t=0 h) and after 24 and 48 hours (t=24h and t=48h, respectively) of exposure in the QUV Test. The variations in E* (refer to Equation (4)), along with the values of L*, a*, and b*, were calculated for these specific time points during the QUV test and compared with the stated point. The average results of three replicate measurements are presented in Table 7.

Table 7 – Results of colorimetry test.

Coordinates	**t=24h**			**t=48h**		
	5%TS	10%TS	15%TS	5%TS	10%TS	15%TS
ΔL*	3.87	6.28	4.76	1.90	5.96	3.72
Δa*	-1.58	-1.88	-1.47	-0.87	-1.48	-0.85
Δb*	0.80	1.11	0.90	4.96	5.59	4.06
ΔE*	4.26	6.65	5.06	5.38	8.30	5.58

Source: Ribas et al. (2025a).

Based on the results, there are noticeable changes in the color coordinates after the weathering process. The variation in L* indicates a general lightness or darkness change. Thus, high positive variations in the ΔL* parameter are desirable for the purpose of this functionalization, in order to modify the color of the HMA2 surface to lighter colors. As expected, ΔL* showed a greater decrease (10-37%) after 48 hours compared to 24 hours. This is particularly evident in the 5%TS, where ΔL* decreases from 3.87 at 24 hours to 1.90 at 48 hours, suggesting that the sample is darkening over time. It could be related to the fact that this percentage has minimum amount of TCM and because of that the HMA is not very well covered, showing the darkest surface and being quickly impacted by ultraviolet exposure. The 10%TS specimen showed better ΔL* performance, with a higher difference of initial condition and less than 5% of reduction between 24 and 48h of weathering, indicating better functionalization resistance.

Bearing in mind that the TCM used in this study is blue, the analyses of b* coordinate are especially interesting. It indicates the yellow-blue axis, and, thus, the smaller Δb* corresponds to a minor variance of blue color among the specimens after weathering exposition. The results show a significant increase after 48 hours for all samples, especially for the 5% and 10% TS, where Δb* are 6 and 5 times higher, respectively. This suggests a notable shift toward the yellow end of the spectrum as the exposure time increases. Such behavior is consistent with the yellowing effect caused by UV degradation, a phenomenon well-documented in literature related to polymer-based coatings exposed to weathering (Gupta; Kumar; Sachdeva, 2024; Kuyyakanont; Iwata, 2024).

Finally, the overall color difference, ΔE*, increases with time, indicating a cumulative effect of UV exposure on the samples. Notably, the 10% TS shows the highest ΔE* values at both time intervals, rising from 6.65 at 24 hours to 8.30 at 48 hours, indicating the most pronounced change in overall color. This could be related to this specific concentration of the TS presenting better specimen cover, without TCM agglomeration, which probably makes it more susceptible to accelerated environmental degradation.

These findings suggest that increased exposure time intensifies color changes, in this study particularly in lightness (HMA substrate color) and the yellow-blue spectrum (blue TCM), which could be indicative of degradation processes such as photo-oxidation and polymer breakdown under UV radiation (Gupta; Kumar; Sachdeva, 2024; Kuyyakanont; Iwata, 2024).

4.4.2 Optical characterization results

The reflectance spectrum of functionalized HMA over the wavelength range of 220–850 nm is shown in Figure 34. It is possible to observe a significant influence of the TS layer on the solar reflectance of HMA mixtures, especially in the visible (VIS) range and above the TT due to the thermochromic effect. The functionalized HMA exhibits noticeably higher spectral reflectance compared to the control HMA under initial conditions (t=0h), indicating improved optical properties (Figures 34a and 34b). As noted in Table 8, the functionalized HMA shows a total reflectance (R%) value ranging from 5.5% to 7.5%, whereas the control HMA has a lower range of 3.5% to 4.4%. Among the tested samples, the HMA2-5%TS exhibits a marked increase in solar reflectance, with an improvement of 112% above the TT.

Figures 34c and 34d display the reflection spectra of functionalized HMA after 24 hours and Figures 34e and 34f after 48 hours of exposure to the QUV test. The data clearly show that, after weathering exposure, the solar reflectance of functionalized HMA decreases compared to its pre-UV exposure state. Specifically, the total R(%) value above TT drops by 32%, 11%, and 15% for HMA with 5%TS, 10%TS, and 15%TS, respectively, after 24 hours of QUV testing (Table 8). These results align with the colorimetry results, which also suggest that the HMA2-5%TS is more vulnerable to UV degradation.

Figure 34 – The reflection spectra of HMA_2 specimens after the QUV test at room temperature (a (t=0h), c (t=24h), and e (t=48h)) and above transition temperature (b (t=0h), d (t=24h), and f (t=48h)).

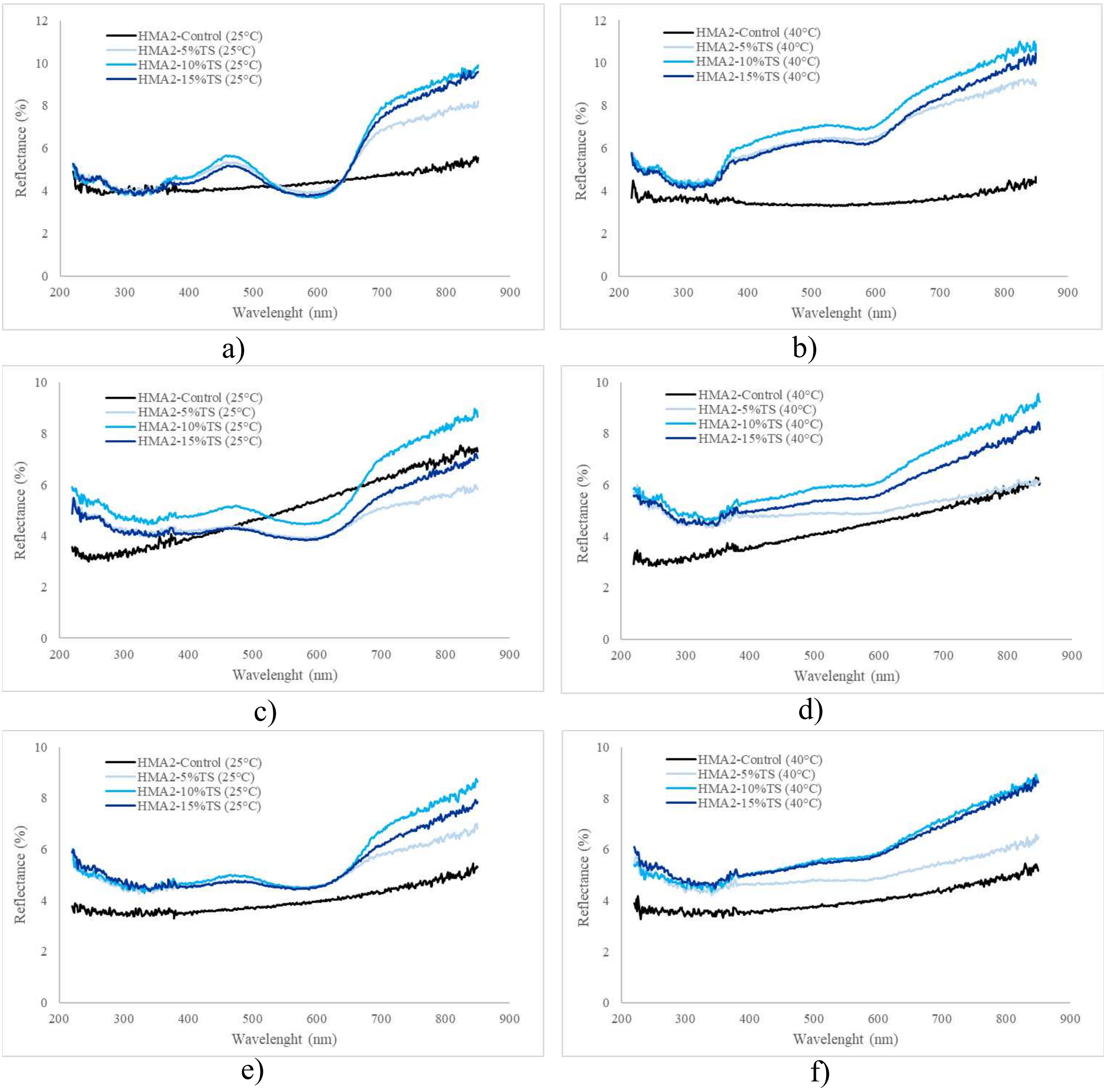

Source: Ribas et al. (2025a).

After 48 hours of UV exposure, the total R(%) value above TT shows only a slight reduction compared to the 24-hour mark, with decreases ranging from 1% to 5%. Notably, HMA2-10%TS demonstrates the best performance in terms of solar reflectance regarding the

UV-Vis range in overall tests. The spraying coating themochromic functionalization of HMA_2 specimens contribute to decrease absorption of VIS solar radiation and eventually leads to reduce the surface temperature of the pavement during the summer. This reduction in heat absorption presents a promising approach to mitigating UHI effects.

Table 8 – Total solar reflectance (%) of thermochromic HMA2 before and after QUV test.

Specimen	**Room Temperature (25°C)**			**Above TT (40°C)**		
	t=0	t=24h	t=48h	t=0	t=24h	t=48h
HMA_2-Control	4.4	5.2	4.0	3.5	4.4	4.0
HMA_2-5%TS	5.5	4.5	5.1	7.5	5.1	5.0
HMA_2-10%TS	5.6	5.6	5.5	7.3	6.4	6.1
HMA_2-15%TS	5.6	4.7	5.2	6.9	5.9	6.0

Source: Ribas et al. (2025a).

4.4.3 Thermal performance of thermochromic HMA1 in indoor solar radiation test

The results of the outdoor solar radiation test are shown in Figure 35a. The test was run from 5 a.m. to 7 p.m., aligning with the solar activity in Fortaleza, Ceará, Brazil. The surface temperature monitoring curve of the specimens closely mirrors the trend of air temperature throughout the day, exhibiting a bell-shaped curve with a peak temperature occurring around noon (12:00 p.m.).

Figure 35 – The outdoor solar radiation test results: (a) the surface temperature and (b) the surface temperature differences between functionalized specimens and control specimen.

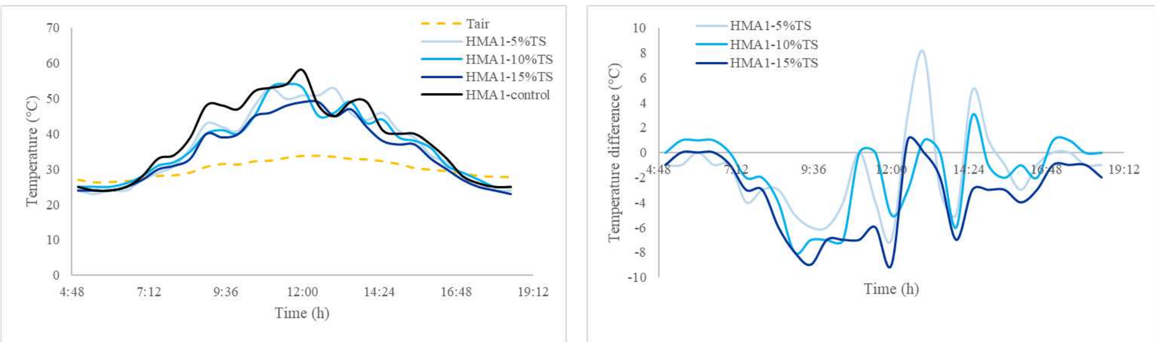

a) b)

Source: Ribas et al. (2025a).

The control HMA_1 reached a maximum temperature of approximately 58°C, while the functionalized HMAs exhibited lower peak temperatures: 51°C for HMA_1-5%TS, 53°C for

HMA_1-10%TS, and 49°C for HMA_1-15%TS. Figure 35b illustrates this temperature difference more clearly, showing that the functionalized HMA consistently maintained lower surface temperatures than the control HMA throughout the test period, particularly during the time of highest solar radiation, from 9:00 a.m. to 12:00 p.m. During this period, the maximum surface temperature of the functionalized HMA was reduced by 5-9°C compared to the control HMA. In Figure 36, the temperature differences of the samples can be observed through thermal photographs taken at different times of the day. It is highlighted that, during all periods of direct sunlight, the images indicate higher temperatures for the HMA-control and lower temperatures for the HMA-15%TS. These results of outdoor solar radiation test results confirm the reflectance improvement of the TS layers can indeed render the cooling effect to asphalt pavement in hot summer.

Figure 36 – Thermal photograph of HMA specimens at (a) 7 a.m.; (b) 12 p.m.; (c) 4 p.m.; and (d) 6 p.m.

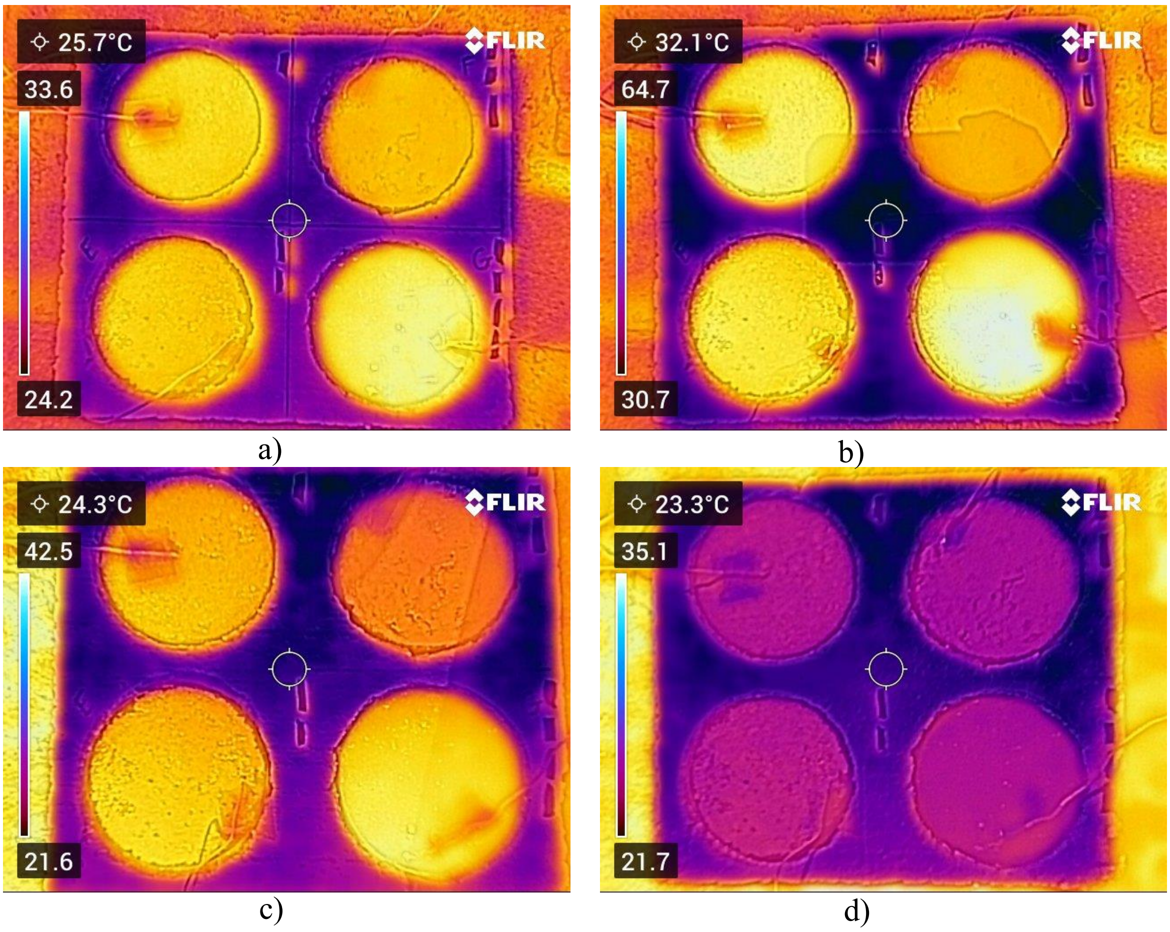

Source: Ribas et al. (2025a).

Additionally, to assess the optical and thermal balance of the pavement surface based on the adapted heat transfer theory for asphalt pavements, the net radiation (R_n) was calculated using Equation 8, as depicted in Figure 37a. According to the findings presented in the "Optical Characterization Results" section and supported by other studies (Hu; Gao; Yu, 2015; Hu; Yu, 2016a), it is evident that the thermochromic solution primarily affects the solar albedo of the asphalt specimens through its optical modification properties, without significantly impacting other thermophysical parameters. Consequently, only two factors, albedo and surface temperature, played a role in determining the net radiation (R_n) values. The emissivity was considered as constant value of 0.81 (Chen *et al.*, 2024).

Figure 37a shows the evolution of R_n over time, peaking in the early afternoon around 12 to 13 hours, a period right after the maximum incoming solar radiation. The order of the curves, which HMA1-control is above all the ones from functionalized HMA, reveals variations in their ability to absorb and emit radiation is a direct indicator of their thermal performance. As expected, the control specimen absorbs more solar radiation and reflects less heat back into the environment, leading to higher surface temperatures during the whole test period. At the time of maximum solar exposure, the R_n reaches approximately 700 W/m² for HMA_1-control and dropped by 5% for HMA_1-5%TS and around 10% for 10%TS and 15%TS specimens. These findings imply that increasing the concentration of TCM improves the material's ability to manage thermal radiation. However, the performance improvement between 10%TS and 15%TS appears to be marginal, suggesting a saturation point where additional TCM pigments may not yield substantial benefits.

Figure 37b shows the accumulated R_n, which represents the total energy absorbed throughout the day, which gives an overall picture of the heat management capability of each coating. The addition of TS in the HMA1 specimens reduces the accumulated net radiation compared to the control specimen, without treatment ranging from 8% for 5%TS to 18% for 15%TS. Lower values indicate that the surface is better at managing solar heat, either by reflecting it or re-radiating it, leading to cooler thermal profile, contributing to more energy-efficient environments. The results highlight the effectiveness of the TS in improving the overall energy balance of asphalt pavements, a critical factor in mitigating heat buildup, particularly in urban environments.

Figure 37 – The outdoor solar radiation test results: a) the net radiation between functionalized specimens and control specimen and b) the total amount of net radiation during the time test.

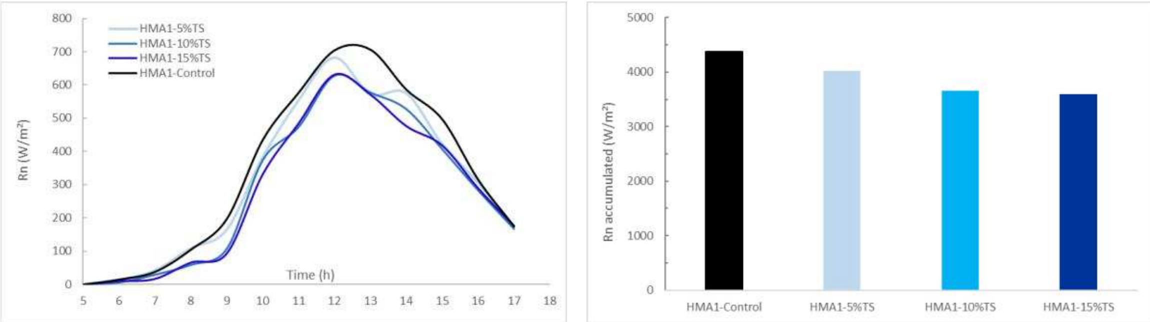

(a) (b)

Source: Ribas et al. (2025a).

4.5 Conclusions

This study investigated the impact of the thermochromic solution content on the optical performance of HMA specimens under accelerated environmental degradation and thermal performance in outdoor solar radiation conditions. The results demonstrated that the spraying coating thermochromic functionalization of asphalt mixtures has significant potential to improve optical-thermal energy balance, especially above the transition temperature (TT), due to the thermochromic effect. The major findings of this research are summarized as follows:

- The thermochromic solutions improved the total solar reflectance in UV-VIS range of functionalized HMA by 112% compared to the control HMA in initial conditions (t=0h) for HMA2-5%TS.
- After exposure to the accelerated weathering, the functionalized HMA showed a reduction in solar reflectance, with a notable decrease of 32% after 24 hours. However, the reduction in reflectance slowed after 48 hours, indicating some resilience to prolonged UV exposure.
- The outdoor solar radiation test confirmed that functionalized HMA maintained lower surface temperatures than the control HMA throughout the day, with temperature reductions of 5–9°C during peak solar radiation periods.
- The optical and thermal balance analysis, based on net radiation calculations, highlighted that the improved solar albedo was the primary factor responsible for the cooling effect.

Overall, the study confirms that the thermochromic functionalization of asphalt is a potential strategy to mitigate heat absorption and reduce surface temperatures, which can help address UHI effects and improve pavement durability. The findings suggest that integrating thermochromic materials into asphalt surfaces offers a promising solution for enhancing thermal performance of pavements, particularly in hot climates.

This study provides valuable insights into the optical-thermal performance of thermochromic-functionalized asphalt, but further exploration is needed to enhance its applicability. Future research should focus on analyzing the full solar reflectance spectrum, including infrared, to better understand thermal energy exchange and cooling performance. Studies on thicker specimens and heat transfer through deeper pavement layers are also essential for evaluating overall performance. Real-scale specimen testing and dynamic thermal cycling simulations using advanced modeling can improve prediction accuracy. Additionally, long-term durability studies under real-world traffic and environmental conditions are crucial to assess wear, weathering, and aging. These efforts will help optimize thermochromic materials for sustainable pavement applications, aiding in urban heat island mitigation and improving pavement performance.

5 EVALUATING THE MICROCLIMATIC AND THERMAL COMFORT IMPACT OF HIGH-REFLECTIVE PAVEMENTS ACROSS DIFFERENT URBAN CANYON SETTINGS IN A TROPICAL CITY

Abstract

Urban heat islands (UHIs) present significant challenges in tropical cities, where elevated temperatures intensify thermal discomfort and environmental stress. These effects are further influenced by urban form, which plays a key role in shaping local microclimatic conditions. This study aims to investigate the microclimatic impacts, including thermal comfort, of different urban canyon configurations (vertical and horizontal) in a tropical city, and to assess how urban morphology influences the performance of reflective pavements (RP) as a UHI mitigation strategy. Critical thermal hotspots were first identified using the local climate zone (LCZ) classification to characterize spatial thermal variability. Two contrasting LCZs, representative of predominantly vertical and horizontal urban canyons, with distinct socioeconomic characteristics, construction materials, and geometries, were simulated under baseline and reflective pavement scenarios using high-resolution ENVI-met modeling, with thermal comfort assessed by universal thermal climate index (UTCI). Results showed that high albedo (α=0.5) pavements reduced surface temperatures by up to 9.6 °C and air temperatures by 1.7 °C during peak solar hours; however, it simultaneously increases mean radiant temperatures by approximately 13°C during peak solar exposure. The presence of vertical canyons promotes radiative trapping and multiple reflections, reducing the overall energetic efficiency of the RP strategy. These findings highlight the critical role of urban form in modulating microclimatic and comfort outcomes and provide actionable insights for context-sensitive UHI mitigation in tropical climates.

5.1 Introduction

Climates in urban areas differ significantly from non-urban areas due to the unique characteristics of the built environment. Urban structure, land use types, human activity, and topography play decisive roles in shaping microclimatic patterns by altering the balance between heat absorption and reflection (Oke *et al.*, 2017). These interactions result in distinct microclimatic subsystems, which can be identified by variations in temperature, humidity, mean total radiation, and other meteorological parameters (Grimmond, 2007, Stewart; Oke, 2012). A key consequence is the intensification of the urban heat island (UHI) effect, which contributes to elevated air temperatures, directly impacting public health, energy demand, and environmental degradation (Xu *et al.*, 2021).

One prominent framework for analyzing urban climate variability is the local climate zones (LCZs) classification system, which standardizes urban morphology and land cover based on surface structure, permeability, material properties, and anthropogenic activity (Stewart; Oke, 2012). LCZs have been successfully applied in various studies to investigate the relationship between urban form and thermal behavior, such as estimating air temperature variation (Rahmani; Sharifi, 2023), mapping UHIs (Wang *et al*., 2018, Dimitrov; Popov; Iliev, 2021), and correlating urban morphology with thermal conditions (Kotharkar; Bagade; Singh, 2020, Du *et al*., 2024). Du *et al*. (2024) used LCZ maps in Hong Kong to reveal how urban structure parameters, such as sky view factor (SVF) and surface albedo, significantly influence UHI intensity, particularly in high-rise commercial areas, where heat trapping and anthropogenic emissions are intensified. Interestingly, they also identified urban cool islands in industrial and open urban areas due to the low SVF and the massive volume of urban structures, which reduced solar heat gain and increased heat capacity. Kotharkar; Bagade; Singh (2020) advanced this framework by combining LCZ classification with microclimate simulations to identify critical UHI zones and evaluate mitigation strategies such as reflective pavements and urban greening. Their findings highlighted the importance of tailoring interventions to specific LCZ types, for example, cool pavements were most effective in dense, unplanned settlements, while greening yielded better results in low-density zones. These studies reinforce the local significance of spatial context when designing heat mitigation strategies and demonstrate the utility of combining LCZ mapping with microscale simulation tools.

Tropical cities, in particular, are highly vulnerable to thermal discomfort due to their naturally high insolation associated with the dense urbanization, characterized by impervious surfaces, vegetation loss, and widespread use of heat-retaining materials such as asphalt and concrete (Gartland 2010). These materials absorb solar radiation and reemit it during afternoon and nighttime hours, exacerbating heat retention in the urban canyon. Moreover, pavements have been major contributors to daytime sensible heat flux and elevated surface temperatures, as they cover a large fraction of urban land area and store and re-radiate heat to the atmosphere. As the need for climate-sustainable infrastructure grows, the scientific community increasingly focuses on identifying effective mitigation strategies, especially those related to pavement technologies, such as highly reflective pavements, supported by advanced urban microclimate simulations (Santamouris *et al*., 2012, Wang; Berardi; Akbari, 2016, Sen *et al*., 2019, Zhang *et al*., 2022, Du *et al*., 2024).

Reflective pavements are a passive cooling solution and have emerged as a promising intervention for UHI mitigation due to their ability to increase surface albedo and reduce heat storage. Numerous studies using numerical simulations have demonstrated their effectiveness. Wang; Berardi; Akbari (2016) simulated a switch from asphalt concrete to Portland cement concrete, observing a midday surface temperature reduction of 7.9°C by increasing albedo from 0.2 to 0.4. Reductions in air temperature have also been documented, ranging from 0.2 to 0.4°C (Sen *et al*., 2019, Jia; Wang 2021) to as much as 1.5°C (Zeeshan; Ali, 2022, Zhang *et al*., 2022). Regarding surface temperature, albedo has a more pronounced impact on this variable, with reported reductions ranging from 6 to 12°C (Synnefa; Santamouris; Livada, 2006, Zhang *et al*., 2024, Ribas *et al*., 2025a).

While the efficacy of these materials in reducing surface and near-surface air temperatures is generally acknowledged (Ribas *et al.*, 2025a), a critical issue regarding the impact of the high reflectance on microclimate conditions and heat stress of the human body remains when considering the holistic performance of these surfaces (Elmagri; Kamel; Ozer, 2024). A few studies have employed thermal comfort indices, such as the universal thermal climate index (UTCI), in these assessments to quantify improvements in pedestrian experience (Jia; Wang, 2021), further supporting the relevance of detailed thermal modeling. UTCI is a tool that combines meteorological factors (air temperature, humidity, wind speed, and radiation) with a thermophysiological model to assess thermal comfort in different climates.

The main findings of Jia and Wang (2021) indicate that the UTCI values of RP heat mitigation strategy are only slightly lower (0.03°C) than the reference without a cool strategy in a humid subtropical climate of Hong Kong. However, results by Tavares et al. (2025), conducted in a business district under a tropical climate in Australia, found that, at 11 a.m., the addition of cool pavements had a negative effect on thermal comfort by leading to an overall increase in UTCI. It was due to the increase in reflected radiation from the cool pavement within street canyons, while in the existing scenario, the radiation was mainly absorbed by the asphalt during the daytime. Therefore, a strategy designed to cool the city should necessarily consider urban form parameters to not reduce human thermal comfort during the daytime. This effect necessitates a detailed, context-specific microclimatic evaluation, particularly across varied urban forms and climatic settings. This highlights the complexity of planning sustainable cooling strategies for urban spaces.

Simulation tools, like computational fluid dynamics (CFD) methods, have played a pivotal role in these investigations, as highlighted in a meta-analysis by Tsoka et al. (2018), which emphasized their growing relevance in urban climate modeling subject studies. However, despite this progress, most studies have been conducted in Northern Hemisphere cities with subtropical (Jia; Wang 2021, Zhang *et al*., 2022), semi-arid (Sen *et al*., 2019), temperate

(Taleghani *et al.*, 2019), or Mediterranean climates (Kyriakodis; Santamouris 2018, Pigliautile *et al*., 2020). These efforts indicate that microclimate simulations largely reflect local urban and climatic conditions. In this context, only a few recent studies have focused on tropical regions, such as Kowalski; Lopes; Masiero (2024) and Tavares; Abuseif; Dupré (2025). The authors' results indicated an overestimation of mean radiant temperature (MRT) attributed to the site's topographical characteristics. The study also challenges the common assumption that the hottest hours of the day are necessarily the most harmful to human well-being, showing that this relationship may vary according to local climate patterns (Tavares; Abuseif; Dupré, 2025). This leaves a significant research gap concerning the performance of high-albedo (> 0.4) reflective pavements in tropical environments, particularly in equatorial areas, where extreme solar incidence (450 – 800 W/m²) combined with diverse urban morphologies poses unique challenges that remain scientific contribution. These findings highlight the importance of urban microclimate simulation studies as a tool to predict the effects and impacts of pavement strategies on UHI mitigation and to support decision-making related to investments in urban infrastructure.

In countries of the Global South, where urbanization has often occurred in an unplanned and heterogeneous manner, markedly different urban forms coexist within the same city, frequently reflecting socioeconomic disparities (UN-Habitat, 2022; Emmanuel; Johansson, 2006). Urban canyons, narrow streets flanked by tall, closely spaced buildings, can modify microclimatic conditions by restricting the penetration of sunlight and wind (Oke *et al.* 2017). This configuration influences temperature, humidity, and wind speed, with direct implications for thermal comfort (Sharmin; Steemers; Matzarakis, 2017). As a result, urban canyon configurations vary according to the built environment and the purchasing power of local populations. Vertical urban canyons, more prevalent in higher-income areas, are characterized by high (> 1) height-to-width (H/W) ratios primarily driven by tall buildings. In contrast, shallow-urban canyons, commonly found in lower-income neighborhoods, are defined by low-rise constructions combined with narrow street widths, sometimes also resulting in high H/W ratios (Johansson, 2006; Ratti; Sabatino; Britter, 2005). Given that urban canyon geometry influences local heat dynamics and human thermal perception a systematic investigation of how different canyon typologies modulate microclimatic conditions and thermal comfort remains a relevant scientific and technical gap, particularly in tropical cities (Stewart; Oke, 2012).

This study aims to address UHI mitigation in a tropical city by microclimate modeling to assess the effectiveness of high albedo reflective pavements across different urban canyon settings. Critical UHI hotspots were first identified by mapping LCZs and analyzing thermal patterns to prioritize intervention areas. Two contrasting urban canyon settings, selected based on pronounced differences in socioeconomic conditions, construction materials, and urban morphology, were modeled under baseline and high-albedo reflective pavement scenarios using high-resolution computational simulations. The simulations evaluated potential improvements in thermal comfort by analyzing changes in surface temperature, near-air temperature, and pedestrian-level comfort index (UTCI). By integrating spatial analysis and microclimate modeling, this research seeks to bridge the gap between theoretical knowledge and practical heat mitigation strategies in tropical urban environments, offering actionable guidance to planners and policymakers on *where* and *how* to implement a cool pavement strategy for maximum benefit.

5.2 Methods

An overview of the research process was provided before detailing the methodology. Figure 38 presents a flowchart illustrating the steps undertaken in this study.

Figure 38 – Flowchart of research.

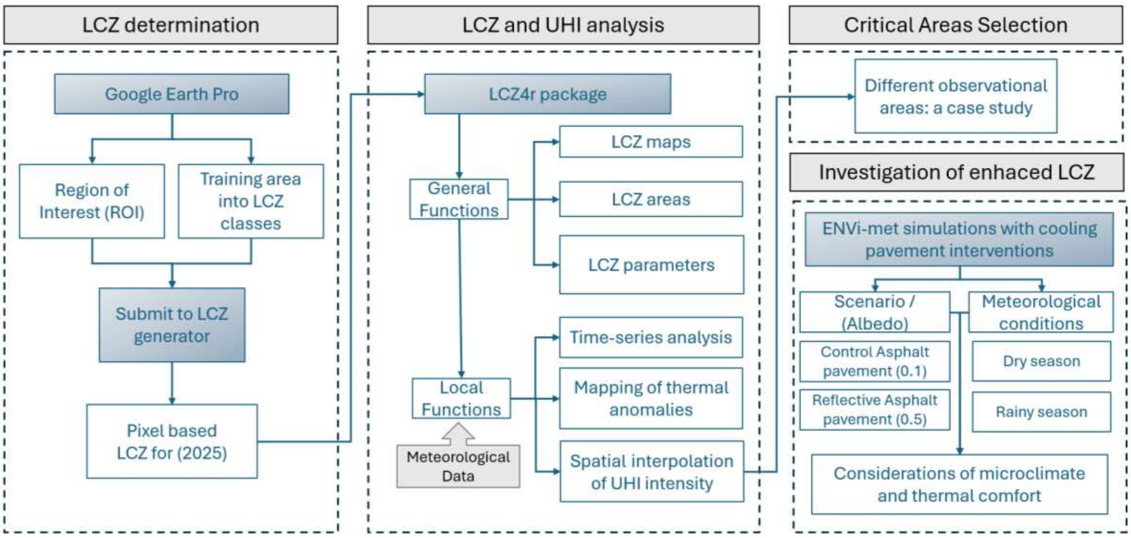

Source: Author, 2026.

5.2.1 Case Study Area

Fortaleza is located at the northeastern coast of Brazil, positioned at geographic coordinates 3°43'02" S latitude and 38°32'35" W longitude (Figure 39). Covering a land area of approximately 312.4 km² with an elevation of 16 m above sea level, the city ranks among Brazil's most populous urban centers, with around 2.7 million inhabitants and a population density of 7,775.5 inhabitants/km² (IBGE, 2023).

Figure 39 – Location of the study area: the city of Fortaleza, case study neighborhoods (HR, LR), and temperature measurement stations.

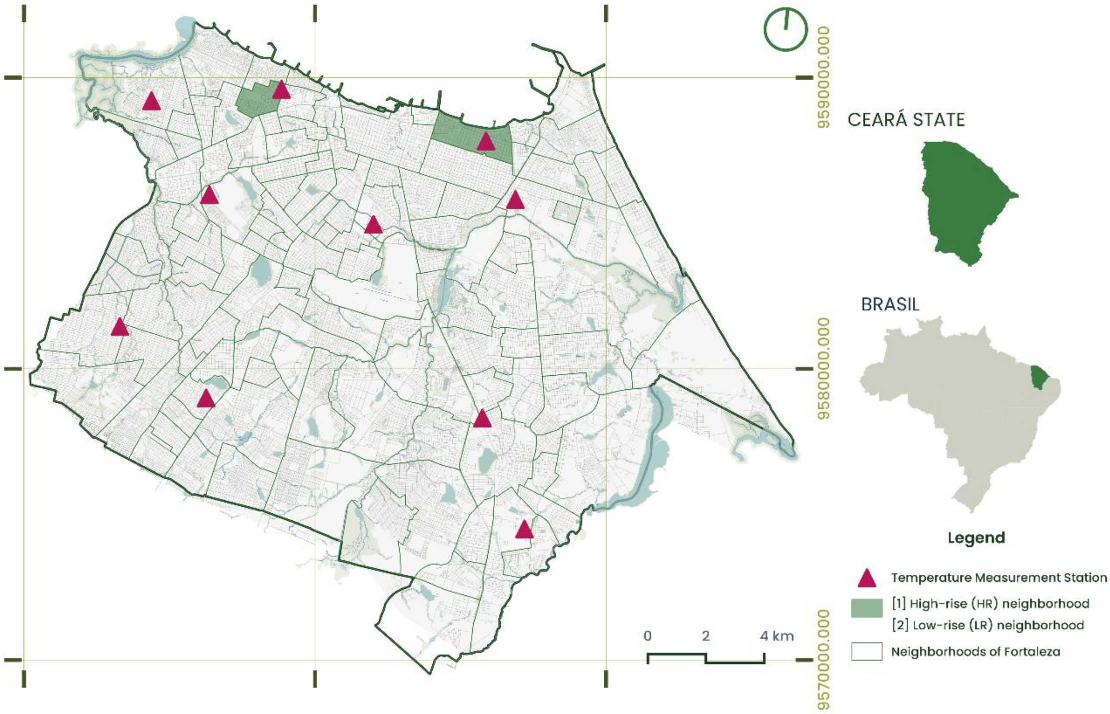

Source: Author, 2026.

Fortaleza has a hot sub-humid tropical climate, with semi-arid features in inland areas (IPECE, 2024). Under the Köppen-Geiger classification, the city exhibits a tropical savanna climate (*Aw*), marked by a distinct dry season. The mean annual temperature is approximately 27 °C, with high relative humidity due to its proximity to the Atlantic Ocean. Annual precipitation averages 1,400 mm, concentrated primarily in the first half of the year (February to May). Wind speeds range from 3 to 5 m/s year-round, with prevailing easterly/southeasterly winds (Lima Júnior; Gomes; Zanella, 2024).

Regarding land use and urbanization characteristics, Fortaleza has undergone rapid urbanization since the 1980s, resulting in large-scale conversion of natural land cover to built-up areas. The city exhibits stark socio-spatial inequalities, with high-density housing and verticalization in central/northeastern zones contrasting with informal settlements in western and southern regions. Currently, 100% of its territory is classified as urban (IPECE, 2024) except for critical environmental preservation areas such as "*Parque do Cocó",* one of Brazil's largest urban green spaces, which plays a vital role in climate regulation and mitigating environmental impacts in the city (Lima Júnior; Ribeiro; Amorim 2024).

Previous studies identified UHIs in Fortaleza with temperature increases of up to 5°C, particularly in southwestern, western, northwestern, and central areas (Moura; Zanella; Sales, 2008). Thermal comfort analyses indicate peak discomfort between 01:00 p.m. and 03:00 p.m. during summer, causing significant physiological stress (Petalas; Mota, 2013). Lima Júnior; Gomes; Zanella (2024) highlights intensifying urban climate impacts, with peripheral areas (especially northwest and west) exhibiting the worst thermal conditions due to dense construction and the use of low-quality materials, which have poor thermal properties. The interplay of climatic conditions, urbanization trends, and land cover characteristics underscores the challenges for Fortaleza's urban and environmental management, particularly regarding thermal comfort and UHI mitigation strategies.

5.2.2 Local Climate Zone Classification

This study employed the LCZ classification system developed by Stewart and Oke (2012) to categorize land surface characteristics across the study area. The classification process was implemented using the specialized LCZ generator tool (Demuzere; Kittner; Bechtel, 2021), an online and open-source platform that maps a city of interest into LCZs, integrating remote sensing data, GIS processing, and machine learning to classify urban and natural landscapes. To that end, a valid training area file and some metadata are required as input.

The input data preparation of the region was delineated according to Stewart and Oke (2012) methodology, which establishes 10 distinct built-up zones (LCZs 1-10) and 7 land-cover types (LCZs A-G), reflecting variations in urban morphology and natural landscapes. Representative training areas of Fortaleza were manually labeled for each LCZ class based on field surveys and local urban morphology data (Figure 40), ensuring alignment with the LCZ framework.

After a random forest classification process, the average overall accuracy metrics reach values above 0.5, a minimum accuracy level proposed by Bechtel *et al*. (2019), was used as a criterion to pass the automated quality control. The results were obtained as LCZ categories at a 100 m resolution, leveraging spectral, textural, and geometric features.

Figure 40 – LCZ classification sample from Fortaleza and the quantity of training areas for each LCZ type.

Built up type	Fortaleza	Land cover type	Fortaleza
LCZ1: Compact high-rise		LCZ A: dense trees	
LCZ 2: Compact mid-rise		LCZ B: scattered trees	
LCZ 3: Compact low-rise		LCZ C: brush, scrub	
LCZ 4: Open high-rise		LCZ D: low plants	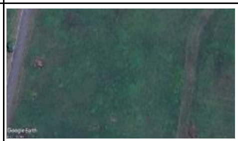
LCZ 5: Open mid-rise		LCZ E: bare rock or paved	
LCZ 6: Open low-rise		LCZ F: bare soil or sand	
LCZ 7: Lightweight low-rise	Not existed	LCZ G: water	
LCZ 8: Large low-rise			
LCZ 9: Sparsely built			
LCZ 10: Heavy industry			

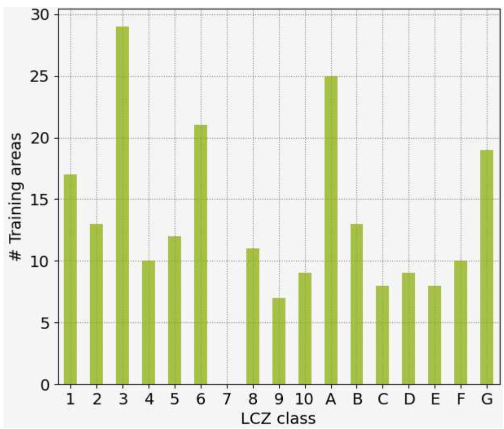

Source: Author, 2026.

5.2.3 UHI analysis by LCZ4r

The UHI effect in Fortaleza was assessed using the LCZ4r package (Anjos *et al.*, 2025), an advanced computational tool designed for LCZ-based thermal analysis. From the Fortaleza LCZ map previously created using the LCZ generator, the first step was processed using LCZ4r's automated classification module for advanced analysis of air temperature data and related environmental variables. For that step, it was necessary to import air temperature data. The temperature and relative humidity data used were obtained by Lima Junior (2023) in a field campaign carried out between November 2021 and March 2022, in order to cover both the dry and rainy seasons. For data collection, ten mini stations with HOBO MX2301A (accuracy of ±0.2°C) thermo-hygrometers were used, properly sheltered to avoid exposure to direct solar radiation and wind, allowing the readings to be more accurate and representative of environmental conditions. The recordings were taken every 10 minutes and adjusted to fit the package requirements. The spatial distribution of data collection stations is presented in Figure 39.

Time-series for air temperature data were systematically categorized by LCZ classification to monitor temporal trends and identify temperature anomalies. These anomalies were calculated as the difference between temperatures recorded at individual LCZ monitoring stations and the mean temperature across all stations during corresponding periods, with positive values indicating relatively warmer zones. For spatial analysis, geostatistical techniques were applied, utilizing Kriging interpolation to generate continuous temperature and anomaly distribution maps. This approach effectively accounted for spatial autocorrelation while minimizing estimation variance, providing robust visualization of thermal patterns across the urban landscape.

Urban heat island intensity (UHII) was quantified using the urban-rural comparison method. Reference stations were carefully selected based on multiple criteria: verified LCZ classifications distinguishing urban from rural areas, in-depth knowledge of local urban morphology, and on-site verification of surface characteristics. For this case study, the monitoring station located in "*Parque do Cocó*" was selected as the rural reference site. UHII was computed using the following equation (Equation 1):

$$UHII = T_{urban} - T_{rural} \tag{12}$$

where, T_{urban} represents urban station temperatures and T_{rural} represents rural reference temperatures.

5.2.4 Microclimate modelling and calibration

5.2.4.1 Modelling Areas Selection

The critical areas were chosen from two distinct residential areas of Fortaleza base on urban canyon settings. These zones were selected based on three main criteria of: (i) the significant contrast in their urban morphology and geometry, (ii) their results of UHI analysis, and (iii) the availability of in situ air temperature data collected during previous field campaigns. The selection of these contrasting zones aimed to capture the variability in microclimatic responses across different urban forms when implementing the high-albedo reflective pavement as a cool strategy.

5.2.4.2 Envi-met Settings and Scenarios

Microclimatic simulations were conducted using the ENVI-met software version 5.6.1, a German computational fluid dynamics (CFD) model designed to simulate urban microclimates based on the interaction between surfaces, vegetation, and the atmosphere (Wang; Berardi; Akbari, 2016). ENVI-met solves the Reynolds-Averaged Navier–Stokes (RANS) equations in three dimensions, with a horizontal resolution ranging from 0.5 to 10.0 meters (Erell; Pearlmutter; Williamson, 2011).

Based on the analysis of field measurements reported by Lima Júnior; Gomes; Zanella (2024), two representative simulation days were selected: November 19, 2021, the hottest day in the dry season; and January 28, 2022, the coolest day in the rainy season. Each simulation began at 04:00 a.m. local time, approximately two hours before sunrise, and ran for a total of 18 hours. Vertical one-dimensional profiles (from ground level up to 2,500 meters) of atmospheric variables, such as specific humidity, were obtained from the University of Wyoming Radiosonde Archive database (https://weather.uwyo.edu/upperair/sounding.shtml). Additional microclimatic input data, including air temperature and relative humidity, were sourced from field measurements as mentioned earlier. Simulations employed the “simple forcing” method, incorporating hourly input values for air temperature and relative humidity.

Wind speed data were obtained from INMET and applied uniformly to both simulation areas. A detailed overview of the input parameters is provided in Table 9.

Table 9 – Detailed input parameters for simulated areas (LR and HR).

Category	Parameter	Value
Domain Configuration	Modelling area (L × W × H) (m)	387 × 381 × 468
	Grid resolution (X × Y × Z) (m)	3 × 3 × 2
Simulation Period	Start date/time (Dry)	04:00 a.m. / Nov. 19th, 2021
	End date/time (Dry)	10:00 p.m. / Nov. 19th, 2021
	Start date/time (Rainy)	04:00 a.m. / Jan. 28th, 2022
	End date/time (Rainy)	10:00 p.m. / Jan. 28th, 2022
	Total duration (h)	18
	Output interval for receptors (min)	30
Meteorological Inputs	Wind direction	104°
	Wind speed at 10 m height (m/s)	5.20
	Specific humidity in 2,500m (g/kg)	5.00
	Air temperature range (°C)	27 - 36
	Relative humidity range (%)	46 - 79
	Mean roughness length (m)	0.01

Source: Author, 2026.

Each model included a vegetation layer with 3D trees, a building layer (with height and material data for each building), and a surface layer (representing the materials used at ground level) as indicated in Table 10. A measurement point (receptor) was placed at the same location as the field monitoring station in each neighborhood, serving as the reference for validating the simulation results. To ensure comparability between the areas, identical boundary conditions were applied in both models as specified in Table 10. Overall, boundary conditions are handled in a consistent manner for the duration of simulations.

Two simulation scenarios were carried out to compare the efficiency of UHI mitigation strategy of reflective pavement. The control scenario (CO) represented the current land cover conditions of each neighborhood area, based on high-resolution imagery from Google Earth and street-level observations from Google Maps. The second scenario, referred to as the reflective pavement (RP) simulation, introduced a modification in surface albedo: the pavement albedo of the control scenario was 0.1, representing conventional asphalt pavement, and it was increased to 0.5 to represent the application of reflective pavement material.

Table 10 – Input layer parameters used in the ENVI-met simulation.

Layer	**Element**	**ENVI-met ID**	**Specification**
Vegetation	3D Trees	0200C2	Cylindrical shape, small trunk, sparse foliage, 5 m height
Buildings	Walls (HR)	Created by the author	Masonry (16 cm), 14 mm hollow block, 4 cm plaster
	Walls (LR)	Created by the author	Masonry (12 cm), 10 cm brick burned, 2 cm plaster
	Roof (HR)	0200C2	Lightweight concrete
	Roof (LR)	0200R1	Clay tiles
Surfaces	Under buildings	CELLAR	Standard subsurface material
	Pavements	Created by the author	Asphalt pavement with varying albedo (0.1 and 0.5)
	Borders Simulation Area	CELLAR	Standard subsurface material

Source: Author, 2026.

5.2.4.3 Model Calibration

For model validation, many studies adopt correlation analysis between air temperature derived from model simulation and on-site measured air temperature (Tsoka; Tsikaloudaki; Theodosiou, 2018). Validation conducted for one or a few sample areas within the same region or city is generally considered sufficient (Chatterjee *et al.*, 2019). Therefore, the overall validation of the ENVI-met model will be assessed based on field measurements carried out by Lima Júnior; Gomes; Zanella (2024) in the LR and HR neighborhoods.

To perform the simulations, hourly average values of air temperature and relative humidity were used as forced input in ENVI-met. The simulation results were compared with the daily profiles of meteorological variables measured in the field. These measurement receptor points were examined alongside the results provided by data receivers in the ENVI-met model.

Finally, the model's accuracy was verified by calculating commonly used validation indices, such as mean absolute error (MAE) and root mean square error (RMSE), computed according to Equation 1 and Equation 2, respectively. MAE is a metric that measures the average of absolute differences between predicted and observed values, where n is the number of observations, P_i is the predicted value (simulated by ENVI-met), O_i is the observed value (measured in the field), and $|P_i - O_i|$ is the absolute difference between predicted and observed values. Meanwhile, RMSE isolates systematic error, i.e., the average tendency to overestimate or underestimate values over time. A lower RMSE indicates less bias in the model, where n is the number of observations, $\bar{P}$ is the average predicted value (simulated by ENVI-met), $\bar{O}$ is the average observed value (measured in the field), and $(\bar{P} - \bar{O})^2$ is the square of the difference between the average predicted and observed values.

$$MAE = \frac{1}{n}\sum_{i=1}^{n}|P_i - O_i| \tag{13}$$

$$RMSE = \sqrt{\frac{1}{n}\sum_{i=1}^{n}(\bar{P} - \bar{O})^2} \tag{14}$$

5.2.4.4 Assessment of Thermal Comfort

To assess thermal comfort under different simulated scenarios, UTCI was applied. This bioclimatic index quantifies thermal stress by expressing it as an equivalent ambient temperature, which corresponds to the environmental conditions that would provoke the same physiological response in a reference individual exposed to a standard environment (Blazejczyk *et al.*, 2012).

The reference individual is characterized by a metabolic rate of 135 W/m² and a walking speed of 1.1 m/s. In the meteorological reference, the mean radiant temperature equals the ambient temperature, and the wind speed observed 10 m above ground is 0.5 m/s. The reference humidity is set at 50% for ambient temperatures of the reference ≤ 29°C and at 20 hPa (Blazejczyk *et al.*, 2012). The UTCI is computed based on four main environmental parameters: air temperature (Ta), mean radiant temperature (Tmrt), wind speed at 10 m above ground level (Va), and atmospheric humidity, which may be expressed as either water vapor pressure (pa) or relative humidity (rH). The index is calculated using the formula according to Bröde *et al*. (2012):

$$\text{UTCI} = f(\text{Ta}, \text{Tmrt}, \text{Va}, \text{rH}) = \text{Ta} + offset(\text{Ta}, \text{Tmrt}, \text{Va}, \text{rH}) \quad (15)$$

In this study, UTCI values were calculated using the BioMet tool available within the ENVI-met software, based on simulation outputs for the selected time periods. Thermal stress categories associated with UTCI values follow established classification ranges, as shown in Table 11. These categories range from "no thermal stress" to "extreme heat/cold stress" and are used to interpret the physiological implications of the simulated microclimate conditions on human comfort.

Table 11 – UTCI equivalent temperature classification.

UTCI (°C) range	Stress Category
above +46	extreme heat stress
+38 to +46	very strong heat stress
+32 to +38	strong heat stress
+26 to +32	moderate heat stress
+9 to +26	no thermal stress
+9 to 0	slight cold stress
0 to -13	moderate cold stress
-13 to -27	strong cold stress
-27 to -40	very strong cold stress
below -40	extreme cold stress

Source: Author, 2026.

5.3 Results

5.3.1 LCZ Maps and UHI analysis

Regions of interest (ROIs) were defined based on the administrative boundaries of Fortaleza. Training samples for all LCZ types were selected using data from the year 2025, with the exception of LCZ 7, a category rarely found in urban environments, which was excluded from the analysis. The resulting LCZ classification map accurately represents the spatial distribution of LCZ types in the city, as shown in Figure 41a.

Figure 41 – (a) LCZ classification map of Fortaleza; (b) LCZ classes percentage distribution.

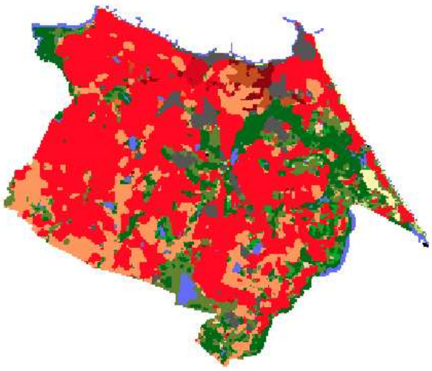

a)

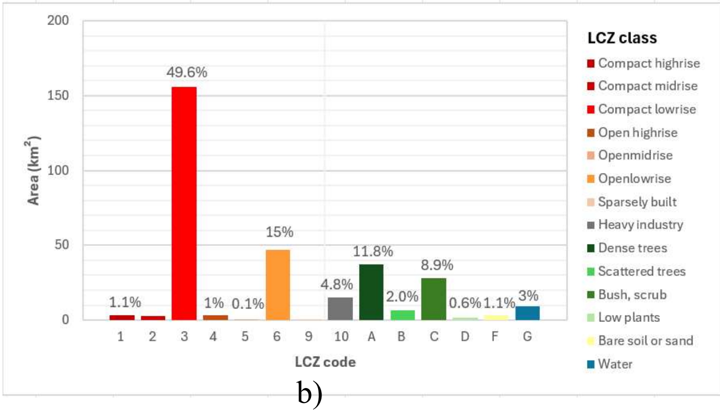

b)

Source: Author, 2026.

Overall, the LCZ map reveals a predominance of "built-up" zones, with LCZ 2 (compact mid-rise buildings) being the most prevalent, covering approximately 50% of the total area (Figure 41b). This classification aligns with the current land use and urban development patterns in Fortaleza. LCZ 6 (open low-rise) ranks second, representing 15% of the area, primarily in the southern region of the city, which corresponds to peripheral zones characterized by unplanned housing developments.

As previously noted, "*Parque do Cocó*", a large preserved urban forest located in the central part of the city, accounts for most of the 11.8% of LCZ 11 (dense trees), highlighting the presence of significant green infrastructure within the urban fabric. Although LCZs 1 and 4 (compact high-rise and open high-rise, respectively) make up only about 2.1% of the city's total area, they are concentrated along the coastal zone, in prime real estate areas. These zones reflect the urban morphology and increased verticalization pattern in high-value regions of the city.

To analyze intra-day variability of the UHI effect, UHII assessments were conducted for specific time windows using the LCZ4r package, which integrates the LCZ framework into air temperature interpolation. Figure 42 presents the spatial distribution of UHII intensity in Fortaleza on November 19, 2021, at 12:00 p.m. and 10:00 p.m.

Figure 42 – LCZ- Air temperature interpolation maps in Fortaleza on November 19, 2021, at: (a) 12 p.m.; (b) 10 p.m.

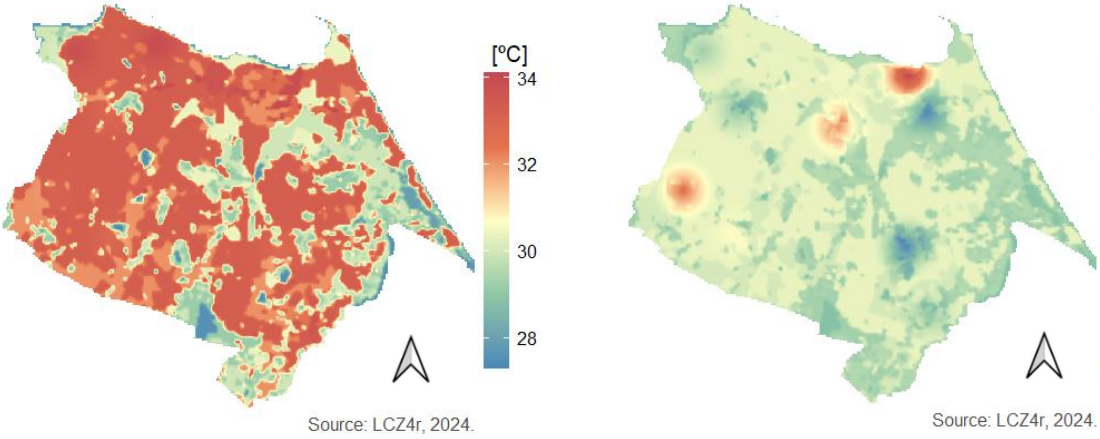

a) b)

Source: Author, 2026.

At 12:00 p.m. (Figure 42a), elevated air temperatures were observed across most of the city, particularly in densely built central areas. The only notable exception was LCZ 11, where lower temperatures were recorded due to the presence of significant vegetated areas such as "*Parque do Cocó*", as well as nearby water bodies, which contribute to localized cooling effects.

By 10:00 p.m. (Figure 42b), UHI intensity became more pronounced, revealing persistent heat retention in certain urban zones. Heat hotspots were primarily located in areas classified as LCZ 4 (open high-rise), LCZ 3 (compact low-rise), and LCZ 10 (heavy industry), highlighting their reduced capacity to dissipate accumulated heat during the night. Even though the air temperature difference among the hottest spots reaches up to 0.5°C, these findings underscore the importance of urban form and land cover in modulating nocturnal temperature distribution and the resilience of urban areas to heat stress.

Figure 43 illustrates the air temperature anomalies for Fortaleza on the hottest day recorded during the measurement period, a representative summer day. These anomalies represent deviations of observed temperatures from the average at each station analyzed. To account for baseline differences across LCZs, the anomalies were normalized using the LCZ4r approach, which adjusts for inherent variations in reference temperatures between LCZ types (Anjos *et al*., 2025).

Figure 43 – Daily air temperature anomalies across different LCZ classes in Fortaleza on November 19, 2021: a) LCZ-temperature anomalies map; b) total deviation graph.

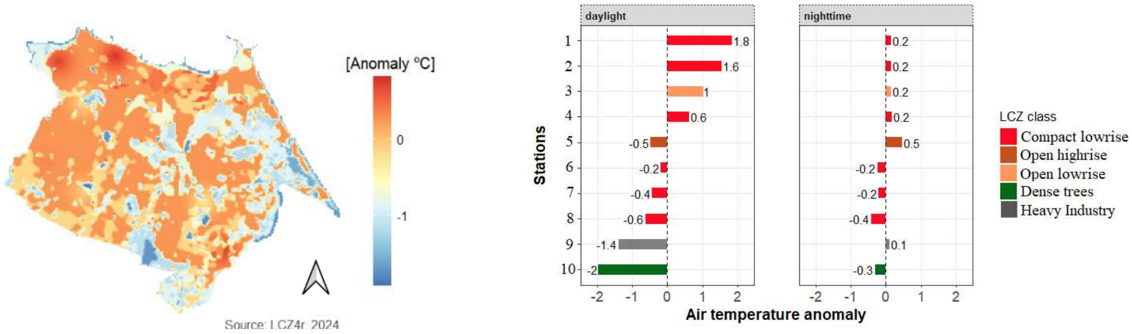

a) b)

Source: Author, 2026.

The results highlight clear contrasts in temperature patterns across different LCZ classes, underscoring the influence of land use and land cover on urban microclimate. Stations located in LCZ 3 (compact low-rise) and LCZ 6 (open low-rise) exhibited positive anomalies of +1.8 C and +1.0°C, respectively, indicating elevated daytime temperatures in more densely built-up areas. In contrast, LCZ 11 (dense trees) and LCZ 10 (heavy industry) stations recorded negative anomalies of –2.0°C and –1.4°C, respectively, reflecting slightly cooler conditions. The nighttime anomalies reveal the LCZ 4 (open high-rise) station as the hottest area in the city, with a temperature variation of +1.0°C.

5.3.2 Urban Characteristics of Modeled Areas

Based on the analysis of LCZs and UHI formation, two areas of the city were selected for comparison of morphological parameters: low-rise (LR) and high-rise (HR) areas. Table 12 shows the main morphological parameters of the LR and HR neighborhoods.

LR is located in the northwest part of Fortaleza and is characterized by an extremely high population density and low average income, reaching approximately 18,000 inhabitants/km² and presenting a human development index (HDI) of 0.365. In terms of urban development, LR exhibits a dense built environment with a pronounced scarcity of green areas and open spaces that could contribute to urban heating. The predominant land use is residential, with closely spaced, attached buildings that lack front, side, or rear setbacks. This results in a high concentration of LR constructions. The street network is composed of long and narrow roads, paved with asphalt concrete, and when sidewalks are present, they are typically narrow and made of concrete. Most buildings in this area have up to four floors and make extensive use of materials such as concrete, ceramic roof tiles, and asphalt pavements, which dominate the local landscape (Figure 44).

Table 12 – Morphological parameters of the LR and HR neighborhoods by LCZ4r.

Parameter	**LR**	**HR**	**Fortaleza**
Total Area	1.42 km²	2.65 km²	313.80 km²
Building Surface Fraction[a]	55.0%	48.7%	39.2%
Impervious Surface Fraction[b]	55.0%	48.7%	38.7%
Vegetation Surface Fraction[c]	15.0%	10.7%	34.3%
Height Roughness Elements[d]	6.50 m	11.32 m	6.78 m
Sky View Factor[e] [0-1]	0.40	0.45	0.59
Mean Aspect Ratio[f] [0-3]	1.12	0.85	0.77

[a]Ratio of building plan area to total plan area (%)

[b]Ratio of impervious plan area (paved, rock) to total plan area (%)

[c]Ratio of vegetation plan area to total plan area (%)

[d]Geometric average of building heights (LCZs 1–10) and tree/plant heights (LCZs A–F) (m)

[e]Ratio of the amount of sky hemisphere visible from ground level to that of an unobstructed hemisphere

[f]Mean height-to-width ratio of street canyons (LCZs 1–7), building spacing (LCZs 8–10), and tree spacing (LCZs A–G)

Source: Author, 2026.

HR, in contrast, is a highly verticalized area with a higher average income (HDI of 0.953), which is reflected in an urban pattern markedly different from that of LR. The streets and avenues are predominantly paved with asphalt, but the wider roadways, averaging 14m, allow for better wind circulation throughout the area. Buildings in HR generally exceed ten floors and are primarily constructed using concrete, steel frameworks, and ceramic cladding (Figure 45). Although green areas are limited, they are mainly concentrated within condominium common spaces and along urban landscaping strips. According to Lima Junior *et al.* (2024), a particularly relevant feature of HR is its proximity to the coastline, which plays a crucial role in cooling the local atmosphere through enhanced marine breezes.

Figure 44 – a) Low-rise (LR) street view's borders; b) LR building heights distribution.

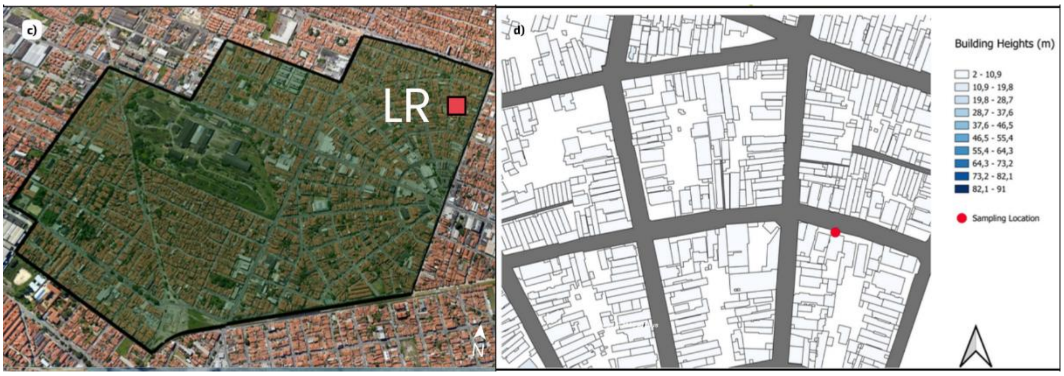

Source: Author, 2026.

Figure 45 – a) High-rise (HR) street view's borders; b) HR building heights distribution.

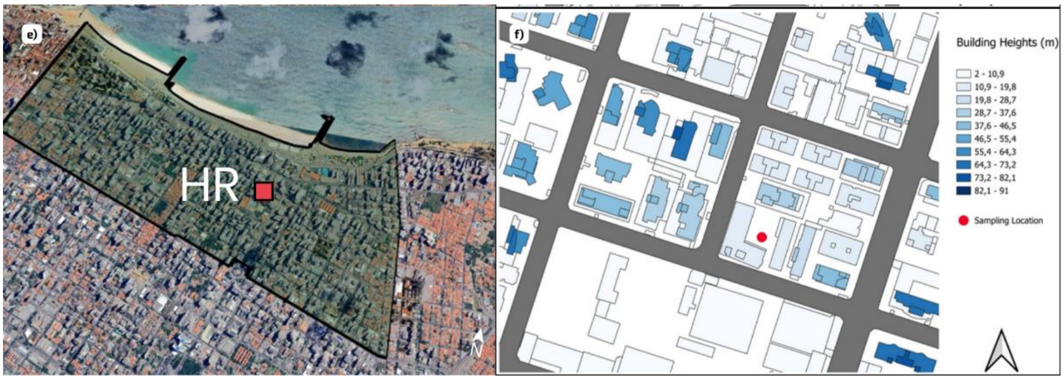

Source: Author, 2026.

The comparative analysis of morphological parameters between the LR and HR areas reveals meaningful differences in urban canyon configurations and their potential microclimatic implications. The mean height of roughness elements is considerably higher in the HR area (11.32 m) than in the LR area (6.50 m), reflecting the predominance of taller buildings and a more vertically developed urban fabric. Increased surface roughness enhances the interaction between airflow and the built environment, potentially promoting greater turbulent mixing and heat dissipation under favorable wind conditions. However, taller buildings also introduce extensive vertical surfaces that absorb and re-emit longwave radiation, which can contribute to higher radiant heat loads at the pedestrian level, particularly during daytime.

The SVF parameter shows relatively similar values in both areas, though it is slightly higher in the HR area (0.45) compared to the LR area (0.40). This suggests that despite the greater building heights, the HR area maintains marginally higher sky openness, likely due to wider streets or more spaced building arrangements. Lower SVF values are commonly associated with increased nocturnal heat retention due to reduced longwave radiative loss, whereas slightly higher SVF values may facilitate nighttime cooling while increasing daytime exposure to direct solar radiation.

The mean aspect ratio (H/W) further highlights these morphological contrasts. The LR area exhibits a higher aspect ratio (1.12), indicative of more confined urban canyons formed by relatively low-rise buildings combined with narrow street widths. Here in this study, it was considered as an area of horizontal canyons. Such configurations tend to restrict ventilation and enhance radiative trapping, thereby exacerbating thermal stress in tropical climates. In contrast, the HR area presents a lower mean aspect ratio (0.85), suggesting more open canyon geometries in which greater building heights are offset by wider streets. Here in this study, it was considered as an area of vertical canyons. This geometry can favor air circulation and heat dispersion, although the presence of extensive vertical surfaces may still increase mean radiant temperature during periods of intense solar exposure.

5.3.3 Validation of Envi-met modelling results with field measurements

In order to perform the validation of the ENVI-met microclimate model, the profiles of air temperature for base scenario are compared against those of the measurement campaign. Figure 46 shows the comparison between the actual air temperature measurements at the receptor locations and the corresponding simulated profiles.

The comparison reveals a good agreement between measured data (solid orange lines) and simulated data from the dry season scenario (solid green lines) throughout November 19^{th}, 2021. While predictions based on wet season scenario (28^{th} January, 2022) deviate the most from actual measurements during the hours of maximum solar irradiance, from 8:00 a.m. to 05:00 p.m. In fact, for both receptors, the simulated profiles of air temperature are above the actual measured profiles: the model shows a smoothing in the simulated data curve if compared to the measured one, which shows higher data variation. In particular, a maximum difference in air temperature of approximately 3.2°C is observed in the simulated data at around 11:00 a.m. during the dry season for the LR-CO scenario.

Figure 46 – Comparison between simulated and measured air temperature for different dates: a) and b) LR (h = 1.4 m); c) and d) HR (h = 1.4 m).

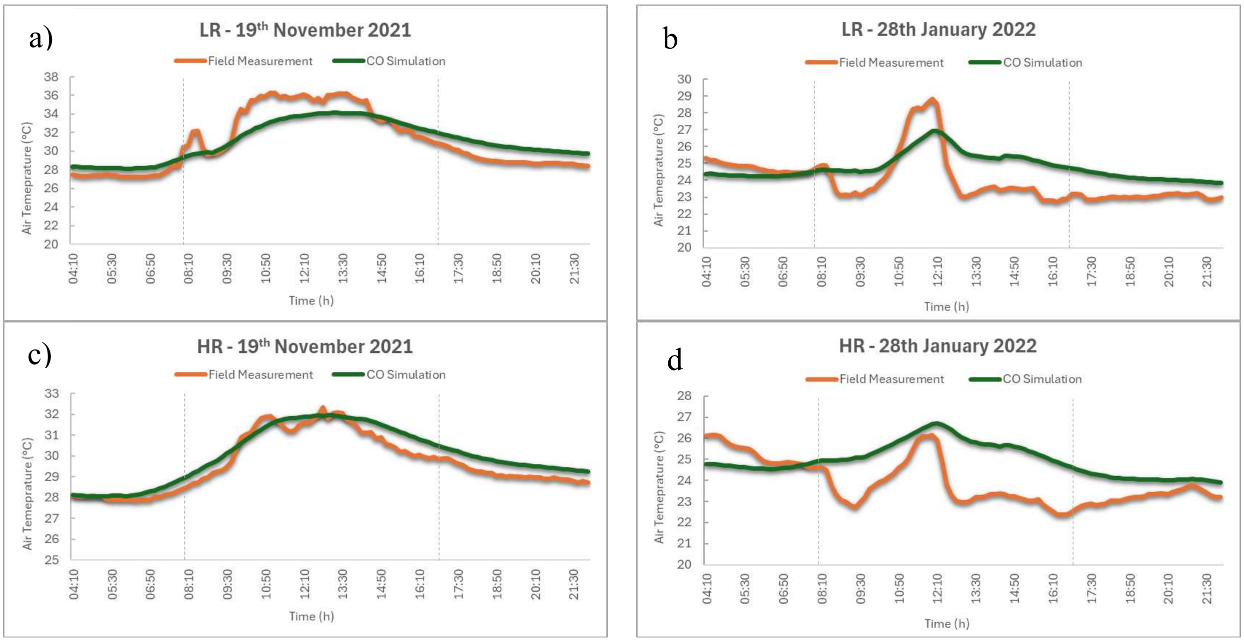

Source: Author, 2026.

Although some studies more frequently report that ENVI-met tends to underestimate air temperatures during the day, in this case, the opposite is observed. According to Detommaso, Costanzo and Nocera (2021), such discrepancies may result from simplifications in ENVI-met's advanced radiation transfer scheme (IVS method). The IVS method aims primarily to improve the accuracy of modeling secondary radiation fluxes, specifically, the radiation emitted or reflected by environmental objects (walls, roofs, ground, and vegetation). These simplifications can lead to inaccuracies in calculating urban canyon radiation, particularly during periods of maximum solar exposure, as also noted by Liu; Hu; Liu, (2020).

To evaluate numerically the deviation between the modelling outputs and the actual measured data, the statistical indices presented in Section 5.2.4.3 are calculated and reported in Table 13 for the two base simulation scenarios. For the dry period, represented by November 19th, 2021 the HR site exhibited significantly lower error indices (MAE = 0.45 C and RMSE = 0.51 C) compared to LR (MAE = 1.34 C and RMSE = 1.53 C), indicating more accurate simulations at HR. This is further supported by the higher R^2 values, which demonstrate a strong agreement between simulated and observed data, suggesting that the model performed very well at the HR site during November. In contrast, during the rainy period (January 28th, 2022), both MAE and RMSE values remained elevated, reflecting the persistence of larger pointwise errors compared to November. Notably, at HR, MAE and RMSE increased to 1.33°C and 1.57°C, respectively, indicating a significant decline in model performance. R^2 also dropped substantially, pointing to a weakened correlation between simulated and observed values, and suggesting the model struggled to accurately represent air temperature during this period.

Table 13 – Validation indices of the ENVI-met model for simulated base scenarios.

Variable	Statistical índices	Unit	Locations / Date			
			19th November, 2021		28th January, 2022	
			LR	HR	LR	HR
Air Temperature	MAE	°C	1.34	0.45	1.17	1.33
	RMSE	°C	1.53	0.51	1.35	1.57
	R^2	-	0.84	0.94	0.36	0.06

Source: Author, 2026.

Overall, the model showed better performance in November, particularly at the HR location, where all statistical indicators pointed to high accuracy and strong correlation. In January, model performance declined at both sites, with a more pronounced deterioration at HR, where the correlation nearly vanished ($R^2 \approx 0$). This variation may be attributed to the different climatic conditions during the rainy season, suggesting that the model's effectiveness is reduced under these circumstances. Rainy periods introduce significant complexity to microclimate simulations, particularly through changes in fluid dynamics and the energy balance (Bruse, 2017). Furthermore, the simplified forcing method used in this ENVI-met study does not include precipitation data as an input parameter, which is a crucial omission that can heavily contribute to the discrepancies observed between simulations and field measurements (Salvati; Kolokotroni, 2019). In this context, the present study proceeded with the analysis of simulation results only for the dry period, where the model demonstrated more reliable performance.

5.3.4 Air and ground surface temperatures in the control simulation (CO)

Figure 47 illustrates the air temperature at 1.4 m above ground level at noon for the LR and HR neighborhoods, shown in panels (a) and (b), respectively. The highest surface air temperature simulated was 39.3 °C in the LR neighborhood (Figure 48a). Higher air temperatures are observed over asphalt pavement, particularly on the eastern side of the neighborhood, which may be influenced by the prevailing wind direction.

The air temperature range in LR is at least 2.5 °C higher than in HR. Although HR is slightly closer to the coast than LR, this temperature difference is likely related to variations in the urban built environment. HR features wider streets and taller buildings, which create more open space between structures, allowing for better wind circulation. The lower air temperatures in HR may also be attributed to the shading effect of tall buildings and the presence of some vegetated areas within residential complexes, where temperatures reached as low as 32.5 °C (Figure 47b). These findings highlight the significant influence of local land cover on air temperature, consistent with previous studies (Santamouris, 2014, Taleghani *et al.*, 2019), which demonstrate that land surface characteristics can substantially alter the urban microclimate.

Figure 47 – Maps of air temperature at a height of 1.4 m at noon (dry season): a) LR and b) HR.

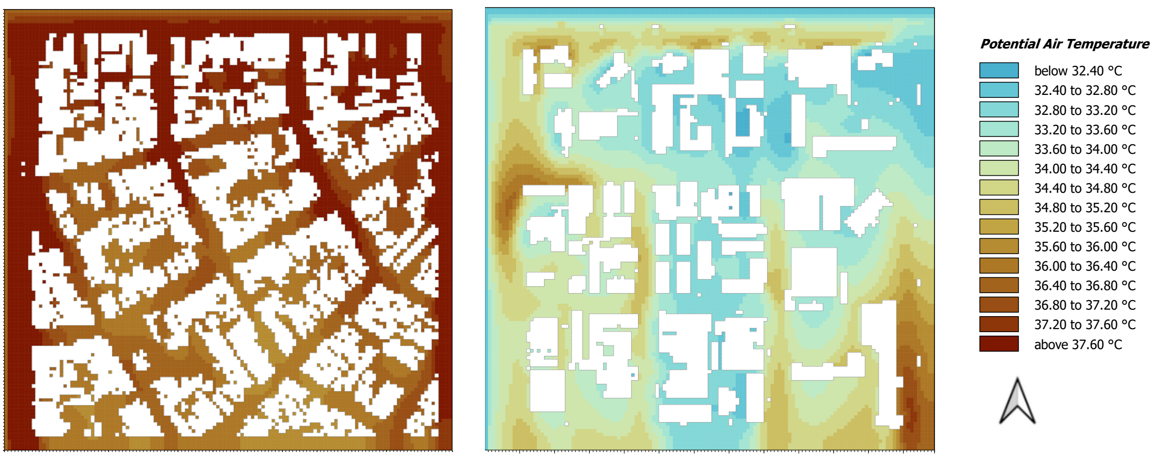

a) b)

Source: Author, 2026.

Similarly, surface temperatures are highest over pavements in the LR neighborhood, reaching a maximum of 56.8 °C, as shown in Figure 48a. The temperature difference, at least 3.3 °C higher than in HR, is likely associated with the lack of shaded areas in LR, where the urban morphology is characterized by relatively uniform building heights and a scarcity of vegetation. In contrast, Figure 48b shows that the lowest surface temperatures in HR are observed near the buildings, likely due to the shading provided by their greater height and spacing. It is possible to observe that the paved area exerts a significant impact on the local microclimate of the studied sites, as the highest air and surface temperatures were recorded above it.

Figure 48 – Maps of ground surface temperature (z = 0 m) at noon (dry season): (a) LR and (b) HR.

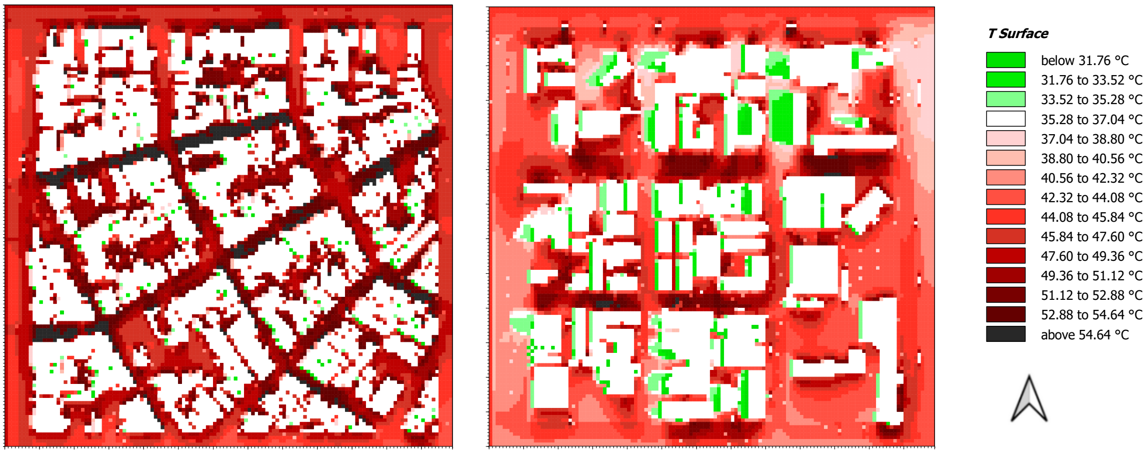

a) b)

Source: Author, 2026.

5.3.5 Impacts of the heat mitigation strategy (RP) on the air and surface temperatures

Figures 49 and 50 illustrate the impact of implementing the high-albedo reflective pavement strategy (RP scenario) in comparison to the control simulation (CO scenario) on air temperature and surface temperature, respectively. The graphs display results at 8:00 a.m., 12:00 p.m., 4:00 p.m., and 8:00 p.m., time points selected to capture the strategy's performance throughout the day. These include the period of peak solar irradiance at noon, typically associated with the most thermally stressful conditions, and the absence of solar radiation at night (8:00 p.m.), when UHI effects tend to be more pronounced.

Comparing the changes in air temperatures, the adoption of high-albedo reflective pavements led to a cooling effect of up to 1.7 C in near-surface air temperature at 12:00p.m. in both neighborhoods. The most significant reductions were observed during periods of active solar radiation, aligning with the reflective material's activity. However, the cooling effect gradually diminished during the late afternoon and was nearly absent by 8:00 p.m. Moreover, differences in urban morphology between LR and HR did not appear to significantly influence the air temperature reduction results in this model.

Figure 49 – Maps of absolute differences in potential air temperature (h = 1.4 m) between RP and CO simulations at 8:00 a.m., 12:00 p.m., 4:00 p.m., and 8:00 p.m. (dry season).

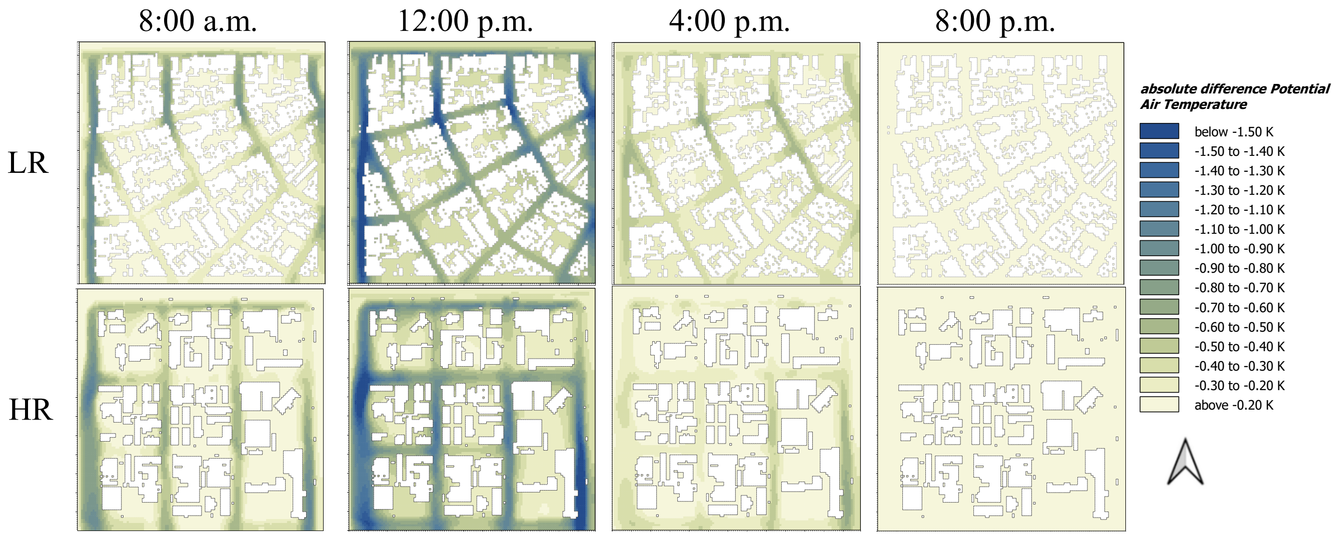

Source: Author, 2026.

Regarding surface temperatures, the RP scenario achieved maximum reductions of up to 9.6 C at 12:00p.m. in both neighborhoods. This magnitude of reduction is consistent with the findings of Ribas *et al*. (2025a), who reported surface temperature decreases of 5–9 C during peak solar radiation hours in outdoor experiments with thermochromic-functionalized hot mix asphalt (HMA) samples, compared to untreated surfaces in exposed to a tropical climate. Like the air temperature results, the most pronounced surface cooling effects were observed during the daytime. The LR neighborhood experienced slightly greater surface temperature reductions than HR, with a maximum difference of 0.6 °C. Although overall differences between the neighborhoods were not substantial, shading effects from trees and taller buildings in HR contributed to slightly cooler temperatures in some streets, as observed in the spatial maps.

For those variables, no significant differences were identified in the performance of the RP strategy between the two urban configurations, with both areas exhibiting comparable cooling gains. This similarity suggests that, at least for these thermodynamic variables, the application of reflective pavements yields consistent reductions regardless of differences in urban canyon geometry. One possible explanation is the limited ability of the ENVI-met model to fully capture the influence of geometric variations in urban form on near-surface thermal responses. This interpretation is consistent with the findings of Sharmin; Steemers; Matzarakis (2017), who reported that under theoretical scenarios with uniform building heights and simplified canyon morphologies, ENVI-met may not be sufficiently sensitive to geometric irregularities when compared to real-world observations. Consequently, while reflective pavements effectively reduce air temperature and surface temperature, their differential microclimatic responses across distinct urban geometries may be underestimated in simulations.

Figure 50 – Maps of absolute differences in ground surface temperature (z = 0 m) between RP and CO simulations at 8:00 a.m., 12:00 p.m., 4:00 p.m., and 8:00 p.m. (dry season).

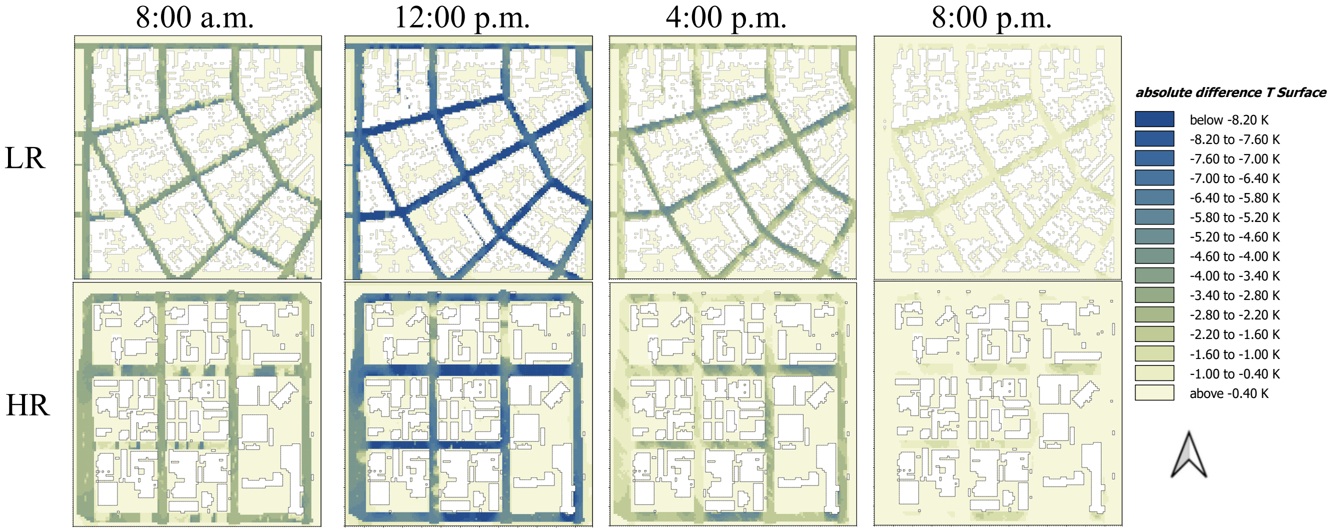

Source: Author, 2026.

5.3.6 Impacts of the heat mitigation strategy (RP) on surface energy balance

Figure 51 presents the impacts of implementing the RP strategy, compared with the control scenario, on the surface energy balance evaluated at different periods along the day. Reflective pavement strategies modify land-cover characteristics and consequently alter the energy balance by directly influencing the energy fluxes between the surface and the atmosphere. The plots in Figure 51 were generated using a Python script that processed the ENVI-met output variables (Q_H, Q_G, and Q_{LE}) and applied Equation (5) to compute the resulting surface energy balance. The following equation can express the surface energy balance:

$$\Delta Q^* = Q_H + Q_{LE} + Q_G \quad (16)$$

where ΔQ^*represents the total net radiation, $Q_H$the sensible heat flux, $Q_{LE}$the latent heat flux, and $Q_G$the ground heat flux. All terms are expressed in W/m², as described by NOAA (National Oceanic and Atmospheric Administration, 2015).

When comparing the variations in total net radiation between the scenarios, it is evident that, in both neighborhoods, the adoption of RP resulted in a substantial reduction of this variable, up to 350 W/m² directly over the paved areas. Because solar radiation is the primary driver of the surface energy balance (Oke *et al.*, 2017), the decrease in net radiation occurs mainly during periods of direct insolation, from 7 a.m. to 4 p.m. A reduction in net radiation indicates that the RP scenario promotes a more energy-efficient urban environment, with likely benefits for outdoor thermal comfort.

Figure 51 – Maps of absolute differences in ground surface temperature (z = 0 m) between RP and CO simulations at 8:00 a.m., 12:00 p.m., 4:00 p.m., and 8:00 p.m. o(dry season).

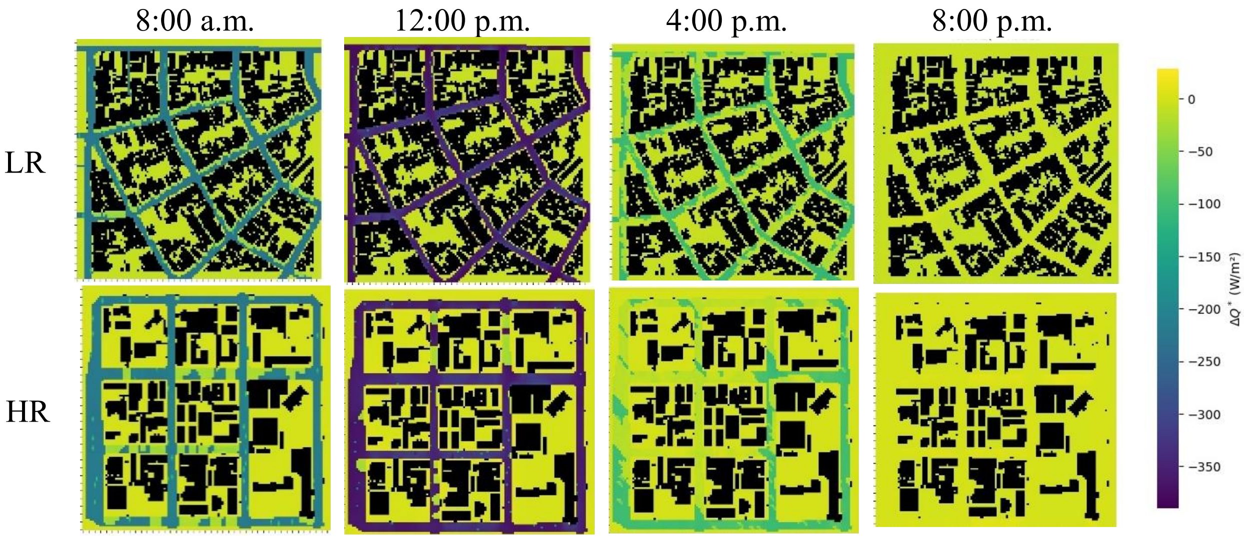

Source: Author, 2026.

At the neighborhood scale, the model results demonstrate that modifying pavement albedo plays a key role in restructuring the local thermal regime and may contribute to mitigating UHI effects. This occurs because increasing surface albedo reduces net radiation and, consequently, the amount of energy available to be re-emitted as convective heat into the atmosphere. Comparable outcomes were reported by Ribas *et al.* (2025a), whose field experiments indicated an 18% reduction in surface energy balance for thermochromic asphalt concrete samples relative to untreated surfaces, equivalent to a 9°C decrease in surface temperature. Taleghani *et al.* (2019) obtained slightly more conservative results when comparing high-albedo pavements to conventional ones, reporting a maximum reduction of 320 W/m² in net radiation and a 6.9°C decrease in surface temperature in a neighborhood-scale assessment.

The integration of the ΔQ* curve quantifies the total gain in energetic efficiency across the analyzed areas. For the LR neighborhood, the RP strategy yielded an accumulated reduction of 823 W/m² of net radiation for the simulated day. In contrast, in the HR neighborhood, the efficiency was 8.5% lower (760 W/m²). Given that both neighborhoods have similar percentages of paved surface (20–25%), differences in energy balance are likely associated with their distinct morphological and construction characteristics. Although LR exhibits high density, most buildings reach only up to four stories, whereas HR is characterized by buildings typically exceeding ten stories, favoring the formation of vertical urban canyons and, consequently, enhancing radiative trapping and heat retention.

These findings highlight the complexity underlying the selection of urban cooling strategies, and their benefits depend on material properties, urban morphology, local climate, and the interplay of surface–atmosphere energy exchanges. Therefore, careful consideration of neighborhood-scale characteristics is essential to optimize the effectiveness of heat-mitigation interventions.

5.3.7 Impacts of the heat mitigation strategy (RP) on outdoor thermal comfort

The assessment of mean radiant temperature (MRT) is essential for outdoor thermal comfort analysis, especially when using the UTCI, as MRT strongly influences the thermal load perceived by pedestrians. Differences in MRT between simulation scenarios are usually more noticeable than differences in air temperature, underscoring its critical role in microclimatic evaluations.

As shown in Figure 52, MRT presents consistently positive values throughout the day, indicating that the RP strategy increases MRT in comparison to the CO. This increase peaks at 12:00 p.m., during maximum solar exposure, with a difference of approximately 13°C in both neighborhoods (LR and HR), particularly over the pavement surface. However, this difference declines sharply by 4:00 p.m., falling to less than 3°C. At night, the difference between RP and CO becomes negative, as the RP surface's reflective behavior during the day limits heat retention, making it slightly cooler than CO, which retains and re-radiates heat, raising MRT by approximately 0.5°C.

Although RP consistently presents the highest MRT values due to the strong reflection of shortwave radiation from its surroundings, the maximum difference in MRT between control and reflective pavement scenarios reported by Elmagri; Kamel; Ozer, (2024) was about 7°C, notably lower than in the present study. This can be attributed to the lower albedo (0.35) used in their study, conducted in the semi-arid climate of Arizona, compared to the higher albedo (0.50) applied in this study under a tropical climate. In contrast, Jia and Wang

(2021) found that cool pavements with an albedo of 0.50 led to a maximum MRT increase of only 2.57°C in a humid subtropical climate of Hong Kong. This indicates that climate/geographical location has a large impact on the MRT variable.

Figure 52 – Maps of absolute differences of MRT (h = 1.4 m) between RP and CO simulations at 8:00 a.m., 12:00 p.m., 4:00 p.m., and 8:00 p.m. (dry season).

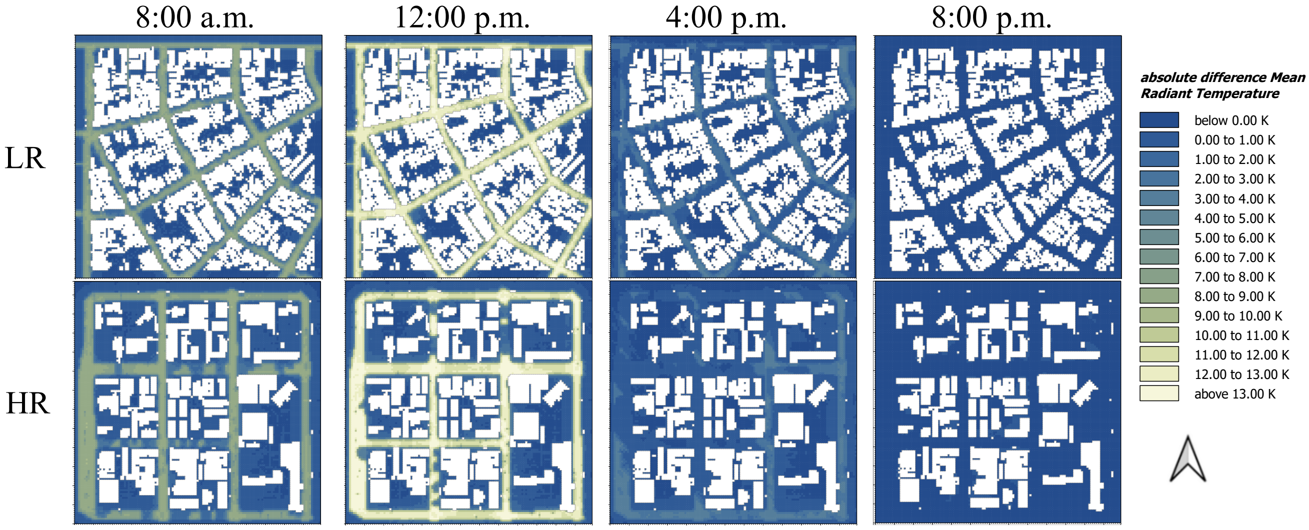

Source: Author, 2026.

Figure 53 presents the diurnal variation of average UTCI values for both simulation scenarios, measured at a height of 1.4 m. As illustrated, the RP scenarios exhibit similar daily patterns, with UTCI values peaking around 12:00 p.m. and reaching their lowest levels around 4:00 a.m. During the daytime, UTCI values in the HR neighborhood generally exceed 32 °C, indicating a strong likelihood of thermal discomfort for pedestrians. Conditions are even more severe in the LR neighborhood, where UTCI values range from 39.1 °C to 47.6 °C, corresponding to the "extreme heat stress" category. At sunset, UTCI values in HR drop significantly, falling from approximately 44 °C to below 32 °C, which corresponds to a shift from very strong to moderate heat stress. In contrast, UTCI values in LR decrease to around 34 °C, remaining within the range of strong thermal stress. During nighttime hours, UTCI values are relatively lower in both neighborhoods, indicating conditions ranging from moderate thermal stress to no thermal stress.

Figure 54 compares the absolute differences in UTCI between the RP scenario and the CO simulation at four time points: 8:00 a.m., 12:00 p.m., 4:00 p.m., and 8:00 p.m. The most significant differences occur over paved surfaces, particularly at noon, with maximum UTCI increases of approximately 2.6 °C for both LR and HR neighborhoods. By mid-afternoon

(4:00 p.m.), this difference drops sharply to around 0.5 °C. During the daytime, UTCI values are consistently higher in the RP scenario, indicating increased thermal discomfort for pedestrians. This effect is primarily due to the high solar reflectivity of the reflective pavement under intense sunlight, which reflects a larger portion of incoming shortwave radiation. Moreover, the ENVI-met model cannot accurately simulate the temporal variations of wind speed, as a consequence of the static initialization parameters (Tsoka; Tsikaloudaki; Theodosiou, 2018). This limitation probably negatively impacts the UTCI results, especially in the HR area located near the coast.

Figure 53 – Diurnal profiles of UTCI for all scenarios.

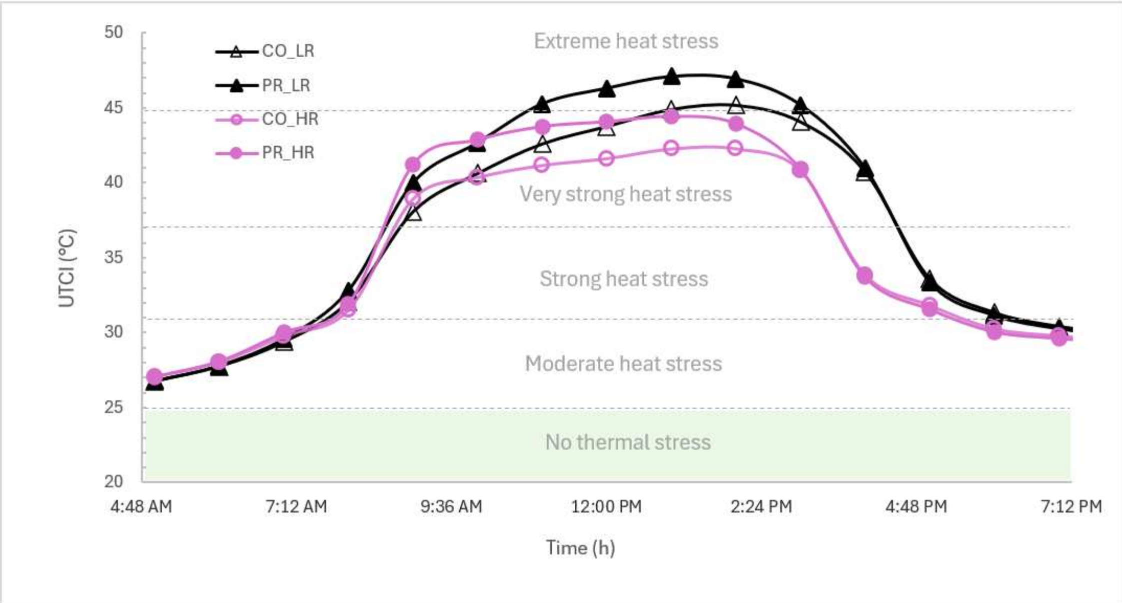

Source: Author, 2026.

After sunset, however, an inversion is observed: UTCI values in the RP scenario become slightly lower than in the CO scenario, with a maximum difference of –0.17 °C, suggesting a marginal improvement in thermal comfort during nighttime conditions. Nevertheless, these results are less favorable than those reported by Elmagri; Kamel; Ozer (2024), where cool pavement strategies provided nighttime UTCI reductions of up to 0.9 °C compared to conventional asphalt pavements in the arid climate of Arizona. One possible explanation for this discrepancy lies in the tropical climate of Fortaleza, where elevated nighttime temperatures persist and limit the cooling benefits of reflective materials. Additionally, as noted by Elmagri; Kamel; Ozer (2024), while high-albedo pavements may lower surface temperatures and contribute to better air quality by reducing ground-level ozone formation, they can also negatively affect pedestrian thermal comfort under high solar loads by increasing the amount of reflected radiation absorbed by the human body.

Figure 54 – Maps of absolute differences in UTCI (h = 1.4 m) between RP and CO simulations at 8:00 a.m., 12:00 p.m., 4:00 p.m., and 8:00 p.m. (dry season).

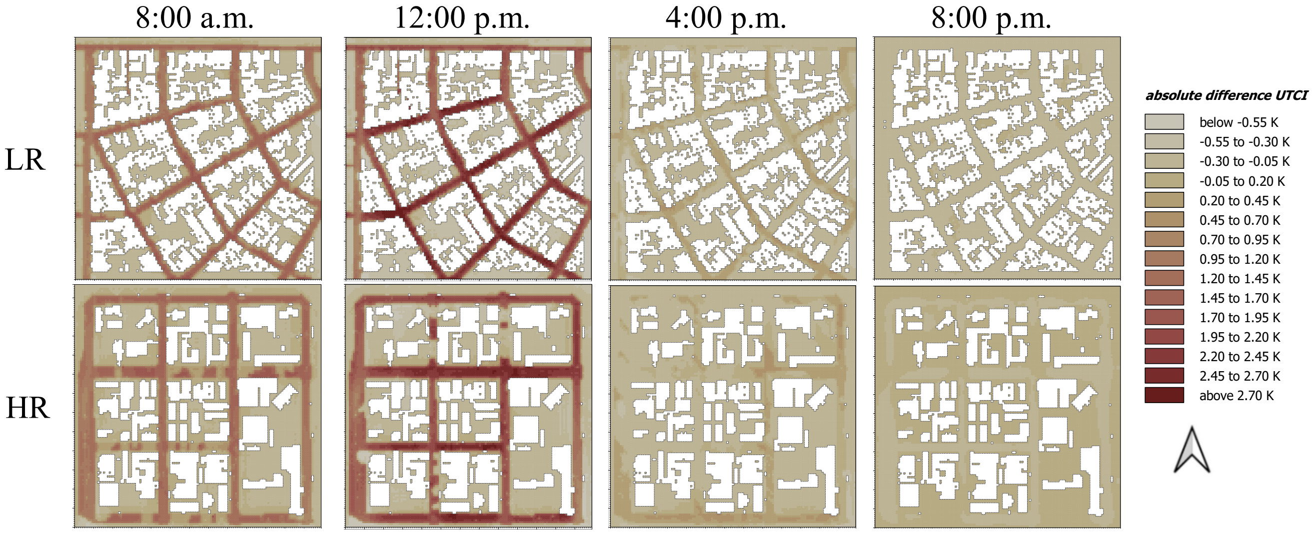

Source: Author, 2026.

The results can be partially explained by the distinct urban morphologies and environmental contexts of the two neighborhood areas. LR appears to experience higher temperatures and greater thermal discomfort, likely due to its narrower streets and the absence of lateral spacing between buildings, which hinders wind circulation and increases the absorption of reflected energy from the high-albedo reflective pavement. This urban configuration contributes to greater heat retention at the pedestrian level. In contrast, although HR has taller buildings, its proximity to the coast and the shading effects provided by these structures likely contribute to lower levels of thermal stress. These differences highlight how urban form and local environmental conditions can significantly influence thermal comfort. Moreover, such disparities may reflect underlying socioeconomic inequalities, as neighborhoods with lower HDI values tend to be more exposed to adverse microclimatic conditions, raising important concerns about climate justice.

5.3.8 Consideration of Local Acclimatization and Perception of Thermal Comfort

Even though UTCI is a widely used indicator for assessing outdoor thermal comfort, its application in tropical regions requires careful interpretation and, in many cases, methodological adjustment. The original UTCI classification was primarily developed and validated in temperate climates, which show a much broader range of thermal stress categories, including cold and very cold conditions that are uncommon in tropical urban environments, and a variation of heat stress not easy to identify in all-year-round hot weather. As a result, the UTCI tends to overestimate heat stress and underestimate the adaptive capacity of populations living in warm climates.

The climatic conditions of tropical cities, characterized by persistently high air temperatures, elevated humidity, and limited diurnal thermal amplitude, make several of the UTCI thermal-stress categories irrelevant or indistinguishable in practice. Because the UTCI scale is highly sensitive to radiant temperature and wind variation, its subclasses (e.g., slight heat stress, moderate heat stress, strong heat stress) may differ by only 1–2 °C. Petalas (2015) explicitly argues that using globally defined thresholds in tropical climates "penalizes" these environments by categorizing long periods as stressful when, in fact, local residents experience acceptable thermal conditions due to chronic heat exposure and long-term adaptation. This mismatch highlights that UTCI's globally standardized thresholds do not adequately reflect the physiological acclimatization or behavioral adaptation of populations living in warm and humid regions.

To address these limitations, Petalas (2015) proposes new locally adapted comfort thresholds for a tropical city. According to the author, the neutral comfort zone should lie between: UTCI = 27.5°C and 31.1°C. Applying this adjusted classification to Fortaleza provides a different interpretation of thermal comfort. According to the original UTCI scale (Figure 53), all simulated hours would be categorized as heat discomfort, including early morning periods, classified mostly as "moderate heat stress." However, using the adapted thresholds (Figure 55), conditions between 5 p.m. and 8 a.m. fall within the comfort range. Moreover, in some cases, conditions fall below 27.5 °C, which Petalas categorizes as "cool discomfort", indicating that residents may feel slightly cold, especially during the night and early morning hours.

To support and contextualize the UTCI analyses performed for the study areas, Figure 56 illustrates the spatial distribution of urban canyons classification based on the height-to-width ratio (H/W). From that, an elaborated hourly matrix of adjusted UTCI values was organized by street orientation (N/S and E/W) and canyon geometry expressed by the H/W ratio to combine analyses. Figure 20a and 20b show the thermal sensation for each hour of the day according to Petalas' (2015) locally adapted comfort thresholds, with color shading indicating thermal categories: blue for “cold discomfort,” green for “comfort,” and red for “heat discomfort.”

Figure 55 – Diurnal profiles of UTCI for all scenarios with an alternative acclimation threshold.

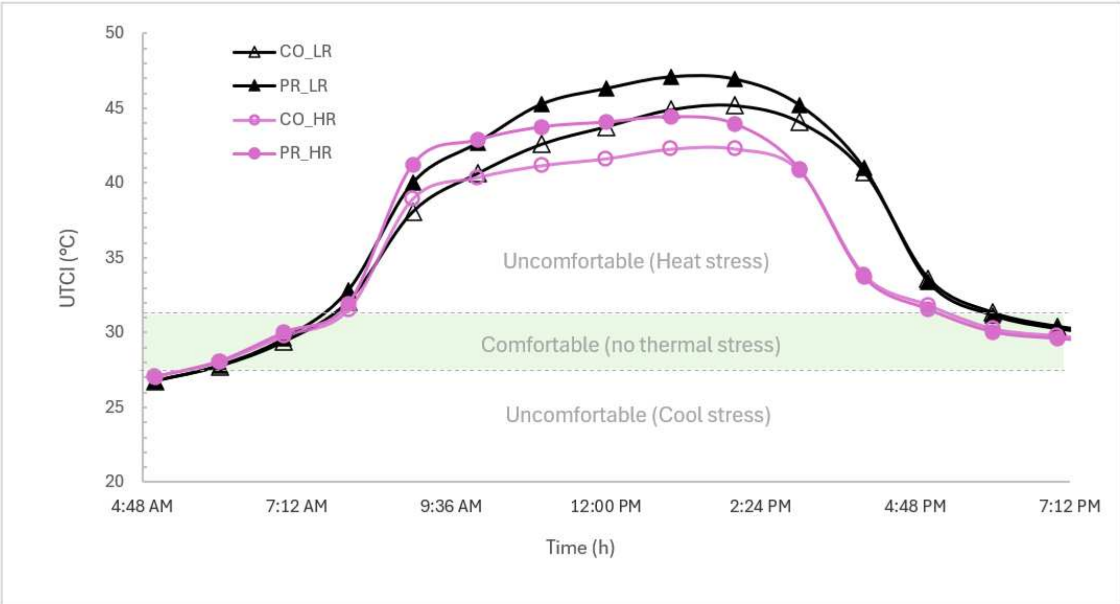

Source: Author, 2026.

Figure 56 – Diurnal profiles of UTCI for all scenarios with an alternative acclimation threshold.

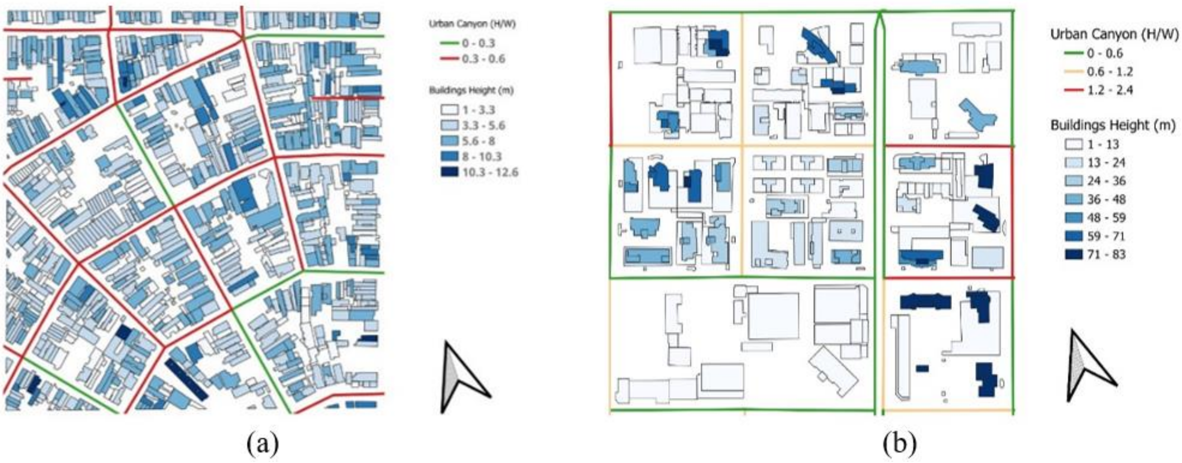

Source: Author, 2026.

When the UTCI is evaluated using the locally adapted limits, both neighborhoods exhibit thermal comfort only between approximately 5 pm and 7 am, whereas heat discomfort dominates from 8 am to 4 pm, following the daytime rise in air temperature and solar radiation.

A relevant pattern emerging from the matrices is that “cold discomfort” appears in the early evening and nighttime hours, especially along E/W-oriented streets. This probably stems from the interaction with the input Fortaleza’s predominant wind direction (≈104°), which aligns more favorably with E/W-oriented streets and enhances ventilation. As a result, these streets experience more efficient advective cooling during the nighttime.

Figure 57 highlights the influence of orientation and canyon depth on diurnal thermal perception: E/W-oriented streets tend to present cooler nighttime conditions due to their alignment with the prevailing wind direction, while variations in H/W reveal how canyon geometry modulates daytime heating and nocturnal cooling. The visualization supports the analysis of microclimatic differences among urban forms and their implications for outdoor thermal comfort.

Figure 57 – Hourly matrix of adjusted UTCI values organized by street orientation (N/S and E/W) and canyon geometry (H/W ratio) for: (a) LR and (b) HR.

Direction	N/S		E/W	
H/W	[0, 0.3]	[0.3, 0.6]	[0, 0.3]	[0.3, 0.6]
5 AM	25.88	24.91	25.4	24.08
6 AM	27.11	26.73	26.79	26.43
7 AM	32.99	34.07	32.15	33.4
8 AM	37.07	38.57	38.61	37.96
9 AM	40.04	40.56	40.59	39.85
10 AM	43.41	43.04	43.13	42.99
11 AM	45.24	44.75	44.77	44.74
12 PM	46.18	45.49	45.57	45.23
1 PM	46.52	45.8	45.92	45.19
2 PM	45.46	45.1	45.32	43.74
3 PM	42.47	42.76	42.77	39.76
4 PM	38.38	36.97	38.54	35.84
5 PM	32.37	31.41	31.76	30.29
6 PM	30.09	29.11	29.54	27.92
7 PM	29.28	28.33	28.77	27.08
8 PM	28.88	27.97	28.41	26.74
9 PM	28.63	27.76	28.2	26.56
10 PM	28.4	27.54	27.97	26.33

(a)

Direction	N/S		E/W		
H/W	[0, 0.6]	[0.6, 1.2]	[0, 0.6]	[0.6, 1.2]	[1.2, 2.4]
5 AM	26,78	26,92	23,69	23,30	23,46
6 AM	28,17	27,95	26,32	25,63	25,48
7 AM	33,37	29,93	32,37	31,69	30,98
8 AM	37,13	32,56	35,56	34,93	33,77
9 AM	39,34	40,19	37,91	37,23	35,43
10 AM	40,90	41,80	39,65	38,86	30,80
11 AM	42,67	43,07	40,76	39,96	32,94
12 PM	43,04	43,52	41,36	40,37	32,40
1 PM	42,40	44,02	41,69	36,93	32,06
2 PM	40,52	41,39	41,21	36,21	31,38
3 PM	36,54	39,71	39,43	31,78	30,61
4 PM	33,41	35,59	35,75	29,82	29,40
5 PM	31,26	31,72	28,76	27,96	27,64
6 PM	29,71	30,16	27,08	26,59	26,41
7 PM	29,25	29,68	26,65	26,18	26,01
8 PM	28,92	29,35	26,41	25,94	25,75
9 PM	28,70	29,12	26,25	25,78	25,57
10 PM	28,48	28,90	26,08	25,61	25,37

(b)

Source: Author, 2026.

For instance, in the LR, higher H/W ratios tend to produce cooler conditions, probably because moderately tall buildings provide intermittent shading during part of the day; in contrast, in the HR neighborhood, the effect of H/W ratios is more dependent on street orientation. Along N/S streets, taller canyons tend to be warmer because they obstruct wind channels aligned with the dominant 104° wind flow, reducing ventilation. Along E/W streets, however, higher H/W can promote cooler conditions, as the canyon alignment is more compatible with the incoming winds, which enhances channeling and convective heat removal. Overall, the HR neighborhood frequently appears more comfortable than the LR area, a result consistent with the creation of wind corridors and the shading from the taller constructions.

5.4 *Discussion of Urban Morphology, Thermal Comfort, and Limitations of Reflective Pavement Strategies in Tropical Cities*

The results of this study demonstrate that, although RP strategies are effective in reducing key thermophysical variables commonly investigated in pavement infrastructure studies (near-surface air temperature, surface temperature, and net radiation), their implications within the urban environment are more complex and highly dependent on urban morphology, climate conditions, and human exposure. In hot and humid tropical climates, these complexities are particularly relevant, as strategies that are beneficial from an energetic or infrastructural perspective may not necessarily translate into improved thermal comfort for pedestrians during periods of intense solar radiation.

Taken together, the urban morphology parameters indicate that the LR area, despite its lower building heights, exhibits a more thermally constrained urban configuration that may be particularly unfavorable from a microclimatic and thermal comfort perspective. Conversely, the HR area combines higher verticalization with relatively open canyons, highlighting that building height alone does not determine urban thermal conditions. These contrasting configurations provide an especially relevant framework for evaluating whether and how microclimatic impacts differ across urban canyon typologies, and for assessing how reflective pavement solutions respond to and interact with these morphological differences in terms of surface temperatures, radiative exchanges, and pedestrian thermal comfort.

From an energetic standpoint, the analysis of net radiation indicates subtle but meaningful differences between the two study areas. The LR neighborhood, characterized by predominantly horizontal urban canyons, exhibited a higher total daily reduction in net radiation when RP was applied. This suggests greater overall energetic efficiency, as shortwave radiation is more rapidly dissipated, leaving less energy available for heating the urban fabric. In contrast, the HR neighborhood, dominated by vertical urban canyons, tended to retain a larger fraction of net radiation. The increased presence of tall buildings promotes radiative trapping and multiple reflections, reducing the overall energetic efficiency of the RP strategy. This retained energy may contribute to increased indoor cooling demands, particularly during nighttime, potentially reinforcing feedbacks that exacerbate external heat loads through anthropogenic heat release.

When thermal comfort is considered, however, a contrasting pattern emerges. During periods of direct solar exposure, UTCI values were generally lower in the HR area, despite its lower energetic efficiency. This outcome is partially explained by the shading provided by taller buildings, the proximity of the HR area to the coastline, and the presence of wind corridors, especially aligned along the east–west (E/W) axis, which coincides with the prevailing regional wind direction. These factors collectively reduce direct solar exposure and enhance convective cooling at the pedestrian level. On the other hand, the LR area, with more confined horizontal canyons and limited shading, exposes pedestrians more directly to solar radiation, increasing heat stress during daytime. These spatial patterns intersect with social vulnerability: the HR area is associated with higher socioeconomic indicators and greater access to adaptive resources such as air conditioning and private mobility, whereas populations in LR areas are generally more exposed to outdoor thermal stress and more dependent on public space and active transport.

Despite the insights gained from applying microclimate simulations to the real scenarios in this study, it is necessary to acknowledge several practical limitations. The ENVI-met simulations were conducted with fixed wind speed and direction, which constrains the model's ability to represent the full variability of urban ventilation under real atmospheric conditions. Practical challenges related to the long-term performance and maintenance of reflective pavements in hot and humid tropical environments, such as soiling, moisture retention, biological growth, and material degradation, were not explicitly addressed and may reduce their effectiveness over time. Additionally, while UTCI is a widely adopted thermal comfort index, it may not fully capture the increase in mean radiant temperature caused by multiple reflections between buildings in dense urban environments and the acclimatization of the local population, as discussed earlier. This limitation may lead to an underestimation of pedestrian thermal stress in areas where reflective surfaces and complex geometries amplify radiative exchanges.

Taken together, these findings reinforce that reflective pavements should not be interpreted as a universal or standalone solution for urban heat mitigation in tropical cities. Their application must be context-sensitive and integrated with complementary strategies. Based on the results of this case study, reflective pavements are more likely to provide net benefits when applied along streets with higher H/W ratios, preferably oriented along the E/W direction, where shading, wind flow, and canyon geometry help offset increases in MRT. Moreover, RP strategies should be combined with nature-based solutions, particularly urban tree planting, which can significantly reduce radiant heat exposure through shading, as highlighted by Jia and Wang (2021), while also delivering co-benefits related to air quality and urban livability.

For urban designers and policymakers, these insights suggest that the deployment of reflective pavements should be selective and strategically targeted rather than widespread. Priority should be given to corridors with lower pedestrian exposure during peak solar hours or to areas where urban form and ventilation can mitigate adverse comfort effects. In socially vulnerable neighborhoods, where exposure to heat is highest, reflective pavements should only be implemented in conjunction with shading, greenery, and broader climate adaptation measures. Ultimately, effective urban heat mitigation in tropical cities requires a holistic approach that balances material-based interventions with urban design, social equity, and long-term climatic resilience.

5.5 Conclusions

This study aimed to evaluate the potential of high-albedo reflective pavement surfaces as a heat mitigation strategy in urban environments, using the city of Fortaleza, Brazil, as a case study. Firstly, the classification of LCZs and temperature anomaly analysis allowed for a detailed spatial understanding of intra-urban thermal variability and the definition of different urban canyon setting areas to investigate how the reflective pavement solution affects surface temperature, near-surface air temperature, and outdoor thermal comfort under typical summer conditions in a tropical climate. Simulations were conducted using the ENVI-met model, complemented by UTCI calculations through the BioMet tool.

This study indicates that RP strategies do not deliver uniform performance across different urban contexts, reinforcing the need for spatially sensitive and morphology-aware applications. The effectiveness of RP is conditioned by urban configuration parameters, including the presence and height of urban canyons, street orientation relative to prevailing wind directions, and the degree of shading provided by the built environment. These factors significantly modulate surface–atmosphere energy exchanges and, consequently, the microclimatic outcomes of RP implementation.

In tropical climates, the results indicate that reductions in air temperature, surface temperature, and net radiation alone are insufficient criteria for guiding the application of reflective pavements. Although RP contributes to cooling these variables, it simultaneously increases MRT by approximately 13 °C during peak solar exposure. This increase has direct implications for pedestrian thermal comfort and highlights MRT as a critical variable for assessing the real-world impacts of RP in hot and humid urban environments.

The combined analyses also emphasize the relevance of population acclimatization in thermal comfort assessments. While the UTCI is widely adopted and provides a standardized framework for comparative analysis, local adaptation to heat may influence thermal perception and tolerance. As such, reliance on UTCI alone may not fully capture how different populations experience and respond to changes induced by RP strategies, particularly in tropical cities where chronic heat exposure is common. After UTCI adaptation suggested, conditions between 5 p.m. and 8 a.m. fall within the comfort range, compatible with the lived experience of residents. Thermal comfort for pedestrians should be a central consideration in urban design, particularly in densely populated and socioeconomically vulnerable areas, where the balance between environmental benefits and human well-being becomes critical.

Overall, the results reinforce that reflective pavements should not be interpreted as a universal or standalone solution for urban heat mitigation in tropical cities. Based on this case study, RP strategies are more likely to yield net benefits when applied along streets with higher height-to-width ratios, preferably oriented in the east–west direction, where shading and ventilation can offset adverse radiative effects. Crucially, RP should be integrated with complementary mitigation and adaptation measure, such as urban vegetation and shading interventions, to ensure that infrastructure-level cooling benefits do not come at the expense of pedestrian thermal comfort and social equity.

Future research should explore the integration of high-albedo reflective pavements with other mitigation measures, such as vegetation, shading devices, and permeable surfaces, to assess potential synergies. Additionally, long-term monitoring and field experiments are needed to validate simulation results and better understand the behavior of these materials under real atmospheric conditions, especially regarding radiative fluxes and their interaction with the human body. Further studies could also investigate the social and spatial equity implications of applying such strategies in cities with pronounced disparities, advancing discussions on climate justice in urban planning.

6 FINAL THOUGHTS AND CONCLUSIONS

This session presents a set of reflections on the scientific papers developed within the scope of this dissertation, considering the period and circumstances in which they were produced. It may be regarded as a synthesis of what it is identified as the main contributions of this work to the state of the art, or, at the very least, to the Transportation and the Environment Research Group (TRAMA), particularly within the research line to which this doctorate is aligned: advanced characterization of pavement materials and pavement functionalization.

6.1 Session 2 (Bibliometric Analysis and Literature Review)

This review session emerged from the need to consolidate the principal and most relevant information on the state of the art of thermochromic technology applied to asphalt pavements. Although other literature reviews on thermochromic materials were found, they primarily addressed diverse applications and focused only on a small portion of their content on transportation infrastructure. This is unsurprising given that thermochromism in pavements is a relatively recent research topic, as emphasized in the reviewed scientific papers, whose bibliometric analysis shows that the earliest publications date back to 2013. Notably, during the first three years, all published studies originated from the same research group, and only later did the number of publications grow and diversify among other research groups.

In this context, this specific research paper stands out as a valuable and well-structured source specifically tailored to researchers in transportation infrastructure who are interested in exploring thermochromic materials in asphalt pavements' applications. It provides a comprehensive overview of bibliometric indicators, enabling an understanding of who the leading authors and institutions are, what research topics have been prioritized, and which methodological approaches have been adopted so far. It also synthesizes the main scientific advances achieved to date and, more importantly, the scientific gaps they leave for future studies and researchers. The writing process of this session was fundamental for identifying the major research gaps that subsequently guided the objectives and methodological choices explored in the following sessions of this dissertation.

One of the most prominent gaps revealed concerns the origin of the thermochromic microcapsules used in current asphalt pavement studies. Nearly all studies rely on commercial thermocapsules, which behave as a "black box", since their true chemical composition is not disclosed. Researchers, therefore, resort to reverse engineering and advanced characterization techniques to infer their internal structure and composition. After the publication of the review, however, a new study by Zhang and Xu (2024) was identified, representing a substantial contribution to the field. The authors synthesized their own thermochromic microcapsules using a chromogenic core composed of thermal red dye (as the recessive dye), bisphenol A (as the chromogenic agent), and tetradecanol (as the solvent), encapsulated in a urea-formaldehyde resin shell through in-situ polymerization. Their results demonstrated both successful encapsulation and reversible thermochromic performance.

Despite this advance, the synthesized microcapsules, like the commercial ones, still rely on bisphenol A, a compound with known carcinogenic potential and environmental concerns. This observation reinforces the opportunity for research on alternative core and shell materials that are safer, environmentally friendly, and more appropriate for surface-applied thermochromic solutions, which naturally experience greater exposure to weathering. Additionally, most existing studies utilize a “standard” transition temperature near 31 °C. For tropical regions such as Northeastern Brazil, where air temperatures often approach or exceed this threshold for much of the year, such a low transition temperature may limit the functional effectiveness of the thermochromic mechanism. Both issues, safer chemical formulations and climatically appropriate transition temperatures, were identified early in the conception of this dissertation and originally integrated into its objectives, although their development is still ongoing and thus not incorporated into the final written document.

Another major gap highlighted relates to the limited scientific investment in surface spray functionalization. Significant uncertainties remain regarding how such surface treatments alter the surface characteristics of asphalt mixtures, including adhesion, texture, anchorage, and long-term durability under environmental and traffic loading, especially for field use. These knowledge gaps became part of research questions in Sessions 3 and 4 of this dissertation, which employed innovative methods such as close-range photogrammetry, colorimetric analysis, and accelerated weathering chambers to evaluate the performance, degradation, and persistence of thermochromic surface coatings.

Importantly, in Session 2, it was also noted that no real-scale implementations of thermochromic solutions for pavements have been documented in the literature to date. The existing evidence is limited to laboratory studies or small-scale outdoor experiments, though many of these demonstrate promising reductions in surface temperatures of functionalized asphalt binder and mixtures. This context motivated the development of Session 5 of the dissertation, which investigates the large-scale application of high-reflectivity thermochromic-inspired solutions by computational microclimate simulations, considering land-use patterns, local microclimate conditions, and the potential impacts on air temperature and human thermal stress.

Finally, there is an additional contribution by adapting the technology readiness level (TRL) framework to assess the maturity of thermochromic pavement technologies. By grouping future perspectives into “research lab”, “simulated world”, and “real world” stages, it was provided a practical and forward-looking tool for researchers and practitioners seeking to understand the current level of development and the critical steps necessary for advancing thermochromism from experimental innovation to operational technology in road engineering.

In summary, this Session represented a fundamental and strategic starting point for the development of the present doctoral research, as it helped define subsequent methodological steps while consolidating the current state of knowledge on thermochromic materials applied to asphalt pavements. Beyond synthesizing updated scientific evidence, the study also presented a relevant degree of innovation in both content and structure. Methodologically, the originality of the work lies in the integrated approach combining bibliometric analysis and systematic literature review, structured around key technical dimensions: modifying agents and incorporation methods, optical and thermal performance of functionalized asphalt pavements, and their mechanical behavior. This structured synthesis not only clarifies the evolution of research trends but also identifies critical knowledge gaps and future research pathways. Furthermore, its publication in an open-access scientific journal enhances the visibility, accessibility, and dissemination potential of the findings, reinforcing its contribution to advancing scientific understanding in the field of thermochromic functionalization of asphalt materials. According to Scopus, the paper has received six citations to date, indicating its emerging impact within the scientific community.

6.2 Session 3 (Considerations of Surface Characteristics and Long-term Fracture Behavior of Functionalized Asphalt Mixtures)

Session 3 represents a significant outcome of the collaborative research undertaken during an academic mobility period at the University of Nebraska–Lincoln (UNL), supported by the CAPES PDSE program. Developed in partnership with the Infrastructure Materials & Pavement Research (IMPAR) Lab, the study benefited from the proven expertise of the research group led by Professor Jamilla Teixeira and from the direct technical support of the Ph.D. student Farzad Yazdipanah. Importantly, the work presents an innovative combination of two sustainable strategies in asphalt pavement engineering: the surface thermochromic functionalization of asphalt mixtures and the incorporation of 25% RAP (Reclaimed Asphalt Pavement) into the mix, a standard mixture widely used in academic and applied research within the Nebraska Department of Transportation (NDOT–NE).

Methodologically, this piece of work advances the state of the art by integrating surface, mechanical, and durability analyses to evaluate the functionalization process. The investigation focuses on (i) surface property variations (macrotexture and microtexture) before and after thermochromic spraying-coating, (ii) the adaptation of the pull-off test to evaluate the adhesion between the thermochromic coating and the asphalt substrate, and (iii) the long-term cracking performance of the functionalized asphalt mixtures subjected to the AASHTO R30 long-term aging protocol (AASHTO, 2002).

With respect to surface characteristics, the study makes a valuable methodological contribution by employing a combined close-range photogrammetry and digital image processing (CRP–DIP) approach. Although based on previous references such as Maia *et al.* (2024), this work innovates by adapting the method for cylindrical specimens and by developing a Python routine to extract surface texture parameters. This methodology was subsequently validated and calibrated using the AIMS surface analysis module, leading to an additional publication in which I am a co-author: Santos, Ribas, and Castelo Branco (2024). At present, this protocol has been incorporated into other research projects within the TRAMA research group to support surface and road safety evaluations. It is important to note, however, that 3D surface modelling tends to smooth the surface profile due to the interpolation procedures used to reconstruct geometry. Because the software does not provide full control over point-cloud generation or point density, ideally as high as possible, the accuracy of the model becomes strongly dependent on image quality. These limitations leave open questions that warrant further standardization and investigation in future work.

This chapter also contributes methodologically through the adapted use of the pull-off tester to assess the adhesion between thin coatings and the asphalt surface. Although pull-off failure mechanisms do not fully replicate field conditions, the technique offers significant advantages over the previously adopted tape test used by Alcantara (2024), originally adapted from paint adhesion protocols. In particular, the pull-off test improves procedural standardization, controlling pull rate, failure area, and damage mode, thereby minimizing operator subjectivity and enabling quantifiable comparisons of bond strength across studies.

Notably, the most compelling contribution of the work lies in its innovative investigation of cracking resistance. The hypothesis that thermochromic functionalization could act as a protective barrier against asphalt mixture aging was examined using the SCB test, comparing coated and uncoated specimens subjected to long-term aging (LTA). Given that one of the primary aging mechanisms in asphalt mixture is thermo-oxidative, the selected protocol AASHTO R30 (AASHTO, 2002) aimed to simulate degradation driven by heat and oxygen exposure. The findings indicate a promising improvement in cracking resistance, particularly for the 6% TCM coating, suggesting that higher coating contents may enhance resistance to aging-induced brittleness.

However, an important consideration must be emphasized: the aging protocol adopted does not incorporate the effects of solar radiation, even though the core thermochromic mechanism for surface temperature reduction operates through optical changes, namely, increased reflectivity resulting from color transitions. It is therefore plausible that different aging procedures, particularly those involving radiation exposure, could yield more pronounced functionalization benefits. This observation highlights a meaningful direction for future research.

Overall, the chapter provides substantive experimental evidence and methodological advances supporting the feasibility of thermochromic spray functionalization as a sustainable and potentially protective surface treatment for RAP-recycled asphalt mixtures. Its combined contributions to surface characterization protocols, adhesion assessment methods, and long-term cracking evaluation underscore its relevance for ongoing developments in sustainability-oriented pavement engineering.

6.3 Session 4 (Consideration of Optical-Thermal Balance and Durability of Functionalized Asphalt Mixtures)

Session 4 was initially submitted to the EATA Conference, subsequently invited for publication in *Road Materials and Pavement Design*, and later disseminated through a podium presentation at the conference held in Italy in July 2025. The study is marked by a particular methodological feature: the use of two different asphalt mixtures, one in the field and another in laboratory tests. This distinction resulted from the collaborative nature of the work, as the outdoor experimental tests were conducted in Brazil (UFC), while the accelerated degradation tests were carried out in the United States (UNL). Despite this peculiarity, the work offers a compelling contribution by integrating outdoors test-based and laboratory-based assessments focused on the cooling performance and durability of a thermochromic solution applied as a top layer into HMA samples. Specifically, the study examines the optical–thermal behavior of the coated surfaces and their resistance to environmental degradation.

The justification for conducting the Outdoor Solar Radiation Test in Fortaleza (Brazil) lies in its objective of capturing the typical heating behavior of asphalt pavements under the natural environmental conditions of a tropical summer day, conditions that contrast sharply with those of Nebraska (US). Beyond the experimental measurement of surface temperature reductions in functionalized samples, the study innovatively applies the field-observed data to the theoretical framework of the optical–thermal balance of pavement surfaces. This allowed for an estimation of the energetic benefits (i.e., cooling efficiency) deriving from the use of thermochromic coatings. Additionally, it was also possible to estimate the variation in surface albedo over the test period indirectly, through calculations and analysis of thermographic images. From this effort emerged the idea of designing a device capable of performing direct albedo measurements. The prototype, informally referred to as the "*albedômetro",* consists of two low-cost optical sensors mounted in opposite directions, one facing upward to capture incident radiation and the other facing downward to measure reflected radiation. The device is currently undergoing testing and validation.

The laboratory component of this part of the research aimed to advance the understanding of thermochromic solution durability under severe environmental stressors by simulating exposure to ultraviolet radiation and temperature–humidity cycles. The results highlight the critical influence of microcapsule materials on the resistance to degradation, particularly to UV radiation, an issue especially relevant because polymer-based shells are inherently susceptible to photodegradation. Building on previous TRAMA research (Alcantara, 2024), future studies may explore the incorporation of biopolymers, such as chitosan, either as the capsule shell or as part of the thermochromic solution formulation. Chitosan has shown promising adhesion properties for semiconductor particles (e.g., TiO_2) to asphalt substrates (Alcantara *et al.*, 2025) and may additionally act as a "sunscreen" protective layer for the surface, potentially enhancing the long-term durability of thermochromic functionalization.

Another point of methodological relevance lies in the apparent convergence of results from the UV–Vis reflectance tests and the colorimetry analyses after accelerated degradation. While not entirely interchangeable, given that spectral reflectance captures curve behavior across a wide range and colorimetry provides only numerical indicators of color coordinates, both methods led to similar conclusions regarding degradation patterns. This alignment suggests a potential methodological advantage: colorimetry, being considerably simpler and not dependent on sophisticated equipment, may serve as a practical alternative, particularly when full spectral analysis is not feasible.

Finally, it is worth noting that the paper received positive feedback from the scientific community during its conference presentation, generating engagement, questions, and expressing interest among attendees. This reception underscores both the innovative character of the study and its relevance to ongoing advancements in the state of the art regarding thermochromic pavement technologies. According to Scopus, the paper has received four citations to date, indicating its emerging impact within the scientific community.

6.4 Session 5 (Considerations of Microclimatic Simulations)

This session constitutes the broadest and most conceptually diverse component of the dissertation, as it encompasses themes ranging from urban landscape mapping and microclimate characterization, based on physical attributes of land cover and built form, such as local climate zones (LCZs), to the application of microclimatic models. In particular, it involves the use of computational fluid dynamics (CFD), a numerical simulation framework used to predict fluid behavior (air and other gases, in this case). Here, CFD was employed to examine how modifications in asphalt pavement surface albedo across distinct urban areas of Fortaleza (Brazil), differentiated by land-use patterns, LCZ classes, and urban geometries, affect air temperature, surface temperature, and components of the radiation balance in the lower atmosphere.

Although the application of LCZ classification to Fortaleza through the LCZ generator tool presents some known limitations, such as its maximum spatial resolution of 100 m, the resulting maps, together with subsequent data processing using LCZ4r, proved decisive in establishing objective criteria for identifying the city’s hottest zones and selecting areas for simulation. This step also contributed to current practice, as the LCZ maps generated became publicly available on the LCZ generator database, enabling other researchers and practitioners to explore and build upon these results.

The paper advances the discussion on reflective and thermochromic asphalt pavements by addressing a critical knowledge gap in microclimate simulations: the relationship between thermophysical improvements and actual human thermal perception. While most transportation-infrastructure studies emphasize reductions in surface temperature, near-surface air temperature, and net radiation as direct proxies for UHI mitigation, this research demonstrates that such improvements do not automatically translate into enhanced pedestrian thermal comfort. The findings reveal a complex interaction between albedo modification, urban morphology, and human exposure, particularly in hot and humid tropical climates. When analyzed through locally adapted UTCI thresholds, the results show that reflective pavements may reduce key energetic variables while simultaneously producing limited or even adverse comfort outcomes during peak solar hours, mainly due to increased mean radiant temperature (MRT) and radiative trapping in dense urban canyons. By incorporating adjusted comfort ranges proposed for tropical contexts, the study offers a more realistic interpretation of thermal stress, highlighting the importance of physiological acclimatization and long-term adaptation of local populations. This nuanced approach reinforces that sustainable urban-infrastructure decisions must integrate environmental performance with social and climatic context, rather than relying solely on generalized thermal indices.

It is equally important to recognize methodological and conceptual limitations affecting the interpretation of the simulation results. The ENVI-met simulations were conducted under simplified forcing conditions, with reduced meteorological inputs and fixed wind speed and direction, limiting the representation of real urban-atmosphere variability, particularly relevant in Fortaleza, where prevailing winds strongly influence pedestrian comfort and nocturnal cooling. Furthermore, although universal thermal climate index (UTCI) is widely adopted, its globally standardized classification does not fully capture local acclimatization patterns nor the amplification of radiant exchanges caused by multiple reflections within complex urban geometries. Even with the application of locally adapted thresholds, uncertainties remain regarding the subjective perception of comfort in tropical environments. Practical aspects not explicitly modeled, such as the thermochromic reversibly effect, may also alter long-term pavement performance. These limitations emphasize that reflective pavement strategies should be interpreted cautiously and implemented selectively, as part of integrated, morphology-sensitive, and socially equitable urban heat mitigation policies.

Other constraints arise from the spatial and computational limitations of the simulations. Each modeled area represented approximately 1 km², due to the chosen ENVI-met's high horizontal resolution (3 × 3 m) and the high level of geometric detail required. Even with access to a high-performance server, each scenario required roughly 120 hours of processing time. This computational burden was further exacerbated by the constraints of the student software license, which restricts the use of parallel computing cores.

Further limitation concerns the field data employed for model validation. These measurements were obtained during a 2021 urban climate monitoring campaign for another Ph.D. dissertation (Lima Júnior, 2023). Although potential climatic variations over the analyzed period cannot be ruled out, the measurements were primarily used for ENVI-met model calibration. Moreover, no significant urban morphological changes have occurred around the monitored sites and field measurements were not a core component of this dissertation. Therefore, any temporal inconsistencies are unlikely to compromise the overall reliability of the study's results.

In light of these considerations, the contribution should be viewed as an initial effort toward developing microclimate simulation studies for Fortaleza. This work opens several avenues for future research: simulations should be extended to other overheated areas of the city, such as industrial zones, as well as to "cool islands," such as the surroundings of Parque do Cocó. Comparative analyses using ENVI-met's *full forcing* mode are also recommended to better evaluate wind effects. Finally, incorporating data on atmospheric pollutant concentrations, such as NOx and CO, currently being collected by ongoing projects within the TRAMA group would enable more comprehensive assessments of microclimate, air quality, and human exposure and vulnerability.

REFERENCES

AASHTO. **Standard method of test for determining the fracture potential of asphalt mixtures using the Illinois Flexibility Index Test** (I-FIT). AASHTO TP 124-20. Washington, D.C., 2020.

AASHTO. **Standard Practice for Mixture Conditioning of Hot Mix Asphalt (HMA), AASHTO R 30**, Washington, D.C., 2002.

AKBARI, H.; MENON, S.; ROSENFELD, A. Global cooling: Increasing world-wide urban albedos to offset CO_2. **Climatic Change**, Boston, v. 94, n. 3-4, p. 275-286, 2009. DOI: https://doi.org/10.1007/s10584-008-9515-9.

ALCANTARA, A. P. M. P.; RIBAS, L. V. S.; SILVA, D. B.; BRITO, J. I. C.; FREITAS, E. F.; SOUSA, F. W.; CASTELO BRANCO, V. T. F. Chitosan-Doped TiO_2 Functionalized Asphalt Mixtures for NO_2 Mitigation Under High Pollution Levels. **Materials**, Switzerland v. 18, n. 18, p. 4292, 2025. DOI: https://doi.org/10.3390/ma18184292

ALCANTARA, Amanda Pontes Maia Pires. **Funcionalização de pavimentos asfálticos para redução de emissões de NO2:** um estudo de viabilidade. 2024. 143 f. Tese (Doutorado em Engenharia de Transportes) - Centro de Tecnologia, Universidade Federal do Ceará, Fortaleza, 2024.

ALDRICH, H. P. Frost Penetration Below Highway and Airfield Pavements. **HRB Bulletin**, [s. l.], v. 135, p. 124-149, 1956.

AL-QADI, I. L.; AURANGZEB, Q.; CARPENTER, S. H.; PINE, W. J.; TREPANIER, J. **Impact of high RAP contents on structural and performance properties of asphalt mixtures**. Urbana, IL: Illinois Center for Transportation, University of Illinois at Urbana-Champaign, 2012. (Research Report FHWA-ICT-12-002). Disponível em: https://www.ideals.illinois.edu/items/45794. Acesso em: 27 jun. 2026.

AL-QADI, I. L.; SAID, I. M.; ALI, U. M.; KADDO, J. R. Cracking prediction of asphalt concrete using fracture and strength tests. **International Journal of Pavement Engineering**, England, v. 23, n. 10, p. 3333-3345, 2022. DOI: https://doi.org/10.1080/10298436.2021.1892108.

ANJOS, M.; MEDEIROS, D.; CASTELHANO, F.; MEIER, F.; SILVA, T.; CORREIA, E.; LOPES, A. LCZ4r package R for local climate zones and urban heat islands. **Scientific Reports**, London, v. 15, p. 7710, 2025. DOI: https://doi.org/10.1038/s41598-025-92000-0.

APOSTOLIDIS, P.; LIU, X.; ERKENS, S.; SCARPAS, T. Oxidative aging of epoxy asphalt. **International Journal of Pavement Engineering,** England, v. 23, n. 5, p. 1471-1481, 2022. DOI: https://doi.org/10.1080/10298436.2020.1806278.

ASAEDA, T.; CA, V. T. Characteristics of permeable pavement during hot summer weather and impact on the thermal environment. **Building and Environment**, Oxford, v. 35, p. 363-375, 2000. DOI: https://doi.org/10.1016/S0360-1323(99)00020-7.

ASTM INTERNATIONAL. **Standard practice for operating fluorescent ultraviolet (UV) lamp apparatus for exposure of non-metallic materials**. ASTM G154-23. West Conshohocken: ASTM, 2023.

ASTM INTERNATIONAL. **Standard solar constant and zero air mass solar spectral irradiance tables**. ASTM E490-00, 2000.

ASTM INTERNATIONAL. **Standard test method for solar absorptance, reflectance, and transmittance of materials using integrating spheres**. ASTM E903-96. West Conshohocken: ASTM, 1996.

BASTOLA, N. R.; KHEDMATI, M.; YAZDIPANAH, F.; HAGHSHENAS, H. F. Investigating the field performance of high-recycled asphalt pavement mixtures with bio-oil recycling agent. **Transportation Research Record,** Washington, v. 2678, n. 10, p. 1004-1014, 2024. DOI: https://doi.org/10.1177/03611981241236189.

BECHTEL, B.; ALEXANDER, P. J.; BECK, C.; BÖHNER, J.; BROUSSE, O.; CHING, J.; DEMUZERE, M.; FONTE, C.; GÁL, T.; HIDALGO, J.; HOFFMANN, P.; MIDDEL, A.; MILLS, G.; REN, C.; SEE, L.; SISMANIDIS, P.; VERDONCK, M.-L.; XU, G.; XU, Y. Generating WUDAPT Level 0 data – Current status of production and evaluation. **Urban Climate,** Amsterdam, v. 27, p. 24-45, 2019. DOI: https://doi.org/10.1016/j.uclim.2018.10.001.

BERARDI, U.; GARAI, M.; MORSELLI, T. Preparation and assessment of the potential energy savings of thermochromic and cool coatings considering inter-building effects. **Solar Energy**, Oxford, v. 209, p. 493-504, 2020. DOI: https://doi.org/10.1016/j.solener.2020.09.015.

BLAZEJCZYK, K.; EPSTEIN, Y.; JENDRITZKY, G.; STAIGER, H.; TINZ, B. Comparison of UTCI to selected thermal indices. **International Journal of Biometeorology**, Netherlands, v. 56, n. 3, p. 515-535, 2012. DOI: https://doi.org/10.1007/s00484-011-0453-2.

BO, W.; LIU, J.; PENG, W.; PENG, W.; YU, B. Properties and characterization of temperature-responsive asphalt by using thermochromic powder. **Journal of Testing and Evaluation**, Conshohocken, PA, v. 49, n. 5, p. 3646–3664, 2021. DOI: https://doi.org/10.1520/JTE20200276.

BRÖDE, P.; FIALA, D.; BŁAŻEJCZYK, K.; HOLMÉR, I.; JENDRITZKY, G.; KAMPMANN, B.; TINZ, B.; HAVENITH, G. Deriving the operational procedure for the Universal Thermal Climate Index (UTCI). **International Journal of Biometeorology**, Netherlands, v. 56, n. 3, p. 481-494, 2012. DOI: https://doi.org/10.1007/s00484-011-0454-1.

BRUSE, D. **Decoding Urban Nature.** Essen, 2017.

CARNEIRO, J. O.; AZEVEDO, S.; TEIXEIRA, V.; FERNANDES, F.; FREITAS, E.; SILVA, H.; OLIVEIRA, J. Development of photocatalytic asphalt mixtures by the deposition and volumetric incorporation of TiO_2 nanoparticles. **Construction and Building Materials**, London, v. 38, p. 594-601, 2013. DOI: https://doi.org/10.1016/j.conbuildmat.2012.09.005.

CHATTERJEE, S.; KHAN, A.; DINDA, A.; MITHUN, S.; KHATUN, R.; AKBARI, H.; KUSAKA, H.; MITRA, C.; BHATTI, S. S.; DOAN, Q. V.; WANG, Y. Simulating micro-scale thermal interactions in different building environments for mitigating urban heat islands. **Science of the Total Environment**, Amsterdam, v. 663, p. 610–631, 2019. DOI: https://doi.org/10.1016/j.scitotenv.2019.01.299

CHEELA, V. R. S.; JOHN, M.; BISWAS, W.; SARKER, P. Combating Urban Heat Island Effect. A Review of Reflective Pavements and Tree Shading Strategies. **Buildings**, Switzerland, v. 11, p. 93, 2021. DOI: https://doi.org/10.3390/buildings11030093.

CHEN, Y.; LI, Z.; DING, S.; YANG, X.; GUO, T. Research on heat reflective coating technology of asphalt pavement. **International Journal of Pavement Engineering**, England, v. 23, n. 13, p. 4455-4464, 2022. DOI: https://doi.org/10.1080/10298436.2021.1952410.

CHENG, Y.; ZHANG, X.; FANG, C.; CHEN, J.; WANG, Z. Discoloration mechanism, structures and recent applications of thermochromic materials via different methods: a review. **Journal of Materials Science & Technology,** China, v. 34, n. 12, p. 2225-2234, 2018. DOI: https://doi.org/10.1016/j.jmst.2018.05.016.

CHEN, Z., ZHANG, H., DUAN, H., WU, C., ZHANG, S., 2021a. Long-term photo oxidation aging investigation of temperature-regulating bitumen based on thermochromic principle. **Fuel,** England, v. 286, part. 2, p. 119403, 2021. DOI: https://doi.org/10.1016/j.fuel.2020.119403.

CHEN, Z., ZHANG, H., DUAN, H., SHI, C. Improvement of thermal and optical responses of short-term aged thermochromic asphalt binder by warm-mix asphalt technology**. Journal of Cleaner Production,** London, v. 279, p. 123675, 2021. DOI: https://doi.org/10.1016/j.jclepro.2020.123675.

CHEN, Z.; LIU, J.; ZHANG, H.; KUANG, H.; ZHAO, M.; ZHANG, S. Comparative investigation of mechanical and cooling performance between thermochromic road materials prepared by wet/dry process. **Journal of Cleaner Production**, London, v. 360, p. 132158, 2022. DOI: https://doi.org/10.1016/j.jclepro.2022.132158.

CHEN, Z.; ZHANG, H.; SHI, C.; WEI, C. Rheological performance investigation and sustainability evaluation of asphalt binder with thermochromic powders under solar radiation. **Solar Energy Materials and Solar Cells**, Amsterdam, v. 191, p. 175-182, 2019. DOI: https://doi.org/10.1016/j.solmat.2018.11.017.

CHEN, Z.; ZHANG, H.; YANG, X.; LENG, Z.; TANG, Y. Cooling efficiency of thermochromic asphalt pavement material and its contribution to field performance enhancement of asphalt mixture. **Construction and Building Materials**, London, v. 411, p. 134562, 2024. DOI: https://doi.org/10.1016/j.conbuildmat.2023.134562.

CIVAN, L.; KURAMA, S. A review: preparation of functionalized materials/smart fabrics that exhibit thermochromic behavior. **Materials Science and Technology**, Thousand Oaks, v. 37, n. 18, p. 1405–1420, 2021. DOI: https://doi.org/10.1080/02670836.2021.2015844

DAWSON, A. R.; DEHDEZI, P. K.; HALL, M. R.; WANG, J.; ISOLA, R. Enhancing thermal properties of asphalt materials for heat storage and transfer applications. **Road Materials and**

Pavement Design, Abingdon, UK, v. 13, n. 4, p. 784–803, 2012. DOI: https://doi.org/10.1080/14680629.2012.735791.

DEMPSEY, B.; THOMPSON, M. A. Heat-Transfer Model for Evaluating Frost Action and Temperature Related Effects in Multilayered Pavement Systems. **Transportation Research Record**, Washington, v. 342, p. 39-56, 1970. Disponível em: https://onlinepubs.trb.org/Onlinepubs/hrr/1970/342/342-005.pdf. Acesso em: 27 jun. 2026.

DEMUZERE, M.; KITTNER, J.; BECHTEL, B. LCZ Generator: A Web Application to Create Local Climate Zone Maps. **Frontiers in Environmental Science**, Switzerland v. 9, p. 1-18, 2021. DOI: https://doi.org/10.3389/fenvs.2021.637455.

DETOMMASO, M.; COSTANZO, V.; NOCERA, F. Application of weather data morphing for calibration of urban ENVI-met microclimate models: results and critical issues**. Urban Climate**, Amsterdam, v. 38, p. 100895, 2021. DOI: https://doi.org/10.1016/j.uclim.2021.100895

DIMITROV, S.; POPOV, A.; ILIEV, M. An Application of the LCZ Approach in Surface Urban Heat Island Mapping in Sofia, Bulgaria. **Atmosphere**, Switzerland, v. 12, n. 11, p. 1370, 2021. DOI: https://doi.org/10.3390/atmos12111370.

DU, P.; CHEN, Z.; ZHANG, H. Rheological and aging behaviors of base and SBS modified asphalt with thermochromic microcapsule. **Construction and Building Materials**, London, v. 200, p. 1-9, 2019. DOI: https://doi.org/10.1016/j.conbuildmat.2018.12.083.

DU, R.; LIU, C.-H.; LI, X.-X. A new method for detecting urban morphology effects on urban-scale air temperature and building energy consumption under mesoscale meteorological conditions. **Urban Climate,** Amsterdam, v. 53, p. 101775, 2024. DOI: https://doi.org/10.1016/j.uclim.2023.101775.

ELMAGRI, H.; KAMEL, T. M.; OZER, H. Assessment of the effectiveness of cool pavements on outdoor thermal environment in urban areas. **Building and Environment,** Oxford**,** v. 266, p. 112095, 2024. DOI: https://doi.org/10.1016/j.buildenv.2024.112095.

EMMANUEL, R.; JOHANSSON, E. Influence of urban morphology and sea breeze on hot humid microclimate: The case of Colombo, Sri Lanka. **Climate Research,** Germany, v. 30, n. 3, p.189–200, 2006. DOI: https://doi.org/10.3354/cr030189

ERELL, E.; PEARLMUTTER, D.; WILLIAMSON, T. **Urban Microclimate**: Designing the Spaces Between Buildings. London: Taylor & Francis, 2011.

FORTUNIAK, K., 2008. Numerical estimation of the effective albedo of an urban canyon. **Theoretical and Applied Climatology,** Vienna v. 91, p. 245–258, 2008. DOI: https://doi.org/10.1007/s00704-007-0312-6

GARSHASBI, S.; SANTAMOURIS, M. Using advanced thermochromic technologies in the built environment: Recent development and potential to decrease the energy consumption and fight urban overheating. **Solar Energy Materials and Solar Cells**, Amsterdam, v. 191, p. 21-32, 2019. DOI: https://doi.org/10.1016/j.solmat.2018.10.023.

GARTLAND, L. **Ilhas de calor**: como mitigar zonas de calor em áreas urbanas. São Paulo: Oficina de Textos, 2010.

GOLDEN, J. S.; KALOUSH, K. E. Mesoscale and microscale evaluation of surface pavement impacts on the urban heat island effects. **International Journal of Pavement Engineering**, England, v. 7, p. 37-52, 2006. DOI: https://doi.org/10.1080/10298430500505325.

GRIMMOND, S. Urbanization and global environmental change: local effects of urban warming. **The Geographical Journal**, [s. l.], v. 173, n. 1, p. 83-88, 2007. DOI: https://doi.org/10.1111/J.1475-4959.2007.232_3.X.

GUPTA, A.; KUMAR, N.; SACHDEVA, A. Factors affecting the ageing of polymer composite: A state of art. **Polymer Degradation and Stability**, Oxford, v. 221, p. 110670, 2024. DOI: https://doi.org/10.1016/j.polymdegradstab.2024.110670.

HARTLEY, K. Infrastructure and SDG localization: the 21st century mandate. **Environmental Research: Infrastructure and Sustainability**, England, v. 2, n. 1, p. 013001, 2022. DOI: https://doi.org/10.1088/2634-4505/ac442a.

HU, J.; GAO, Q.; YU, X. Characterization of the optical and mechanical properties of innovative multifunctional thermochromic asphalt binders. **Journal of Materials in Civil Engineering,** New York, v. 27, n. 5, p. 04014171, 2015. DOI: https://doi.org/10.1061/(ASCE)MT.1943-5533.0001132.

HU, J.; WANASEKARA, N.; YU, X. Thermal properties of thermochromic asphalt binders by modulated differential scanning calorimetry. **Transportation Research Record**, Washington, v. 2444, p. 142-150, 2014. DOI: https://doi.org/10.3141/2444-16.

HU, J.; YU, X. Performance evaluation of solar-responsive asphalt mixture with thermochromic materials and nano-TiO_2 scatterers. **Construction and Building Materials**, London, v. 247, p. 118605, 2020. DOI: https://doi.org/10.1016/j.conbuildmat.2020.118605.

HU, J.; YU, X. B. Adaptive building roof by coupling thermochromic material and phase change material: energy performance under different climate conditions. **Construction and Building Materials**, London, v. 262, p. 120481, 2020. DOI: https://doi.org/10.1016/j.conbuildmat.2020.120481.

HU, J.; YU, X. Experimental study of sustainable asphalt binder. **Transportation Research Record**, Washington, v. 2372, n. 1, p. 108-115, 2013. DOI: https://doi.org/10.3141/2372-12.

HU, J.; YU, X. Innovative thermochromic asphalt coating: characterization and thermal performance. **Road Materials and Pavement Design**, France, v. 17, p. 187-202, 2016. DOI: https://doi.org/10.1080/14680629.2015.1068215.

HU, J.; YU, X. Reflectance spectra of thermochromic asphalt binder: characterization and optical mixing model. **Journal of Materials in Civil Engineering**, New York, v. 28, p. 04015121, 2016. DOI: https://doi.org/10.1061/(ASCE)MT.1943-5533.0001387.

HU, Z.; XU, T.; LIU, P.; OESER, M. Developed photocatalytic asphalt mixture of open graded friction course for degrading vehicle exhaust. **Journal of Cleaner Production**, London, v. 279, p. 123453, 2021. DOI: https://doi.org/10.1016/j.jclepro.2020.123453.

HU, K.; CHEN, Y.; CHEN, G.; DUAN, Y.; YU, C. Proposed cool coatings with high near-infrared reflectance and heat insulation for asphalt pavement. **Coatings** Switzerland, v. 11, n. 85, p. 1-15, 2021. DOI: https://doi.org/10.3390/coatings11010085.

INSTITUTO BRASILEIRO DE GEOGRAFIA E ESTATÍSTICA. **Censo Demográfico 2022**: resultados preliminares. Rio de Janeiro: IBGE, 2023.

INTERGOVERNMENTAL PANEL ON CLIMATE CHANGE. **Climate Change 2021 –** The Physical Science Basis. Cambridge: Cambridge University Press, 2023.

INTERGOVERNMENTAL PANEL ON CLIMATE CHANGE. C**limate Change 2022** – Impacts, Adaptation and Vulnerability. Cambridge: Cambridge University Press, 2023.

INTERNATIONAL COMMISSION ON ILLUMINATION. **Colorimétrie** – Partie 4: Espace Chromatique Lab CIE 1976. Vienna: CIE, 1976.

INTERNATIONAL ENERGY AGENCY. **CO_2 Emissions from Fuel Combustion 2021.** Paris: International Energy Agency, 2021. Disponível em: https://www.iea.org/reports/global-energy-review-co2-emissions-in-2021. Acesso em: 12 mar. 2026.

INTERNATIONAL ENERGY AGENCY. **Global energy review:** CO_2 emissions in 2021**.** Paris: IEA, 2021. Disponível em: https://www.iea.org/reports/global-energy-review-co2-emissions-in-2021. Acesso em: 12 mar. 2026.

INSTITUTO DE PESQUISA E ESTRATÉGIA ECONÔMICA DO CEARÁ. **Portal de Mapas e Dados do IPECE**. 2024. Disponível em: https://mapas.ipece.ce.gov.br/i3geo/interface/gm.phtml. Acesso em: 27 jun. 2026.

JIA, S.; WANG, Y. Effect of heat mitigation strategies on thermal environment, thermal comfort, and walkability: a case study in Hong Kong. **Building and Environment,** Oxford, v. 201, p. 107988, 2021. DOI: https://doi.org/10.1016/j.buildenv.2021.107988.

JIANG, J.; JIN, Y.; BAO, T.; OU, X. Sensible heat discharging from pavements with varying thermophysical properties. **Sustainable Cities and Society**, Amsterdam, v. 45, p. 431-438, 2019. DOI: https://doi.org/10.1016/j.scs.2018.11.023.

JOHANSSON, E. Influence of urban geometry on outdoor thermal comfort in a hot dry climate: A study in Fez, Morocco. **Building and Environment,** Oxford**, v.** 41, n. 10, p. 1326–1338, 2006. DOI: https://doi.org/10.1016/j.buildenv.2005.05.022

KARLESSI, T.; SANTAMOURIS, M.; APOSTOLAKIS, K.; SYNNEFA, A.; LIVADA, I. Development and testing of thermochromic coatings for buildings and urban structures. **Solar Energy**, Oxford, v. 83, p. 538-551, 2009. DOI: https://doi.org/10.1016/j.solener.2008.10.005.

KEYMANESH, M. R.; AMANI, S.; OMRAN, A. T.; KARIMI, M. M. Evaluation of the impact of long-term aging on fracture properties of warm mix asphalt (WMA) with high RAP contents. **Construction and Building Materials**, London, v. 400, p. 132671, 2023. DOI: https://doi.org/10.1016/j.conbuildmat.2023.132671

KIM, I. R.; CASTERONA, C.; ELWARDANY, M.; RAD, F. Y. Long-Term Aging of Asphalt Mixtures for Performance Testing and Prediction. *In*: NATIONAL cooperative highway research program. Washington, DC: The National Academies Press, 2017. (NCHRP Research Report 871). Disponível em: https://doi.org/10.17226/24959. Acesso em: 12 mar. 2026.

KOLOKOTSA, D.; GIANNARIAKIS, G.; GOBAKIS, K.; GIANNARAKIS, G.; SYNNEFA, A.; SANTAMOURIS, M. Cool roofs and cool pavements application in Acharnes, Greece. **Sustainable Cities and Society**, Amsterdam, v. 37, p. 466-474, 2018. DOI: https://doi.org/10.1016/j.scs.2017.11.035

KOTHARKAR, R.; BAGADE, A.; SINGH, P. R. A systematic approach for urban heat island mitigation strategies in critical local climate zones of an Indian city. **Urban Climate**, Amsterdam, v. 34, p. 100701, 2020. DOI: https://doi.org/10.1016/j.uclim.2020.100701.

KOWALSKI, L. F.; LOPES, A. M. S.; MASIERO, E. Integrated effects of pavement simulation models and scale differences on the thermal environment of tropical cities. **City and Built Environment,** [s. l.], v. 2, n. 1, p. 9, 2024. DOI: https://doi.org/10.1007/s44213-024-00032-5.

KUYYAKANONT, A.; IWATA ,M. Study of different degradation effects in UV-sensitive polymers using xenon lamp and deuterium lamp to simulate UV irradiation in space environment. **Nuclear Instruments and Methods in Physics Research Section B: Beam Interactions with Materials and Atoms**, Amsterdam, v. 549, p. 165267, 2024. DOI: https://doi.org/10.1016/j.nimb.2024.165267

KYRIAKODIS, G.-E.; SANTAMOURIS, M. Using reflective pavements to mitigate urban heat island in warm climates - Results from a large scale urban mitigation project. **Urban Climate**, Amsterdam, v. 24, p. 326-339, 2018. DOI: https://doi.org/10.1016/j.uclim.2017.02.002.

LI, L.; CHEN, Z.; ZHANG, H.; DUAN, H. Effect of thermochromic materials on the properties of SBS-modified asphalt mixture. **Journal of Materials in Civil Engineering,** New York, v. 32, n. 12, p. 1-6, 2020. DOI: https://doi.org/10.1061/(ASCE)MT.1943-5533.0003489.

LI, L.; ZHANG, H.; CHEN, Z. Effect of thermochromic materials on physical and aging properties of SBS modified asphalt. **Petroleum Science and Technology**, Philadelphia, v. 36, n. 24, p. 2119-2124, 2018. DOI: https://doi.org/10.1080/10916466.2018.1533863.

LI, L.; ZHANG, H.; CHEN, Z.; WEI, C. Physical and rheological evaluation of aging behaviors of SBS modified asphalt with thermochromic powders. **Construction and Building Materials**, London, v. 193, p. 135-141, 2018. DOI: https://doi.org/10.1016/j.conbuildmat.2018.10.197.

LI, Q.; HU, T.; LUO, S.; GAO, L.; WANG, C.; GUAN, Y. Evaluation of cooling effect and pavement performance for thermochromic material modified asphalt mixtures under solar radiation. **Construction and Building Materials**, London, v. 261, p. 120589, 2020. DOI: https://doi.org/10.1016/j.conbuildmat.2020.120589.

LI, Q.; JIANG, J.; HU, T.; MENG, Y.; GAO, L.; LUO, S. Laboratory evaluation of rutting resistance for asphalt binders and mixtures modified with different thermochromic microcapsule powders. **Construction and Building Materials**, London, v. 252, p. 119099, 2020. DOI: https://doi.org/10.1016/j.conbuildmat.2020.119099.

LI, R.; LENG, Z.; ZHANG, Y.; MA, X. Preparation and characterization of waterborne epoxy modified bitumen emulsion as a potential high-performance cold binder. **Journal of Cleaner Production**, London, v. 235, p. 1265-1275, 2019. DOI: https://doi.org/10.1016/j.jclepro.2019.06.267.

LIMA JUNIOR, A. F.; GOMES, F. I. B. P.; ZANELLA, M. E. The Heat Index (HI) in the city of Fortaleza, Ceará. **Sociedade & Natureza**, [s. l.], v. 37, n. 1, 2024. DOI: 10.14393/SN-v37-2025-73091. Disponível em: https://seer.ufu.br/index.php/sociedadenatureza/article/view/73091. Acesso em: 27 jun. 2026.

LIMA JÚNIOR, A.; RIBEIRO, I.; AMORIM, J. H. Parques urbanos e ilhas de frescor: a importância do Parque do Cocó para o conforto térmico na cidade de Fortaleza/CE. **Geo UERJ**, Rio de Janeiro, n. 45, 2024. DOI: 10.12957/geouerj.2024.80373. Disponível em: https://www.e-publicacoes.uerj.br/geouerj/article/view/80373. Acesso em: 27 jun. 2026.

LIMA JÚNIOR, Antonio Ferreira. **Clima urbano:** análise do campo térmico e sugestão de áreas prioritárias para implementação de medidas mitigadoras. 2023. 261f. Tese (Doutorado em Geografia) - Centro de Ciências, Universidade Federal do Ceará, Fortaleza, 2023.

LIMA JÚNIOR, O.; CARDOSO, P.; ROCHA SEGUNDO, I.; FREITAS, E.; COSTA, M. F. M.; NASCIMENTO, H.; AFONSO, C.; LANDI JÚNIOR, S.; TEIXEIRA, V.; CARNEIRO, J. O. Thermochromism applied to Transportation Engineering: asphalt roads and paints. **Journal of Physics: Conference Series,** v. 2407, p. 1-6, 2022. DOI: https://doi.org/10.1088/1742-6596/2407/1/012042

LIMA JÚNIOR, O.; FREITAS, E.; CARDOSO, P.; ROCHA SEGUNDO, I.; MARGALHO, E.; MOREIRA, L.; NASCIMENTO, J. H. O., LANDI, S;, CARNEIRO, J. Mitigation of urban heat island effects by thermochromic asphalt pavement. **Coatings,** Switzerland, v. 13, p. 1-15, 2023. DOI: https://doi.org/10.3390/ coatings13010035.

LIU, D.; HU, S.; LIU, J. Contrasting the performance capabilities of urban radiation field between three microclimate simulation tools. **Building and Environment**, Oxford, v. 175, p. 106789, 2020. DOI: https://doi.org/10.1016/j.buildenv.2020.106789

LU, Y.; RAHMAN, M. A.; MOORE, N. W.; GOLROKH, A. J. Lab-Controlled Experimental Evaluation of Heat-Reflective Coatings by Increasing Surface Albedo for Cool Pavements in Urban Areas. **Coatings,** Switzerland**,** v. 12, n. 1, p.1-24, 2022. DOI: https://doi.org/10.3390/coatings12010007

MAIA, R.S.; HAJJ, R. M.; CUNTO, F. J. C.; BRANCO, V. T. F. C. Safety-oriented urban pavement design and evaluation: integrating microscopic simulation and tyre-pavement friction. **International Journal of Pavement Engineering**, England, v. 25, n. 1, p. 2345138,

2024. DOI: https://doi.org/10.1080/10298436.2024.2345138

MALICK, R. B.; CHEN, B. L.; BHOWMICK, S. Harvesting energy from asphalt pavements and reducing the heat island effect. **International Journal of Sustainable Engineering,** Oxon, v. 2, p. 214-228, 2009. DOI: https://doi.org/10.1080/19397030903121950.

MANSELL, P.; VAN ROOYEN, D.; PHILBIN, S.; SABINI, L. Infrastructure projects' assessment through SDG targets: towards a comprehensive framework. **Engineering Project Organization Journal**, Madras Chennai, India, v. 10, n. 2, p. 34, Sept. 2024. DOI: https://doi.org/10.25219/epoj.2021.00108.

MARTÍN, Y.; PANEQUE, P. Moving from adaptation capacities to implementing adaptation to extreme heat events in urban areas of the European Union: Introducing the U-ADAPT! research approach. **Journal of Environmental Management**, London, v. 310, p. 114773, 2022. DOI: https://doi.org/10.1016/j.jenvman.2022.114773.

MONTEIRO, C. A. F. A. A cidade como processo derivador ambiental e a geração de um clima urbano. **Geosul**, Florianópolis, v. 5, n. 9, p. 75-107, 1990.

MOURA, M. O.; ZANELLA, M. E.; SALES, M. C. L. Ilhas térmicas na cidade de Fortaleza/CE. **Boletim Goiano de Geografia**, Goiânia, v. 28, n. 2, p. 33-44, 2008. DOI: https://doi.org/10.5216/bgg.v28i2.5718.

MUENCH, S.; DAM, T. V.; RAM, P.; SMITH, K. **Pavement resilience:** state of the practice: FHWA-HIF-23-006. Washington, DC: Federal Highway Administration, 2023. Disponível em: https://www.fhwa.dot.gov/pavement/concrete/pubs/hif23006.pdf. Acesso em: 12 mar. 2026.

NATIONAL OCEANIC AND ATMOSPHERIC ADMINISTRATION. **NOAA holistic climate and Earth system model strategy:** phase I report**.** Washington, DC: NOAA, 2015.

OKE, T. R.; MILLS, G.; CHRISTEN, A.; VOOGT, J. A. **Urban Climates**. Cambridge: Cambridge University Press, 2017.

OZER, H.; AL-QADI, I. L.; SINGHVI, P.; KHAN, T.; RIVERA-PEREZ, J.; EL-KHATIB, A. Fracture characterization of asphalt mixtures with high recycled content using Illinois semicircular bending test method and flexibility index. **Transportation Research Record**, Washington, v. 2575, n. 1, p. 130-137, 2016. DOI: https://doi.org/10.3141/2575-14.

PANÁK, O.; DRŽKOVÁ, M.; KAILOVÁ, N.; SYROVÝ, T. Colorimetric analysis of thermochromic samples in different forms employing a digital camera. **Measurement**, London, v. 127, p. 554-564, 2018. DOI: https://doi.org/10.1016/j.measurement.2018.06.025.

PETALAS, K. V. **Estudo da sensação térmica e definição de limites de conforto para espaços abertos na cidade de Fortaleza, CE.** 2015. 272 f. Tese (Doutorado em Engenharia Civil: Saneamento Ambiental) - Centro de Tecnologia, Universidade Federal do Ceará, Fortaleza, 2015.

PETALAS, K.; MOTA, F. S. B. Avaliação das condições bioclimáticas da região costeira do nordeste brasileiro: o município de Fortaleza - CE. **Revista Brasileira de Climatologia**, Curitiba, v. 13, p. 185-201, 2013.

PIGLIAUTILE, I.; CHÀFER, M.; PISELLO, A. L.; PÉREZ, G.; CABEZA, L. F. Inter-building assessment of urban heat island mitigation strategies: Field tests and numerical modelling in a simplified-geometry experimental set-up. **Renewable Energy,** Oxford, v. 147, part. 1, p. 1663-1675, 2020. DOI: https://doi.org/10.1016/j.renene.2019.09.082.

PINHEIRO, C.; LANDI, S.; LIMA, O.; RIBAS, L.; HAMMES, N.; SEGUNDO, I. R.; HOMEM, N. C.; CASTELO BRANCO, V.; FREITAS, E.; COSTA, M. F.; CARNEIRO, J. Advancements in phase change materials in asphalt pavements for mitigation of urban heat island effect: Bibliometric analysis and systematic review. **Sensors**, Basel, v. 23, p. 7741, 2023. DOI: https://doi.org/10.3390/s23187741.

PISELLO, A. L. State of the art on the development of cool coatings for buildings and cities. **Solar Energy**, Oxford, v. 144, p. 660-680, 2017. DOI: https://doi.org/10.1016/j.solener.2017.01.068.

QIN, Y.; HILLER, J. E. Understanding pavement-surface energy balance and its implications on cool pavement development. **Energy and Buildings,** Lausanne, v. 85, p. 389-399, 2014. DOI: https://doi.org/10.1016/j.enbuild.2014.09.076.

RAHMANI, N.; SHARIFI, A. Comparative analysis of the surface urban heat island (SUHI) effect based on the local climate zone (LCZ) classification scheme for two Japanese cities, Hiroshima, and Sapporo. **Climate**, Basel, v. 11, n. 7, p. 142, 2023. DOI: https://doi.org/10.3390/cli11070142.

RATTI, C.; DI SABATINO, S.; BRITTER, R. Urban texture analysis with image processing techniques: Winds and dispersion. **Theoretical and Applied Climatology**, Vienna, v. 84, p. 77–90, 2005. DOI: https://doi.org/10.1007/s00704-005-0146-z

RIBAS, L. V. S.; ROCHA SEGUNDO, I.G.; CARNEIRO, J.; FREITAS, E.F.; CASTELO BRANCO, V.T.F. Research trends on thermochromic asphalt mixtures functionalization: bibliometric analysis and review. **Cleaner Materials**, v. 14, p. 100273, 2024. DOI: 10.1016/j.clema.2024.100273.

RIBAS, L. V. S.; SANTOS, J. R. P.; LIMA, K.; TEIXEIRA, J. E. S. L.; CASTELO BRANCO, V. T. F. Assessment of optical-thermal balance and environmental degradation of a thermochromic-coated asphalt mixture for urban heat mitigation. **Road Materials and Pavement Design**, France, v. 26, n. sup1, p. 537-552, 2025. DOI: https://doi.org/10.1080/14680629.2025.2482846.

RIBAS, L. V. S.; ALCANTARA, A. P. M. P.; BARBOSA, L. M.; CASTRO BRITO, J. I.; CASTELO BRANCO, V. T. F. Asphalt emissions in paving production, transportation, placement and in-service temperature conditions. **Road Materials and Pavement Design**, France, p. 1-17, 20 may, 2025. DOI: https://doi.org/10.1080/14680629.2025.2479215.

RIBAS, L. V. S.; YAZDIPANAH, F.; SANTOS, J. R. P.; TEIXEIRA, J. E. S. L.; CASTELO BRANCO, V. T. F. Evaluation of surface characteristics and long-term fracture behaviour of asphalt mixtures functionalised by thermochromic spraying coating. **International Journal of Pavement Engineering**, v. 26, p. 1-18, n. 1, 2025. DOI: 10.1080/10298436.2025.2544897.

RIBAS, L.; ROCHA SEGUNDO, I.; CARNEIRO, J.; CASTELO BRANCO, V. Tendências de pesquisa sobre funcionalização de misturas asfálticas termocromáticas e materiais de mudança de fase na mitigação de ilhas de calor: uma análise bibliométrica. *In*: CONGRESSO DE ENSINO E PESQUISA EM TRANSPORTES, 36, 2022, Fortaleza. **Anais […]** Fortaleza: ANPET, 2022. Disponível em: https://proceedings.science/anpet/anpet-2022/trabalhos/tendencias-de-pesquisa-sobre-funcionalizacao-de-misturas-asfalticas-termocromati?lang=pt-br. Acesso em: 27 jun. 2026.

ROCHA SEGUNDO, I.; FREITAS, E.; BRANCO, V. T. F. C.; LANDI, S.; COSTA, M. F.; CARNEIRO, J. O. Review and analysis of advances in functionalized, smart, and multifunctional asphalt mixtures. **Renewable and Sustainable Energy Reviews,** Oxford, v. 151, p. 111552, 2021. DOI: https://doi.org/10.1016/j.rser.2021.111552.

ROCHA SEGUNDO, I.; LANDI JÚNIOR, S.; OLIVEIRA, S. M. B.; FREITAS, E. F.; CARNEIRO, J. A. O. Photocatalytic asphalt mixtures: mechanical performance and impacts of traffic and weathering abrasion on photocatalytic efficiency. **Catalysis Today**, Amsterdam, v. 326, p. 94-100, 2019. DOI: https://doi.org/10.1016/j.cattod.2018.07.012.

ROCHA SEGUNDO, I.; LANDI JÚNIOR, S.; OLIVEIRA, S.; FREITAS, E.; COSTA, M. F.; CARNEIRO, J. Photocatalytic asphalt mixtures: Semiconductors' impact in skid resistance and texture. **Road Materials and Pavement Design**, France, v. 20, n. sup2, p. S578-S589, 2019. DOI: https://doi.org/10.1080/14680629.2019.1624398.

ROCHA SEGUNDO, I.; LIMA JÚNIOR, O.; AFONSO, C.; FREITAS, E.; CARNEIRO, J. Mapping the evolution of the world literature on smart asphalt: a bibliometric analysis. *In*: INTERNATIONAL SYMPOSIUM OF ASPHALT PAVEMENTS, 1., 2022, Costa Rica. **Anais** [...]. San José, Costa Rica: ASAP, 2022. p. 1-8.

ROSENFELD, A. H.; ROMM, J. J.; AKBARI, H.; POMERANTZ, M. Policies to reduce heat islands magnitudes of benefits and incentives to achieve them. *In*: ACEEE SUMMER STUDY ON ENERGY EFFICIENCY IN BUILDINGS, 10., 1996. **Proceedings** […]. Pacific Grove, CA: American Council for an Energy-Efficient Economy, 1996. p. 177-186.

ROSSI, S.; SIMEONI, M.; QUARANTA, A. Behavior of chromogenic pigments and influence of binder in organic smart coatings. **Dyes and Pigments**, London, v. 184, p. 108879, 2021. DOI: https://doi.org/10.1016/j.dyepig.2020.108879.

SAADEH, S.; ZOUHBI, A.; ALMASHHADANI, S.; AL-HADITHI, A. Application of fully permeable pavements as a sustainable approach for mitigation of stormwater runoff. **International Journal of Transportation Science and Technology**, Beijing, v. 8, n. 4, p. 338-350, 2019. DOI: https://doi.org/10.1016/j.ijtst.2018.11.004.

SALVADOR. **Plano de Ação Climática**. Salvador: Prefeitura Municipal, 2020. Disponível em: https://americadosul.iclei.org/wp-content/uploads/sites/19/2021/01/salvador-plano-de-acao-climatica.pdf. Acesso em: 11 mar. 2026.

SALVATI, A.; KOLOKOTRONI, M. Microclimate data for building energy modelling: Study on ENVI-met forcing data. *In*: INTERNATIONAL CONFERENCE AND EXHIBITION, 16., 2019, Rome. **Proceedings** […]. Rome, Italy: IBPSA, 2019. p. 3361-3368. Disponível em: https://publications.ibpsa.org/conference/paper/?id=bs2019_210544. Acesso em: 27 jun. 2026.

SANTAMOURIS, M. Cooling the cities: A review of reflective and green roof mitigation technologies to fight heat island and improve comfort in urban environments. **Solar Energy**, Oxford, v. 103, p. 682-703, 2014. DOI: https://doi.org/10.1016/j.solener.2012.07.003.

SANTAMOURIS, M. Using cool pavements as a mitigation strategy to fight urban heat island: A review of the actual developments. **Renewable and Sustainable Energy Reviews**, Oxford, v. 26, p. 224-240, 2013. DOI: https://doi.org/10.1016/j.rser.2013.05.047.

SANTAMOURIS, M.; GAITANI, N.; SPANOU, A.; SALIARI, M.; GIANNOPOULOU, K.; VASILAKOPOULOU, K.; KARDOMATEAS, T. Using cool paving materials to improve microclimate of urban areas - Design realization and results of the flisvos project**. Building and Environment**, Oxford, v. 53, p. 128-136, 2012. DOI: https://doi.org/10.1016/j.buildenv.2012.01.023.

SANTOS, J. R. P.; RIBAS, L. V. S.; CASTELO BRANCO, V. T. F. Caracterização da macrotextura de pavimentos através do mean profile depth utilizando modelagem 3D da superfície. *In*: RIO DE TRANSPORTES, 21., 2024, Rio de Janeiro. **Anais [**...] Rio de Janeiro:UFRJ, 2024. p.1-10. Disponível em: https://repositorio.ufc.br/bitstream/riufc/83915/3/2025_tcc_jrpsantos.pdf. Acesso em: 31 out. 2025.

SANTOS, S. M. B; BENTO-GONÇALVES, A.; VIEIRA, A. Research on wildfires and remote sensing in the last three decades: a bibliometric analysis. **Forests**, Basel, v. 12, p. 1-17, n. 5, 2021. DOI: https:// doi.org/10.3390/f12050604.

SEN, S.; ROESLER, J.; RUDDELL, B.; MIDDEL, A. Cool pavement strategies for urban heat island mitigation in suburban Phoenix, Arizona. **Sustainability**, Basel, v. 11, n. 16, p. 4452, 2019. DOI: https://doi.org/10.3390/su11164452.

SHA, A.; LIU, Z.; TANG, K.; LI, P. Solar heating reflective coating layer (SHRCL) to cool the asphalt pavement surface. **Construction and Building Materials**, London, v. 139, p. 355-364, 2017. DOI: https://doi.org/10.1016/j.conbuildmat.2017.02.087.

SHAMSAEI, M.; CARTER, A.; VAILLANCOURT, M. A review on the heat transfer in asphalt pavements and urban heat island mitigation methods. **Construction and Building Materials,** London, v. 359, p. 129350, 2022. DOI: https://doi.org/10.1016/j.conbuildmat.2022.129350.

SHARMIN, T.; STEEMERS, K.; MATZARAKIS, A. Microclimatic modelling in assessing the impact of urban geometry on urban thermal environment. **Sustainable Cities and Society**, Amsterdam, v. 34, p. 293-308, 2017. DOI: https://doi.org/10.1016/j.scs.2017.07.006

SORIANO, M.A.G.; CASTELO BRANCO, V.T.F. Justiça climática nos planos de ação climática: uma análise do setor de transportes. **Transporte y Territorio,** v. 32, p. 37-68, 2025.

DOI: https://doi.org/10.34096/rtt.i32.16698

STEWART, I. D.; OKE, T. R. Local Climate Zones for urban temperature studies. **Bulletin of the American Meteorological Society,** Boston, v. 93, n. 12, p. 1879–1900, 2012. DOI: https://doi.org/10.1175/BAMS-D-11-00019.1

STEWART, I. D.; OKE, T. R.; KRAYENHOFF, E. S. Evaluation of the 'local climate zone' scheme using temperature observations and model simulations. **Int. J. Climatol**. v. 34, p. 1062–1080, 2013. DOI: https://doi.org/10.1002/joc.3746

SYNNEFA, A.; SANTAMOURIS, M.; APOSTOLAKIS, K. Experimental testing of cool colored thin layer asphalt and estimation of its potential to improve the urban microclimate. **Building and Environment**, Oxford, v. 46, n. 1, p. 38-44, 2011. DOI: https://doi.org/10.1016/j.buildenv.2010.06.006.

SYNNEFA, A.; SANTAMOURIS, M.; LIVADA, I. A study of the thermal performance of reflective coatings for the urban environment. **Solar Energy**, Oxford, v. 80, n. 8, p. 968-981, 2006. DOI: https://doi.org/10.1016/j.solener.2005.08.005.

TALEGHANI, M.; CRANK, P.; MOHEGH, A.; SAILOR, D.; BAN-WEISS, G. The impact of heat mitigation strategies on the energy balance of a neighborhood in Los Angeles. **Solar Energy,** Oxford, v. 177, p. 604-611, 2019. DOI: https://doi.org/10.1016/j.solener.2018.11.037

TAVARES, S. G.; ABUSEIF, M.; DUPRÉ, K. Urban Heat Mitigation in a Tropical Climate: A Computer Simulation-Based Study in Townsville, Australia**. City and Environment Interactions**, Amsterdam, v. 27, p. 100211, 2025. DOI: https://doi.org/10.1016/j.cacint.2025.100211

TEIXEIRA, J. E. S. L.; AMAECING JUNIOR, C. M.; REZENDE, L. R.; BRANCO, V. T. F. C.; KIM, Y. R. Evaluation of asphalt concrete's fatigue behavior using cyclic semi-circular bending test. **Construction and Building Materials**, London, v. 400, p. 132772, 2023. DOI: https://doi.org/10.1016/j.conbuildmat.2023.132772

TÖZÜM, M. S.; ALAY AKSOY, S.; ALKAN, C. Manufacturing surface active shell and bisphenol A free thermochromic acrylic microcapsules for textile applications. **International Journal of Energy Research**. Hoboken, v. 45, p. 7018–7037, 2021. DOI: https://doi.org/10.1002/er.6287.

TSOKA, S.; TSIKALOUDAKI, A.; THEODOSIOU, T. Analyzing the ENVI-met microclimate model's performance and assessing cool materials and urban vegetation applications–A review. **Sustainable Cities and Society**, Amsterdam, v. 43, p. 55-76, 2018. DOI: https://doi.org/10.1016/j.scs.2018.08.009.

UNITED NATIONS HUMAN SETTLEMENTS PROGRAMME (UN-HABITAT). **World cities report 2022:** envisaging the future of cities. Nairobi: UN-Habitat, 2022. Disponível em: https://unhabitat.org/sites/default/files/2022/06/wcr_2022.pdf. Acesso em: 13 mar. 2026.

UNITED NATIONS. **Transforming our world:** the 2030 Agenda for Sustainable Development. New York, 2015. Disponível em: https://docs.un.org/en/A/RES/70/1. Acesso em: 27 jun. 2026.

WANG, Q.; MIN, Z.; LI, M.; HUANG, W. Mechanical behavior and thermal oxidative aging of anhydride-cured epoxy asphalt with different asphalt contents. **Journal of Materials in Civil Engineering,** USA, v. 34, n. 10, p. 04022245, 2022. DOI: https://doi.org/10.1061/(ASCE)MT.1943-5533.0004408

WANG, R.; REN, C.; XU, Y.; LAU, K. K. L.; SHI, Y. Mapping the local climate zones of urban areas by GIS-based and WUDAPT methods: A case study of Hong Kong. **Urban Climate**, Amsterdam, v. 24, p. 567–576, 2018 DOI: https://doi.org/10.1016/j.uclim.2017.10.001

WANG, Y.; BERARDI, U.; AKBARI, H. Comparing the effects of urban heat island mitigation strategies for Toronto, Canada. **Energy and Buildings**, Lausanne, v. 114, p. 2-19, 2016. DOI: https://doi.org/10.1016/j.enbuild.2015.06.046.

WILLIAMS, B. A.; WILLIS, J. R.; SHACAT, J. **Asphalt pavement industry survey on recycled materials and warm-mix asphalt usage 2022**. Greenbelt: NAPA, 2022. Disponível em: https://www.asphaltpavement.org/uploads/documents/IS138-2022_RAP-RAS-WMA_Survey__WITH_APPENDICES_508.pdf. Acesso em: 12 mar. 2026.

WU, S.; LIU, G.; LI, H.; ZHU, C.; CHEN, Z. Evaluation of mechanical properties and aging index of 10-year field aged asphalt materials. **Construction and Building Materials**, London, v. 155, p. 1158-1167, 2017. DOI: https://doi.org/10.1016/j.conbuildmat.2017.08.135.

XIE, J.; CHEN, J.; HU, L.; WU, S.; WANG, Z.; LI, M.; YANG, C. Preparation, thermochromic properties and temperature controlling ability of novel pellets in ultra-thin wearing course. **Construction and Building Materials,** London, v. 389, p. 131797, 2023. DOI: https://doi.org/10.1016/j.conbuildmat.2023.131797.

XU, L.; WANG, J.; XIAO, F.; EL-BADAWY, S.; AWED, A. Potential strategies to mitigate the heat island impacts of highway pavement on megacities with considerations of energy uses. **Applied Energy**, United Kingdom, v. 281, p. 116077, 2021. DOI: https://doi.org/10.1016/j.apenergy.2020.116077.

YANG, R.; OZER, H.; KANG, S.; AL-QADI, I. L. **Environmental impacts of producing asphalt mixtures with varying degrees of recycled asphalt materials**. University of California. 2014. Disponível em: https://digitalcommons.unl.edu/cgi/viewcontent.cgi?article=1279&context=ndor. Acesso em: 9 mar. 2026.

YAZDIPANAH, F.; KHEDMATI, M.; REA, R.; TEIXEIRA, J.; HAGHSHENAS, H. F. Development of a balance mix performance framework for assessing high-recycled asphalt mixtures' resistance: A study integrating laboratory and field findings. **Road Materials and Pavement Design**, France, v. 26, n. 11, p. 1–20, 2025. DOI: https://doi.org/10.1080/14680629.2025.2465577

YAZDIPANAH, F.; KHEDMATI, M.; HAGHSHENAS, H. F. **Nebraska Balanced Mix Design – Phase I**. SPR-FY22 (002). Nebraska: Department of Transportation, 2023. Disponível em:

https://digitalcommons.unl.edu/cgi/viewcontent.cgi?article=1279&context=ndor. Acesso em: 9 mar. 2026.

YI, Y.; JIANG, Y.; FAN, J.; ZHANG, Y.; DENG, C.; TIAN, T.; JI, X. Durability of a heat-reflective coating on an asphalt pavement. **Road Materials and Pavement Design**, France, v. 23, n. 11, p. 2651-2668, 2022. DOI: https://doi.org/10.1080/14680629.2021.1991838.

YIN, F.; WEST, R. C. **Balanced mix design resource guide (No. IS-143)**. Greenbelt: National Asphalt Pavement Association, 2021. Disponível em: https://www.eng.auburn.edu/research/centers/ncat/files/NAPA-IS-143-BMD-Resource-Guide-2021.pdf. Acesso em: 12 mar. 2026.

YU, B.; PENG, W.; LIU, J.; ZHANG, J.; LI, W.; HONG, Q. Research on the performance of temperature responsive asphalt mixture with thermochromic material. **Road Materials and Pavement Design**, Oxon, v. 23, n. 3, p. 713–724, 2022. DOI: https://doi.org/10.1080/14680629.2020.1842792

ZEESHAN, M.; ALI, Z. Heat stress mitigation in urban streets having hot humid climatic conditions: Strategies and performance results from a real scale retrofitting project. **Science and Technology for the Built Environment,** United Kingdon, v. 28, n. 4, p. 513-526, 2022. DOI: https://doi.org/10.1080/23744731.2022.2043214

ZHANG, H.; CHEN, Z.; LI, L.; ZHU, C. Evaluation of aging behaviors of asphalt with different thermochromic powders. **Construction and Building Materials,** London, v. 155, p. 1198-1205, 2017. DOI: https://doi.org/10.1016/j.conbuildmat.2017.08.161.

ZHANG, H.; CHEN, Z.; XU, G.; SHI, C. Physical, rheological and chemical characterization of aging behaviors of thermochromic asphalt binder. **Fuel**, England, v. 211, p. 850-858, 2018. DOI: https://doi.org/10.1016/j.fuel.2017.09.111.

ZHANG, H.; LI, L.; CHEN, Z. Effect of aging on the rheological behaviors of SBS-modified asphalt with thermochromic materials. **Journal of Testing and Evaluation**, USA, v. 49, n. 6, p. 4032–4039, 2020. DOI: https://doi.org/10.1520/JTE20190633

ZHANG, J.; XU, T. Developments and thermal properties of thermochromic microcapsule and thermochromic asphalt-based composite coatings. **Construction and Building Materials**, London, v. 438, p. 137184, 2024. DOI: https://doi.org/10.1016/j.conbuildmat.2024.137184.

ZHANG, X.; LI, H.; JIA, M.; XIE, N; KOUSIS, I.; SANTAMOURIS, M. Laboratorial investigation on optical, thermal and pavement performance of biomimetic dark reflective coatings with composite structure for pavement cooling. **Building and Environment,** Oxford, v. 266, p. 112057, 2024. DOI: https://doi.org/10.1016/j.buildenv.2024.112057.

ZHANG, X.; LI, H.; XIE, N.; JIA, M.; YANG, B.; LI, S. Laboratorial investigation on optical and thermal properties of thermochromic pavement coatings for dynamic thermoregulation and urban heat island mitigation. **Sustainable Cities and Society,** Amsterdam, v. 83, p. 103950, 2022. DOI: https://doi.org/10.1016/j.scs.2022.103950.

ZHANG, Y.; ZHAI, X. Preparation and testing of thermochromic coatings for buildings. **Solar Energy**, Oxford, v. 191, p. 540–548, 2019. DOI: https://doi.org/10.1016/j.solener.2019.09.042.

ZHAO, M.; LONG, J.; ZHANG, H.; CHEN, Z. Performance evaluation of temperature-regulating asphalt mixture with thermochromic materials and low freezing point materials. **Construction and Building Materials,** London, v. 364, p. 129873, 2023. DOI: https://doi.org/10.1016/j.conbuildmat.2022.129873.

ZHOU, Y.; SHEPHERD, J. M. Atlanta's urban heat island under extreme heat conditions and potential mitigation strategies. **Natural Hazards**, New York, v. 52, n. 3, p. 639-668, 2010. DOI: https://doi.org/10.1007/s11069-009-9406-z